JSCSEN 76(5)647–803(2011)

International Year of CHEMISTRY 2011

Journal of the Serbian Chemical Society

Electronic Version

VOLUME 76

No 5

BELGRADE 2011

Available on line at

www.shd.org.rs/JSCS/

The full search of JSCS is available through

DOAJ DIRECTORY OF OPEN ACCESS JOURNALS

www.doaj.org

Journal of the Serbian Chemical Society
JSCS-info@shd.org.rs • www.shd.org.rs/JSCS

J. Serb. Chem. Soc. Vol. 76, No. 5 (2011)

CONTENTS

Published by the Serbian Chemical Society
Karnegijeva 4/III, 11000 Belgrade, Serbia
Printed by the Faculty of Technology and Metallurgy
Karnegijeva 4, P.O. Box 35-03, 11120 Belgrade, Serbia

Journal of the Serbian Chemical Society
JSCS-info@shd.org.rs • www.shd.org.rs/JSCS
J. Serb. Chem. Soc. 76 (5) 647–677 (2011) UDC 543.42:542.943:573.02:541.515+615.27
JSCS–4147 *Review*

REVIEW

The role of EPR spectroscopy in studies of the oxidative status of biological systems and the antioxidative properties of various compounds

IVAN SPASOJEVIĆ[1], MILOŠ MOJOVIĆ[2], ALEKSANDAR IGNJATOVIĆ[2] and GORAN BAČIĆ[2]*

[1]*Institute for Multidisciplinary Research, Kneza Višeslava 1, University of Belgrade, 11000 Belgrade and* [2]*Faculty of Physical Chemistry, University of Belgrade, Studentski trg 12–16, 11000 Belgrade, Serbia*

(Received 15 October, revised 28 December 2010)

Abstract: In this era of intense study of free radicals and antioxidants, electron paramagnetic resonance (EPR) is arguably the best-suited technique for such research, particularly when considering biochemical and biological systems. No attempt was made to cover all the topics of EPR application but instead attention was restricted to two areas that are both novel and received less attention in previous reviews. In the first section, the application of EPR in assessing the oxidative status of various biological systems, using endogenous stabile paramagnetic species, such as the ascorbyl radical, semiquinone, melanin, and oxidized pigments, is addressed. The second section covers the use of EPR in the emerging field of antioxidant development, using EPR spin-trapping and spin-probing techniques. In both sections, in addition to giving an overview of the available literature, examples (mostly from the authors' recent work) are also presented in sufficient detail to illustrate how to explore the full potential of EPR. This review aims at encouraging biologists, chemists and pharmacologists interested in the redox metabolism of living systems, free radical chemistry or antioxidative properties of new drugs and natural products to take advantage of this technique for their investigations.

Keywords: EPR spectroscopy; oxidative status; antioxidants; spin-probes; spin--traps.

CONTENT

* Corresponding author. E-mail: ggbacic@ffh.bg.ac.rs
doi: 10.2298/JSC101015064S

1. INTRODUCTION

The delicate balance between the advantageous and detrimental effects of free radicals is clearly an important aspect of life. Although reactive oxygen species (ROS) have been labelled as "villains" for a long time,[1,2] they also have been found to regulate the activity of a number of enzymes *via* oxidation in receptor-mediated signalling pathways, a process known as redox signalling.[3–8] This signalling is involved in the regulation of vascular tone, oxygen tension, activity of the immune system, growth in plants, and some other physiological processes.[9] On the other hand, uncontrolled generation of radicals is highly related to many pathophysiological events, such as neurodegenerative diseases (Alzheimer's disease, amyotrophic lateral sclerosis, Down's syndrome, *etc*),[10–13] malignancy,[14] diabetes mellitus,[15] sepsis[16] and atherosclerosis,[17] and also seems to play an important role in the aging process.[1,2,18,19] Hence, a certain level of oxidation performed by free radicals is mandatory in biosystems, but increased oxidation may jeopardize normal functioning and lead to pathophysiological conditions. Therefore, knowledge of the relative level of oxidation in a biosystem, known as oxidative status, clearly represents an imperative in studies of the mechanisms of (patho)physiological processes.[20]

Antioxidant supplements may be of great benefit in treating conditions related to a disturbed oxidative status. However, since free radicals are involved in signalling pathways, biosystems have developed a refractory response against the excessive presence of antioxidants,[21,22] in order to maintain a flexible intracellular redox poise.[19] This could explain why megadoses of ascorbate and some other antioxidants do not prolong life in humans with a balanced diet.[23,24] Although there is a myriad of compounds and foods that possess good antioxidative characteristics, new antioxidants that could be able to overcome the refractory response of the body, such as fructose and its phosphorylated forms,[25] should be investigated. However, the evaluation of antioxidative properties still represents the first step in determining whether a particular food or its compounds could be of any use in health problems related to oxidative stress.

A broad spectrum of techniques has been applied in redox research. Most of them, however, determine only the total antioxidative status or antioxidative capacity and do not provide details on specific reactive species. On the other hand, those which are able to provide more specific data require the use of tedious laboratory procedures or suffer from low sensitivity or artefacts. Electron Paramagnetic Resonance (EPR) spectroscopy stands out from other methods because of its unique ability to detect either short or long lived radicals with high specificity and sensitivity (*e.g.*, EPR spin-trapping detection of the superoxide radical is 40 times more sensitive than spectrophotometric analysis with cytochrome *c* [26,27]). EPR is also capable of directly detecting a number of specific markers of the oxidative status, such as the ascorbyl radical,[28,29] the tocopherol radical,[30,31] melanin,[32,33] semiquinone,[34] and plant pigments,[35,36] in a variety of biosystems – human and animal tissues and fluids, whole insects, plant tissues and others. In an antioxidant investigation, EPR can also be applied to determine the capacity of the selected compound, extract or food to remove specific reactive species, such as superoxide ($O_2^{\bullet-}$), hydroxyl radical ($^{\bullet}OH$), organic radicals, lipid peroxides, or to sequester iron.[37–42] In addition, EPR is, in principle, a non-destructive technique, which is a clear advantage over chemical procedures when dealing with biological systems. This paper represents an overview of recent applications of EPR spectroscopy in determining the oxidative status of biosystems and antioxidative properties of compounds, extracts, and foods. The full capacity of a variety of EPR techniques in redox studies is yet to be explored; hence, the aim was to encourage scientists to apply EPR in their studies and to develop new EPR techniques. As a matter of convenience, most of the examples and illustrations are from a series of the authors' recent studies, with the aim of presenting the main principles of the application of EPR in redox research.

2. EVALUATION OF OXIDATIVE STATUS

2.1. EPR in comparison to other methods

A variety of spectrophotometric assays is available for investigating the oxidative status of biochemical systems. Widely applied is the ABTS (2,2-azino--bis(3-ethylbenzothiazoline-6-sulphonic acid) assay, in which ABTS is added to a system, oxidized by horseradish peroxidase/H_2O_2 to the radical cation $ABTS^+$ which absorbs light at 660, 734 and 820 nm. Results obtained using the ABTS assay are expressed as equivalents of ascorbic acid, indicating the total antioxidant activity of some tissue homogenate, cells (*e.g.*, cultured cells) or liquids (*e.g.*, serum, CSF, *etc.*).[43,44] Increased total antioxidant activity is usually related to activation of the antioxidative system (AOS), indicating a disturbed oxidative status. Useful information on the oxidative status could also be obtained by measuring the total amount of R–SH groups by the method of Ellman,[45] which can provide information on both pro-oxidative and pro-reductive modifications of the

oxidative status. R–SH groups are present in glutathione (GSH), a very important component of the AOS, as well as in proteins. [46] A total amount of R–SH groups less than normal usually means that some GSH has been oxidized to GSSG *via* ROS reduction. In addition, it could be a consequence of an increased production of reactive nitrogen species (RNS), which leads to the formation of R–SNO groups.[47] On the other hand, an increased level of the total amount of R–SH groups indicates a decrease in the production of superoxide, which leads to a decrease of peroxynitrite production and R–SH nitosylation.[48]

The ROS/RNS-system and the AOS are just two intertwined components present within the global physiological mechanisms of homeostasis.[49] Changes in the oxidative status modify the AOS activity, its composition and structure, striving to provide the best possible protection and preservation of cellular homeostasis.[33] Therefore, the activity of a battery of AOS enzymes (catalase, GSH peroxidase and reductase, MnSOD, and CuZnSOD) represent excellent marker of the oxidative status and may provide information on the specific mechanisms of oxidative processes.[29,50] For example, CuZnSOD is inactivated by H_2O_2;[51] hence a decrease in its activity in some biosystem indicates the development of H_2O_2-mediated oxidative stress.

Confocal fluorescent microscopy represents a powerful tool for redox studies on cell cultures and *ex vivo* tissues. With the increased interest in this area of research, a variety of labels have become available that can be used to investigate the oxidative status of cells under different conditions. For example, the intensity of fluorescence of cells stained with MitoTracker Orange is affected by the intracellular level of hydrogen peroxide (H_2O_2) and the oxidative status.[25,52] Some other dyes, the fluorescence of which is dependent on oxidation, such as carboxy-H_2-DCFDA and others, can also be used.[53]

Although these techniques are useful, they do not provide direct information on the reactive species that participate in oxidative processes; hence, EPR spectroscopy should be used. There are two distinct EPR approaches for the study of the oxidative status of biosystems: EPR spin-trapping of short lived radicals and EPR spectroscopy of stabile, paramagnetic bio molecules.[54] EPR spin-trapping represents a technique with a special place in oxidative studies because of its unique ability to identify and quantify relative changes in the level of any specific short-lived free radical involved in oxidative stress, including even $^{\bullet}OH$ with a lifetime of $\approx 10^{-9}$ s or $O_2^{\bullet-}$ ($\approx 10^{-6}$ s).[55] The application of EPR spin-trapping in the evaluation of oxidative status has been covered in recent reviews.[56,57] Hence, in this section, an alternative manner of application of EPR in investigations of the oxidative status is illustrated. Physiologically active molecules can react with a number of reactive species within cells and therefore propagate or attenuate free radical processes and serve as antioxidants and possible biochemical and/or physiological switches. Some endogenous biomolecules, such as as-

corbate, tocopherol, melanin, or plant pigment system P700, can be modified by ROS to stabile organic radicals with a very long lifetime, allowing their direct detection by EPR spectroscopy.[58] Due to the non-destructive nature of EPR, this can be realised without any interference with biochemical processes, which is not the case with any other method.[59] By detecting and discriminating these paramagnetic molecules, the level of which represents a marker of oxidative status, EPR provides essential information on redox mechanisms in biosystems. However, in spite of the unique capabilities of EPR, it should be emphasized that, in our experience, the most complete insight into redox processes can be achieved by complementing EPR with other methods, such as analysis of the AOS or SH groups (see the next section).

The detection of different paramagnetic biomolecules requires the explanation of some technical details. Usually their signals can be detected by means of a conventional X-band EPR spectrometer operating at a resonant frequency of around 9.5 GHz. The measurements are generally performed at physiological or room temperature, but in some cases lower temperatures (liquid N_2) are required to obtain a better S/N ratio, which requires minor technical adjustments. When dealing with oxygen consuming systems or oxygen sensitive processes, it is essential to control the gas environment in the sample. This can be easily achieved by placing samples in gas-permeable Teflon tubes or holders and flowing the required gas mixture over the sample.[60] In a such manner, a constant level of O_2 can be supplied to the system,[56,60] or if the radical is sensitive to oxygen (*e.g.*, the tocopheroxyl radical, $^{\bullet}$TO), to deprive it by using pure N_2 or Ar.[54] An important component in analyzing any EPR spectrum is to perform spectral simulations of each detected signal, to identify species and to determine their signal intensities (in our studies, Brukers' WINEPR SimFonia was used but there are many other software available).[28,60–62] The following sections illustrate different applications of EPR spectroscopy in detecting the most common stabile paramagnetic species in biosystems.

2.2. EPR spectroscopy of the ascorbyl radical

Ascorbate is thermodynamically at the bottom of the pecking order of oxidizing free radicals.[63] That is, all oxidizing species with higher redox potentials, which include $^{\bullet}$OH, alkyl peroxyl radical ($^{\bullet}$ROO), lipid peroxyl radicals ($^{\bullet}$LOO), tocopheroxyl radical ($^{\bullet}$TO),[63] peroxynitrite,[64] and others, can be repaired by ascorbate, leading to the generation of the ascorbyl radical ($^{\bullet}$Asc). This property makes $^{\bullet}$Asc probably the best endogenous marker of the oxidative status in biosystems. EPR can easily detect the ascorbyl radical in almost any system since it gives a characteristic doublet (Figs. 1a, 1b and 1c). Another important generator of $^{\bullet}$Asc in the biological setup are catalytically active transition metals (*e.g.*, iron or copper), which can provoke oxidation of ascorbate: *i*) directly: Fe^{3+}

(Cu^{2+}) + Asc^- → Fe^{2+} (Cu^{1+}) + •Asc, *ii*) in cooperation with H_2O_2: $Fe^{2+}(Cu^{1+})\cdots Asc + H_2O_2 \rightarrow Fe^{3+}(Cu^{2+}) + {}^{\bullet}Asc + OH^- + H_2O$ or *iii*) *via* •OH, generated in a metal involving the Fenton system: $^{\bullet}OH + Asc^- \rightarrow {}^{\bullet}Asc + OH^-$.[65–67] Obviously, the level of •Asc can indicate how much redox active metals there are in a system,[65,66] but the level of •Asc also depends on the production of free radicals in reactions unrelated to the presence of transition metals and these should be discriminated. It is suggested that the influence of catalytically active metals could be emphasized by the addition of H_2O_2, which should promote reactions *ii* and *iii* depending on the level of the catalytically active metals. On the other hand, it should be stressed that commercial buffers inevitably contain metal impurities which may represent a source of artefacts in biochemical studies by increasing the basic level of •Asc.[65] This potential problem can be eliminated by the addition of strong chelating agents, such as DTPA, which sequester transition metals and diminish their oxidative capacity.[67]

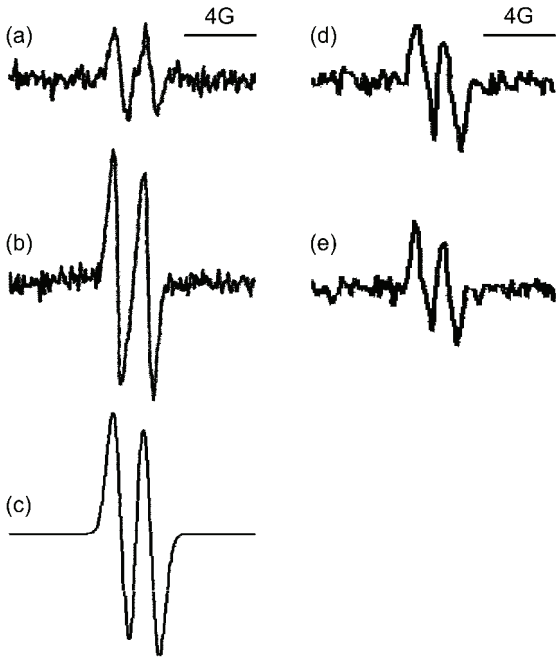

Fig. 1. Left: EPR spectra of the ascorbyl radical (•Asc). EPR detects the single unpaired electron of •Asc, which has a spin $S = ½$. However, the electron interacts with surrounding nuclei that also possess spin (here ^1H with a nuclear spin of $I = ½$), which leads to hyperfine splitting; hence, two lines emerge in the spectrum. An example of •Asc in human plasma: a) untreated serum;[28] b) serum treated with 0.5 mM peroxynitrite;[64] c) spectral simulation of •Asc EPR signal proving that the signal from serum emerges from this radical, enabling quantification of the signal intensity. Characteristic EPR spectra of •Asc in amnion fluid of d) normal and e) thrombophilic pregnancies[29] (showing no differences between the two samples).

The level of •Asc detected by EPR spectroscopy as an indicator of pro-oxidative changes was first introduced by Buettner and Jurkiewicz in 1993.[28] Experiments were performed on a phosphate buffer supplemented with different ascorbate concentrations and on human plasma. Using the •OH and $O_2^{\bullet-}$ generating systems, the authors showed high correlations between the production of these radicals (determined by EPR spin-trapping) and the level of •Asc. Since

then, •Asc has been detected by EPR in a variety of biological samples: plasma,[68,69] cerebrospinal fluid (CSF),[69] skin,[70,71] extracellular fluid,[72] plant leaves[73] and the midgut fluid of insects.[74] Increase of the steady-state concentration of •Asc was reported in several conditions related to pro-oxidative changes, such as ischemia/reperfusion, sepsis,[75] brain injuries,[76] paraquat poisoning, iron overload, gastric cancerogenesis,[77] pre-eclampsia,[78] and others. Recently, EPR spectroscopy of •Asc was employed to investigate the oxidative status of amnion fluid (Figs. 1d and 1e). The similar level of •Asc in the amnion fluid of control and thrombophilic subjects indicates that the disturbed oxidative status of the placenta which was observed by AOS assays,[29] was not provoked by an increased generation of reactive species in amnion fluid,[29] thus enabling a potential mechanisms of thrombophilia to be suggested. There are many other interesting examples. Menditto *et al.*[79] used EPR spectroscopy of •Asc to study the association between the oxidative status of seminal fluid and the iron and copper content. A very innovative and elegant experimental design was developed by Sharma *et al.*,[80] enabling *in vivo* EPR measurements of the level of •Asc, as a real-time quantitative marker of changes of the oxidative status in dog myocardium during ischemia/reperfusion.

The absolute •Asc concentration which can be detected is as low as ≈5 nM by measuring the intensity of the EPR signal using spectral simulation (Fig. 1) and calibration. However, the basal •Asc level in tissues and fluids can vary significantly between subjects or populations,[64,68] and is highly dependent on the level of ascorbate in the system.[72] For instance, due to different diets and life styles, the basal level of ascorbate and, consequently, ascorbyl radical in the plasma of the Brazilian population (65 nM)[64] is different from that of the European one (100 nM).[68] Galleano *et al.*[81] developed an approach that could overcome this potential obstacle in oxidative studies. By combining EPR measurements of the •Asc concentration and HPLC analysis for the total ascorbate level, they were able to calculate the ascorbyl radical/ascorbate (•Asc/Asc) ratio, which represents an indicator of oxidative stress independent of individual and population variations in the ascorbate level. This represents an example of the effectiveness of EPR in combination with other techniques, as emphasized before.

2.3. EPR spectroscopy of the tocopheroxyl radical

Tocopherols (vitamin E) are the main lipid-soluble antioxidants of cellular membranes and blood plasma.[30] They react with oxidizing species, such as •LOO (lipid peroxyl radical),[82] •OH, and $•O_2^-$, but also with NO[83] and $ONOO^-$,[84] to produce •TO, which can be detected by EPR spectroscopy (Fig. 2). However, the generation of •TO in biosystems is thermodynamically interlinked with the metabolism of ascorbate, *via* the reaction: •TO + Asc → TOH + •Asc.[87] For example, it was demonstrated that in human plasma exposed to oxidative stress, the EPR

signal of •TO emerges (Fig. 2b) only after the virtual disappearance of the ascorbyl radical.[31] Therefore, the EPR spectroscopy of the tocopheroxyl radical could be used in investigations of oxidative status, emphasizing an occurrence of intense oxidative stress capable of depletion of the antioxidative capacity of the ascorbate in the system.

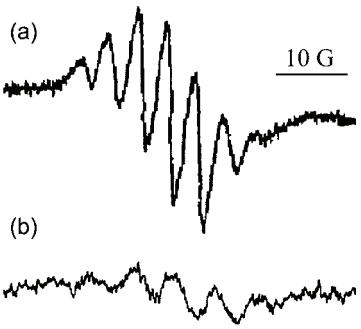

Fig. 2. Characteristic seven-line EPR signal of •TO. a) Generated by purging the suspension with 0.1 mM tocopherol and 100 mM SDS with NO gas;[86] b) in human plasma exposed to $O_2^{\bullet-}$ generated by the hypoxanthine/xanthine oxidase system.[31] The interactions which provoke hyperfine splitting resulting in a complex seven-line signal and the spectral parameters were described in detail by Matsuo *et al.*[87]

The detection of •TO in biosystems *ex vivo* is complicated by the fact that •TO can react with oxygen to produce TO and superoxide (an EPR silent species), which can occur during sample collection and storage, as well as during EPR measurements, hence even EPR measurements have to be performed in an inert atmosphere (N_2). For this reason, most of the EPR studies of •TO have been performed on model systems *in vitro*. Naužil *et al.*[30] applied EPR spectroscopy of •TO to study the inhibitory effects of α-tocopherol against radical-initiated oxidation of low-density lipoproteins (LDL) lipids. Zhou *et al.*[88] used a similar approach to investigate the regeneration of α-tocopherol by green tea polyphenolics in phospholipid micelle exposed to oxidative stress. The metabolism of TO can also be explored using the more stabile and hydrosoluble vitamin E derivative – Trolox (6-hydroxy-2,5,7,8-tetramethylchroman-2-carboxylic acid). For example, Opländer *et al.*[89] applied EPR to investigate the effects of the Trolox against UV-A induced cell death of human skin fibroblasts. It was determined that the production of the Trolox radical is increased in the presence of nitrite, indicating that the EPR spectroscopy of •TO could be useful for studying not only ROS, but also for nitrogen reactive species.

2.4. EPR spectroscopy of melanin

Melanins represent a broad class of biopolymers without a unique structure, composed of 5,6-dihydroxyindole, 5,6-dihydroxyindole-2-carboxylic acid, and their various oxidized forms (Fig. 3).[90] Melanins are divided into three groups: eumelanins and pheomelanins in animals, and allomelanins in plants. Melanins react with ROS, organic radicals and oxidize transition metals.[91] In these reactions, DHI is converted to a stabile SQ radical and other paramagnetic species,[90]

which can be detected by EPR. These properties make the intensity of the EPR signal of melanin an excellent marker signifying the oxidative status of specific melanin-containing systems, such as mammalian skin[92] and eyes,[93,94] some plants,[95] fungi,[96,97] insects,[33,98] and others. Nevertheless, it should be stressed that although EPR spectroscopy can distinguish between different types of melanins, it is virtually impossible to connect the recorded spectrum to a specific eumelanin structure by any spectral analysis.

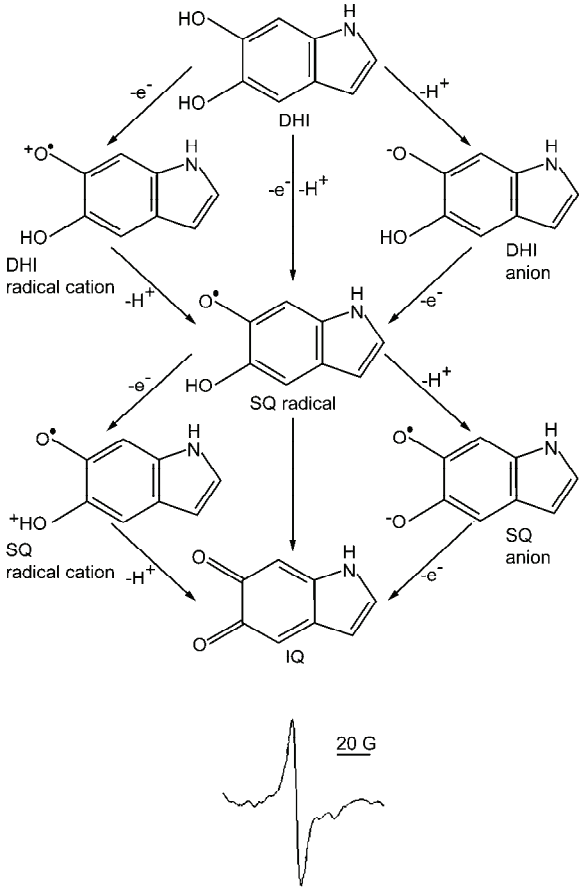

Fig. 3. Redox chemistry (a) and characteristic EPR signal of eumelanin (b). The key monomeric building blocks of eumelanin are: DHI (5,6-dihydroxyindole), SQ (semiquinone) and IQ (5,6-indolequinone). Spin–spin interactions, fast electron transfer reactions and anisotropy related to low mobility of paramagnetic species inside the melanin macromolecules make only one broad line in the melanin EPR spectrum emerge.

Neuromelanin, a pigment found in deep brain regions, such as *substantia nigra*, has drawn much attention because of its role in Parkinson's disease (PD).

Due to the complex chemistry of neuromelanin in the brain, EPR measurements do not provide a straightforward evaluation of the oxidative status, but studies on neuromelanin provide a valuable insight into the mechanisms of neurodegeneration in PD.[99–101] The EPR signal of melanin has been used to study the pro-oxidative effects of UV irradiation in skin and eyes. Wood *et al.*[32] used the melanin signal as an indicator of the oxidative status of melanin-containing skin cells from a genetically melanoma-susceptible cross of *Xiphophorus* fish (a model system for human melanoma research) exposed to UV irradiation of different wavelengths and intensities. A strong correlation between the intensity of the melanin signal and melanoma induction was observed, indicating that pro-oxidative changes represent an important causative step in melanoma development.[32] Pertinent to this, some attempts have been made to develop an *in vivo* EPR technique in the diagnostics of melanoma in humans. In a study performed by Vahidi *et al.*,[102] the EPR spectra of melanin in frog skin were recorded *in situ* using a surface EPR coil and 2D imaging, and the intensity of the melanin signal was observed to depend on the level of oxygenation, which is one of the parameters defining the oxidative status. It was proposed that 2D EPR spectroscopy could potentially be useful in early melanoma detection. Seagle *et al.*[93] employed EPR of melanin to study the effects of UV radiation on human retinal pigment epithelium with different coloured pigments and to compare the observed changes to the modifications in synthetic melanin. Samples were placed in an EPR "flat cell" and irradiated inside the cavity. As expected, the melanin signal from the cells increased with the power of irradiation, but not in two distinguishable portions as observed for synthetic melanin, indicating that *in vivo* radical photogeneration is different from photogeneration in a chemical system. This shows that chemical systems with synthetic melanin do not represent an adequate model of the structure and metabolism of melanin in biosystems.

Melanin represents an important constituent of the oxidative metabolism of insects. Barbehenn *et al.*,[98] applied EPR spectroscopy of melanin to investigate the pro-oxidative defence of plants against herbivorous insects. It was determined that melanin-like reactive substances are formed in the midgut fluid of insects, from the tannic acid present in leaves. In this way, plants disturb the oxidative status of the digestive system of insects and indirectly protect themselves.[103,104] On the other hand, some insects generate melanin to use its ROS scavenging ability in the regulation of their oxidative status. For example, it was recently shown using biochemical assays and EPR of melanin that exposure of the European corn borer (*Ostrinia nubilalis*) to low temperatures leads to an overproduction of H_2O_2 followed by an increase of the melanin signal (Fig. 4).[33] Hydrogen peroxide is an important player in the freeze tolerance development of insects, but as was shown, it can disturb the oxidative status of insect tissues.[33]

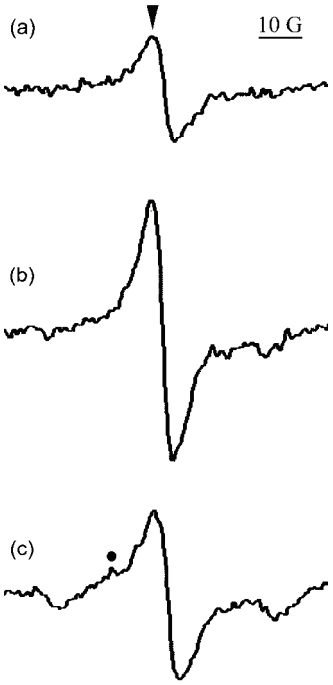

Fig. 4. EPR spectra of melanin in larvae maintained at: a) 5, b) –3 and c) –16 °C. The downward triangle (▼) marks the characteristic eumelanin-related EPR signal. The signal of pheomelanin (circle) can be observed on the left side of the eumelanin signal in panel c). It can be observed that the underlying signal of pheomelanin slightly shifts the eumelanin signal. The measurements were performed at liquid N_2 temperature in order to obtain a higher S/N ratio than at room temperature.[33]

Thus, in this case, insects use melanin to protect their cells from the oxidative burst involved in the adaptation process.

The presented examples illustrate the vast potential of EPR in studying various organic radicals,[105] which should be further utilized in redox studies of biosystems. For example, EPR is able to detect redox-active amino acid radicals: tyrosyl, tryptophanyl, glycyl, and histidyl radical.[106] The EPR of these stabile radicals was previously employed to study enzyme activity and protein damage,[57,107] but, potentially, it may also find applications in investigations of the oxidative status.[108]

2.5. The oxidative status of plants

Although previously unappreciated, the application of EPR spectroscopy is becoming more and more important in plant studies. It was previously illustrated that the EPR spin-trapping technique with advanced spin-traps (*e.g.* DEPMPO) is able to provide crucial data about plant oxidative processes,[34,56,60,109] but when it comes to endogenous paramagnetic species, the great diversity in plants opens even more possibilities for redox research. Although, there are many similarities between evaluating the oxidative status in plants and studies on human and animal systems, it was decided to dedicate a separate section to plants, in order to provide a compact overview and to emphasize the potential of the EPR methods. In a recent review of techniques applicable in the investigation of plant redox

processes, Shulaev and Oliver [27] concluded that, at present, measurements of oxidative stress in plants are limited and there are no truly non-invasive methods. Although they considered the EPR spin-trapping technique, the application of EPR spectroscopy of stabile organic radicals in plants was not taken into account. Since it enables the acquisition of signals of paramagnetic species in plant cells, parts or even whole plants without any interference with the metabolism, EPR spectroscopy could be the missing 'truly non-invasive' technique in plant research. It should be emphasized that the measurements can be performed under selected temperature, atmosphere, and light regimes, which can be varied inside the EPR spectrometer cavity during the course of the experiment.

As in animal tissues and fluids, the ascorbyl radical can be used to determine the oxidative status of plants. Malanga *et al.*[110] used the endogenous signal of the ascorbyl radical in an algal culture (*Chlorella vulgaris*) and intact soybean leaves to study UV-provoked oxidative stress. Puntarulo *et al.*[111] applied EPR measurements of $^{\bullet}$Asc to investigate the effects of NO on the oxidative status of soybean chloroplasts, proposing an antioxidative role of NO based on the decreased level of $^{\bullet}$Asc after treatment with NO.

The photosystem I (PSI), which contains an EPR active specie – oxidized pigment – $P700^{+}$, could also be used as a marker of the oxidative status.[35,36] The increased generation of reactive species leads to photoinhibition of the PSI and a related decrease in the $P700^{+}$ level.[112] Thus, in contrast to previous illustrations, a decrease in the EPR signal signifies pro-oxidative changes of the oxidative status. This approach was employed to investigate the oxidative stress in intact pea leaves exposed to chilling conditions. [36] The light inducible EPR signal, which was recognized to reflect the oxidized form of the PSI pigment P700 ($P700^{+}$), is shown in Fig. 5. The level of $P700^{+}$ was lower in plants exposed to cold, showing that the chilling conditions led to pro-oxidative changes of the status in leaves. A similar non-invasive approach could be used to investigate the oxidative status of plants exposed to some other stressors.

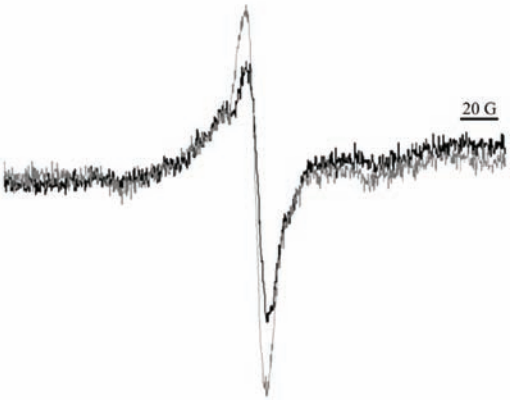

Fig. 5. Spectra of light-induced EPR active species – oxidized PSI pigment ($P700^{+}$) in pea leaves. Pale trace – samples from leaves of control plants exposed to 22 °C/70 μmol m^{-2} s^{-1} temperature/light conditions; dark trace – samples of leaves of peas under a 2 °C/70 μmol m^{-2} s^{-1} regime. The spectra were recorded at –100 °C.[36]

To study paramagnetic species not present in sufficient concentrations in plants to enable non-invasive detection, plant isolates or extracts could be used in EPR studies. For example, the EPR signal of quinhydrone was identified in isolated cell walls from pea roots, which could not be detected in the whole plant parts. The intensity of the EPR signal of quinhydrone was highly correlated with the concentration of H_2O_2 supplemented to the cell wall and with $^{\bullet}OH$ production evaluated by the EPR spin-trapping technique, showing itself to be a useful marker of oxidative status.[34] Pedersen[113–115] published several comprehensive studies on alcohol plant extracts showing that hundreds of species from the families Lamiaceae and Gesneriaceae contain quinone related paramagnetic species easily detectable by EPR, and potentially valuable as markers of oxidative status. Examples of EPR signals of such species in extracts of *Peltodon radicans*, *Salvia hispanica* and *Monarda clinopodia* are illustrated in Fig. 6.

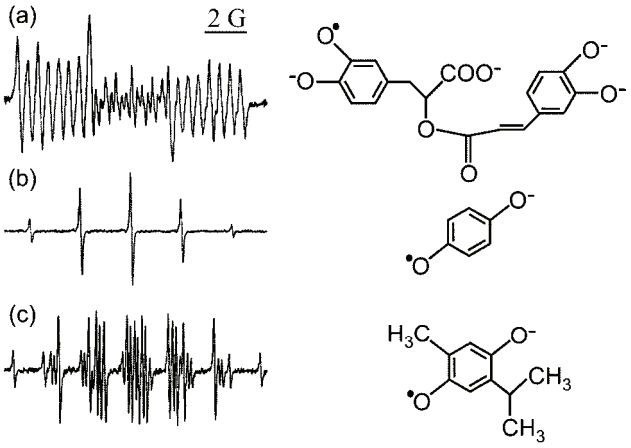

Fig. 6. The EPR semiquinone spectra and chemical structures of a) rosmarinic acid from *Peltodon radicans*, b) hydroquinone from *Salvia hispanica* and c) thymohydroquinone from *Monarda clinopodia* all obtained from crude alcoholic leaf extracts. The signals were identified using the EPR spectra of the corresponding chemicals.[115]

Based on these examples, it is proposed that any plant part or extract that has not been investigated previously by EPR should be first examined using EPR with a wide scan range. If a signal is observed, the recording parameters should be optimized to obtain a good S/N ratio and detailed hyperfine structure of the spectrum. The signal should then be compared with signals of paramagnetic species that are available in the literature. This is usually sufficient to identify the EPR active compound(s). If not, then the chemical composition of the sample should be analysed, in order to narrow the list of compounds with paramagnetic properties that may be present. After this, each "suspect" should be examined separately using EPR spectroscopy and compared to the signal from the sample.

Spectral simulations should be used to compare the levels of paramagnetic species in different samples, and to determine whether the signal of the sample is composed of EPR spectra of more than one paramagnetic species.

3. EVALUATION OF ANTIOXIDATIVE ACTIVITY

3.1. EPR spectroscopy – a technique of choice for investigating the antioxidative properties of compounds, extracts and foods

Overproduction or inefficient removal of reactive species by scavenging enzymes, as well as an increase of the level of catalytically active metals (*e.g.*, iron or copper) related to the generation of the notorious •OH radical, have been shown to lead to damage of biomolecules and cellular membranes in a process known as oxidative stress,[9,116] which has been proposed to be a hallmark of a variety of pathophysiological conditions.[9,10–17,29,54] Under such circumstances, the supplement of antioxidants aimed at re-balancing the disturbed oxidative status could be a very beneficial component of a treatment or a diet.[19,20,24,25] To establish whether some food or a compound could be useful in health problems related to oxidative stress, it is necessary to establish their antioxidative properties. A broad range of methods available for the evaluation of the so-called "total antioxidative capacity" of some compounds, plant extracts or foodstuffs were reviewed previously.[20,117,118] These assays (such as ABTS, ORAC, TRAP, and DPPH assays[118]) are easy to perform; hence, they are frequently employed in studies pointing to an antioxidative capacity of various foods or plant extracts. However, the majority of studies were performed in chemical systems not taking into account the specific properties of target biosystems and metabolic processes that can occur *in vivo*. Although such studies are a prerequisite for further investigations of the antioxidant effectiveness of a certain compound, several other points should be taken into consideration before it should be recommended as a potential cure: task #1: to determine the activity against specific radicals; #2: to determine the distribution of active compounds in both principal environments present in biosystems – hydrophilic and lipophilic; #3: to determine whether the antioxidant acts against radicals in cells, extracellular milieu, or both; #4: to take into account metabolic changes of the investigated compound(s) depending on the route of administration; #5: to determine which specific compound(s) present in the metabolized extract or food is (are) active against free radicals; #6: to determine whether the active compounds could somehow overcome the refractory response. In the following sections, it will be illustrated that the majority of these tasks can be performed by EPR or by combination of EPR with other methods in a carefully planned experimental setup.

EPR spectroscopy can be solely used to perform tasks #1–#3. Two EPR techniques can be applied in antioxidant studies: spin trapping and spin probing. The general concept of the application of EPR spin-trapping for these three tasks

is to generate a specific radical by a selected chemical system and to quantify the inhibiting effects of a compound or extract against radical production (#1). On the other hand, EPR spin-probing can be employed to determine the distribution of potential antioxidants in a hydrophilic, lipophilic, or extracellular environment (#2 and #3). The application of spin-probing in antioxidant research is based on the measurement of the ability of studied compound(s) to reduce synthetic long lived radicals (spin-probes) to EPR-silent hydroxylamines. The spin-probing approach in the study of antioxidants has a long history and has been extensively documented in the literature; in comparison, spin-traps represent an emerging field in EPR spectroscopy.

Tasks #4 and #5 also include the EPR approach, but require specific processing or analysis of the studied systems prior to EPR measurements. For example, antioxidants are usually applied orally, therefore an *in vitro* digestion model system[119] or a more simple methanolysis[39] can be used to process potential antioxidants to compounds that are absorbed *in vivo* (#4). After establishing the antioxidative properties (#1–#3) and metabolic modifications (#4) of some food or extract, analysis of its chemical composition, using HPLC, GC/MS and other methods, should be performed, to reveal compound(s) that could be "responsible" for antioxidative activity. Selected compounds can be then separately tested for antioxidative activity using EPR techniques (#5).

It should be stressed that even if an investigated compound or extract appears to be an excellent antioxidant on the account of these five points, it might not be effective *in vivo* if it is unable to overcome the refractory response (#6).[18–20] In order to resolve this, the protective effects of a potential antioxidant in cell cultures and experimental animals exposed to oxidative stress should be determined. Fluorescent microscopy with redox sensitive dyes has shown itself to be very useful in studies of antioxidative actions in cell cultures, due to its high sensitivity and ability to detect sub-cellular changes related to oxidative stress. On the other hand, a non-destructive *in vivo* EPR technique is the only available method to follow up the oxidative status of animals, with the ability to determine the oxidative stress in specific organs.

As an ideal approach covering all six points is rarely seen in one study, it was decided in this review to separately present applications of spin-trapping and spin-probing techniques, indicating each phase of antioxidant research.

3.2. Applications of EPR spin-trapping in antioxidant research

EPR spin-trapping can provide data on antioxidative effects against the free radicals that are most relevant in physiology $-O_2^{\bullet-}$ and $^{\bullet}OH$ (#1), as well as many others (carbon-centred, $^{\bullet}LOO$, $^{\bullet}SG$).[56,120–127] As these reactive species cannot be directly detected due to their short life-times, a specific compound (spin-trap) is introduced into the system. Spin-traps react with free radicals, thus

forming stabile paramagnetic species (spin adducts), which are readily detected by EPR spectroscopy (Fig. 7). Each reactive species that has been trapped shows its own specific signature EPR spectrum. The advantage of such an approach over other methods that measure the total antioxidative capacity of the compound lies in the ability of EPR to distinguish antioxidative activity against different free radicals, even when simultaneously present in the system. This can be performed using spectral simulations, which enable the identification of each radical and the quantification of the signal intensity. In addition, recently a number of various hydrophilic and lipophilic spin-traps have evolved [120] enabling antioxidative measurements in any selected medium.

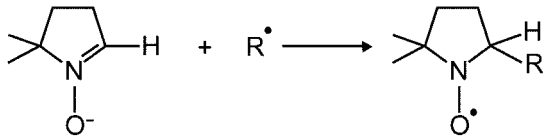

Spin-trap *EPR "silent"* Short lived radical *EPR "silent"* Spin-aduct *EPR active*

Fig. 7. The basic principles of the EPR spin-trapping technique.

For antioxidative studies, *in vitro* chemical systems are used to generate a specific free radical (*e.g.*, the xanthine/xanthine oxidase system or SOTS1 (di-(4-carboxybenzyl)hyponitrite) for $O_2^{\bullet-}$ or the Fenton system and Haber–Weiss-like reaction for $^{\bullet}OH$). The spin-trap is added to a selected system prior to the start of the reaction, and after a specific incubation time, the EPR signal of the spin adduct is recorded and the intensity of the specific trapped radical determined.[56] The application of an antioxidant to the system (before the initiation of the free radical production) should lead to a decreased generation of the spin adducts, due to radical scavenging or interactions with the reactants of the generating system, which is detected by the lower intensity of the EPR signal of a given radical as compared to the control antioxidant-free system.[37–42] The antioxidative activity (*AA*) is then calculated by comparing the signal intensities obtained in the control setup and in the system with the antioxidant, using the simple equation:

$$AA = (I_0 - I_x)/I_0$$

where I_0 and I_x are the intensities of the EPR spectra obtained in the control and the samples with the antioxidant, respectively. The determined antioxidative activity can then be compared to the *AA* of some antioxidant intrinsically present in metabolism, such as ascorbate or tocopherol.[39] This method enables a comparison of the *AA* of the investigated compound with the antioxidative properties of other previously studied compounds. An alternative approach is to determine the EC_{50} value (mg mL^{-1}) – an effective concentration at which the studied compound or extract shows an *AA* of 0.5.[128–130] The EC_{50} value is determined by

interpolation from the linear regression analysis of several *AA* values obtained for different concentrations of the compound or extract. Although attractive for comparative analysis of data obtained in different studies, this approach suffers from a disadvantage as the EC_{50} value depends on the concentration of reactants used in the radical generating system, which may differ from study to study. Therefore, EC_{50} can be used for comparison of the *AA* only when they were obtained in studies using an identical experimental setup.[129,130]

Antioxidative activity against $O_2^{\bullet-}$ can be determined using the xanthine/xanthine oxidase (X/XO) reaction, as an "$O_2^{\bullet-}$ generating" system which is also present in biological systems. EPR spin-trapping with the X/XO system was used in a number of studies to determine AA ($O_2^{\bullet-}$) of β-carotene,[131] vitamin E,[131] glutathione,[124] aminoguanidine,[123] lazaroids,[132] various tea extracts, [133] fullerenes[42] and others. In antioxidant studies, the spin-trap DMPO (5,5-dimethyl-L-pyrroline-*N*-oxide) was usually applied, because of its wide availability and low price. However, the DMPO adduct with the $O_2^{\bullet-}$ radical (DMPO/OOH) has a short lifetime and it is spontaneously transformed into DMPO/OH (the adduct of the $^{\bullet}$OH radical),[56] which may result in unrealistically high values of *AA* ($O_2^{\bullet-}$). Hence, the application of alternative spin-traps, such as DEPMPO (5-(diethoxyphosphoryl)-5-methyl-1-pyrroline-*N*-oxide) is strongly recommended since the DEPMPO/OOH adduct undergoes transformation at a much lower rate than DMPO/OOH[56] or BMPO (5-*tert*-butoxycarbonyl-5-methyl-1-pyrroline *N*-oxide), the $O_2^{\bullet-}$ adduct of which does not undergo transformation at all. However, DEPMPO is the spin-trap of choice when the identification of different radicals is necessary.[134]

As an example of the scheme outlined in the previous paragraphs, the antioxidative properties of extracts of chestnut (*Castanea sativa* L.), and fructose and its phosphorylated forms were examined in two recent studies. [25,37,39] EPR, with DEPMPO and X/XO and the Fenton system, was applied to investigate the antioxidative properties of extracts of chestnut (*C. sativa* L.) leaves, catkin, and spiny burs in an aqueous medium in comparison to the *AA* of ascorbate (#1 and #2), while spin-probing with lipophilic probes was used to determine the antioxidative activity in membranes (#2; see the following section). The EPR signals of DEPMPO/OOH in the X/XO system without and with the catkin extract are shown in Figs. 8a and 8b, respectively. Interestingly, the extracts did not show significant antioxidative activity against $^{\bullet}$OH. Based on the data present in the literature that chestnut extracts are predominantly composed of tannins, which are not absorbed as such but are metabolized by intestinal flora, methanolysis of the extracts was performed to simulate the degradation of tannins in human intestines (#4). In order to determine which compound(s) in the extracts may be responsible for the observed high *AA* values, chemical analysis of the methanolysates was performed using LC/MS and HPLC/DAD (#5). Among the variety of identified

compounds, ellagic and valoneic acids were recognized previously for their antioxidative and anticancer properties. [135,136] Hence, it was proposed that the high AA ($O_2^{\bullet-}$) of chestnut extracts is most likely based on the antioxidative properties of these two acids and similar compounds that were detected, such as flavogallonic acid. Tasks #3 and #6 were not covered in this study and will be the subject of future research. However, it was shown by others that the derivatives of tannins are present in human plasma[137] and have long persistency in the body upon dietary uptake,[138] indicating that they may be able to overcome the refractory response (#6).

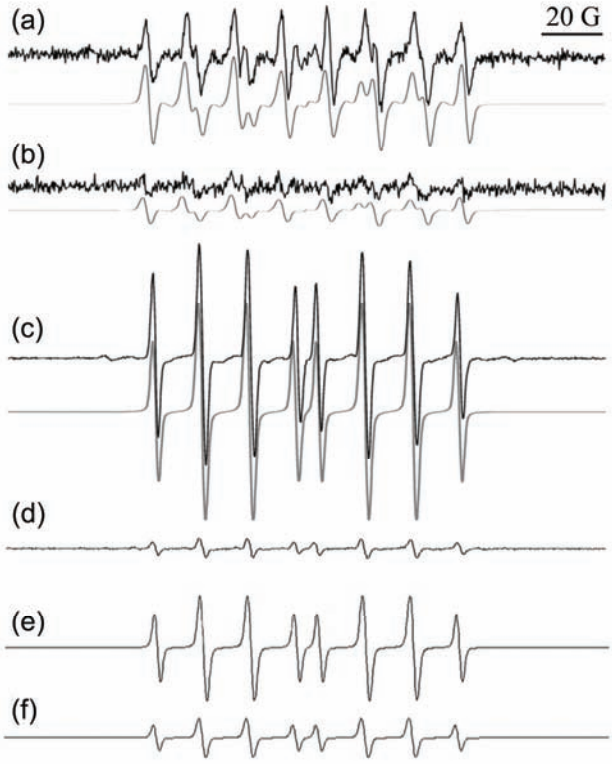

Fig. 8. The characteristic eight-line EPR signals of the DEPMPO/OOH adduct generated in: a) the X/XO system (X 1.6 mM; XO 1.6 IU mL^{-1}); b) X/XO with catkin extract (0.2 mg mL^{-1}). Gray – spectral simulations of the corresponding DEPMPO/OOH signals. Catkin extract *AA*($O_2^{\bullet-}$) = 0.65±0.02; *AA*($O_2^{\bullet-}$) for the same concentration of ascorbate (0.2 mg mL^{-1}) was 0.85±0.04.[39] Characteristic 8-line EPR spectra of the DEPMPO/OH adduct in: c) the Fenton reaction (Fe^{2+} 0.3 mM; H_2O_2 1.2 mM); d) Fenton reaction + 3 mM F16BP, *AA*($^{\bullet}$OH) = = 0.91±0.01. Gray – spectral simulation of the DEPMPO/OH signal.[37] Characteristic EPR signals of the DEPMPO/OH adduct in the metal-free Haber–Weiss-like $^{\bullet}$OH-generating system (KO_2 1.4 mM; H_2O_2 5 mM): e) Haber–Weiss reaction; f) Haber–Weiss reaction + 3 mM F16BP, *AA*($^{\bullet}$OH) = 0.40±0.05.[37]

It should be noted that in studies of specific compounds, some of the points in the present scheme could be found in the literature. For example, the antioxidative properties of fructose and its phosphorylated forms (fructose 1,6-bisphosphate, F16BP; fructose 1-phoshate, F1P; and fructose 6-phosphate, F6P), the biodistribution and metabolism were extensively studied previously, were investigated.[25] Their antioxidative activity against •OH was determined using the Fenton reaction ($Fe^{2+} + H_2O_2 \rightarrow Fe^{3+} + OH^- + {}^{\bullet}OH$), as the "•OH generating system", which represents a constituent of various pathophysiological processes. EPR spin-trapping with the Fenton reaction is the most frequently used method for studying antioxidative properties. It was applied to determine the *AA* of monosaccharides,[37] fullerenes,[42] polysaccharides,[128] vitamins,[139] extracts of various plants,[140,141] seeds,[142] mushrooms,[129,130] teas,[133] spices[143] and others. It was shown that F16BP represents a very efficient antioxidant (#1; Figs. 8c and 8d), which may be useful as an infusion sugar for the treatment of pathophysiological conditions related to oxidative stress.[37] It is known that charged F16BP is preferentially located in the hydrophilic medium (#2), that it is transported into the cells (#3) and that it is not metabolized outside the cell (#4), so all these points in addition to #5 were not the subject of our study. However, if not able to overcome the refractory response and to protect cells from oxidative stress (#6), the application of F16BP in treatment could be futile.[144] Hence, EPR investigations were complemented by the study of intracellular antioxidative properties of F16BP in a cultured astroglial cell exposed to H_2O_2-mediated oxidative stress using confocal fluorescent microscopy and fluorescent markers of oxidative stress, which showed that F16BP is indeed able to overcome the refractory response and protect the cells by diminishing oxidative stress. Further research was conducted to resolve the mechanisms of the antioxidative effects of F16BP. In principle, antioxidative actions against •OH generation in the Fenton system can occur *via* two mechanisms: direct •OH scavenging and sequestration of a transition metal (iron, copper, manganese). In order to establish the mechanisms of antioxidative actions against •OH production, the *AA*(•OH) of a studied compound should be measured in two "•OH generating" systems: *i*) the Fenton reaction, which contains metal ($Fe^{2+} + H_2O_2 \rightarrow Fe^{3+} + {}^{\bullet}OH + OH^-$), and *ii*) the Haber–Weiss-like reaction, which is a metal-free system ($O_2^{\bullet-} + H_2O_2 \rightarrow {}^{\bullet}OH + OH^- + O_2$). The difference between *AA*(•OH) obtained in the first and the second system represents a measure of the metal sequestration of a certain agent. To the best of our knowledge, we were the first to apply this approach in the study of antioxidative activity of F16BP and some other monosaccharides.[37] F16BP showed significantly higher *AA*(•OH) in the Fenton system (Figs. 8c and 8d), when compared to the Haber–Weiss-like reaction (Figs. 8e and 8f). Consequently, it was concluded that F16BP performs antioxidative actions in biological systems *via* both iron

sequestration and $^{\bullet}OH$ scavenging, whereby the first mechanism is predominant.[37]

The ability of any compound to sequester metals is a very important feature as it enables an antioxidant to prevent progression of Fenton chemistry, which is a more efficient strategy for stopping or slowing down oxidative stress, than attempting to scavenge already produced highly reactive $^{\bullet}OH$. For example, different neurodegenerative conditions, such as Parkinson's disease, Alzheimer's disease, are most likely related to the misbalanced metabolism of redox active metals and with consequential propagation of Fenton chemistry.[145,146] Contemporary attempts to treat these conditions are primarily focused on compounds that are efficient in the sequestration of metals.[146] The potential of the EPR approach presented here can be used to screen various compounds for their potential applicability in the chelation therapy of neurodegenerative diseases and to further examine their *in vivo* effects on experimental models.

The presented examples are aimed at illustrating the principles of the application of EPR spin-trapping in antioxidant research and were focused on the biologically most important free radicals ($O_2^{\bullet-}$ and $^{\bullet}OH$). However, it should be stressed that antioxidative activity against various other radicals can be determined using the corresponding generating system and EPR spin-trapping. In an EPR spin-trapping study of the antioxidative activity of chitosan gallate, Pasanphan and co-workers[128] used UV irradiation of AAPH (2,2'-azobis(2-amidinopropane) dihydrochloride) as the generating system of carbon-centred radicals. Schafer *et al.*[131] applied the Photofrin/light/Fe^{2+} system to provoke the generation of lipid radicals in HL-60 cells, and the antioxidative effects of β-carotene, vitamin E and NO against lipid radicals were evaluated using the EPR spin-trapping method. Finally, a recent paper of Šentjurc *et al.*[134] on the antioxidative capacity of leaf extract of the evergreen plant, *Sempervivum tectorum*, superbly illustrates the outstanding possibilities of EPR spin-trapping in antioxidant research. UV irradiation of the liposomal system was used to generate $^{\bullet}OH$, $O_2^{\bullet-}$, and carbon-centred radicals simultaneously, simulating a real biological setup. Using EPR with the spin-trap DEPMPO and spectral simulations, the authors were able to identify specific radicals, quantify their production and determine the antioxidative activities of the extract against each of these three radicals (Fig. 9).

3.3. Applications of EPR spin-probing in antioxidant research

Nitroxyl radicals (or nitroxides) are *N*,*N*-disubstituted $>^{\bullet}NO$ radicals that are widely used as spin-probes (or spin labels) in various systems, primarily because of the relatively high chemical stability of the nitroxide moiety (up to 30 min *in vivo*) which enables their detection not only by EPR spectroscopy, but also by NMR spectroscopy. A variety of EPR spin-probes (over few hundreds, available at reasonably low prices) is available for studying various properties and pro-

cesses in biochemical and biological systems. The applications of spin-probes go beyond redox research, since their EPR spectra can depict their mobility and different characteristics of their environment (viscosity, pH, pO_2, temperature, *etc.*).[127,147,148] The three types of rings that are most commonly used for nitroxide spin-probes: piperidine (*e.g.*, Tempone, Cat_1), pyrrolidine (*e.g.*, PCA) and doxyl (doxyl stearates, *e.g.*, 7-DS) are shown in Fig. 10.[127]

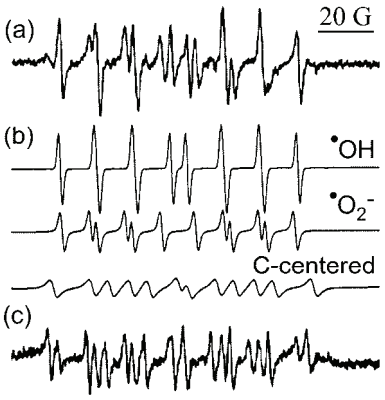

Fig. 9. EPR spectra and spectral simulations of the DEPMPO adducts obtained in liposomes after 2 h irradiation with UV light (λ = 365 nm). a) Control antioxidant-free system; b) computer simulations of the spectra of DEPMPO/OH, DEPMPO/OOH, and carbon-centred radical adduct; c) liposomes + *S. tectorum* (12.5 % v/v) after 2 h irradiation with UV light. *AA*($^{\bullet}$OH) = 0.88; *AA*($^{\bullet}O_2^-$) = 0.95; *AA*(C-centred) = = 0.18.[134]

The stability of nitroxides is primarily based on steric blocking *via* bulky groups (usually methyl) on the adjacent ring carbons, but is not absolute since they can be reduced to EPR-silent hydroxylamines in reactions with various antioxidants. The great assortment of available nitroxides, which can be more or less stabile (*e.g.*, pyrrolidines are more stabile than piperidines), hydrophilic (tempone) or lipophilic (doxyl stearates), charged (Cat_1) or neutral,[127] enable various applications of the EPR spin-probing technique in redox research. The most frequent approach is to add a spin-probe to some biological system (*ex vivo* or *in vivo*) and to follow the decrease of the pertinent signal over time, in order to evaluate the intrinsic oxidative status of the system.[54,127] Here, the application of EPR spin-probing in the measurement of the antioxidative capacity of a specific compound, extract or food will be illustrated. The basic principle is to combine a spin-probe with a potential antioxidant *in vitro* and to evaluate the total capacity of the studied compound to reduce a spin probe, which could be specifically positioned in an aqueous solution, membranes of liposomes or cells, or in the extracellular space (tasks #2 and #3). It should be noted that this approach is not very specific, since spin-probes only represent models of biological free radicals.

3.4. Evaluation of antioxidative activity with EPR spin-probing

The hydrophilic spin-probes most frequently applied in antioxidant research are tempo (2,2,6,6-tetramethylpiperidine-1-oxyl) and its derivatives tempone and Cat_1. Vilhar *et al.*[149] measured the reduction of tempo in tissues of *in vitro*

grown potato plants exposed to jasmonic acid, in order to evaluate antioxidative and metabolic effects. Kocherginsky and co-workers[150] used EPR monitored reduction of tempo and tempone to show that the "reducing power" of beer decreases with increasing temperature and period of storage. EPR and tempone were also applied in the measurements of the antioxidative activity of various plant extracts.[134,151,152] This approach was also utilised in several studies in which the antioxidative activity of chocolate,[41] wild garlic (*Allium ursinum* L.) volatile oil,[38] and the reducing power of plant plasma membranes were investigated.[153]

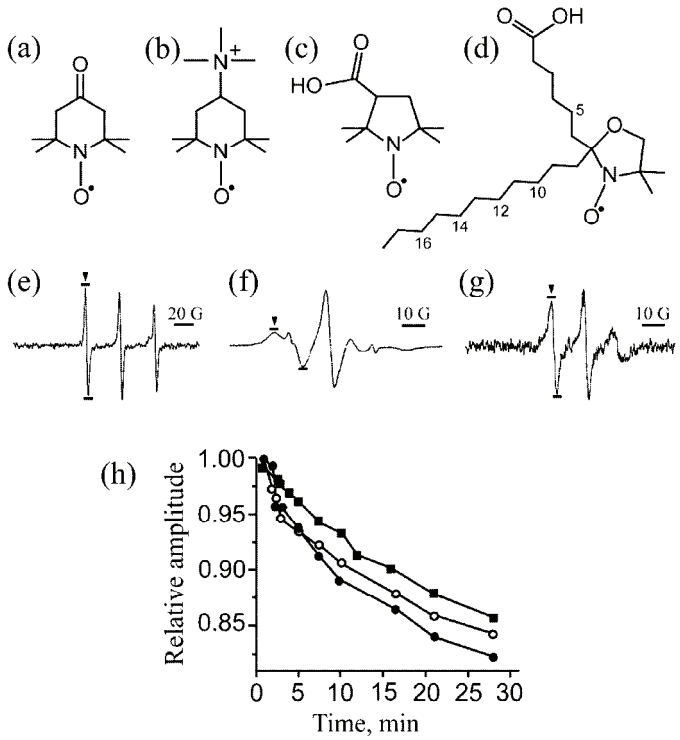

Fig. 10. Chemical structure of spin-probes: a) tempone (4-oxo-2,2,6,6-tetramethylpiperidine--1-oxyl); b) Cat_1 (4-(trimethylammonio)-2,2,6,6-tetramethylpiperidine-1-oxyl); c) PCA (3-carboxy-2,2,5,5-tetramethylpyrrolidine-1-oxyl); d) 7-DS (2-(5-carboxypentyl)-2-undecyl--4,4-dimethyloxazolidine-3-oxyl). The numbers mark the position of the doxyl group on the fatty acid chain in other frequently used doxyl stearates – 5-DS, 10-DS, 12-DS, 14-DS, and 16-DS. Characteristic EPR spectra of tempone (e) in solution; and 7-DS (f) and 12-DS (g) intercalated into liposomes; h) relative amplitude (compared to the amplitude at the start of incubation) of the EPR signal of tempone (■), 7-DS (○) and 12-DS (●) in the presence of AUVO (4.8 mM). The downward triangles in (e–g) mark the lines the amplitudes of which were measured.[38]

The charged spin-probe Cat 1 cannot pass the membrane of cells. Hence, it can be used to study the antioxidative activity of some compounds or extracts in the extracellular medium. Hochkirch *et al.*[154] used EPR with Cat_1 to measure the antioxidative capacity of extracellular solutions in human skin biopsies exposed to UV irradiation. By evaluating the decrease in the EPR signal, they showed that UV light diminishes the activity of antioxidants in the extracellular milieu. Mehlhorn[155] developed an assay for determining the concentration of ascorbate in plasma and hemolysates, based on following the rate of EPR signal disappearance, provoked by ascorbate-mediated reduction of Cat_1.[64]

EPR with doxyl stearates is used to explore whether a compound or extract component(s) acts as an antioxidant inside cellular membranes. Doxyl stearates inserted in a membrane orient their hydrophilic carboxyl group toward the outer aqueous phase of the lipid bilayer and the fatty acid chain extends toward the core of the membrane. Since nitroxide groups could be placed at different positions on the fatty acid chain, the antioxidative activity at different depths of the membrane could be established by measuring and comparing the kinetics of reduction of specific doxyl stearates. EPR measurements of the rates of reduction of 5-, 7-, 10-, 12-, and 16-DS were applied to evaluate the antioxidative activity of ascorbate in the membrane of unilamellar liposomes, showing that ascorbate does not occupy a specific position in the membrane and that the primary site of antioxidative activity of ascorbate is in the external medium.[156] In a similar study, Schreier-Mucillo *et al.*[157] showed that ascorbate is transported through the membrane by diffusion, which explains the similar antioxidative activities at different depths of the membrane. May and co-workers[158] used 5-DS and 16-DS to study the antioxidative activity of ascorbate 6-palmitate (A6P) in the membrane of erythrocytes. A6P reduced 5-DS more efficiently than 16-DS, indicating that the ascorbyl group of A6P is located superficially, but with access to the hydrophobic membrane interior. Takahashi *et al.*[159] studied the intra-membrane antioxidative activity of tocopherols by measuring the reduction of 5-, 7-, 10-, 12-, and 16-DS. It was demonstrated that tocopherols show a higher antioxidative activity closer to the membrane surface, than deep in the lipid region of the bilayer membrane.

Measurements of the reduction of tempone and two doxyl stearates (7- and 12-DS) incorporated into liposomes were combined, to study the antioxidative properties of wild garlic (*Allium ursinum* L.) volatile oil (AUVO) (Fig. 10).[38] The ability of the oil to reduce tempone in water indicated that AUVO is capable of removing radicals in an aqueous environment of biosystems. However, the rank order of signal decay, 12-DS > 7-DS > tempone, demonstrates that the antioxidant compounds in AUVO are preferentially lipophilic, intercalating and protecting the deeper layers of the membrane. The complex kinetics of the decay of the signal of all three used spin-probes indicates that AUVO contains more

than one antioxidative compound active in both media. Such complex kinetics may be deconvoluted into components in order to evaluate the number of active components in the system, as was shown on plant plasma membranes.[153]

3.5. Evaluation of the antioxidative capacity against lipid peroxidation

The ability of antioxidants to remove lipid peroxidation can be assessed by using a specific combination of spin-probing and radical-generating systems. The microenvironment of a spin-probe has a significant impact on its EPR spectrum; thus, specific probes could be used to evaluate membrane fluidity and some other important physiological parameters.[127] Although interesting in itself, EPR spin-probing measurements of fluidity could be used in antioxidant research based on the fact that the fluidity of membranes is dependent on lipid peroxidation.[160] The basic principle of this indirect approach is to provoke lipid peroxidation by exposing membranes to free radicals generated by the Fenton reaction or some other system. The fluidity of the membrane is measured prior and after the addition of a potential antioxidant. If the antioxidant is effective against lipid peroxidation, its introduction into the system should remove lipid radicals and compensate the decrease of membrane fluidity related to peroxidation.

This approach was applied in several studies using liposomes or erythrocytes exposed to the Fenton system as a model of a cellular membrane exposed to oxidative stress, before and after the addition of plant extracts[39,122] or chocolate.[41] Doxyl stearates in a membrane environment have restricted motion which results in a broadening of their spectra, a feature that could be used to measure the order parameter S (Fig. 11), which is reciprocally proportional to membrane fluidity.[127] Peroxidation leads to a decrease in fluidity, so an antioxidant active inside a membrane should be able to enable normal fluidity of the membrane to be regained. For example, the S value of an erythrocyte membrane labelled with 7-DS was around 0.752 in normal cells and ≈0.776 for erythrocytes the membrane of

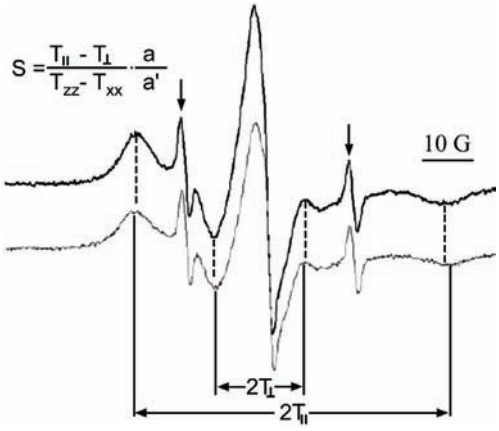

Fig. 11. EPR spectra of erythrocyte membrane labelled with 7-DS. Dark trace – untreated cells; pale trace – cells exposed to the Fenton system. S: order parameter. $2T_{II}$: outer hyperfine splitting. $2T_{\perp}$: inner hyperfine splitting; a: isotropic hyperfine coupling constant in crystal ($a = 1/3(T_{xx} + T_{yy} + T_{zz})$); a': isotropic hyperfine coupling constant in membrane ($a' = 1/3(T_{II} + 2T_{\perp})$). T_{xx}, T_{yy} and T_{zz}: hyperfine constants (for 7-DS, they were taken to be $T_{xx} = T_{yy} = 6.1$ G, $T_{zz} = 32.4$ G [161]). The two narrow lines originate from 7-DS in the solution (arrows).[39]

which was subjected to lipid peroxidation *via* the Fenton reaction. The subsequent application of the extracts of chestnut catkin reverted the order parameter to 0.754, showing that some lipophilic compound(s) in the extract possess the capacity to remove lipid peroxides in biomembranes.

4. CONCLUSIONS

EPR spectroscopy has played a vital role in redox research and its applications are still growing. Herein two approaches that have not hitherto received full attention were addressed. In the first section, it was demonstrated that endogenously present stabile radicals could be used for measuring the oxidative status. Although such an approach is less versatile than the application of EPR spin-traps and spin-probes, its advantage lies in the measurement of the oxidative status of biological systems without any interference with metabolic processes. Secondly, the manners in which different EPR spin-trapping and spin-probing techniques can be used to establish the efficacy of various antioxidants to remove physiologically relevant free radicals and sequestrate metal ions, and thus protect cells from oxidative damage, were presented. The intention was to encourage fellow colleagues interested in redox research to complement the methods used in their studies with some of the EPR techniques outlined in this review and to enhance knowledge further in this exciting area.

Acknowledgements. This work was supported by grant 41005 from the Ministry of Science and Technological Development of the Republic of Serbia. We are grateful to Professor Zlatko Giba from the Institute for Biological Research, Belgrade, Serbia, for helpful discussions.

И З В О Д

УЛОГА ЕПР СПЕКТРОСКОПИЈЕ У ИСПИТИВАЊУ ОКСИДАТИВНОГ СТАТУСА БИОЛОШКИХ СИСТЕМА И АНТИОКСИДАТИВНИХ КАРАКТЕРИСТИКА РАЗЛИЧИТИХ ЈЕДИЊЕЊА

ИВАН СПАСОЈЕВИЋ[1], МИЛОШ МОЈОВИЋ[2], АЛЕКСАНДАР ИГЊАТОВИЋ[2] и ГОРАН БАЧИЋ[2]

[1]Институт за мултидисциплинарна истраживања, Универзитет у Београду, Кнеза Вишеслава 1, 11000 Београд и [2]Факултет за физичку хемију, Универзитет у Београду, Студентски трг 12–16, 11000 Београд

У ери слободних радикала и антиоксиданата, електронска парамагнетна резонанција (EPR) је вероватно најбоља техника за редокс истраживања, посебно када су у питању биохемијски и биолошки системи. У овом прегледном раду, нису покривене све могућности примене EPR-а, него је пажња ограничена на две области које су нове и нису довољно описане у литератури. У првом делу описане су различите примене EPR-а у одређивању оксидативног статуса, употребом ендогених стабилних парамагнетних врста, као што су аскорбил радикал, семихинон, меланин и оксидовани биљни пигменти. Други део се односи на примену ЕПР-а у области испитивања антиоксиданата. Осим прегледа доступне литературе, приказани су детаљно примери (већином из досадашњег рада аутора) како би се илустровали различити начини за коришћење пуних капацитета ЕПР-а у овим областима. Разлог за овакав приступ је жеља да се подстакну биолози заинтересовани за редокс метаболизам, као и

хемичари и фармаколози који се баве хемијом слободних радикала или антиоксидативним особинама нових лекова и природних производа, да укључе ову технику у своја истраживања.

(Примљено 15. октобра, ревидирано 28. децембра 2010)

REFERENCES

1. D. Harman, *J. Gerontol.* **11** (1956) 298
2. D. Harman, *Proc. Natl. Acad. Sci. USA* **78** (1981) 7124
3. C. K. Mittal, F. Murad, *Proc. Natl. Acad. Sci. USA* **74** (1977) 4360
4. K. M. Crawford, C. S. Patt, P. J. Lad, *J. Biol. Chem.* **251** (1976) 7304
5. M. W. Radomski, R. M. J. Palmer, S. Moncada, *Br. J. Pharmacol.* **92** (1987) 639
6. S. Roth, W. Dröge, *Cell Immunol.* **108** (1987) 417
7. R. Schreck, P. A. Baeuerle, *Trends Cell. Biol.* **1** (1991) 39
8. S. G. Rhee, *Science* **312** (2006) 1882
9. W. Dröge, *Physiol. Rev.* **82** (2002) 47
10. K. J. Barnham, C. L. Masters, A. I. Bush, *Nature Rev.* **3** (2004) 205
11. M. R. Cookson, P. J. Shaw, *Brain Pathol.* **9** (1999) 165
12. Y. Luo, G. S. Roth, *Antioxid. Redox Signal.* **2** (2000) 449
13. J. B. De Haan, E. J. Wolvetang, F. Christiano, R. C. Iannello, C. Bladier, M. J. Kelner, I. Kola, *Adv. Pharmacol.* **38** (1997) 379
14. D. Dreher, A. F. Junod, *Eur. J. Cancer* **32** (1996) 30
15. L. W. Oberley, *Free Radical Biol. Med.* **5** (1988) 113
16. J. Bullen, E. Griffiths, H. Rogers, G. Ward, *Microbes Infect.* **2** (2000) 409
17. R. W. Alexander, *Hypertension* **25** (1995) 155
18. N. Lane, *Oxygen: The Molecule that made the World*, Oxford University Press, Oxford, 2002
19. N. Lane, *J. Theor. Biol.* **225** (2003) 531
20. B. Halliwell, *Free Radical Biol. Med.* **46** (2009) 531
21. M. Levine, C. Conry-Cantilena, Y. Wang, R. W. Welch, P. W. Washko, K. R. Dhariwal, J. B. Park, A. Lazarev, J. F. Graumlich, J. King, L. R. Cantilena, *Proc. Natl. Acad. Sci. USA* **93** (1996) 3704
22. E. Herrera, C. Barbas, J. *Physiol. Biochem.* **57** (2001) 43
23. S. Parthasarathy, N. Khan-Merchant, M. Penumetcha, B. V. Khan, N. S antanam, *Curr. Atheroscler. Rep.* **3** (2001) 392
24. J. M. C. Gutteridge, B. Halliwell, *Ann. NY Acad. Sci.* **899** (2000) 136
25. I. Spasojević, A. Bajić, K. Jovanović, M. Spasić, P. Andjus, *Carbohyd. Res.* **344** (2009) 1676
26. V. Roubaud, S. Sankarapandi, P. Kuppusamy, P. Tordo, J. L. Zweier, *Anal. Biochem.* **247** (1997) 404
27. V. Shulaev, D. J. Oliver, *Plant Physiol.* **141** (2006) 367
28. G. R. Buettner, B. A. Jurkiewicz, *Free Radical Biol. Med.* **14** (1993) 49
29. J. Bogdanović Pristov, I. Spasojević, Ž. Miković, V. Mandić, N. Cerović, M. Spasić, *Oxi. Med. Cellular Longevity* **2** (2009) 1
30. J. Neužil, P. K. Witting, R. Stocker, *Proc. Natl. Acad. Sci. USA* **94** (1997) 7885
31. M. K. Sharma, G. B. Buettner, *Free Radical Biol. Med.* **14** (1993) 649

32. R. S. Wood, M. Berwick, R. D. Ley, R. B. Walter, R. B. Setlow, G. S. Timmins, *Proc. Natl. Acad. Sci. USA* **103** (2006) 4111
33. D. Kojić, I. Spasojević, M. Mojović, D. Blagojević, M. R. Worland, G. Grubor-Lajšić, M. B. Spasić, *Eur. J. Entomol.* **106** (2009) 451
34. B. Kukavica, M. Mojović, Ž. Vučinić, V. Maksimović, U. Takahama, S. Veljović Jovanović, *Plant Cell Physiol.* **50** (2009) 304
35. A. G. Ivanov, R. M. Morgan, G. R. Gray, M. Y. Velitchova, N. P. A. Huner, *FEBS Lett.* **430** (1998) 288
36. J. Bogdanović, M. Mojović, N. Milosavić, A. Mitrović, Ž. Vučinić, I. Spasojević, *Eur. Biophys. J.* **37** (2008) 1241
37. I. Spasojević, M. Mojović, D. Blagojević, S. Spasić, D. Jones, A. Nikolić-Kokić, M. Spasić, *Carbohyd. Res.* **344** (2009) 80
38. D. Gođevac, L. Vujisić, M. Mojović, A. Ignjatović, I. Spasojević, V. Vajs, *Food Chem.* **107** (2008) 1692
39. J. Živković, Z. Zeković, I. Mujić, D. Gođevac, M. Mojović, A. Mujić, I. Spasojević, *Food Biophys.* **4** (2009) 126
40. Z. Oreščanin-Dušić, S. Milovanović, A. Nikolić-Kokić, R. Radojčić, I. Spasojević, M. Spasić, *Redox Rep.* **14** (2009) 48
41. J. Simonović, A. Ignjatović, I. Spasojević, M. Daković, M. Mojović, in *Proceedings of the 9th international conference on fundamental and applied aspects of physical chemistry*, Belgrade, Serbia, 2008, p. 391
42. M. Lens, Lj. Medenica, U. Citernesi, *Biotechnol. Appl. Biochem.* **51** (2008) 135
43. A. Cano, J. Hernández-Ruiz, F. Garcia-Cánovas, M. Acosta, M. B. Arnao, *Phytochem. Anal.* **9** (1998) 196
44. R. Re, N. Pellegrini, A. Proteggente, A. Pannala, M. Yang, C Rice-Evans, *Free Radical Biol. Med.* **26** (1999) 1231
45. G. L. Ellman, *Arch. Biochem. Biophys.* **82** (1959) 70
46. D. J. Townsend, *Mol. Intervent.* **7** (2007) 313
47. M. S. B. Paget, M. J. Buttner, *Annu. Rev. Genet.* **37** (2003) 91
48. A. Nikolić Kokić, Z. Stević, S. Stojanović, P. D. Blagojević, D. R. Jones, S. Pavlović, V. Niketić, S. Apostolski, M. B. Spasić, *Redox Rep.* **10** (2005) 265
49. D. Blagojević, *Cryo. Lett.* **28** (2007) 137
50. M. Slavić, A. Appiah, A. Nikolić-Kokić, R. Radojičić, D. R. Jones, M. B. Spasić, *Acta Physiol. Hung.* **93** (2006) 335
51. D. C. Salo, R. E. Pacifici, S. W. Lin, C. Giulivi, K. J. A. Davies, *J. Biol. Chem.* **265** (1990) 11919
52. J. F. Buckman, H. Hernández, G. J. Kress, T. V. Votyakova, S. Pal, I. J. Reynolds, *J. Neurosci. Methods* **104** (2001) 165
53. M. Karbowski, C. Kurono, M. Wozniak, M. Ostrowski, M. Teranishi, T. Soji, T. Wakabayashi, *Biochim. Biophys. Acta* **1449** (1999) 25
54. S. R. Eaton, G. R. Eaton, L. J. Berliner, *Biomedical EPR, Part A: Free radicals, metals, medicine and physiology*, Kluwer Academic/Plenum, New York, 2005
55. H. Karoui, N. Hogg, C. Fréjaville, P. Tordo, B. Kalyanaraman, *J. Biol. Chem.* **271** (1996) 6000
56. G. Bačić, I. Spasojevic, B. Šećerov, M. Mojović, *Spectrochim. Acta A* **69** (2008) 1354
57. S. K. Jackson, J. T. Hancock, P. E. James, *Electron Paramag. Resonan.* **20** (2007) 192

58. D. Armstrong, *Methods in Molecular Biology, Vol. 108, Free Radical and Antioxidant Protocols*, Humana Press Inc., Totowa, NJ, USA, 1999
59. B. Halliwell, M. Whiteman, *Br. J. Pharmacol.* **142** (2004) 231
60. G. Bačić, M. Mojović, *Ann. N. Y. Acad. Sci.* **1048** (2005) 230
61. M. Mojović, I. Spasojević, G. Bačić, *J. Chem. Inf. Model*. **25** (2005) 1716
62. H. Zhao, J. Joseph, H. Zhang, H. Karoui, B. Kalay anaraman, *Free Radical Biol. Med.* **31** (2001) 599
63. G. R. Buettner, *Arch. Biochem. Biophys.* **300** (1993) 535
64. J. Vasquez-Vivar, A. M. Santos, V. B. C. Junqueira, A. Ohara, *Biochem. J.* **314** (1996) 869
65. G. R. Buettner, *J. Biochem. Biophys. Meth.* **16** (1988) 20
66. G. R. Buettner, *Free Radical Res. Commun.* **10** (1990) 5
67. G. R. Buettner, B. Jurkiewicz, *Radiat. Res.* **145** (1996) 532
68. M. Minetti, T. Forte, M. Soriani, V. Quaresima, A. Menditoo, M. Ferrari, *Biochem. J.* **282** (1992) 459
69. K. Nakagawa, H. Kanno, Y. Miura, *Anal. Biochem.* **254** (1997) 31
70. G. R. Buettner, A. G. Motten, R. D. Hall C. F. Chignell, *Photochem. Photobiol.* **46** (1987) 161
71. B. A. Jurkiewicz, G. R. Buettner, *Photochem. Photobiol.* **59** (1994) 1
72. Q. Chen, M. G. Espey, A. Y. Sun, J.-H. Lee, M. C. Krishna, E. Shacter, P. L. Choyke, C. Pooput, K. L. Kirk, G. R. Buettner, M. Levine, *Proc. Natl. Acad. Sci. USA* **104** (2007) 8749
73. U. Heber, C. Miyake, J. Mano, C. Ohno, K. Asada, *Plant Cell Physiol.* **37** (1996) 1066
74. R. V. Barbehenn, U. Poopat, B. Spencer, *Insect Biochem. Mol. Biol.* **33** (2003) 125
75. H. F. Galley, M. J. Davies, N. R. Webster, *Crit. Care Med.* **24** (1996) 1649
76. Y. Matsuo, T. Kihara, M. Ikeda, M. Ninomiya, H. Onodera, K. Kogure, *J. Cereb. Blood Flow Metabol.* **15** (1995) 941
77. I. M. Drake, M. J. Davies, N. P. Mapstone, M. F. Dixon, C. J. Schorah, K. L. White, D. M. Chalmers, A. T. Axon, *Carcinogenesis* **17** (1996) 559
78. C. A. Hubel, V. E. Kagan, E. R. Kisin, M. K. McLaughlin, J. M. Roberts, *Free Radical Biol. Med.* **23** (1997) 597
79. A. Menditto, D. Pietraforte, M. Minetti, *Hum. Reprod.* **12** (1997) 1699
80. M. K. Sharma, G. R. Buettner, K. Spencer, R. E. Kerber, *Circ. Res.* **74** (1994) 650
81. M. Galleano, L. Aimo, S. Puntarulo, *Toxicol. Lett.* **133** (2002) 193
82. B. B. Frei, B. N. Ames, in *Vitamin E in Health and Diseases*, L. Packer, J. Fuchs, Eds., Marcel Dekker, New York, 1993, 131
83. E. G. Janzen, A. L. Wilcox, V. Manoharan, *J. Org. Chem.* **58** (1993) 3597
84. H. Botti, M. Trujillo, C. Batthyany, H. Rubbo, G. Ferrer-Sueta, R. Radi, *Chem. Res. Toxicol*. **17** (2004) 1377
85. V. E. Kagan, N. V. Gorbunov, in *Free Radical and Antioxidant Protocols*, D. Armstrong, Ed., Humana Press Inc., Totowa, NJ, USA, 1999, p. 277
86. M. Matsuo, S. Matsumoto, T. Ozawa, *Org. Magn. Reson.* **21** (1984) 261
87. J. E. Packer, T. F. Slater, R. L. Willson, *Nature* **278** (1979) 737
88. B. Zhou, L. M. Wu, L. Yang, Z. L. Liu, *Free Radical Biol. Med.* **38** (2005) 78
89. C. Opländer, M. M. Cortese, H.-G. Korth, M. Kirsch, C. Mahotka, W. Wetzel, N. Pallua, C. V. Suschek, *Free Radical Biol. Med.* **43** (2007) 818

90. P. Meredith, B. J. Powell, J. Riesz, S. P. Nighswander-Rempel, M. R. Pederson, E. G. Moore, *Soft Matter* **2** (2006) 37
91. K. Reszka, K. Jimbow, in *Oxidative stress in dermatology,* J. Fuchs, L. Packer, Eds., Marcel Dekker Inc., New York, 1993, 287
92. B. Collins, T. O. Poehler, W. A. Bryden, *Photochem. Photobiol.* **62** (1995) 557
93. B.-L. L. Seagle, K. A. Rezai, Y. Kobori, E. M. Gasyna, K. A. Rezaei, J. R. Norris, *Proc. Natl. Acad. Sci. USA* **102** (2005) 8978
94. M. Rozanowska, A. Bober, J. M. Burke, T. Sarna, *Photochem. Photobiol.* **65** (1997) 472
95. A. El-Obeida, S. Al-Harbia, N. Al-Jomaha, A. Hassib, *Phytomedicine* **13** (2006) 324
96. E. Buszman, B. Pilawa, M. Zdybel, S. Wilczyński, A. Gondzik, T. Witoszyńska, T. Wilczok, *Sci. Total Environ.* **363** (2006) 195
97. M. Matuszczyk, E. Buszman, B. Pilawa, T. Witoszyńska, T. Wilczok, *Chem. Phys. Lett.* **394** (2004) 366
98. R. V. Barbehenn, U. Poopat, B. Spencer, *Insect Biochem. Mol. Biol.* **33** (2003) 125
99. W. S. Enochs, T. Sarna, L. Zecca, P. A. Riley , H. M. Swartz, *J. Neural. Transm. Parkinson's Dis. Dementia Sect.* **7** (1994) 83
100. L. Zecca, H. M. Swartz, *J. Neural. Transm. Parkinson's Dis. Dementia Sect.* **5** (1993) 203
101. D. Sulzer, J. Bogulavsky, K. E. Larsen, G. Behr, E. Karatekin, M. H. Kleinman, N. Turro, D. Krantz, R. H. Edwards, L. A. Greene, L. Zecca, *Proc. Natl. Acad. Sci. USA* **79** (2000) 11869
102. N. Vahidi, G. Bačić, H. M. Swartz, in *Proceedings of 8th annual meeting of society of magnetic resonance in medicine*, Amsterdam, Holland, 1989, p. 121
103. C. B. Summers, G. W. Felton, *Insect Biochem. Mol. Biol.* **24** (1994) 943
104. H. M. Appel, L. W. Maines, *J. Insect Physiol.* **41** (1995) 241
105. F. Gerson, W. Huber, *Electron Spin Resonance Spectroscopy of Organic Radicals*, Wiley-VCH Verlag, Weinheim, 2003
106. S. Un, *Magn. Reson. Chem.* **43** (2005) S229
107. D. A. Svistunenko, C. E. Cooper, *Biophys. J.* **87** (2004) 582
108. B. Alvarez, V. Demicheli, R. Durán, M. Trujillo, C. Cerveñansky, B. A. Freeman, R. Radi, *Free Radical Biol. Med.* **37** (2004) 813
109. M. Mojović, M. Vuletić, G. G. Bačić, Ž. Vučinić, *J. Exp. Bot.* **55** (2004) 2523
110. G. Malanga, R. G. Kozak, S. Puntarulo, *Plant Sci.* **141** (1999) 129
111. S. Puntarulo, S. Jasid, M. Simontacchi, *Plant Signal. Behav.* **2** (2007) 96
112. I. Terashima, S. Funayama, K. Sonoike, *Planta* **193** (1994) 300
113. J. A. Pedersen, *Phytochemistry* **17** (1978) 775
114. L. P. Kvist, J. A. Pedersen, *Biochem. Syst. Ecol.* **14** (1986) 385
115. A. J. Pedersen, *Biochem. Syst. Ecol.* **28** (2000) 229
116. E. Crimi, L. J. Ignarro, C. Napoli, *Free Radical Res.* **41** (2007) 1364
117. G. Bartosz, *Adv. Clin. Chem.* **37** (2003) 219
118. B. Halliwell, J. M. C. Gutteridge, *Free radicals in biology and medicine*, Clarendon, Oxford, 2007
119. A.-M. Aura, In vitro *digestion models for dietary phenolic compounds*, Espoo VTT Publications, Helsinki, 2005
120. J.-L. Clément, P. Tordo, *Electron Paramag. Reson.* **20** (2007) 29
121. M. Polovka, *J. Food Nutr. Res.* **45** (2006) 1
122. J. Živković, I. Mujić, Z. Zeković, S. Vidović, A. Mujić, *J. Cent. Eur. Agric.* **2** (2008) 353

123. P. Dobšak, C. Courderot-Masuyer, J. Siegelova, H. Sva činova, J. Jančik, C. Vergely--Vanriessen, L. Rochette, *Scripta Medica (Brno)* **74** (2001) 45
124. C. M. Jones, A. Lawrence, P. Wardman, M. J. Burkitt, *Free Radical Biol. Med.* **32** (2002) 982
125. S. Dikalov, V. Khramtsov, G. Zimmer, *Arch. Biochem. Biophys.* **326** (1996) 207
126. N. E. Poly akov, A. I. Kruppa, T. V . Leshina, T. A. Konovalova, L. D. K ispert, *Free Radical Biol. Med.* **31** (2001) 43
127. N. Kocherginsky, H. M. Swartz, *Nitroxide spin labels. Reactions in Biology and Chemistry*, CRC Press, New York, 1995
128. W. Pasanphan, G. R. Buettner, S. Chirachanchai, *Carbohyd. Res.* **345** (2010) 132
129. Y.-L. Lee, S.-Y. Jian, P.-Y. Lian, J.-L. Mau, *J. Food Compos. Anal.* **21** (2008) 116
130. J.-L. Mau, S.-Y. Tsai, Y.-H. Tseng, S.-J. Huang, *Food Chem.* **93** (2005) 641
131. F. Q. Schafer, H. P. Wang, E. E. Kelley, K. L. Cueno, S. M. Martin, G. R. Buettner, *Biol. Chem.* **383** (2002) 671
132. W. Zhao, J. S. Richardson, M. J. Mombourquette, J. A. Weil, *Free Radical Biol. Med.* **19** (1995) 21
133. G.-C. Yen, H.-Y. Chen, *J. Agric. Food Chem.* **43** (1995) 27
134. M. Šentjurc, M. Nemec, H. D. Connor, V. Abram, *J. Agric. Food Chem.* **51** (2003) 2766
135. F. Festa, T. Aglitti, G. Duranti, R. Ricordy, P. Perticone, R. Cozzi, *Anticancer Res.* **21** (2001) 3903
136. L. Li, R. Tsao, R. Yang, C. Liu, H. Zhu, J.C. Young, *J. Agric. Food Chem.* **54** (2006) 8033
137. J. C. Espin, R. Gonzalez-Barrio, B. Cerda, C. Lopez-Bote, A. I. Rey, F. A. Tomas-Barberan, *J. Agric. Food Chem.* **55** (2007) 10476
138. N. P. Seeram, S. M. Henning, Y. Zhang, M. Suchard, Z. Li, D. Heber, *J. Nutr.* **136** (2006) 2481
139. P. Stocker, J.-F. Lesgards, N. Vidal, F. Chalier, M. Prost, *Biochim. Biophys. Acta* **1621** (2003) 1
140. A. D. Boveris, S. Puntarulo, *Nutr. Res.* **18** (1998) 1545
141. J. Ivanović, S. Đilas, M. Jadranin, V. Vajs, N. Babović, S. Petrović, I. Žižović, *J. Serb. Chem. Soc.* **74** (2009) 717
142. M. Wettasinghe, F. Shahidi, *Food Chem.* **70** (2000) 17
143. H. L. Madsen, B. R. Nielsen, G. Bertelsen, L. H. Skibsted, *Food Chem.* **57** (1996) 331
144. N. Lane, *J. Theoret. Biol.* **225** (2003) 531
145. M. Valko, H. Morris, M. T. D. Cronin, *Curr. Med. Chem.* **12** (2005) 1161
146. R. C. Hider, Y. Ma, F. Molina-Holgado, A. Gaeta, S. Roy , *Biochem. Soc. Trans.* **36** (2008) 1304
147. B. Gallez, G. Bačić, F. Goda, J. Jiang, J. A. O'Hara, J. F. Dunn, H. M. S wartz, *Magn. Reson. Med.* **35** (1996) 97
148. B. Gallez, K. Mader, H. M. Swartz, *Magn. Reson. Med.* **36** (1996) 694
149. B. Vilhar, M. Ravnikar, M. Schara, N. Nemec, N. Gogala, *Plant Cell Rep.* **10** (1991) 541
150. N. M. Kocherg insky, Y. Y. Kostetski, A. I. S mirnov, *J. Agric. Food Chem.* **53** (2005) 1052
151. M. Bergman, A. Perelman, Z. Dubinsky, S. Grossman, *Phytochemistry* **62** (2003) 753
152. A. Rawala, M. Muddeshwarb, S. Biswas, *Biochem. Biophys. Res. Commun.* **324** (2004) 588

153. M. Mojović, I. Spasojević, M. Vuletić, Ž. Vučinić, G. Bačić, *J. Serb. Chem. Soc.* **70** (2005) 177
154. U. Hochkirch, W. Herrmann, R. Stößer, H.-H. Borchert, M. W. Linscheid, *Spectroscopy* **20** (2006) 1
155. R. J. Mehlhorn, *J. Biol. Chem.* **266** (1991) 2724
156. M. Šentjurc, G. Bačić, H. M. Swartz, *Arch. Biochem. Biophys.* **282** (1990) 207
157. S. Schreier-Muccillo, D. Marsh, I. C. P. Smith, *Arch. Biochem. Biophys*. **172** (1976) 1
158. J. M. May, Z.-C. Qu, C. E. Cobb, *Free Radical Biol. Med.* **21** (1996) 471
159. M. Takahashi, J. Tsuchiya, E. Niki, *J. Am. Chem. Soc.* **111** (1989) 6350
160. H. Watanabe, A. Kobayashi, T. Yamamoto, S. Suzuki, H. Hayashi, N. Yamazaki, *Free Radical Biol. Med*. **8** (1990) 507
161. B. J. Gaffney in *Spin Labeling, Theory and Applications*, L. J. Berliner Ed., Academic Press, New York, 1976, p. 567.

Journal of the Serbian Chemical Society
JSCS-info@shd.org.rs • www.shd.org.rs/JSCS
J. Serb. Chem. Soc. 76 (5) 679–684 (2011)
JSCS–4148
UDC 534–8+542.913:547.853+547.286.2
Original scientific paper

Ultrasound-assisted synthesis of dihydropyrimidine-2-thiones

JAVAD SAFAEI-GHOMI* and MOHAMMAD ALI GHASEMZADEH

Department of Organic Chemistry, Faculty of Chemistry, University of Kashan, 51167 Kashan, I. R. Iran

(Received 12 February 2010, revised 9 January 2011)

Abstract: Chalcone derivatives were prepared by the condensation of various substituted aryl aldehydes and acetophenone in alkaline ethanol, while pyrimidine-2-thione derivatives were prepared by the combination of chalcones and thiourea under conventional and ultrasonic conditions. Advantages of the ultrasound effect were observed and high yields of the products were obtained after 20–30 min sonication. Characterization and structural elucidation of the products was realized based on chemical, analytical and spectral analyses. The results clearly demonstrated a high efficiency of the ultrasonic systems was achieved in the chemical processes.

Keywords: chalcone derivatives, ultrasound, pyrimidine-2-thione derivatives.

INTRODUCTION

Heterocyclic compounds have so far been synthesized mainly because of their wide range of biological activities. These compounds play an important role in medicinal chemistry, serving as key templates central to the development of numerous important therapeutic agents.[1] Pyrimidine derivatives have found application in a wide range of medical applications because of their diverse biological activities, such as antimicrobial,[2] antitumor and antifungal activities.[3] In addition, these compounds are considered to be important for drugs and agricultural chemicals.[4–6] These chemotherapeutic applications of pyrimidine derivatives prompted the present synthesis of some substituted pyrimidines in a facile pathway.

Multi-component reactions (MCRs) play an important role in combinatorial chemistry because they enable the synthesis of small drug-like molecules with several degrees of structural diversity. This reaction tool allows compounds to be synthesized in a few steps and usually in a one-pot operation. Another typical benefit from these reactions is the simplified purification, because all the reagents

* Corresponding author. E-mail: safaei@kashanu.ac.ir
doi: 10.2298/JSC100212057S

are incorporated into the final product. The Biginelli reaction is a multiple-component chemical reaction that creates dihydropyrimidine from ethyl acetoacetate, an aryl aldehyde and urea or thiourea.[7,8]

Recently, several methods have been reported for the synthesis of pyrimidine derivatives. One method involves the reaction of aldehydes, ß-dicarbonyl compounds and urea/thiourea in the presence of a catalytic amount of tetrachlorosilane in DMF at ambient temperature.[9] The synthesis of 2-thiopyrimido benzimidazole derivatives by the condensation of 4-isothiocyanato-4-methyl-2-pentanone and 3,3'-diaminobenzidine in absolute methanol under reflux is another method.[10] Pyrimidine derivatives can also be prepared by the reaction of certain amides with nitriles under electrophilic activation of the amide with 2-chloropyridine and trifluoromethanesulfonic anhydride.[11] However, these methods suffer from drawbacks, such as longer reaction times, complicated workup and low yields.

The present paper describes the synthesis of pyrimidine-2-thione derivatives under conventional and ultrasonic irradiation by the reaction of chalcones and thiourea. The effects of ultrasound on organic reactions are attributed to cavitations, a physical process that create, enlarge, and implode gaseous and vaporous cavities in an irradiated liquid.[12] The cavitations induce very high local temperatures and pressures inside the bubbles (cavities), leading to a turbulent flow in the liquid and enhanced mass transfer.[13] In some reactions, ultrasonic irradiation allows the process to occur with ease to provide high yields within very short times.[14–16]

EXPERIMENTAL

All melting points are uncorrected and were determined in a capillary tube on a Boetius melting point microscope. The FTIR spectra were recorded on a Nicolet Magna 550 spectrometer (KBr). The ^{1}H-NMR and ^{13}C-NMR spectra were obtained on a Bruker 400 MHz spectrometer with DMSO-d_6 as the solvent using tetramethylsilane (TMS) as the internal standard. Sonication was performed in an ELO-150 ultrasonic cleaner with a frequency of 46 kHz and a nominal power of 200 W. All reactions were followed and checked by TLC using *n*-hexane/ethyl acetate (7:3) as the mobile phase. The spots were visualized using a UV lamp. The elemental analyses (C, H, N) were obtained from a Carlo ERBA Model EA 1108 analyzer. The mass spectra were recorded on a Joel D-30 instrument at an ionization potential of 70 eV.

*General procedure for the preparation of pyrimidine-2-thione derivatives (**3a–h**)*

Conventional heating. A mixture of chalcone (0.005 mol), thiourea (0.005 mol) and potassium hydroxide (0.5 g) in ethanol (20 ml) was refluxed with stirring on an oil bath at 70––80 °C for the periods indicated in Table I. Subsequently, the reaction mixture was left overnight and then concentrated under reduced pressure. The solid residue was collected, washed with water and recrystallized from ethanol.

Ultrasound. All contents were placed in an ultrasonic bath for the periods indicated in Table I, at 20–25 °C and worked up as described above.

TABLE 1. Preparation of pyrimidines (**3**) under conventional and ultrasound conditions

Compound	Conventional conditions		Ultrasound irradiation	
	Time, h	Yield, %	Time, min	Yield, %
3a	5.5	65	20	82
3b	6	55	22	78
3c	6	54	22	80
3d	5.5	58	24	76
3e	6	60	26	78
3f	6	61	24	75
3g	6.5	65	25	73
3h	5.5	55	29	75

RESULTS AND DISCUSSION

Spectral data for the compounds

*4,6-Diphenyl-3,4-dihydropyrimidine-2(1*H*)-thione (**3a**)*. Yellow crystals; m.p.: 182–184 °C (lit.[17] m.p. 184 °C). FTIR (KBr, cm^{-1}): 3173 (NH), 1644 (C=N), 1559, 1478 (C=C), 1183 (C=S). ^{1}H-NMR (400 MHz, DMSO-d_6, δ / ppm): 4.86 (1H, *d*, *J* = 5.0 Hz, 4–CH), 5.15 (1H, *d*, *J* = 5.0 Hz, 5–CH), 6.78–7.29 (10H, *m*, Ar–H), 8.85 (1H, *bs*, NH), 9.60 (1H, *bs*, NH). ^{13}C-NMR (100 MHz, DMSO-d_6, δ / / ppm): 55.1, 101.6, 1 26.3, 126.8, 127.2, 128.85, 129.2, 129.3, 133.8, 1 34.8, 144.5, 175.4.

*4-(2-Methylphenyl)-6-phenyl-3,4-dihydropyrimidine-2(1*H*)-thione (**3b**)*. Yellow crystals; m.p.: 175–177 °C; Anal. Calcd. for $C_{17}H_{16}N_2S$: C 72.85, H 5.71, N 10.00 %. Found: C 72.7 5, H 5.80, N 10.1 5 %. FTIR (KBr, cm^{-1}): 3235 (NH), 1642 (C=N), 1566, 1480 (C=C), 1165 (C=S). ^{1}H-NMR (400 MHz, DMSO-d_6, δ / / ppm): 2.10 (3H, *s*, CH_3), 4.87 (1H, *d*, *J* = 5.0 Hz, 4–CH) 5.12 (1H, *d*, *J* = 5.0 Hz, 5–CH), 6.91–7.30 (9H, *m*, Ar–H), 8.85 (1H, *bs*, NH), 9.60 (1H, *bs*, NH). ^{13}C--NMR (100 MHz, DMSO- d_6, δ / pp m): 22.3, 56, 101.8, 1 25.4, 125.8, 127.5, 127.9, 128.7, 129.2, 133.4, 133.8, 134.7, 137.5, 144.3, 175.2; MS (EI) (*m*/*z*): 280 (M^+).

*4-(3-Methylphenyl)-6-phenyl-3,4-dihydropyrimidine-2(1*H*)-thione (**3c**)*. Yellow crystals; m.p.: 183–185 °C; Anal. Calcd. for $C_{17}H_{16}N_2S$: C 72.85, H 5.71, N 10.00 %. Found: C 72.88, H 5.77, N 10.10 %. FTIR (KBr, cm^{-1}): 3169 (NH), 1640 (C=N), 1575, 1482 (C=C), 1194 (C=S). ^{1}H-NMR (400 MHz, DMSO-d_6, δ / / ppm): 2.08 (3H, *s*, CH_3), 4.85 (1H, *d*, *J* = 5.0 Hz, 4–CH) 5.15 (1H, *d*, *J* = 5.0 Hz, 5–CH), 6.83 –7.31 (9H, *m*, Ar–H), 8.85 (1H, *bs*, NH), 9.64 (1H, *bs*, NH). ^{13}C-NMR (100 MHz, DMSO-d_6, δ / ppm): 21.6, 55.1, 101.7, 124, 126.2, 127.3, 127.9, 128.6, 129.1, 1 29.3, 133.75, 134.6, 138.2, 144.5, 177.3. MS (EI) (*m*/*z*): 280 (M^+).

*4-(4-Methylphenyl)-6-phenyl-3,4-dihydropyrimidine-2(1*H*)-thione (**3d**)*. Yellow crystals; m.p.: 198–200 C (lit.[18] m.p. 199–200 °C). FTIR (KBr, cm^{-1}): 3198 (NH), 1644 (C=N), 1566, 1480 (C=C), 1184 (C=S). ^{1}H-NMR (400 MHz,

DMSO-d_6, δ/ ppm): 2.03 (3H, *s*, CH_3), 4.86 (1H, *d*, *J* = 5.0 Hz, 4–CH) 5.14 (1H, *d*, *J* = 5.0 Hz, 5–CH), 6.87–7.29 (9H, *m*, Ar–H), 8.85 (1H, *bs*, NH), 9.64 (1H, *bs*, NH). ^{13}C-NMR (100 MHz, DMSO-d_6, δ/ ppm): 21.2, 56.0, 102.8, 127.4, 127.9, 128.5, 129.5, 130.4, 130.7, 134.9, 138.4, 142.2, 178.1.

*4-(2-Methoxyphenyl)-6-phenyl-3,4-dihydropyrimidine-2(1*H*)-thione (**3e**)*. White crystals; m.p.: 178–180°C; Anal. Calcd. for $C_{17}H_{16}N_2OS$: C 68.91, H 5.40, N 9.45 %. Found: C 68.99, H 5.50, N 9.39 %. FTIR (KBr, cm^{-1}): 3152 (NH), 1642 (C=N), 1555, 1479 (C=C), 1182 (C=S). ^{1}H-NMR (400 MHz, DMSO-d_6, δ/ ppm): 3.60 (3H, *s*, $-OCH_3$), 5.13 (2H, *m*, 4–CH, 5–CH), 6.93–7.23 (9H, *m*, Ar–H), 8.75 (1H, *bs*, NH), 9.71 (1H, *bs*, NH). ^{13}C-NMR (100 MHz, DMSO- d_6, δ / ppm): 50.2, 56.0, 100.8, 111.5, 121.1, 126.2, 126.9, 128.8, 129.1, 129.2, 132.1, 133.8, 134.8, 155.73, 177.3. MS (EI) (*m*/*z*): 296 (M^+).

*4-(4-Methoxyphenyl)-6-phenyl-3,4-dihydropyrimidine-2(1*H*)-thione (**3f**)*. White crystals; m.p.: 123–125 C (lit.[19] m.p. 123–124 °C). FTIR (KBr, cm^{-1}): 3149 (NH), 1642 (C=N), 1555, 1479 (C=C), 1182 (C=S). ^{1}H-NMR (400 MHz, DMSO-d_6, δ/ / ppm): 3.60 (3H, *s*, $-OCH_3$), 5.13 (2H, *m*, 4–CH, 5–CH), 6.79–7.25 (9H, *m*, Ar–H), 8.62 (1H, *bs*, NH), 9.60 (1H, *bs*, NH). ^{13}C-NMR (100 MHz, DMSO-d_6, δ/ ppm): 50.2, 56.0, 100.8, 111.6, 121.1, 126.2, 128.8, 129.1, 129.2, 132.1, 134.8, 155.8, 178.2.

*4-(2,4-Dimethoxyphenyl)-6-phenyl-3,4-dihydropyrimidine-2(1*H*)-thione (**3g**)*. White crystals; m.p.: 180–182 °C. Anal. Calcd. for $C_{18}H_{18}N_2O_2S$: C 66.25, H 5.52, N 8.58 %. Found: C 66.29, H 5.43, N 8.67 %. FTIR (KBr, cm^{-1}): 3195 (NH), 1644 (C=N), 1581, 1465 (C=C), 1162 (C=S). ^{1}H-NMR (400 MHz, DMSO--d_6, δ/ ppm): 3.60 (6H, *s*, 2',4'–OCH_3), 5.13 (2H, *m*, 4–CH, 5–CH), 6.83–7.25 (8H, *m*, Ar–H), 8.60 (1H, *bs*, NH), 9.63 (1H, *bs*, NH). ^{13}C-NMR (100 MHz, DMSO-d_6, δ/ ppm): 51.1, 58.2, 101.2, 111.2, 121.2, 125.2, 125.9, 127.3, 129.1, 129.8, 132.6, 134.8, 153.7, 154.6, 177.1. MS (EI) (*m*/*z*): 326 (M^+).

*4-(4-*N,N*-Dimethylphenyl)-6-phenyl-3,4-dihydropyrimidine-2(1*H*)-thione (**3h**)*. Yellow crystals; m.p.: 162–164 °C; Anal. Calcd. for $C_{18}H_{19}N_3S$: C 69.91, H 6.14, N 13.9 %. Found: C 70.03, H 6.19, N 13.95 %. FTIR (KBr, cm^{-1}): 3196 (NH), 1640 (C=N), 1552, 1475 (C=C), 1191 (C=S). ^{1}H-NMR (400 MHz, DMSO--d_6, δ/ ppm): 2.74 (6H, *s*, $N(Me)_2$), 5.00 (2H, *m*, 4–CH, 5–CH), 6.83–7.25 (8H, *m*, Ar–H), 8.64 (1H, *bs*, NH), 9.60 (1H, *bs*, NH). ^{13}C-NMR (100 MHz, DMSO-d_6, δ/ /ppm): 56.5, 79.7, 102.0, 112.2, 125.6, 126.3, 128.0, 128.2, 130.3, 134.5, 138.7, 150.5, 176.1. MS (*m*/*z*): 309 (M^+).

In the present work, chalcone derivatives **1** were treated with thiourea **2** in the presence of potassium hydroxide in ethanol to produce the pyrimidine-2-thione derivatives **3**. The reaction occurred in two steps: first conjugate addition took place on the β-position of carbonyl group and then nucleophilic attack on the carbonyl group followed by dehydration led to the six-membered ring products (Scheme 1).[17,19,20]

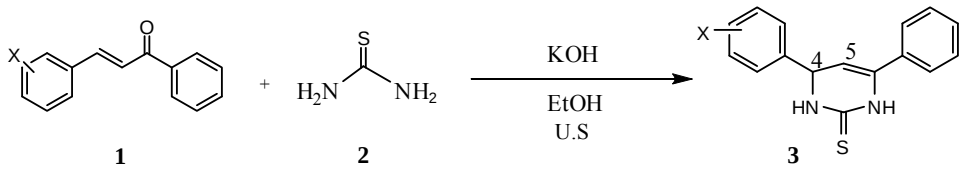

1 **2** **3**

3a: X = H
3b: X = 2-CH_3
3c: X = 3- CH_3
3d: X = 4-CH_3
3e: X = 2-OCH_3
3f: X = 4-OCH_3
3g: X = 2,4-OCH_3
3h: X = N$(Me)_2$

Scheme 1. Approach to the synthesis of pyrimidine-2-thiones under ultrasound irradiation (in **3h** N$(Me)_2$ stands for 4-N$(Me)_2$).

Application of ultrasound shortened the reaction time of the generation of pyrimidines from 6 h under classical conditions to 30 min. In addition, the yields of the products were improved by 20–30 % in comparison with those obtained by the thermal heating method (Table I).

Conventional heating of the sonicating reaction mixture to the same (bulk) temperature did not lead to any significant differences in the yields and times.

In the view of the interest in green chemistry for the synthesis of organic compounds, an optimized procedure for the preparation of pyrimidine-2-thione derivatives was developed. These reactions were realized under milder and cleaner conditions. While with thermal heating these reactions required 6 h at 70–80 °C, the new method was performed at room temperature for shorter times.

CONCLUSIONS

An optimized procedure for the preparation of pyrimidine-2-thione derivatives under mild and clean conditions was described. The advantages of ultrasound in chemical reactions, such as shorter reaction times, higher yields and milder conditions, could be of use in industrial applications in the pharmaceutical or fine chemical industries.

Acknowledgements. The authors gratefully acknowledge the financial support of this work by the Research Affairs Office of the University of Kashan, Kashan, I. R. Iran. Dr A. H. Bamoniri is acknowledged for his help in the preparation of this paper.

ИЗВОД

СИНТЕЗА ДИХИДРОПИРИМИДИН-2-ТИОНА УЛТРАОЗВУЧИВАЊЕМ

JAVAD SAFAEI-GHOMI и MOHAMMAD ALI GHASEMZADEH

Department of Organic Chemistry, Faculty of Chemistry, University of Kashan, 51167 Kashan, I. R. Iran

Деривати халкона добијени су кондензацијом различитих супституисаних арил-алдехида и ацетофенона под базним условима у етанолу, а деривати пиримидин-2-тиона добијени су реакцијом халкона и тиоурее, под уобичајеним реакционим условима и ултраозвучивањем. Уочене су предности ултраозвучивања реакционе смеше, као што су повећање приноса и добијање производа за краће реакционо време, 20–30 min. Карактеризација и

одређивање структуре производа извршено је уобичајеним спектроскопским и аналитичким методама.

(Примљено 12. фебруара 2010, ревидирано 9. јануара 2011)

REFERENCES

1. C. D. Cox, M. J. Breslin, B. J Mariano, *Tetrahedron Lett*. **45** (2004) 1489
2. B. K. Karale, C. H. Gill, M. Khan, V. P. Chavan, A. S. Mane, M. S. Shingare, *Indian. J. Chem*. **41** (2002) 1957
3. M. A. El-Hashash, M. R. Mahmoud, S. A. Madboli, *Indian. J. Chem*. **32** (1993) 449
4. D. J. Brown, *The Chemistry of Heterocyclic Compounds, The Pyrimidines*, Vol. 52, Wiley, New York, USA, 1994
5. M. Kidwai, M. Mishra, *J. Serb. Chem. Soc.* **69** (2004) 247
6. D. J. Brown, in *Comprehensive Heterocyclic Chemistry*, Vol. 3, A.J. Boulton, A. McKillop, Eds., Pergamon, Oxford, UK, 1984, p. 150
7. C. O. Kappe, *Tetrahedron* **49** (1993) 6937
8. A. Dondoni, A. Massi, S. Sabbatini, *Tetrahedron Lett*. **43** (2002) 5913
9. C. Ramalingan, Y. Kwak, *Tetrahedron* **64** (2008) 5023
10. S. M. Sondhi, R. N. Goyal, A. M. Lahoti, N. Singh, R. Shukla, R. Raghubir, *Bioorg. Med. Chem.* **13** (2005) 3185
11. M. Movassaghi, M. D. Hill, *J. Am. Chem. Soc*. **128** (2006) 14254
12. J. L. Luche, *Synthetic Organic Sonochemistry*, Plenum Press, New York, USA, 1999, Ch. 2, pp. 55–56
13. H. A. Stefani, R. Cella, F. A. Dorr, C. M. P. de Pereira, F. P. Gomes, G. Zeni, *Tetrahedron Lett*. **46 (**2005) 2001
14. E. Ruiz, H. Rodriguez, J. Coro, E. Salfran, M. Suarez, R. Martnez-Alvarez, N. Martin, *Ultrason. Sonochem.* **18** (2011) 32
15. J. Safaei-Ghomi, M. Fadaeian, A. Hatami, *Turk. J. Chem.* **31** (2007) 89
16. G. A. Heropoulos, S. Georgakopoulos, B. R. Steele, *Tetrahedron Lett*. **46 (**2005) 2469
17. D. Simon, O. Lafont, C. C. Farnoux, M. Miocque, *J. Heterocycl. Chem.* **22** (1985) 1551
18. H. F. Al-Hajjar, A. Y. Al-Farkh, S. H. Hamoud, *Can. J. Chem*. **57** (1979) 2734
19. M. Kidwai, P. Misra, *Synth. Commun*. **29** (1999) 3237
20. V. M. Barot, S. R. Modi, H. B Naik, *Asian. J. Chem*. **12** (2000) 581.

Journal of the Serbian Chemical Society
JSCS-info@shd.org.rs • www.shd.org.rs/JSCS
J. Serb. Chem. Soc. 76 (5) 685–692 (2011)
JSCS–4149
UDC 66.094.414+547.52+547.323+546.32+547.53+547.551.1
Original scientific paper

Simple and improved regioselective brominations of aromatic compounds using *N*-benzyl-*N*,*N*-dimethylanilinium peroxodisulfate in the presence of potassium bromide under mild reactions conditions

HASSAN GHASEMNEJAD-BOSRA[1]*, FARHAD RAMZANIAN-LEHMALI[2] and SOMAYE JAFARI[1]

[1]*Islamic Azad University – Babol Branch, School of Science, P.O. Box 755, Babol and* [2]*University of Payamenoor, Babol, Iran*

(Received 16 March, revised 9 December 2010)

Abstract: A simple, efficient, and mild method for the selective bromination of some activated aromatic compounds using *N*-benzyl-*N*,*N*-dimethylanilinium peroxodisulfate in the presence of potassium bromide in non-aqueous solution is reported. The results obtained revealed good to excellent selectivity between the *ortho* and *para* positions of phenols and methoxyarenes.

Keyword: bromination; *N*-benzyl-*N*,*N*-dimethylanilinium peroxodisulfate; potassium bromide; phenols; methoxyarenes.

INTRODUCTION

Selective bromination of aromatic compounds is an important reaction in organic synthesis. Therefore, various methods have been developed for the bromination of aromatic rings using different reaction conditions. Direct treatment of aromatic compounds with molecular bromine normally results in a mixture of mono-, di-, and polysubstituted products. In addition, direct bromination of activated aromatic compounds by bromine generates hydrogen bromide, which is corrosive, toxic, and pollutes the environment.[1–4] To overcome these difficulties, numerous methods have been proposed to increase the selectivity and also the yields of the desired *para*-products.[5–14]

In recent years, several peroxodisulfate reagents for oxidative transformations under non-aqueous conditions have been reported.[15] As a part of a program related to the development of peroxodisulfate reagents, a new, simple, and general procedure is reported now for the bromination of a number of phenols and methoxyarenes using *N*-benzyl-*N*,*N*-dimethylanilinium peroxodisulfate

* Corresponding author. E-mail: h_ghasem2000@yahoo.com
doi: 10.2298/JSC100212058G

(DMBAPODS) in the presence of potassium bromide as the source of bromine. *N*-benzyl-*N*,*N*-dimethylanilinium peroxodisulfate was obtained as follows:[14] an aqueous solution of *N*-benzyl-*N*,*N*-dimethylanilinium bromide was added under stirring to a solution of potassium peroxodisulfate in water at room temperature. The products were successively washed with water and acetone and dried under reduced pressure. This reagent is a stable white powder which could be stored for months without losing its activity (Scheme 1).

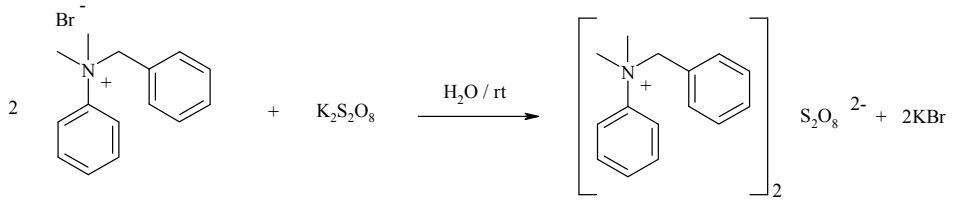

DMBAPODS

Scheme 1. Synthesis of *N*-benzyl-*N*,*N*-dimethylanilinium peroxodisulfate.

EXPERIMENTAL

The reactions were monitored by TLC using silica gel plates and the products purified by flash column chromatography on silica gel (Merck; 230–400 mesh). The products were identified by comparison of their spectra and physical data with those of authentic samples. The ^{1}H-NMR spectra of the brominated compounds were measured at 90 MHz on a JEOL spectrometer with tetramethylsilane as the internal reference and $CDCl_3$ as the solvent. Elemental analysis was performed on a LECO 250 instrument.

Typical procedure for the synthesis of N-*benzyl*-N,N-*dimethylanilinium peroxodisulfate*

To an aqueous solution of 14.60 g *N*,*N*-dimethylanilinium bromide (50 mmol) in 100 mL H_2O was added a solution of 13.51 g potassium peroxodisulfate (50 mmol) in 100 mL H_2O. The mixture was stirred at room temperature for 30 min. The formed precipitate was filtered, washed with cooled distilled water (50 mL), and dried in a desiccator under vacuum over calcium chloride to afford a white powder (92 %), which decomposes at 181–183 °C to a dark brown material. Anal. Calcd. for: $C_{30}H_{36}N_2O_8S_2$: C, 58.43; H, 5.87; N, 4.54 %. Found: C, 58.46; H, 5.89; N, 4.56; ^{1}H-NMR (90 MHz, DMSO-d_6, δ / ppm): 6.9–8.2 (10H, *m*, C_6H_5), 5.8 (2H, *s*. CH_2), 3.95 (6H, *s*. CH_3).

Typical procedure for the bromination of aromatic compounds with potassium bromide in the presence of N-*benzyl*-N,N-*dimethylanilinium peroxodisulfate*

To a solution of aromatic compound (1 mmol) in acetonitrile (5 mL), KBr (1.2 mmol) and *N*-benzyl-*N*,*N*-dimethylanilinium peroxodisulfate (1–1.2 mmol) were added and the mixture heated under reflux for 1.5–9.5 h. The progress of the reaction was monitored by TLC (eluent: carbon tetrachloride/diethyl ether, 4:2, and carbon tetrachloride/*n*-hexane, 8:2) or GC (capillary column). The reaction mixture was cooled to room temperature and filtered. The excess bromine was removed from the filtrate by the dropwise addition of a sodium thiosulfate solution (1 M). Then dichloromethane (5 mL) was added and the solution transferred to a separatory funnel. The organic layer was separated and dried over magnesium sulfate or

calcium chloride. Evaporation of the solvent followed by recrystallization or column chromatography on silica gel of the crude product gave the corresponding brominated compounds in good to excellent yields.

The products were characterized based on their physical and spectral analysis and by direct comparison with literature data (Supplementary Material).[16]

RESULTS AND DISCUSION

This article reports the use of potassium bromide as the source of bromine and *N*-benzyl-*N*,*N*-dimethylanilinium peroxodisulfate as the oxidizing agent in acetonitrile as solvent for the bromination of a number of phenols and methoxyarenes (Scheme 2). The results are given in Table I.

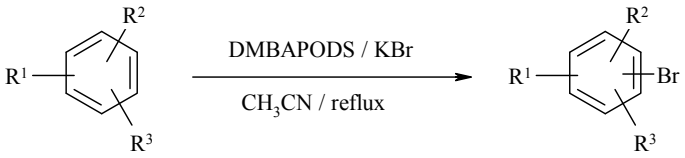

R^1, R^2, R^3 = H, OH, OMe, Cl, NO_2, CH_3, COOH

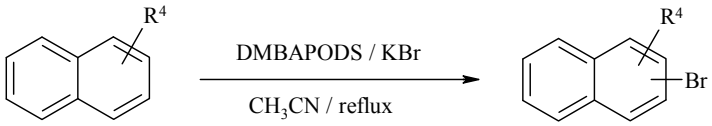

R^4 = OH, OMe

Scheme 2. General reaction for the bromination of aromatic compounds.

Thus, the methoxybenzenes were successfully reacted to afford the desired monobrominated products (Table I, entries **1**–**9**), except 2-methoxynaphthalene, which gave 1-bromo-2-methoxynaphthalene (Table I, entry **7**). Catechol, phenol, *ortho*-cholorophenol, *ortho*-cresol and *ortho*-methoxyphenol were quantitatively converted to the *para*-brominated products with respect to the hydroxyl groups (Table I, entries **10**–**14**). *para*-Nitrophenol and 2,4-dinitrophenol were also converted to the monobrominated products over longer reaction times (Table I, entries **15** and **16**). Resorcinol and *para*-methoxyphenol were quantitatively reacted to give the corresponding monobrominated products (Table I, entries **17** and **18**). Some other aromatic compounds, such as 1-naphthol and 2-naphthol, were also subjected to these reaction conditions, and the corresponding products were obtained in good yields (Table I, entries **20** and **21**). Salicylic acid and 2,4-dihydroxybezoic acid produced the brominated products over longer times and in low-

er yields compared to the other activated phenols and methoxyarenes (Table I, entries **19** and **22**).

TABLE I. Bromination of some aromatic compounds with potassium bromide in the presence of *N*-benzyl-*N*,*N*-dimethylanilinium peroxodisulfate (reactions were performed in CH_3CN at reflux temperature)

Entry	Substrate	Product(s)[a]	Oxidant/sub-strate/KBr	Time h	Yield %[b]	M.p. °C	M.p.[lit.] °C
1	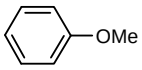	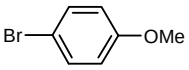	1.2/1/1.2	3	91	Liq	Liq[18e]
2	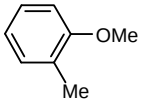	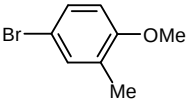	1.2/1/1.2	3.5	95	69	69–70[18a]
3	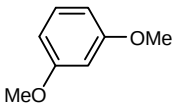	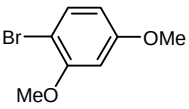	1.2/1/1.2	4	93	25	25–26[18a]
4	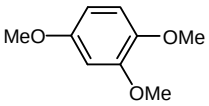	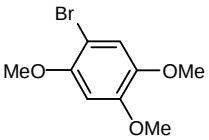	1.2/1/1.2	3	94	55	54–55[18a]
5	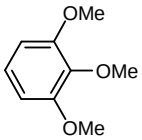	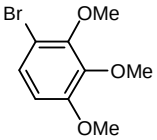	1/1/1.2	2.5	92	Liq	Liq[18a]
6	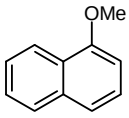	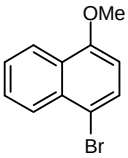	1/1/1.2	7	84	64	63–65[18a]
7	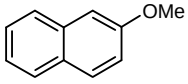	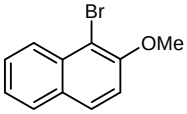	1.2/1/1.2	6	90	55	53–56[18a]
8	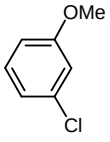	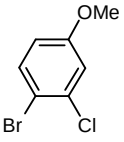	1/1/1.2	5	89	Liq	Liq[18a]

TABLE I. Continued

Entry	Substrate	Product(s)[a]	Oxidant/sub-strate/KBr	Time h	Yield %[b]	M.p. °C	M.p.[lit.] °C
9	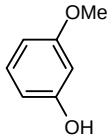	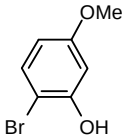	1/1/1.2	3.5	96	152	152–154[18a]
10	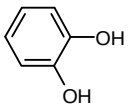	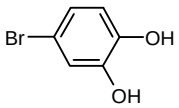	1.2/1/1.2	3	95	87	87–89[18b]
11	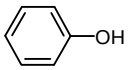	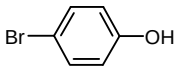	1/1/1.2	4.5	96	63	61–64[18b]
12	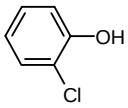	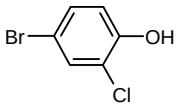	1/1/1.2	1.5	97	51	49–50[18c]
13	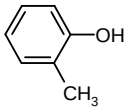	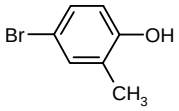	1/1/1.2	4	93	57	58–59[18d]
14	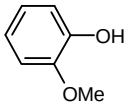	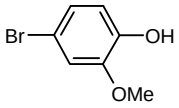	1/1/1.2	3.5	96	34	34–37[18c]
15	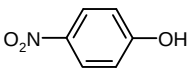	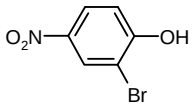	1/1/1.2	8	97	112	111–115[18a]
16	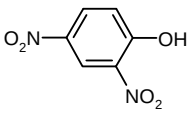	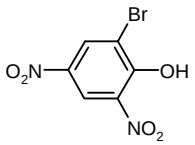	1/1/1.2	9.5	91	99	97–99[18a]
17	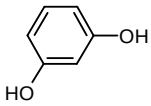	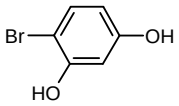	1/1/1.2	2	94	104	103–105[18d]
18	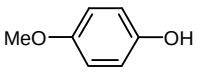	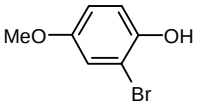	1/1/1.2	4.5	95	45	44–45[18d]

TABLE I. Continued

Entry	Substrate	Product(s)[a]	Oxidant/sub-strate/KBr	Time h	Yield %[b]	M.p. °C	M.p.[lit.] °C
19	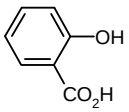	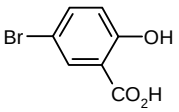	1/1/1.2	6	79	60	58–62[18a]
20	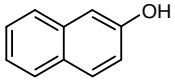	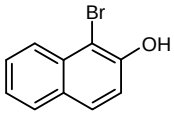	1/1/1.2	5.5	90	79	78–81[18a]
21	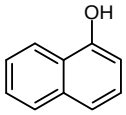	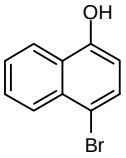	1/1/1.2	5	91	129	129–131[18a]
22	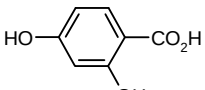	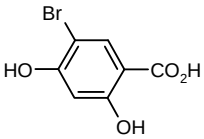	1/1/1.2	6	73	165	165–167[18a]

[a]All products were characterized spectroscopically (^{1}H-NMR and IR) and showed physical and spectral data in accordance with their expected structure and by comparison with authentic samples;[16] [b]yields of isolated products

Although the mechanism for the bromination with lithium bromide and *N*-benzyl-*N*,*N*-dimethylanilinium peroxodisulfate is not clear, the reaction appears to be initiated *via* the formation of the *N*-benzyl-*N*,*N*-dimethylanilinium sulfate radical A by homolysis of *N*-benzyl-*N*,*N*-dimethylanilinium peroxodisulfate.[17] The sulfate radical A may oxidize the bromide anion to the bromonium cation. The electrophilic attack of the bromonium cation at the *p*-position of activated aromatic compounds produces the intermediate B, which is readily converted to the brominated product. However, there is an alternative possibility to form the radical cation C [18] by a one-electron transfer, which may convert to the radical intermediate D (Scheme 3).[4]

It is worth mentioning that the chemoselective conversion of methoxyaromatics to their *para*-substituted products was achieved in excellent yield. Another noteworthy advantage of this system lies in its ability to selectively brominate the *para vs*. the *ortho* position in catechol, phenol , *ortho*-chlorophenol, 2-methoxyphenol and *ortho*-cresol.

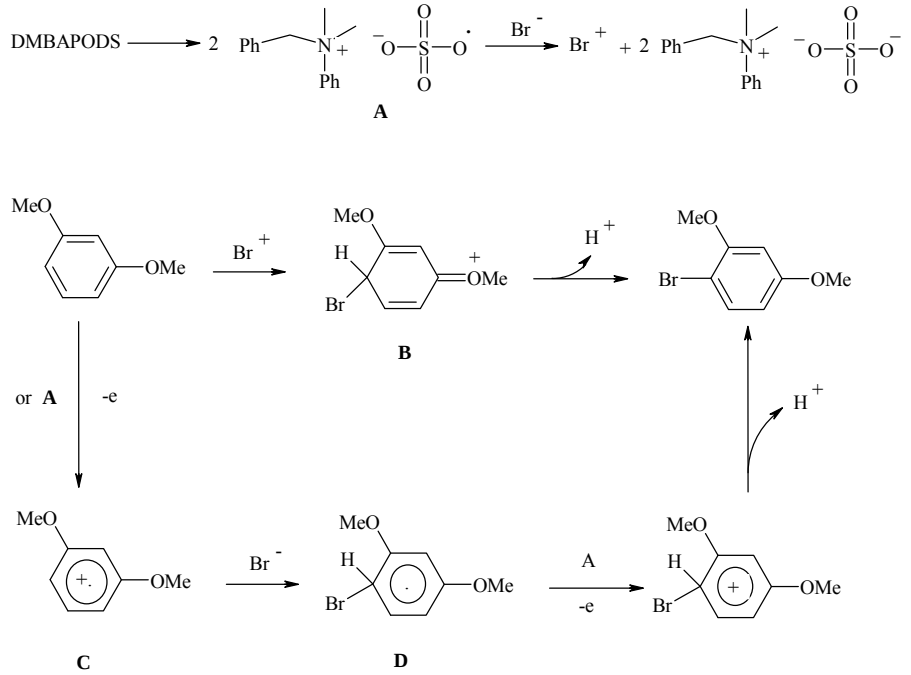

Scheme 3. Proposed mechanism for the synthesis of brominations of aromatic compounds.

CONCLUSIONS

The presented method represents an efficient, chemoselective and environmentally friendly synthesis methodology for the bromination of some activated aromatic compounds.

SUPPLEMENTARY MATERIAL

The ^{1}H-NMR and ^{13}C-NMR spectral data of the products are available electronically at http://www.shd.org.rs/JSCS/, or from the corresponding author on request.

Acknowledgements. We are thankful to the Payamenoor University Research Councils and also the Islamic Azad University – Babol Branch, Babol, Iran for their partial support of this work.

И З В О Д

РЕГИОСЕЛЕКТИВНО БРОМОВАЊЕ АРОМАТИЧНИХ ЈЕДИЊЕЊА ПОМОЋУ *N*-БЕНЗИЛ-*N*,*N*-ДИМЕТИЛАНИЛИНИЈУМ-ПЕРОКСОДИСУЛФАТА У ПРИСУСТВУ КАЛИЈУМ-БРОМИДА ПОД БЛАГИМ РЕАКЦИОНИМ УСЛОВИМА

HASSAN GHASEMNEJAD-BOSRA[1], FARHAD RAMZANIAN-LEHMALI[2] и SOMAYE JAFARI[1]

[1]*Islamic Azad University-Babol Branch, School of Science, P.O. Box 755, Babol u*
[2]*University of Payamenoor, Babol, Iran*

Описан је једноставан и ефикасан поступак селективног бромовања активираних ароматичних једињења помоћу *N*-бензил-*N*,*N*-диметиланилинијум-пероксодисулфата у при-

суству калијум-бромида у неводеним растварачима. Постигнута је добра селективност између *орто* и *пара* супституције фенола и метоксиарена.

(Примљено 16. марта, ревидирано 9. децембра 2010)

REFERENCES

1. D. Morrell *Catalysis of Organic Reactions*, Marcel Dekker, New York, 2002, p. 381
2. J. M. Gnaim, R. A. Sheldon, *Tetrahedron Lett.* **46** (2005) 4465
3. A. Bekaert, O. Provot, O. Rasolojaona, M. Mouad Alami, J. D. Brion, *Tetrahedron Lett*. **46** (2005) 4187
4. M. Y. Park, S. G. Yang, V. Jadhav, Y. H. Kim, *Tetrahedron Lett*. **45** (2004) 4887
5. H. Tajik, I. Mohammadpoor-Baltork, J. Albadi, *Synth. Commun.* **37** (2007) 323
6. Q. H. Chen, F. P. Wang, *Chin. Chem. Lett*. **12** (2001) 421
7. M. Ghiaci, J. Asghari, *Bull. Chem. Soc. Jpn.* **74** (2001) 1151
8. S. T. Wong, C. C. Hwang, C. Y. Mou, *Appl. Catal. B* **63** (2006) 1
9. S. C. Bisaraya, R. A. Rao, *Synth. Commun*. **23** (1993) 779
10. N. B. Barhate, A. S. Gajare, R. D. Wakharkar, A. V. Bedekar, *Tetrahedron Lett.* **39** (1998) 6349
11. M. C. Carreno, J. L. Garcia Ruano, G. Sanz, M. A. Toledo, A. Urbano, *J. Org. Chem.* **60** (1995) 5328
12. P. V. Vyas, A. K. Bhatt, G. Ramachandraiah, A. V. Bedekar, *Tetrahedron. Lett.* **44** (2003) 4085
13. a) J. Zhao, X. Jia, H. Zhai, *Tetrahedron Lett*. **44** (2003) 9371; b) B. Das, K. Venkateswarlu, A. Majhi, V. Siddaiah, K. R. Reddy, *Chin. Chem. Lett.* **20** (2009) 256
14. a) M. M. Lakouraj, M. Tajbakhsh, F. Ramzanian-Lehmali, K. Ghodrati, *Monatsh. Chem.* **139** (2008) 537; b) M. M. Lakouraj, M. Tajbakhsh, F. Ramzanian-Lehmali, *Phosphorus, Sulfur Silicon Relat. Elem*. **183** (2008) 3388; c) H. Ghasemnejad-Bosra, M. Tajbakhsh, F. Ramzanian-Lehmali, M. Shabani-Mahali, M. A. Khalilzadeh, *Phosphorus, Sulfur Silicon Relat. Elem*. **183** (2008) 1496; d) M. Tajbakhsh, M. M. Lakouraj, F. Ramzanian-Lehmali, *Synlett* **11** (2006) 724; e) M. Tajbakhsh, I. Mohammadpoor-Baltork, F. Ramzanian-Lehmali, *Phosphorus, Sulfur Silicon Relat. Elem*. **178** (2003) 2621; f) M. Tajbakhsh, I. Mohammadpoor-Baltork, F. Ramzanian-Lehmali, *J. Chem. Res.-S.* (2001) 185; g) H. Ghasemnejad-Bosra, M. Faraje, S. Habibzadeh, F. Ramzanian-Lehmali, *J. Serb. Chem. Soc.* **75** (2010) 299
15. A. N. Pankratov, O. Fedotova, A. Barbanova, T. Alyonkina, Y. Eliseev, *J. Serb. Chem. Soc.* **69** (2004) 421
16. a) T. Raju, K. Kulangiappar, M. A. Kulandainathan, U. Uma, R. Malini, A. Muthukumaran, *Tetrahedron Lett*. **47** (2006) 4581; b) T. Stropnok, S. Bombek, M. Kočevar, S. Polanc, *Tetrahedron Lett*. **49** (2008) 1729
17. S. C. Roy, C. Guin, K. K. Rana, G. Maiti, *Tetrahedron Lett*. **42** (2001) 6941
18. a) C. Galli, *J. Org. Chem.* **56** (1991) 3238; b) C. Galli, S. Giammarino, *J. Chem. Soc. Perkin. Trans. 2* (1994) 1261; c) M. Fabbrini, C. Galli, P. Gentili, D. Macchitella, H. Petride, *J. Chem. Soc. Perkin. Trans. 2* (2001) 1516
19. a) www.sigmaaldrich.com (accessed December 2010); b) R. H. Mitchell, Y.-H. Lai, R. V. Williams, J. *Org. Chem*. **44** (1979) 4733; c) Z. G. Lee, Z. C. Hu, Y. Chen, *Chin. J. Chem*. **23** (2005) 1537; d) M. Fujio, M. Mishima, Y. Tsuno, Y. Yukawa, Y. Takai, *Bull. Chem. Soc. Jpn.* **48** (1975) 2127; e) A. S. Hussey, I. J. Wilk, *J. Am. Chem. Soc*. **72** (1950) 830.

Journal of the Serbian Chemical Society
JSCS@tmf.bg.ac.rs • www.shd.org.rs/JSCS
J. Serb. Chem. Soc. 76 (5) S1–S3 (2011) *Supplementary material*

SUPPLEMENTARY MATERIAL TO

Simple and improved regioselective brominations of aromatic compounds using *N*-benzyl-*N*,*N*-dimethylanilinium peroxodisulfate in the presence of potassium bromide under mild reactions conditions

HASSAN GHASEMNEJAD-BOSRA[1]*, FARHAD RAMZANIAN-LEHMALI[2] and SOMAYE JAFARI[1]

[1]*Islamic Azad University – Babol Branch, School of Science, P.O. Box 755, Babol and* [2]*University of Payamenoor, Babol, Iran*

J. Serb. Chem. Soc. 76 (5) (2011) 685–692

TABLE I-S. ^{1}H-NMR and ^{13}C-NMR spectral data of the products

Entry	Product	^{1}H-NMR, δ/ ppm	^{13}CNMR, δ/ ppm
1	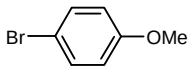	3.70 (3H, *s*, –OCH_3), 6.57–6.61 (2H, *qq*, Ar), 7.19–7.23 (2H, *qq*, Ar)	55.15 (–OCH_3), 108.60 (C1), 111.90 (C3,5), 129.00 (C2,6), 156.91 (C4)
2	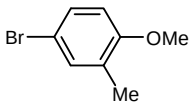	2.22 (3H, *s*, –CH_3), 3.72 (3H, *s*, –OCH_3), 6.63 (1H, *d*, Ar), 7.11 (1H, *d*, Ar), 7.23 (1H, *d*, Ar)	17.16 (–CH_3), 55.30 (–OCH_3), 103.03 (C1), 114.04 (C5), 128.86 (C3), 131.74 (C2), 133.25 (C6), 157.52 (C4)
3	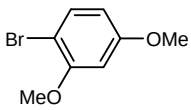	3.70 (3H, *s*, –OCH_3), 3.83 (3H, *s*, –OCH_3), 6.45–6.50 (2H, *m*, Ar), 7.13 (1H, *dd*, Ar)	55.87(–OCH_3), 55.93(–OCH_3), 115.35 (C5), 116.27 (C2), 118.70 (C1), 125.66 (C6), 148.84 (C4), 149.78 (C3)
4	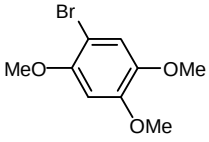	3.68 (3H, *s*, –OCH_3), 3.75 (3H, *s*, –OCH_3), 3.80 (3H, *s*, –OCH_3), 6.25 (1H, *s*, Ar), 6.87 (1H, *s*, Ar)	55.93 (–OCH_3), 56.52 (–OCH_3), 56.65 (–OCH_3), 100.46 (C3), 105.67 (C1), 117.06 (C6), 146.14 (C5), 150.26 (C4), 154.02 (C2)
5	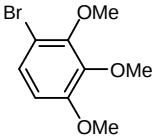	3.65 (3H, *s*, –OCH_3), 3.77 (3H, *s*, –OCH_3), 3.95 (3H, *s*, –OCH_3), 6.24 (1H, *d*, Ar), 7.90 (1H, *d*, Ar)	57.03 (–OCH_3), 58.22 (–OCH_3), 60.68 (–OCH_3), 109.03 (C1), 111.56 (C4), 128.44 (C6), 139.54 (C3), 149.15 (C2), 152.43 (C4)

* Corresponding author. E-mail: h_ghasem2000@yahoo.com

TABLE I-S. Continued

Entry	Product	^{1}H-NMR, δ/ ppm	^{13}CNMR, δ/ ppm
6	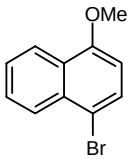	3.80 (3H, *s*, –OCH_3), 7.27 (1H, *d*, Ar), 7.41 (1H, *t*, Ar), 7.47 (1H, *d*, Ar), 7.58 (1H, *t*, Ar), 7.68–7.70 (2H, *m*, Ar)	55.22 (–OCH_3), 104.30 (C3), 113.00 (C1), 122.30 (C5), 125.70 (C6), 126.60 (C8), 127.40 (C10), 127.50 (C7), 129.30 (C2), 133.20 (C9), 155.00 (C4)
7	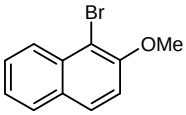	3.78 (3H, *s*, –OCH_3), 7.21 (1H, *d*, Ar), 7.40 (1H, *t*, Ar), 7.45 (1H, *d*, Ar), 7.58 (1H, *t*, Ar), 7.63–7.65 (2H, *m*, Ar)	56.80 (–OCH_3), 108.40 (C1), 113.40 (C3), 124.10 (C6), 125.80 (C8), 127.50 (C7), 127.80 (C5), 128.80 (C4), 129.60 (C9), 139.90 (C10), 153.60 (C2)
8	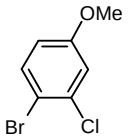	3.71 (3H, *s*, –OCH_3), 6.64 (1H, *dd*, Ar), 6.77 (1H, *m*, Ar), 7.35–7.37 (1H, *dd*, Ar)	55.76 (–OCH_3), 101.33 (C1), 103.07 (C3), 112.44 (C5), 134.63 (C6), 154.05 (C2), 157.68 (C4),
9	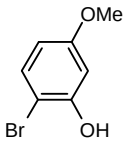	3.83 (3H, *s*, –OCH_3), 6.42–6.45 (1H, *qq*, Ar), 6.50 (1H, *m*, Ar), 7.09–7.11 (1H, *dd*, Ar)	55.70 (–OCH_3), 101.12 (C3), 103.28 (C5), 112.39 (C1), 133.97 (C2), 153.98 (C6), 157.58 (C4)
10	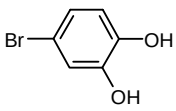	6.48 (1H, *d*, Ar), 6.70–6.72 (1H, *dd*, Ar), 7.07–7.10 (1H, *dd*, Ar)	113.51 (C4), 103.01 (C6), 117.63 (C3), 128.45 (C5), 141.33 (C1), 147.84 (C2)
11	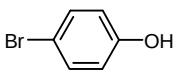	6.89–6.92 (2H, *qq*, Ar), 7.23–7.26 (2H, *qq*, Ar)	107.20 (C4), 113.50 (C2,6), 128.90 (C3,5), 154.10 (C1)
12	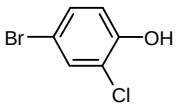	6.94–6.96 (1H, *dd*, Ar), 7.20–7.21 (1H, *dd*, Ar), 7.27–7.29 (1H, *dd*, Ar)	112.40 (C4), 117.60 (C6), 120.80 (C2), 129.45 (C3), 131.30 (C5), 150.51 (C1)
13	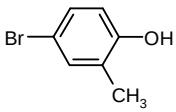	2.21 (3H, *s*, –CH_3), 6.73 (1H, *m*, Ar), 7.09 (1H, *m*, Ar), 7.21 (1H, *m*, Ar)	17.45 (CH_3), 100.10 (C4), 117.18 (C6), 125.51 (C2), 130.19 (C3), 138.10 (C5), 152.20 (C1)
14	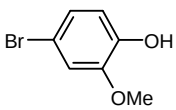	3.80 (3H, *s*, –CH_3), 6.88–6.90 (1H, *dd*, Ar), 6.97 (1H, *m*, Ar), 7.04–7.06 (1H, *dd*, Ar)	55.93 (OCH_3), 114.27 (C3), 116.96 (C4), 118.59 (C6), 125.60 (C5), 145.62 (C1), 148.53 (C2)
15	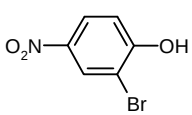	7.16–7.18 (1H, *dd*, Ar), 7.80–7.82 (1H, *dd*, Ar), 7.30 (1H, *d*, Ar)	107.04 (C2), 119.80 (C6), 122.91 (C5), 127.62 (C3), 142.04 (C4), 157.63 (C1)

TABLE I-S. Continued

Entry	Product	^{1}H-NMR, δ/ ppm	^{13}CNMR, δ/ ppm
16	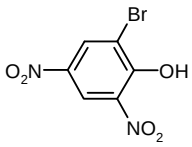	8.68 (1H, *d*, Ar), 8.82 (1H, *d*, Ar), 7.30 (1H, *d*, Ar)	104.26 (C2), 120.24 (C5), 134.21 (C3), 136.96 (C6), 141.62 (C4), 154.87 (C1)
17	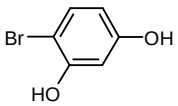	6.47–6.49 (1H, *dd*, Ar), 6.70–6.73 (1H, *dd*, Ar), 7.30 (1H, *d*, Ar)	99.38 (C4), 104.08 (C2), 109.52 (C6), 133.60 (C5), 151.75 (C3), 155.28 (C3),
18	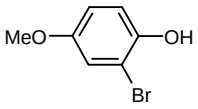	3.71 (3H, *s*, –OCH_3), 6.76 (1H, *m*, Ar), 6.91–6.93 (1H, *dd*, Ar), 6.98–7.01 (1H, *qq*, Ar)	55.34 (OCH_3),112.18 (C3), 113.98 (C2), 114.83 (C5), 118.15 (C6), 143.03 (C1), 155.71 (C4),
19	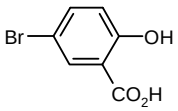	6.99–7.02 (1H, *dd*, Ar), 7.57–7.59 (1H, *dd*, Ar), 7.77–7.78 (1H, *dd*, Ar), 11.31 (1H, *s*, –COOH)	100.46 (C5), 112.38 (C1), 118.26 (C3), 132.81 (C4), 136.09 (C6), 157.86 (C2), 171.54 (CO_2H)
20	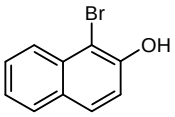	7.89 (1H, *d*, Ar), 7.29 (1H, *d*, Ar), 7.45 (1H, *t*, Ar), 7.58 (1H, *t*, Ar), 7.70–7.72 (2H, *m*, Ar)	106.00 (C1), 117.00 (C3), 124.00 (C6), 125.20 (C8), 127.70 (C7), 128.10 (C5), 129.20 (C4), 129.50 (C10), 132.10 (C9), 150.40 (C2)
21	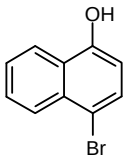	7.95 (1H, *d*, Ar), 7.33 (1H, *d*, Ar), 7.46 (1H, *t*, Ar), 7.62 (1H, *t*, Ar), 7.75–7.78 (2H, *m*, Ar)	109.10 (C3), 113.43 (C1), 121.30 (C5), 125.50 (C10), 126.00 (C6), 127.00 (C8), 127.80 (C7), 129.30 (C2), 132.70(C9), 151.10 (C4)
22	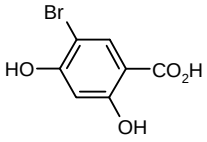	6.46 (1H, *s*, Ar), 7.75 (1H, *s*, Ar)	98.53 (C5), 104.28 (C3), 105.50 (C1), 137.44 (C6), 153.28 (C4), 158.23 (C2), 171.52 (CO_2H),

Journal of the Serbian Chemical Society
JSCS-info@shd.org.rs • www.shd.org.rs/JSCS

J. Serb. Chem. Soc. 76 (5) 693–698 (2011)
JSCS–4150

UDC 542.913:547.466–326+
547.416:615.281/.282–188
Original scientific paper

Synthesis, characterisation and antimicrobial activity of (5-bromo-5-nitro-2-oxido-1,3,2-dioxaphosphinan-2-yl) amino acid esters

PEMMASANI SANTHIPRIYA[1], CHINTHAPARTHI RADHA RANI[2], NANDANUR JAGANNADHA REDDY[1], CHEREDDY SYAMA SUNDAR[2] and CIRANDUR SURESH REDDY[2]*

[1]*Department of Chemistry, S. G. H. R & M. C. M. R. Degree College, Guntur and* [2]*Department of Chemistry, Sri Venkateswara University, Tirupati-517 502, India*

(Received 20 May, revised 13 December 2010)

Abstract: Synthesis of a new series of (5-bromo-5-nitro-2-oxido-1,3,2-dioxaphosphinan-2-yl)amino acid esters (**3a**–**l**) was accomplished *via* a two step process, which involves the prior preparation of the monochloride intermediate (**2**) and its subsequent reaction with the amino acid esters in dry tetrahydrofuran in the presence of triethylamine at reflux temperature. The title compounds (**3a**–**l**) structures were established by analytical, IR, ^{1}H-, ^{13}C- and ^{31}P-NMR, and mass spectral data. They exhibited significant antibacterial and antifungal activity.

Keywords: dioxaphosphinane; 2-bromo-2-nitropropane-1,3-diol; amino acid ester hydrochlorides; antibacterial activity; antifungal activity.

INTRODUCTION

1,3,2-Dioxaphosphinanes are an important class of organophosphorus heterocycles, which continue to attract considerable interest due to their unique stereochemical features and diverse potential biological applications.[1–4] Compounds bearing an esterified amino acid group on the phosphorus atom have been found to display useful anti-neoplastic properties.[5–8] The phosphate moiety when attached to an amino acid group is expected to increase their cellular uptake and thus enhance their chemotherapeutic properties. In view of this, the synthesis of a new class of heterocyclic compounds was accomplished and their activity on bacteria and fungi was tested.

* Corresponding author. E-mail: csrsvu@gmail.com
doi: 10.2298/JSC100520059S

RESULTS AND DISCUSSION

Synthesis of (5-bromo-5-nitro-2-oxido-1,3,2-dioxaphosphinan-2-yl)amino acid esters (**3a**–**l**) was accomplished in a two-step process. The synthetic route (Scheme 1) involves the cyclization of equimolar quantities of 2-bromo-2-nitro-propane-1,3-diol (**1**) with phosphorus oxychloride in the presence of triethylamine in tetrahydrofuran (THF) to afford the corresponding monochloride (**2**). In the second step, the subsequent reaction of **2** with different amino acid ester hydrochlorides was realized at room temperature under stirring for 8–10 h to afford **3a**–**l**.

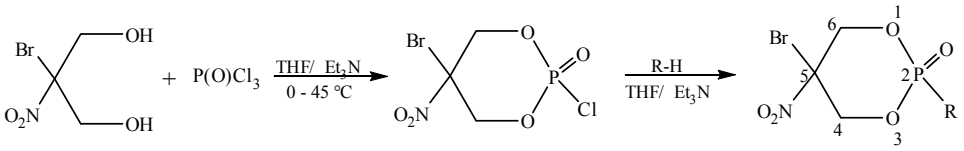

(1) **(2)** **(3a-l)**

Compound	R	Compound	R
3a	$-HN-CH_2-CO_2CH_3$	**3h**	$-NH-CH(COOCH_3)-CH_2-C_3H_3N_2$
3b	$-HN-CH(CH_3)-CO_2CH_3$	**3i**	$-NH-CH(COOCH_3)-CH_2-C_6H_5$
3c	$-HN-CH(CH_3)-CO_2C_2H_5$	**3j**	$-NH-CH(COOC_2H_5)-CH_2-C_6H_5$
3d	$-HN-CH(CH(CH_3)_2)-CO_2CH_3$	**3k**	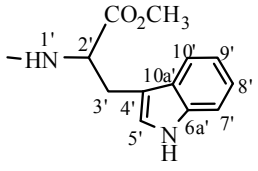
3e	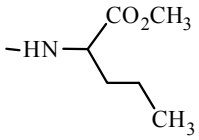	**3l**	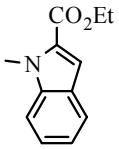
3f	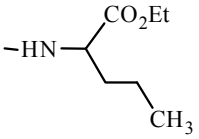		
3g	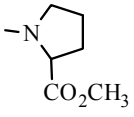		

Scheme 1. Reaction route to the title compounds.

Product yields and elemental analysis, and IR, ^{1}H-, ^{13}C- and ^{31}P-NMR data of **3a–l** are given in Supplementary material. The spectral data agree with the proposed chemical structures for compounds **3a–l.** Characteristic absorption bands in IR spectra for the title compounds were observed in the regions 3418––3441, 1739–1748, 1554–1564, 1249–1258 and 552–563 cm^{-1} for N–H, C=O, NO_2, P=O and C–Br, respectively.[9]

In the ^{1}H-NMR spectra,[10] the aromatic protons of **3a–l** gave a multiplet at δ 6.1–8.4 ppm. The N–H protons appeared as a broad singlet signal at δ 8.02–8.75 ppm. The methoxy protons and methylene protons directly attached to the oxygen of ester moiety in compounds **3a–l** resonated in the range of δ 3.42–3.62 and 4.10–4.14 ppm, respectively. Similarly, the methyl functions in **3a–l** resonated in the region of δ 1.12–1.45 ppm. The ^{13}C-NMR spectra for **3a**, **b**, **c**, **e**, **f**, **j**, **k** and **l** showed carbon chemical shifts in the expected region.[10] The ^{31}P chemical shifts[11] were observed at δ 7.24–13.2 ppm for **3a–l** as a singlet. The mass spectra of compounds **3a**, **b**, **f**, **h**, **j** and **k** showed their respective molecular ion peak at the expected *m*/*z* mass value.

Antimicrobial activity

The compounds **3a–l** showed moderate activity against *Staphylococcus aureus* and *Escherichia coli*. The highlight is that the three compounds **3g, 3h** and **3j** were more effective (Table I).

TABLE I. Antibacterial activity of compounds **3a–j** (zone of inhibition, mm)

Compound	Concentration, ppm			
	100	50	100	50
	E. coli		*S. aureus*	
3a	8	6	8	5
3b	8	6	9	8
3c	9	7	9	7
3d	10	8	9	8
3e	10	8	9	7
3f	10	7	9	8
3g	11	8 10 7		
3h	12	8	6	6
3i	10	7	9	6
3j	12	8 10 7		
3k	10	8	9	7
3l	10	7	9	6
Penicillin	12	8 10 7		

The results of the antifungal screening against *Aspergillus niger* and *Helminthosporium oryzae* are presented in Table II. It is gratifying to observe that the majority of the compounds (**3a–l**) exhibited higher antifungal activity against both tested fungal strains when compared with that of griseofulvin. The signi-

ficant results are that **3g** and **3h** exhibited higher activities than the standard griseofulvin against both the fungi.

Thus, a new group of compounds with very high antibacterial and fungicidal activity, higher than the presently used commercial bactericides and fungicides, have been discovered.

TABLE II. Antifunal activity of compounds **3a–j** (Zone of inhibition, mm)

Compound	Concentration, ppm			
	100	50	100	50
	A. niger		*H. oryzae*	
3a	8	6	8	7
3b	9	7	9	7
3c	9	8	8	7
3d	11	8 10 8		
3e	10	8 10 7		
3f	10	6 11 8		
3g	13	7	9	5
3h	13	7 12		10
3i	9	8	10 8	
3j	12	7 12 9		
3k	10	8 10 7		
3l	10	8 10 8		
Griseofulvin	12	7 12 9		

EXPERIMENTAL

The melting points were determined in open capillary tubes on a Mel-Temp apparatus and are uncorrected. The IR spectra (ν_{max} / cm^{-1}) were recorded as KBr pellets on a Perkin Elmer 1000 instrument. The ^{1}H-, ^{13}C- and ^{31}P-NMR spectra were recorded on a Varian AMX 400 MHz NMR spectrometer operating at 400 MHz for ^{1}H, 100.57 MHz for ^{13}C and 161.7 MHz for ^{31}P-NMR. All the compounds were dissolved in DMSO-d_6 and the chemical shifts were referenced to TMS (^{1}H and ^{13}C) and 85 % H_3PO_4 (^{31}P). The microanalyses data were obtained from the Central Drug Research Institute (CDRI), Lucknow, India.

*General procedure for the synthesis of (5-bromo-5-nitro-2-oxido-1,3,2-dioxaphosphinan-2--yl)amino acid esters (**3a–l**)*

Cyclization of equimolar quantities of 2-bromo-2-nitropropane-1,3-diol (**1**) with phosphorus oxychloride in the presence of triethylamine in THF afforded the corresponding monochloride (**2**). In the second step, reaction of **2** with different amino acid ester hydrochlorides at room temperature under stirring for 8–10 h afforded **3a–l**. Progress of the reaction was monitored by TLC analysis. The crude products obtained as residues after removal of the solvent on a rotary evaporator were purified by repeated washing with water to remove any residual triethylamine hydrochloride and then with cold methanol to remove the unreacted starting materials and other impurities. The crude title compounds (**3a–l**) were further purified by flash chromatography on silica gel, using hexane–ethyl acetate (8:2) as eluent. All of them were obtained in high yields (68–75 %).

Antimicrobial activity

The antimicrobial activities[12] of **3a–l** were tested against the growth of *S. aureus* (ATCC 25923) (gram +ve) and *E. coli* (ATCC 25922) (gram –ve) by the disc diffusion method at two concentrations (100 and 50 ppm) on 6 mm diameter discs.

They were also screened for antifungal activity against *A. niger* (ATCC 16404) and *H. oryzae* (ATCC 11000) species along with the standard fungicide griseofulvin by the disc diffusion method at two different concentrations (100 and 50 ppm) on the same disc size.

SUPPLEMENTARY MATERIAL

The analytical and spectral data of the title compounds are available electronically at http://www.shd.org.rs/JSCS/, or from the corresponding author on request.

Acknowledgements. The authors thank Prof. C. Devendranath Reddy, Department of Chemistry, S.V. University, Tirupati for his valuable advice and the UGC (34-306/2008, SR) for providing financial assistance.

ИЗВОД

СИНТЕЗА, КАРАКТЕРИЗАЦИЈА И АНТИМИКРОБНА АКТИВНОСТ ЕСТАРА (5-БРОМ-5-НИТРО-2-ОКСИДО-1,3,2-ДИОКСАФОСФИНАН-2-ИЛ)-АМИНО-КИСЕЛИНА

PEMMASANI SANTHIPRIYA[1], CHINTHAPARTHI RADHA RANI[2], NANDANUR JAGANNADHA REDDY[1], CHEREDDY SYAMA SUNDAR[2] и CIRANDUR SURESH REDDY[2]

[1]*Department of Chemistry, S. G. H. R & M. C. M. R. Degree College, Guntur u* [2]*Department of Chemistry, Sri Venkateswara University, Tirupati-517 502, India*

Остварена је синтеза естара (5-бром-5-нитро-2-оксидо-1,3,2-диоксафосфинан-2-ил)-амино-киселина у два реакциона корака. У првом је извршена синтеза монохлоридног интермедијера (**2**), а у следећем реакција интермедијера са естрима амино-киселина, у сувом тетрахидрофурану у присуству триетиламина на температури кључања. Структура деривата (**3a–l**) је утврђена аналитичким и спектралним методама (IC, NMR (^{1}H, ^{13}C и ^{31}P) и масена спектрометрија). Испитивањем антимикробне активности добијених деривата утврђено је да показују значајно добру антибактеријску и антифунгалну активност.

(Примљено 20. маја, ревидирано 13. децембра 2010)

REFERENCES

1. a) A. M. Polozov, A. V. Khotinen, E. N. Klimovitskii, *Phosphorus, Sulfur Silicon Relat. Elem.* **109** (1996) 581; b) D. Bouchu, *Phosphorus, Sulfur Silicon Relat. Elem.* **15** (1983) 33; c) R. L. Shao, G. F. Yang, W. S. Miao, *Chem. J. Chin. Univ.* **16** (1995) 391
2. a) R. S. Edmundson, O. Johnson, D. W. Jones, *Phosphorus, Sulfur Silicon Relat. Elem.* **46** (1989) 61; b) R. S. Edmundson, O. Johnson, D. W. Jones, T. J. King, *J. Chem. Soc. Perkin Trans. 2* (1985) 69; c) O. Johnson, D. W. Jones, R. S. Edmundson, *Acta Crystallogr. Sect. C* **45** (1989) 142
3. J. A. Mosbo, J. G. Verkade, *J. Am. Chem. Soc.* **95** (1973) 204
4. a) C. Meier, *Angew. Chem., Int. Ed. Engl.* **35** (1996) 70; b) M. Sasaki, K. Moriguchi, K. Yanagi, *Agric. Biol. Chem.* **52** (1988) 159
5. C. McGuigan, P. Narashiman, *Synthesis* (1993) 311
6. K. G. Devine, C. McGuigan, T. J. O' Connor, S. R. Nicholis, D. Kinchington, *AIDS* **4** (1990) 371

7. P. J. Cox, *Biochem. Pharmacol.* **28** (1979) 2045
8. M. Szekerke, *Cancer Treatment Rep.* **60** (1976) 347
9. P. Vasu Govardhana Reddy, Y. Hari Babu, C. Suresh Reddy, *J. Heterocycl. Chem.* **40** (2003) 535
10. M. Veera Narayana Reddy, A. Bala Krishna, C. Suresh Reddy, *Eur. J. Med. Chem.* **45** (2010) 1828
11. M. Anil Kumar, K. Suresh Kumar, C. Devendranath Reddy, C. Naga Raju, C. Suresh Reddy, P. Hari Krishna, *S. Afr. J. Chem*. **62** (2009) 26
12. D. V. Mangte, S. P. Deshmukh, D. D. Bhokare, A. Arti Deshpande, *Indian J. Pharm. Sci.* **69** (2007) 295.

Journal of the Serbian Chemical Society
JSCS@tmf.bg.ac.rs • www.shd.org.rs/JSCS
J. Serb. Chem. Soc. 76 (5) S5–S8 (2011) *Supplementary material*

SUPPLEMENTARY MATERIAL TO

Synthesis, characterisation and antimicrobial activity of (5-bromo-5-nitro-2-oxido-1,3,2-dioxaphosphinan-2-yl) amino acid esters

PEMMASANI SANTHIPRIYA[1], CHINTHAPARTHI RADHA RANI[2], NANDANUR JAGANNADHA REDDY[1], CHEREDDY SYAMA SUNDAR[2] and CIRANDUR SURESH REDDY[2]*

[1]*Department of Chemistry, S. G. H. R & M. C. M. R. Degree College, Guntur and*
[2]*Department of Chemistry, Sri Venkateswara University, Tirupati-517 502, India*

J. Serb. Chem. Soc. 76 (5) (2011) 693–698

ANALYTICAL AND SPECTRAL DATA OF THE TITLE COMPOUNDS

*Methyl [(5-bromo-5-nitro-2-oxido-1,3,2-dioxaphosphinan-2-yl)amino]acetate (**3a**)*. Yield: 75 %; m.p.: 177–179 °C; Anal. Calcd. for: $C_6H_{10}BrN_2O_7P$ (FW 332): C, 21.64; H, 3.03; N, 8.41 %. Found: C, 21.60; H, 3.98; N, 8.38 %. IR (KBr, cm^{-1}): 3418 (–N–H, secondary amine), 1745 (–C=O, ester), 1555 ($–NO_2$), 1255 (–P=O, phosphinan), 552 (–C–Br). ^{1}H-NMR (400 MHz, DMSO-d_6, δ / / ppm): 4.14–4.25 (4H, *m*, $–CH_2$ ($C_{4\text{ and }6}$)), 8.22 (1H, *brs*, NH, D_2O exchangeable), 3.42 (3H, *s*, $–OCH_3$), 4.13 (2H, *s*, $–NCH_2$). ^{13}C-NMR (100 MHz, DMSO-d_6, δ / ppm): 54.6 ($C_{4\text{ and }6}$), 70.7 (C_5), 170.1 (COO), 37.2 (NCH_2), 53.4 ($–OCH_3$). ^{31}P-NMR (161.7 MHz, DMSO-d_6, δ / ppm): 13.2. MS (*m/z*, relative abundance, %): 334 (M+2, 31.6), 332 (M^+, 32.5).

*Methyl 2-[(5-bromo-5-nitro-2-oxido-1,3,2-dioxaphosphinan-2-yl)amino]propanoate (**3b**)*. Yield: 71 %; m.p.: 123–124 °C; Anal. Calcd. for: $C_7H_{12}BrN_2O_7P$ (FW 346): C, 24.23; H, 3.49; N, 8.07 %. Found C, 24.18; H, 3.45; N, 8.01 5. IR (KBr, cm^{-1}): 3419 (–N–H, secondary amine), 1745 (–C=O, ester), 1558 ($–NO_2$), 1254 (–P=O, phosphinan), 553 (–C–Br). ^{1}H-NMR (400 MHz, DMSO-d_6, δ / / ppm): 4.17–4.42 (4H, *m*, $–CH_2$ ($C_{4\text{ and }6}$)), 8.42 (1H, *brs*, NH, D_2O exchangeable), 3.48 (1H, *s*, –NCH), 3.45 (3H, *s*, $–OCH_3$), 1.45 (3H, *d*, J = 6.2 Hz, CH_3). ^{13}C-NMR (100 MHz, DMSO-d_6, δ / ppm): 53.2 ($C_{4\text{ and }6}$), 68.4 (C_5), 168.4 (COO), 38.4 (NCH), 52.7 ($–OCH_3$), 26.3 (CH_3). ^{31}P-NMR (161.7 MHz, DMSO-

* Corresponding author. E-mail: csrsvu@gmail.com
doi: 10.2298/JSC100520059S

d_6, δ / ppm): 9.02. MS (*m/z*, relative abundance, %): 348 (M+2, 28.6), 346 (M^+, 30.5).

*Ethyl 2-[(5-bromo-5-nitro-2-oxido-1,3,2-dioxaphosphinan-2-yl)amino]propanoate (**3c**)*. Yield: 69 %; m.p.: 160–162 °C; Anal. Calcd. for $C_8H_{14}BrN_2O_7P$ (FW 360): C, 26.61; H, 3.91; N, 7.76 %. Found C, 26.58; H, 3.87; N, 7.71 %. IR (KBr, cm^{-1}): 3432 (–N–H, secondary amine), 1743 (–C=O, ester), 1561 ($–NO_2$), 1258 (–P=O, phosphinan), 557 (–C–Br). ^{1}H-NMR (400 MHz, DMSO-d_6, δ / / ppm): 4.14–4.42 (4H, *m*, $–CH_2$ ($C_{4\text{ and }6}$)), 8.08 (1H, *brs*, –NH, D_2O exchangeable), 4.13 (2H, *q*, J = 5.8 Hz, $–OCH_2$), 3.49 (1H, *q*, J = 5.7 Hz, –NCH), 1.26 (6H, *m*, 2×$–CH_3$). ^{31}P-NMR (161.7 MHz, DMSO-d_6, δ / ppm): 7.24.

*Methyl 2-[(5-bromo-5-nitro-2-oxido-1,3,2-dioxaphosphinan-2-yl)amino]-3-methyl butanoate (**3d**)*. Yield: 71 %; m.p.: 190–192 °C; Anal. Calcd. for: $C_9H_{16}N_2O_7P$ (FW 374): C, 28.82; H, 4.30; N, 7.47 %. Found C, 28.79; H, 4.28; N, 7.44 %. IR (KBr, cm^{-1}): 3420 (–N–H, secondary amine), 1742 (–C=O, ester), 1561 ($–NO_2$), 1256 (–P=O, phosphinan), 557 (–C–Br). ^{1}H-NMR (400 MHz, DMSO-d_6, δ / ppm): 4.20–4.52 (4H, *m*, $–CH_2$ ($C_{4\text{ and }6}$)), 8.02 (1H, *brs*, –NH, D_2O exchangeable), 3.47 (3H, *s*, $–OCH_3$), 3.45 (1H, *d*, J = 5.6 Hz, –NCH), 1.35 (1H, *m*, –CH), 1.03 (6H, *d*, J = 6.4 Hz, $2CH_3$). ^{13}C-NMR (100 MHz, DMSO-d_6, δ / ppm): 55.2 ($C_{4\text{ and }6}$), 71.1 (C_5), 169.3 (COO), 37.9 (–NCH), 53.8 ($–OCH_3$), 21.6 (2×$–CH_2$), 18.7 (CH_3). ^{31}P-NMR (161.7 MHz, DMSO-d_6, δ / / ppm): 8.52.

*Methyl 2-[(5-bromo-5-nitro-2-oxido-1,3,2-dioxaphosphinan-2-yl)amino]pentanoate (**3e**)*. Yield: 74 % ; m.p.: 189–191 °C; Anal. Calcd. for: $C_9H_{16}N_2O_7P$ (FW 374): C, 28.82; H, 4.30; N, 7.47 %. Found C, 28.79; H, 4.28; N, 7.44 %. IR (KBr, cm^{-1}): 3435 (–N–H secondary amine), 1745 (–C=O, ester), 1560 ($–NO_2$), 1258 (–P=O, phosphinan), 560 (–C–Br). ^{1}H- NMR (400 MHz, DMSO-d_6, δ / / ppm): 4.17–4.52 (4H, *m*, CH_2 ($C_{4\text{ and }6}$)), 8.68 (1H, *brs*, NH, D_2O exchangeable), 3.56 (1H, *t*, J = 5.7 Hz, N–CH), 3.58 (3H, *s*, OCH_3), 1.12–1.58 (4H, *m*, 2×CH_2), 1.22 (3H, *t*, J = 6.8 Hz, $–CH_3$). ^{13}C-NMR (100 MHz, DMSO-d_6, δ / / ppm): 56.3 ($C_{4\text{ and }6}$), 72.3 (C_5), 170.3 (COO), 38.4 (–NCH), 54.4 ($–OCH_3$), 22.4 (2 × $–CH_2$), 17.3 (CH_3). ^{31}P-NMR (161.7 MHz, DMSO-d_6, δ / ppm): 10.41.

*Ethyl 2-[(5-bromo-5-nitro-2-oxido-1,3,2-dioxaphosphinan-2-yl)amino]pentanoate (**3f**)*. Yield: 74 %; m.p.: 128–130 °C; Anal. Calcd. for: $C_{10}H_{18}BrN_2O_7P$ (FW 388): C, 30.86; H, 4.66; N, 7.20 %. Found C, 30.81; H, 4.62; N, 7.18 %. IR (KBr, cm^{-1}): 3432 (–N–H, secondary amine), 1748 (–C=O, ester), 1561 ($–NO_2$), 1249 (–P=O, phosphinan), 560 (–C–Br). ^{1}H-NMR (400 MHz, DMSO-d_6, δ / / ppm): 4.17–4.50 (4H, *m*, $–CH_2$ ($C_{4\&6}$)), 8.66 (1H, *brs*, NH, D_2O exchangeable), 3.47 (1H, *m*, –NCH), 4.10 (2H, *q*, J = 5.7 Hz, $–OCH_2$), 1.26 (3H, *t*, J = 3.2 Hz, $–CH_3$), 1.23–1.58 (4H, *m*, 2×$–CH_2$), 1.12 (3H, *t*, J = 3.3 Hz, $–CH_3$). ^{13}C-NMR (100 MHz, DMSO-d_6, δ / ppm): 56.8 ($C_{4\text{ and }6}$), 72.6 (C_5), 169.8 (COO), 37.7 (–NCH), 54.2 ($–OCH_2$), 22.4 (2 ×$–CH_2$), 17.3 ($–CH_3$), 19.6 ($–CH_3$). ^{31}P-

-NMR (161.7 MHz, DMSO-d_6, δ / ppm): 11.7. MS (*m/z*, relative abundance, %): 390 (M+2, 23.2), 388 (M^+, 24.6).

Methyl 1-(5-bromo-5-nitro-2-oxido-1,3,2-dioxaphosphinan-2-yl)pyrrolidine--2-carboxylate (***3g***). Yield: 75 % ; m.p.: 177–179 °C; Anal. Calcd. for: $C_9H_{14}BrN_2O_7P$ (FW 372): C, 28.97; H, 3.78; N, 7.51 % . Found C, 28.95; H, 3.75; N, 7.48 %. IR (KBr, cm^{-1}): 1739 (–C=O, ester), 1564 ($–NO_2$), 1251 (–P=O, phosphinan), 563 (–C–Br). ^{1}H-NMR (400 MHz, DMSO-d_6, δ / ppm): 4.15–4.48 (4H, *m*, $–CH_2$ ($C_{4\text{ and }6}$)), 3.19 (1H, *t*, J = 5.8 Hz, –NCH), 1.65–2.31 (6H, *m*, 3×$–CH_2$), 3.54 (3H, *s*, $–OCH_3$). ^{31}P-NMR (161.7 MHz, DMSO-d_6, δ / / ppm): 10.5.

*Methyl 2-[(5-bromo-5-nitro-2-oxido-1,3,2-dioxaphosphinan-2-yl)amino]-3--(1*H*-imidazol-4-yl)propanoate* (***3h***). Yield: 72 % ; m.p.: 135–137 °C; Anal. Calcd. for $C_{10}H_{14}BrN_4O_7P$ (FW 412): C, 29.07; H, 3.42; N, 13.56 %. Found C, 29.02; H, 3.39; N, 13.53 %. IR (KBr, cm^{-1}): 3430 (–N–H, secondary amine), 1740 (–C=O, ester), 1554 ($–NO_2$), 1254 (–P=O, phosphinan), 554 (–C–Br). ^{1}H--NMR (400 MHz, DMSO-d_6, δ / ppm): 6.75–7.25 (2H, *m*, Ar–H), 4.15–4.43 (4H, *m*, $–CH_2$ ($C_{4\text{ and }6}$)), 8.72 (2H, *brs*, NH, D_2O exchangeable), 3.45 (1H, *m*, –NCH), 3.59 (3H, *s*, OCH_3), 2.81 (2H, *m*, Ar–CH_2). ^{31}P-NMR (161.7 MHz, DMSO-d_6, δ / ppm): 11.5; MS (*m/z*, (relative abundance), %): 414 (M+2, 17.3), 412 (M^+, 18.9).

Methyl 2-[(5-bromo-5-nitro-2-oxido-1,3,2-dioxaphosphinan-2-yl)amino]-3--phenylpropanoate (***3i***). Yield: 70 %; m.p.: 138–140 °C; Anal. Calcd. for $C_{13}H_{16}BrN_2O_7P$ (FW 421): C, 36.90; H, 3.81; N, 6.62 %. Found C, 36.86; H, 3.78; N, 6.59 %. IR (KBr, cm^{-1}): 3441 (–N–H, secondary amine), 1743 (–C=O, ester), 1555 ($–NO_2$), 1248 (–P=O, phosphinan), 555 (–C–Br). ^{1}H-NMR (400 MHz, DMSO-d_6, δ / ppm): 6.78–7.20 (5H, *m*, Ar–H), 4.35–4.52 (4H, *m*, $–CH_2$ ($C_{4\text{ and }6}$)), 8.59 (1H, *s*, –N–H, D_2O exchangeable), 3.91 (2H, *m*, Ar–CH_2), 3.64 (3H, *s*, $–OCH_3$), 3.51 (1H, *m*, –NCH). ^{31}P-NMR (161.7 MHz, DMSO-d_6, δ / / ppm): 11.5.

Ethyl 2-[(5-bromo-5-nitro-2-oxido-1,3,2-dioxaphosphinan-2-yl)amino]-3-phenylpropanoate (***3j***). Yield: 68 %; m.p.: 115–117 °C; Anal. Calcd. for $C_{14}H_{18}BrN_2O_7P$ (FW 436): C, 38.46; H, 4.15; N, 6.41 %. Found C, 38.43; H, 4.12; N, 6.38 %. IR (KBr, cm^{-1}): 3439 (–N–H, secondary amine), 1748 (–C=O, ester), 1558 (NO_2), 1250 (–P=O, phosphinan), 561 (–C–Br). ^{1}H-NMR (400 MHz, DMSO-d_6, δ / ppm): 6.76–7.21 (6H, *m*, Ar–H), 4.28–4.42 (4H, *m*, $–CH_2$ ($C_{4\text{ and }6}$)), 8.58 (1H, *s*, –N–H, D_2O exchangeable), 3.87 (2H, *m*, Ar–CH_2), 4.12 (2H, *q*, J = 5.7 Hz, $–OCH_2$), 3.54 (1H, *m*, –NCH), 1.25 (3H, *t*, J = 6.8 Hz, $–CH_3$). ^{13}C-NMR (100 MHz, DMSO-d_6, δ / ppm): 168.2 (COO), 123.2–143.7 ($C_{aromatic}$), 56.8 (NCH), 56.1 (OCH_2), 43.2 (Ar–CH_2), 19.8 (CH_3). ^{31}P-NMR (161.7 MHz, DMSO-d_6, δ / ppm): 12.2. MS (*m/z*, relative abundance, %): 438 (M+2, 31.2), 436 (M^+, 35.6).

*Methyl 2-[(5-bromo-5-nitro-2-oxido-1,3,2-dioxaphosphinan-2-yl)amino]-3--(1*H*-indol-3-yl)propanoate (**3k**)*. Yield: 72 %; m.p.: 108–110 °C; Anal. Calcd. for: $C_{15}H_{17}BrN_3O_7PS$ (FW 461): C, 39.98; H, 3.71; N, 9.09 %. Found C, 39.96; H, 3.68; N, 9.05 %. IR (KBr, cm^{-1}): 3433 (–N–H, secondary amine), 1742 (C=O, ester), 1558 ($–NO_2$), 1255 (–P=O, ph osphinan), 561 (–C–Br). ^{1}H-NMR (400 MHz, DMSO-d_6, δ / ppm): 6.78–7.29 (5H, *m*, Ar–H), 4.29–4.52 (4H, *m*, $–CH_2$ ($C_{4\text{ and }6}$)), 8.75 (2H, *brs*, –N–H, D_2O exchangeable), 3.62 (3H, *s*, $–OCH_3$), 3.63 (1H, *m*, –NCH), 6.81–7.36 (2H, *m*, Ar–CH_2). ^{13}C-NMR (100 MHz, DMSO-d_6, δ / ppm): 58.2 ($C_{4\text{ and }6}$), 72.4 (C_5), 170.2 (COO), 37.2 (N–CH), 54.5 (OCH_3), 35.2 ($C_{3'}$), 112.5 ($C_{4'}$), 126.8 ($C_{5'}$), 117.6 ($C_{10'}$), 131.2 ($C_{10a'}$), 141.2 ($C_{6a'}$), 108.3 ($C_{7'}$), 125.3 ($C_{8'}$), 121.2 ($C_{9'}$). ^{31}P-NMR (161.7 MHz, DMSO-d_6, δ / ppm): 10.9. MS (*m/z*, (relative abundance), %): 463 (M+2, 23.2), 461 (M^+, 25.3).

*Ethyl 1-(5-bromo-5-nitro-2-oxido-1,3,2-dioxaphosphinan-2-yl)-1*H*-indole-2-carboxylate (**3l**)*. Yield: 69 % ; m.p.: 104–106 °C; An al. Calcd. for: $C_{14}H_{14}BrN_2O_7P$ (FW 432): C, 38.82; H, 3.26; N, 6.47 %. Found C, 38.79; H, 3.22; N, 6.43 %. IR (KBr, cm^{-1}): 1742 (–C=O, ester), 1558 ($–NO_2$), 1253 (–P=O, phosphinan), 561 (–C–Br). ^{1}H-NMR (400 MHz, DMSO-d_6, δ / ppm): 6.77–7.26 (5H, *m*, Ar–H), 4.23–4.52 (4H, *m*, $–CH_2$ ($C_{4\&6}$)), 4.14 (2H, *q*, J = 5.6 Hz, $–OCH_2$), 1.22 (3H, *t*, J = 6.7 Hz, $–CH_3$). ^{13}C–NMR (100 MHz, DMSO-d_6, δ / ppm): 58.4 ($C_{4\text{ and }6}$), 72.1 (C_5), 169.5 (COO), 54.6 (OCH_2), 18.9 ($–CH_3$), 133.3 ($C_{2'}$), 104.6 ($C_{3'}$), 131.5 ($C_{3a'}$), 122.2 ($C_{4'}$), 117.6 ($C_{5'}$), 124.6 ($C_{6'}$), 114.6 ($C_{7'}$), 145.6 ($C_{7a'}$). ^{31}P-NMR (161.7 MHz, DMSO-d_6, δ / ppm): 11.2.

Journal of the Serbian Chemical Society
JSCS-info@shd.org.rs • www.shd.org.rs/JSCS
J. Serb. Chem. Soc. 76 (5) 699–707 (2011)
JSCS–4151
UDC 579.864+547.466.1:579.61:615.28–188
Original scientific paper

The partial characterization of the antibacterial peptide bacteriocin G_2 produced by the probiotic bacteria *Lactobacillus plantarum* G_2

SVETLANA L. ŠEATOVIĆ[1]*, JELENA S. JOVANOVIĆ NOVAKOVIĆ[1], GORDANA N. ZAVIŠIĆ[1], ŽELJKA Č. RADULOVIĆ[1], MARIJA Đ. GAVROVIĆ-JANKULOVIĆ[2#] and RATKO M. JANKOV[2#]

[1]*Galenika a.d., Batajnički drum bb, 11080 Zemun, Belgrade, Serbia and* [2]*Faculty of Chemistry, University of Belgrade, Studentski trg 12–16, 11000 Belgrade, Serbia*

(Received 5 June, revised 15 October 2010)

Abstract: The aim of this study was the partial characterization of the antimicrobial peptide bacteriocin G_2 produced by probiotic bacteria *Lactobacillus plantarum* G_2, which was isolated from a clinical sample of a healthy person. Antimicrobial substance was secreted in the supernatant of an *L. plantarum* G_2 culture, and showed a diverse spectrum of antimicrobial activity of all the tested strains of the genera *Lactobacillus* and the pathogenic bacteria *Staphylococcus aureus* and *Salmonella abony*. Isoelectric focusing revealed that bacteriocin G_2 is a cationic peptide (p*I* about 10) with a molecular mass of 2.2 kDa according to tricine–sodium dodecyl sulphate–polyacrylamide gel electrophoresis, SDS-PAGE. The antimicrobial activity of bacteriocin G_2 was diminished by the proteolytic action of trypsin and proteinase K. Bacteriocin G_2 preserved its biological activity in the temperature range 40–60 °C (15 min), which was lost at 80 °C. Bacteriocin G_2 was stable in the pH range 2–9, while treatment with 1 % Tween 80 and 1 % urea resulted in increased antimicrobial activity. The probiotic strain *L. plantarum* G_2 produces the antimicrobial substance proteinaceous in nature with bacteriocin characteristics. Bacteriocin production is one of the key properties of probiotic bacteria with clinical potential as anti-infective agents, which will increase the likelihood of its *in vivo* efficacy.

Keywords: *Lactobacillus plantarum*; probiotic; bacteriocin.

INTRODUCTION

Bacteria employed in probiotic applications help to maintain or restore the natural microbial flora of a host. The ability of probiotic bacteria to successfully outcompete undesired species is often due to, or enhanced by, the production of

* Corresponding author. E-mail: seatovic.svetlana@gmail.com
# Serbian Chemical Society member.
doi: 10.2298/JSC100605060S

potent antimicrobial toxins.[1] Some antimicrobial substances are non-specific, such as short-chain fatty acids or hydrogen peroxide, while others are specific with a very narrow killing range, such as bacteriocins, bacteriocin-like inhibitory substances (BLIS), and bacteriophages.[2–4] Bacteriocins have been designated as bacterial substances with the capacity to inhibit, even in low concentrations, the multiplication of other taxonomically similar bacteria.[5] They comprise a large and functionally diverse family of toxins found in all major lineages of Bacteria and Archaea, but there are certain features that unite them as a family; they are all ribosomally synthesized proteinaceous compounds and are active against bacteria closely related to the producing bacteria.[6] In an attempt to organise this diverse family, bacteriocins are roughly classified into two main groups, the toxins produced by Gram-negative bacteria and those produced by Gram-positive bacteria.[7]

Bacteriocins from Gram-positive bacteria are generally cationic, amphiphilic, membrane-permeabilizing peptides, approximately 2–6 kDa in size.[8] They are particularly attractive when the goal of probiotic application is to supplement, rather than dramatically alter, the natural bacterial flora of a host.[1] Bacteriocin nisin was found to be safe for human consumption by the Food and Drug Administration and has thus gained popularity in probiotic research.[1]

Numerous strains of bacteriocin producing *Lactobacillus plantarum* have been isolated in the last two decades. Several of these plantaricins were characterized and their amino acid sequence determined.[9]

The aim of this work was to test bacteria with probiotic characteristics, *L. plantarum* G_2, for antimicrobial peptide production. The antimicrobial spectrum and some properties of the bacteriocin G_2 are described herein for the first time.

EXPERIMENTAL

Bacterial strains and growth media

The bacteriocin G_2 producing strain used in this study was isolated from a clinical sample of a healthy person, and according to its phenotypic and genotypic characteristics, it was classified as *L. plantarum* G_2. The strain was stored at –20 °C in MRS (de Man, Rogosa and Sharpe, Merck) medium containing 15 % glycerol. MRS broth (Merck) was used for cell propagation.

Indicator bacteria strains

The bacteria used as indicator strains were: *L. acidophilus* ATCC 314, *L. rhamnosus* ATCC 7469, *L. leishmany* ATCC 7830, *L. plantarum* G1, *L. casei* G_3, *Enterococcus faecalis* ATCC 29219, *Staphylococcus aureus* ATCC 6538–P, *Pseudomonas aeruginosa* ATCC 9027, *Escherichia coli* ATCC 8739, *Klebsiella* sp. ATCC 10031, *Bacillus subtilis* ATCC 6633, *B. cereus* ATCC 11178, *Micrococcus luteus* ATCC 93419, *Salmonella abony* ATCC 6017.

L. leishmany ATCC 7830 was used as the indicator bacterium for the estimation of antimicrobial activity.

Production of bacteriocin G_2

For bacteriocin production, *L. plantarum* G_2 cells were grown anaerobically (in 1000 ml Erlenmeyer flasks) in MRS broth (pH 6.4), at 37 °C and 58 rpm for 24 h, in rotary shaker incubator (Adolf Kühner, Switzerland). The culture was centrifuged at 4000 × *g*, for 20 min at 4 °C. The pH of the supernatant was adjusted to 6.5–7.0 with 1.0 M NaOH, to exclude the antimicrobial effect of organic acids, followed by filtration of the supernatant through a 0.2 μm pore-size cellulose acetate filter (Sigma–Aldrich). The supernatant S was used for screening the antimicrobial activity.

Detection of antimicrobial activity

The antimicrobial activity of the bacteriocin produced by *L. plantarum* G_2 was screened using the agar well diffusion (AWD) assay.[10] Pre-poured MRS agar plates were overlain with 0.1 mL suspension of the indicator strain (containing 10^6 CFU mL^{-1}). Wells of 6 mm in diameter were cut into the agar plate using a cork borer and 100 μL of the supernatant S was placed into each well. After 18 h of incubation at 37 °C, the zone of inhibition (diameter) was measured.

Bacteriocin assay

The critical dilution assay described by Mayer-Hartings *et al.*[11] was used to quantify the inhibitory activity of the bacteriocin against the respective sensitive indicator strain *L. leishmany*. A serial two-fold dilution of the supernatant was made in 0.1 M Tris-HCl buffer, pH 7. The activity of each dilution was determined by the AWD assay. The antimicrobial activity is expressed in arbitrary units (AU mL^{-1}). One AU is defined as the reciprocal of the highest dilution showing a clear zone of growth inhibition.

Sensitivity to enzyme activity of bacteriocin G_2

To investigate the sensitivity of the bacteriocin to different enzymes (all obtained from Sigma), neutralized supernatant S samples of the tested strain were mixed with enzyme solutions of catalase, pronase E, proteinase K, trypsin, chymotrypsin, lipase, lysozyme and α--amylase (final enzyme concentration was 1 mg mL^{-1}), incubated for 1 h at the optimum temperature for each of the enzymes and the residual activities were measured using the AWD assay. Two controls, one with sterile MRS and the respective enzyme (1 mg mL^{-1}), and the other one with untreated bacteriocin were included.

Heat resistance and pH stability of bacteriocin G_2

To determine the heat stability of bacteriocin G_2, aliquots of the neutralized cell-free supernatant of tested strain were heated at 40, 60 and 80 °C for 15, 30, 60 and 90 min, and immediately cooled in an ice water bath. The heat resistance was also checked after autoclaving the bacteriocin at 121 °C for 15 min. The residual bacteriocin activity was determined by the AWD assay.

To test the stability at different pH, aliquots of neutralized supernatant were adjusted to pH values from 2–12 using 4 M HCl and 4 M NaOH, respectively and subsequently incubated for 1 h at 37 °C. The residual activities were measured after neutralizing the aliquots to pH 7.

Sensitivity of bacteriocin G_2 to surfactants

To examine sensitivity of bacteriocin G_2 to surfactants, SDS, Tween 80, Triton X-100 and urea were used. Neutralized cell-free supernatant samples of tested strain were mixed with surfactants at a final concentration of 1 % (w/v) and incubated for 2 h at 37 °C. Residual

bacteriocin activities were measured using the AWD assay. The surfactants at a concentration of 1 % in neutralized MRS broth were used as controls.

Preparation of crude supernatant

Crude supernatant was prepared from 500 mL of an *L. plantarum* G_2 culture. The cells were grown to the stationary phase in MRS broth at 37 °C. The cell-free supernatant of the culture was collected by centrifugation at 4000 × *g* for 20 min at 4 °C. To concentrate the produced bacteriocin G_2 10-fold, the supernatant was filter sterilized (0.22 μm), and ultrafiltrated on 5 kDa cut-off membrane (Millipore). The obtained solution, designated crude supernatant fluid, was used for bacteriocin characterization by electrophoretic methods, *i.e.*, sodium dodecyl sulphate–polyacrylamide gel electrophoresis, SDS-PAGE, and isoelectric focusing.

Reducing and non-reducing tricine SDS PAGE

The molecular mass of bacteriocin G_2 was estimated in a tricine–SDS-PAGE, as described by Schagger and Von Jagow.[12] To test for the presence of interchain disulphide bonds between the bacteriocin subunits or intrachain disulphide bonds essential for its activity, reducing and non-reducing sample buffers for the tricine–SDS-PAGE were used.

Electrophoresis was performed in vertical gels (16.5 % acrylamide) at 30 V for 1 h, and 90 V for 5 h. To determine the apparent molecular mass of the bacteriocin after tricine–SDS-PAGE, the gel was cut into two slices. One half was fixed and stained with Coomassie Brilliant Blue. The other slice was assayed for antimicrobial activity according to Bhunia *et al.* (1987), with a slight modification.[13] The gel prepared for growth inhibition was fixed in 20 % 2-propanol and 10 % acetic acid for 5 min and washed in deionised water for 24 h. Afterwards, the gel was placed on a MRS prepared agar plate and overlaid with 20 mL of soft MRS agar seeded with *L. leishmany* (10^6 CFU mL^{-1}). After incubation of the plate for 24 h at 37 °C, the location of the zone of growth inhibition was identified and photographed. For molecular mass determination, Amersham Low-Range Rainbow Molecular Weight Markers (3500–40000 Da) were used. The protein standards molecular masses (Da) and colours were as follows: 38000, blue; 31000, orange; 24000, green; 17000, blue; 12000, red; 8500, yellow and 3500, blue.

Isoelectric focusing

Isoelectric focusing, IEF, was performed at 10 °C in a Multiphor II electrophoresis unit according to the manufacturer's instructions (Pharmacia). The isoelectric point was determined by using a broad p*I* calibration kit (p*I* 3.5–10, Pharmacia). After IEF, the gel was washed with distilled water for 30 s and cut into two slices. One slice was fixed and stained with Coomassie Brilliant Blue and the other one was assayed for antimicrobial activity by the agar overlay method described above.

RESULTS AND DISCUSSION

Spectrum of antimicrobial activity of bacteriocin G_2

To examine the effect of the bacteriocin from *L. plantarum* G_2 on other microorganisms, neutralized cell-free supernatant was tested for antimicrobial activity against Gram-positive and Gram-negative bacteria by the well diffusion agar test. As shown in Table I, the bacteriocin was active against all the tested strains of the genera *Lactobacillus*: *L. acidophilus*, *L. rhamnosus*, *L. leishmany*, *L. plan-*

tarum G_1 and *L. casei* G_3. The bacteriocin G_2 also inhibited the growth of the pathogenic bacteria *S. aureus* and *S. abony*. Bacteriocin G_2 displayed a relatively broad spectrum of antimicrobial activity as it inhibited 7 of the 14 indicator strains.

TABLE I. Inhibitory activity of neutralized cell-free supernatant of *L. plantarum* G_2 against various indicator strains, which is expressed as the diameter of the zone of inhibition

Indicator organism	Antimicrobial activity of bacteriocin G_2[a]
L. acidophilus ATCC 314	+
L. rhamnosus ATCC 7469	+
L. leishmany ATCC 7830	++
L. plantarum G_1	+
L. casei G_3	+
E. faecalis ATCC 29219	–
S. aureus ATCC 6538–P	+
P. aeruginosa ATCC 9027	–
E. coli ATCC 8739	–
Klebsiella sp. ATCC 10031	–
B. subtilis ATCC 6633	–
B. cereus ATCC 11178	–
M. luteus ATCC 93419	–
S. abony ATCC 6017	+

[a]–: No inhibition zone; +: 5 mm < zone < 10 mm; ++: 10 mm < zone < 15 mm

The inhibitory spectrum of bacteriocins produced by different species of lactobacilli varies greatly.[14] Most bacteriocins inhibit only lactobacilli or closely related Gram-positive bacteria, whereas others are active against a broad spectrum of Gram-positive and Gram-negative bacteria.[15–19]

Effect of enzymes, heat and pH on the antimicrobial activity of bacteriocin G_2

Bacteriocin G_2 was tested for its sensitivity to various enzymes. The antibacterial activity was retained after catalase treatment, indicating that antibacterial activity was not due to H_2O_2. As shown in Table II, trypsin and proteinase K were the only proteases that partially or completely inhibited the antimicrobial activity. The fact that the bacteriocin was inactivated by trypsin and proteinase K indicates its proteinaceous nature, however, despite this, the substance was rather persistent to proteolytic cleavage of pronase E and chymotrypsin. Most bacteriocins are resistant to all proteolytic enzymes, but a few of them, including nisin, plantaricin C, plantaricin D, are sensitive to the actions of some proteases.[20–24] The antimicrobial activity of bacteriocin G_2 was not affected by lipase, lysozyme or α-amylase, suggesting that its biological activity was not dependent on the presence of a lipid or sugar moiety.

Incubation of the neutralized supernatant containing bacteriocin G_2 at different temperatures for 15, 30 and 90 min showed that it was completely stable up

to 40 °C (Table III). No loss of activity was detected after 15 min at 60 °C, but inactivation occurred when the incubation was continued for a longer period. A total loss of activity was observed after incubation at 80 °C. Heat-stability is a major feature of low-molecular-weight bacteriocins; however, some bacteriocins produced by *Lactobacillus* strains were inactivated by 10- to 15-min treatment at 60–100 °C.[25,26]

TABLE II. Antimicrobial activity of bacteriocin G_2 detected after enzyme treatment, expressed as residual bacteriocin activity

Surfactant	Residual bacteriocin activity[a], %
Catalase	100
Proteinase K	40
Pronase E	100
Chymotrypsin	100
Trypsin	0
Lysozyme	100
Lipase	100
α-Amylase	100

[a]The percentage of the initial activity

The activity of bacteriocin G_2 was stable throughout the pH range 3–7 (Fig. 1). Above pH 7, the activity decreased and was completely lost at pH 10. Bacteriocins differ greatly with respect to their sensitivity to pH. Many are considerably more tolerant to acid than to alkaline pH values.[27] As most bacteriocins and bacteriocin-like substances, bacteriocin G_2 was also stable in acidic and neutral pH values, indicating that the substances are well adapted to the environment of the bacteria that produce them.[28]

TABLE III. Antimicrobial activity of bacteriocin G_2 detected after thermal treatment, expressed as residual bacteriocin activity

Treatment	Residual bacteriocin activity, %
40 °C, 15 min	100
40 °C, 30 min	100
40 °C, 60 min	100
40 °C, 90 min	100
60 °C, 15 min	100
60 °C, 30 min	0
60 °C, 60 min	0
60 °C, 90 min	0
80 °C, 15 min	0
80 °C, 30 min	0
80 °C, 60min	0
80 °C, 90 min	0
Autoclaving 121 °C, 15 min	0

To examine the hydrophobic nature of bacteriocin G_2, the neutralized supernatant was treated with surfactants at a final concentration of 1 % (w/v). The sensitivity to the surfactants is given in Table IV. Treatment with Tween 80 and urea resulted in increased antimicrobial activity. SDS and Triton X-100 had no effect on the bacteriocin activity. Many bacteriocins contain hydrophobic domains and tend to form large aggregates. The large macromolecules can be disaggregated by the use of surface-active compounds. Desegregation can result in a significant increase in bacteriocin activity.[29]

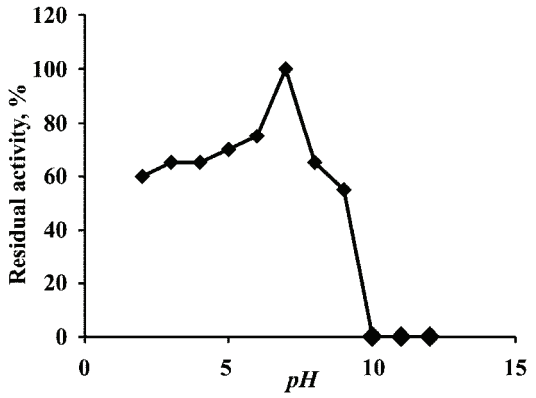

Fig. 1 Effect of pH treatment on the activity of bacteriocin G_2.

TABLE IV. Effect of surfactants on bacteriocin G_2 activity, expressed as residual bacteriocin activity

Surfactant	Residual bacteriocin activity, %	
	Treated supernatant	Surfactant control
None (control)	100	–
SDS	167	150
Tween 80	133	0
Triton X-100	117	108
Urea	117	0

Molecular mass determination

Electrophoretic analysis of the concentrated supernatant of *L. plantarum* G_2 prepared using a sample buffer containing the reducing agent 2-mercaptoethanol showed a wide protein band occupying most of the gel. The gel slice overlaid with the indicator strain revealed a single clear inhibition band, corresponding to a molecular mass of 2.2 kDa. Similar molecular masses have been reported for a few other bacteriocins, including plantaricin A.[9] A tendency of bacteriocins produced by other lactic acid bacteria to aggregate was reported, which might have contributed to the reason why the bacteriocins could not pass through a 5 kDa cut-off membrane.[30,31] Bacteriocin G_2 retained antimicrobial activity after treatment with reducing agents indicating that it does not have intramolecular disul-

phide bonds that are essential for its activity. Bacteriocin G_2 resolved in non-reducing tricine–SDS-PAGE, and subsequently overlaid with indicator strain showed a single clear band with the same molecular mass as found with the reducing gel.

*p*I *determination*

To determine the isoelelectric point of bacteriocin G_2, isoelectric focusing was performed. A single clear inhibition band was detected on the part of the gel overlaid with the indicator strain, corresponding to a p*I* value of about 10. Bacteriocin G_2 is a cationic protein, as are most bacteriocins.[10] The high isoelectric point allows bacteriocins to interact at physiological pH with the anionic surface of bacterial membranes.

CONCLUSIONS

Based on the presented results, it may be concluded that the antimicrobial substance from the culture supernatant of *L. plantarum* G_2 is a peptide with a diverse spectrum of antimicrobial activity. Stability in acidic and neutral pH range (up to pH 9), resistance to proteolytic cleavage but sensitivity to trypsin and heat stability at physiological temperatures allow bacteriocin G_2 to be a competitive advantage of *L. plantarum* G_2 probiotic preparations.

ИЗВОД

ПАРЦИЈАЛНА КАРАКТЕРИЗАЦИЈА АНТИБАКТЕРИЈСКОГ ПЕПТИДА КОЈИ ПРОИЗВОДИ ПРОБИОТСКА БАКТЕРИЈА *Lactobacillus plantarum* G_2

СВЕТЛАНА Л. ШЕАТОВИЋ[1], ЈЕЛЕНА С. ЈОВАНОВИЋ НОВАКОВИЋ[1], ГОРДАНА Н. ЗАВИШИЋ[1], ЖЕЉКА Ч. РАДУЛОВИЋ[1], МАРИЈА Ђ. ГАВРОВИЋ–ЈАНКУЛОВИЋ[2] и РАТКО М. ЈАНКОВ[2]

[1]Галеника а.д., Батајнички друм бб, 11080 Земун и [2]Хемијски факултет,Универзитет у Београду, Студентски трг 12–16, 11000 Београд

Циљ овог истраживања је била парцијална карактеризација антимикробног пептида из пробиотске бактерија *Lactobacillus plantarum* G_2 изоловане из клиничког узорка здраве особе. Антимикробно једињење из *L. plantarum* G_2, означено као бактериоцин G_2, добијено из супернатанта бактеријске културе, показало је широк спектар антимикробне активности, инхибирајући раст свих испитиванх врста рода *Lactobacillus,* као и патогених бактерија *Staphylococcus aureus* и *Salmonella abony*. Бактериоцин G_2 је осетљив на протеолитичко дејство трипсина и протеиназе K. Антимикробна активност је стабилна у опсегу 40–60 °C (15 мин), али се губи на температури од 80 °C. Установљено је да је бактериоцин стабилан на pH вредностима између 2 и 9. Дејство Tween-a 80 и урее је довело до повећане инхибиторне активности. Према IEF, бактериоцин G_2 је катјонски протеин, са p*I* вредношћу око 10, а молекуласка маса одређена на основу трицин–SDS-PAGE је 2,2 kDa. Пробиотски сој *L plantarum* G_2 продукује антимикробно једињење протеинске структуре са карактеристикама бактериоцина. Синтеза бактериоцина је једна од кључних особина пробиотских бактерија које имају клинички потенцијал као антиинфективни агенси, јер значајно повећава вероватноћу њихове *in vivo* ефикасности.

(Примљено 5. јуна, ревидирано 15. октобра 2010)

REFERENCES

1. O. Gillor, A. Etzion, M. A. Riley, *Appl. Microbiol. Biotechnol*. **81** (2008) 591
2. F. J. Carr, D. Chill, N. Maida, *Crit. Rev. Microbiol*. **28** (2002) 281
3. D. A. Eschenbach, B. L. Williams, S. J. Klebanoff, K. Young-Smith, C. M. Critchlow, K. K. Holmes, *J. Clin. Microbiol.* **27** (1989) 251
4. J. R. Tagg, K. P. Dierksen, *Trends Biotechnol.* **21** (2003) 217
5. E. L. de Souza, C. A. da Silva, C. P. de Sousa, *Braz. Arch. Biol. Technol.* **48** (2005) 503
6. M. A. Riley, J. E. Wertz, *Annu. Rev. Microbiol.* **56** (2002) 117
7. C. van Kraaij, W. M. de Vos, R. J. Siezen, O. P. Kuipers, *Nat. Prod. Rep*. **16** (1999) 575
8. O. Gillor, L. M. Nigro, M. A. Riley, *Curr. Pharm. Des.* **11** (2005) 1
9. S. D. Todorov, *Braz. J. Microbiol.* **40** (2009) 17
10. R. W. Jack, J. R. Tagg, B. Ray, *Microbiol. Rev.* **59** (1995) 171
11. A. Mayer-Harting, A. J. Hedges, R. C. W. Berkeley, *Methods Microbiol.* **7A** (1972) 315
12. H. Schägger, G. von Jagow, *Anal. Biochem.* **166 (**1987) 368
13. A. K. Bhunia, M. C. Johnson, B. Ray, *J Ind Microbiol.* **2** (1987) 319
14. S. Boris, R. Jimenez-Diaz, J. L. Caso, C. Barbes, *J. Appl. Microbiol*. **91** (2001) 328
15. A. Delgardo, D. Brito, P. Fevereiro, C. Peres, J. Figueiredo Marques, *Lait* **81** (2001) 203
16. M. Yamato, K. Ozaki, F. Ota, *Microbiol. Res.* **158** (2003)169
17. J. Chumchalova, J. Stiles, J. Josephsen, M. Plockova, *J. Appl. Microbiol*. **96** (2004) 1082
18. H .S. Chin, J. S. Shim, J. M. Kim, R. Yang, S. Yoon, *Food Sci. Biotechnol.* **10** (2001) 335
19. F V. Miteva, I. Ivanova, I. Budakova, A. Pa ntev, T. Stefanova, S. Danova, P Moncheva, V. Mitev, *J. Appl. Microbiol*. **85** (1988) 603
20. H. C. Mantovani, H. Hajigin, R. W. Worobo, J. B. Russell, *Microbiology* **148** (2005) 3347
21. L. A. Martin-Visscher, M. J. Belkum, S. Garneau-Tsodikova, R. M. Whittal, J. Zheng, L. M. McMullen, J. C. Vederas, *Appl. Environ. Microbiol.***74** (2008) 4756
22. H. Matsusaki, K. Sonomoto, A. Ishizaki, *Food Sci. Tehnol. Int. Tokyo* **4** (1998) 290
23. B. Gonzalez, P. Arca, B. Mayo, J. Suarez, *Appl. Environ. Microbiol.* **60** (1994) 2158
24. C. M. A. P. Franz, M. Du To it, N. A. Olasupo, U. Schillin ger, W. H. Hol zapfel, *Lett. Appl. Microbiol.* **26** (1998) 231
25. J. C. Oscariz, A. G. Pisarbarro, *Int. Microbiol*. **4** (2001) 13
26. V. Karthikeyan, S. W. Santosh, *Afr. J. Microbiol. Res.* **3** (2009) 233
27. M. Abdelbasset, K. Djamila, *Afr. J. Biotechnol.* **7** (2008) 2908
28. L. Navarro, M. Zarazaga, J. Saen z, F. Ruiz- Larrea, C. Torres, *J. Appl. Microbiol.* **88** (2000) 44
29. J. C. Piard, M. Desmazeaud, *Lait* **72** (1992) 113
30. A. K. Bhunia, M. C. Johnson, B. Ray, *J. Appl. Bacteriol*. **65** (1988) 261
31. T. Toba, S. K. Samant, E. Yoshioka, T. Itoh, *Lett. Appl. Microbiol*. **13** (1991) 281

Journal of the Serbian Chemical Society
JSCS-info@shd.org.rs • www.shd.org.rs/JSCS
J. Serb. Chem. Soc. 76 (5) 709–717 (2011)
JSCS–4152
UDC *Pouzolzia zeylanica*:547.56:541.515:615.27–188
Original scientific paper

Free radical-scavenging capacity, antioxidant activity and phenolic content of *Pouzolzia zeylanica*

PEIYUAN LI[1]*, LINI HUO[1], WEI SU[2]**, RUMEI LU[1], CHAOCHENG DENG[1], LIANGQUAN LIU[2], YONGKUN DENG[1], NANA GUO[2], CHENGSHENG LU[1] and CHUNLING HE[1]

[1]*College of Pharmacy, Guangxi Traditional Chinese Medical University, Nanning 530001, and* [2]*College of Chemistry and Life Science, Guangxi Teachers Education University, Nanning 530001, P. R. China*

(Received 18 August, revised 1 November 2010)

Abstract: *Pouzolzia zeylanica* was extracted with different solvents (acetone, ethyl acetate and petroleum ether), using different protocols (cold-extraction and Soxhlet extraction). To evaluate the antiradical and antioxidant abilities of the extracts, four *in vitro* test systems were employed, *i.e.*, DPPH, ABTS and hydroxyl radical scavenging assays and a reducing power assay. All extracts exhibited outstanding antioxidant activities that were superior to that of butylated hydroxytoluene. The ethyl acetate extracts exhibited the most significant antioxidant activities, and cold-extraction under stirring seemed to be the more efficacious method for acquiring the predominant antioxidants. Furthermore, the antioxidant activities and total phenolic (TP) content of different extracts followed the same order, *i.e.*, there is a good correlation between antioxidant activities and TP content. The results showed that these extracts, especially the ethyl acetate extracts, could be considered as natural antioxidants and may be useful for curing diseases arising from oxidative deterioration.

Keywords: total phenolic content; DPPH; ABTS; hydroxyl radical; reducing power; *Pouzolzia zeylanica*.

INTRODUCTION

Free radicals, which are generated in several biochemical reactions in the body, have been implicated as mediators of many diseases, including cancer, atherosclerosis and heart diseases.[1–3] Although these free radicals can be scavenged by the *in vivo* produced antioxidant compounds, the endogenous antioxidants are insufficient to completely remove them and maintain a balance. As a result, dietary antioxidants are required to counteract excess free radicals.[4–7]

Corresponding authors. E-mail: *lipearpear@yahoo.cn; **aaasuwei@yahoo.com.cn
doi: 10.2298/JSC100818063L

Synthetic antioxidants, such as butylated hydroxytoluene (BHT) and butylated hydroxyanisole (BHA), which are effective in their role as antioxidants, are commercially available and currently used in industrial processes. However, since suspected actions as promoters of carcinogenesis and other side effects have been reported, their use in food, cosmetic and pharmaceutical products has been decreasing.[8–12]. Thus, there has been an upsurge of interest in naturally-occurring antioxidants from vegetables, fruits, leaves, oilseeds, cereal crops, tree barks, roots, spices and herbs [13–16].

Pouzolzia zeylanica (L.) Benn. is a perennial herbaceous plant belonging to the Urticaceae family.[17] It is used as a remedy for diarrhea, indigestion, infantile malnutrition, urination difficulties and injuries from falls. Moreover, it is especially useful in conditions such as acute mastitis and pyogenic infections.[2,3] However, no chemical and biochemical information concerning *P. zeylanica* has been reported.

In the present study, the antiradical and antioxidant activities of the whole plant of *P. zeylanica* in four *in vitro* models, including DPPH, ABTS and hydroxyl radical scavenging assays and the reducing power assay, were investigated The total phenolic (TP) content and the relationships between the TP content and antioxidant activities were also investigated.

EXPERIMENTAL

Sample and reagents

Pouzolzia zeylanica whole plant was collected during the summer of 2009 in the Guangxi province, China. A voucher specimen was identified by Dr. Songji Wei at the Department of Zhuang Pharmacy, Guangxi Traditional Chinese Medical University. 2,2'-Azinobis(3--ethylbenzothiazoline-6-sulfonic acid) diammonium salt (ABTS) and butylated hydroxytoluene (BHT) were purchased from Sigma Aldrich, St. Louis, USA. 1,1-Diphenyl-2-picrylhydrazyl (DPPH) (purity 98 %) was purchased from Wako Chemicals, Japan. Gallic acid standard was purchased from J & K Scientific Ltd., Beijing, China. Other chemicals were obtained from the China National Medicine Group Shanghai Corporation, Shanghai, China. All employed chemicals and solvents were of analytical grade.

Preparation of extracts

The extraction of *Pouzolzia zeylanica* was performed using two different methods: *i*) cold-extraction under magnetic stirring and *ii*) Soxhlet extraction. For each extraction method, three different solvents were used: acetone, ethyl acetate and petroleum ether (boiling point range 60–90 °C).

Cold-extraction under stirring. Fifty grams of air-dried plant material was extracted with 500 mL of the individual solvents under constant stirring. The filtrate was collected three times at 48 h intervals during a total extraction period of 144 h. The acetone extract (CAE), ethyl acetate extract (CEE) and petroleum ether extract (CPE) were obtained by concentrating the extract liquid under reduced pressure at 40 °C using a vacuum rotary evaporator and the dry extracts were stored at –20 °C until use.

Soxhlet extraction. Ten grams of *P. zeylanica* material was extracted with 100 mL of the individual solvents using a Soxhlet apparatus for 7 h. The extract liquid was then concentrated

in a vacuum rotary evaporator at 40 °C and the obtained dry extracts (SAE, SEE and SPE) were stored at –20 °C until use.

Determination of total phenolic content

Total phenolic (*TP*) concentration in the extracts was determined using Folin–Ciocalteu reagent (FCR), according to the method of Kumar *et al.*[18] with slight modification. Gallic acid was used as a standard. Briefly, the solution of each extract (0.5 mL, 1 mg mL^{-1}) was diluted to 10 mL with distilled water in a volumetric flask. FCR (1 mL) was added and mixed thoroughly, and then sodium carbonate solution (3 mL, 2 %) was added. The absorbance at 760 nm was measured after 2 h. The total phenolic content was determined by comparison with the standard calibration curve of gallic acid, and results are presented as micrograms of gallic acid equivalents (mg of GAE) per gram dry weight (g DW). All tests were conducted in triplicate.

DPPH radical scavenging assay

Plant extracts were tested for the scavenging effect on DPPH radical according to the method of Pan *et al.*[19] 0.2 mL of extract solution in ethanol (95 %) at different concentrations (0.2, 0.5, 0.8 and 1.2 mg mL^{-1}) was added to 8 mL of 0.004 % (w/v) stock solution of DPPH in ethanol (95 %). The scavenging activity on the DPPH radical was determined by measuring the absorbance at 517 nm until the reaction reached the steady state, using a UV–Visible TV--1901 spectrophotometer (Beijing Purkinje General Instrument Co. Ltd., China). As a positive control, synthetic antioxidant BHT was used. All determinations were performed in triplicate. The DPPH radical scavenging activity (*S%*) was calculated using the following equation: $S\% = ((A_{control} - A_{sample})/A_{control})\times 100$, where $A_{control}$ is the absorbance of the blank control (containing all reagents except the extract solution) and A_{sample} is the absorbance of the test sample.

ABTS radical scavenging assay

The antioxidant capacity was estimated in terms of the $ABTS^{\bullet+}$ radical scavenging activity following the procedure described by Delgado-Andrade *et al.*[20] Briefly, $ABTS^{\bullet+}$ was obtained by reacting 7 mM ABTS stock solution with 2.45 mM potassium persulfate and the mixture was left to stand in the dark at room temperature for 12–16 h before use. The $ABTS^{\bullet+}$ solution (stable for 2 days) was diluted with 5 mM phosphate-buffered saline (pH 7.4) to an absorbance at 730 nm of 0.70±0.02. After the addition of 10 μL of sample to 4 mL of diluted $ABTS^{\bullet+}$ solution, the absorbance was measured at 30 min. All samples were analyzed in triplicate. The $ABTS^{\bullet+}$ radical-scavenging activity of the samples was expressed as $S\% = ((A_{control} - A_{sample})/A_{control}))\times 100$, where $A_{control}$ is the absorbance of the blank control ($ABTS^{\bullet+}$ solution without test sample) and A_{sample} is the absorbance of the test sample.

Hydroxyl radical scavenging activity

The hydroxyl radical scavenging activity was determined according to the method of Beara *et al.*[21] with some modification. 2 mL of extract solution (0.2, 0.5, 0.8 and 1.2 mg mL^{-1}), 1.0 mL of *ortho*-phenanthroline (7.5 mmol L^{-1}), 5.0 mL of phosphate buffer (0.2 M, pH 6.6), 1.0 mL of ferrous sulfate (7.5 mmol L^{-1}) and 1.0 mL of H_2O_2 (0.1 %) were mixed and diluted to 25 mL with distilled water. After incubation at room temperature for 30 min, the absorbance was measured at 510 nm. The scavenging percentage (*P%*) was calculated as $P\% = ((A - A_1)/(A_2 - A_1))\times 100$, where A, A_1 and A_2 are the absorbance value of the system with all solution including H_2O_2 and the extract solution, the system without extract solution, and the system without H_2O_2 and the extract solution, respectively.

Measurement of the reducing power

The reducing power was determined as described by Gulcin.[7] Briefly, 120 µL of extract solution at different concentrations was mixed with 2.5 mL of phosphate buffer (0.2 M, pH 7.4) and 2.5 mL of potassium ferricyanide (1 %). After the mixture had been incubated at 50 °C for 20 min, 2.5 mL of trichloroacetic acid (10 %, w/v) was added, and the mixture was then centrifuged at 3000 rpm for 10 min. A 2.5 mL aliquot of the supernatant was mixed with 2.5 mL of distilled water and 0.5 mL of ferric chloride (0.1 %), and then the absorbance was measured at 700 nm. The higher the absorbance value the stronger is the reducing power. All measurements were made in triplicate.

Statistical analysis

All tests were conducted in triplicate. The results are expressed as means±*SD*. Analysis of variance and significant differences among the means were tested by the one-way ANOVA, using SPSS (Version 13.0 for Windows, SPSS Inc., Chicago, IL). Values of $P < 0.05$ were regarded as significant.

RESULTS AND DISCUSSION

Total phenolic (TP) content

It is well known that phenolic compounds are potential antioxidants and free radical-scavengers; hence, there should be a close correlation between the content of phenolic compounds and antioxidant activity.[18] In the present study, the TP content of various solvent extracts from *Pouzolzia zeylanica* was investigated. The results are given in Table I ($P<0.01$). The TP content varied in the different extracts and ranged from 38.9 to 90.5 mg GAE g^{-1} DW. The extract with the highest TP content was CEE (90.5 mg GAE g^{-1} DW), followed by SEE (81.2 mg GAE g^{-1} DW), indicating that CEE might have the most outstanding antioxidant activity. The TP contents were in the following order: CEE > SEE > CAE > SAE > CPE > SPE.

TABLE I. TP content of various extracts from *Pouzolzia zeylanica*. Results are the mean±*SD* of three parallel measurements. The values bearing different letters are very significantly different ($P < 0.01$)

Sample	Total phenolics, mg GAE g^{-1} DW
CAE	73.6±0.16^{c}
SAE	69.2±0.25^{d}
CEE	90.5±0.28^{a}
SEE	81.2±0.32^{b}
CPE	39.4±0.20^{e}
SPE	38.9±0.13^{e}

DPPH radical scavenging activity

DPPH has been widely used for free radical-scavenging assessments due to its ease and convenience. In the present study, all extracts were found to be effective scavengers against DPPH radical. They were superior to BHT and their activities increased in a concentration dependent manner (Fig. 1). The ethyl ace-

tate extracts showed the highest DPPH radical scavenging activity, while the weakest scavengers were the petroleum ether extracts. On the other hand, the extracts obtained by cold-extraction exhibited stronger DPPH radical scavenging ability than the corresponding extracts obtained by Soxhlet extraction. For instance, CEE possessed a scavenging capacity of 64.9 % on the DPPH radical, whereas that of SEE was only 55.9 %.

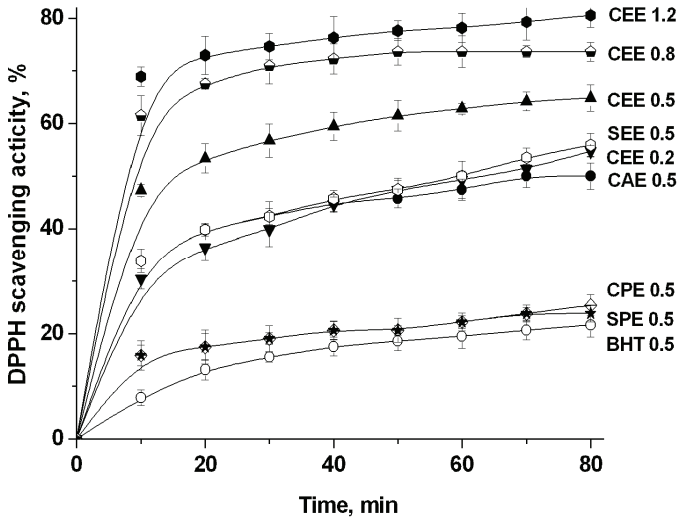

Fig. 1. DPPH radical scavenging activity of the various solvent extracts from *Pouzolzia zeylanica* compared with BHT. The values are the mean ± *SD* of three parallel measurements. The values are significantly different ($P < 0.05$) when compared to the control.

ABTS radical scavenging activity

The scavenging capacities of the various extracts for the ABTS radical were measured and compared (Fig. 2). As can be seen, the scavenging effect of all extracts increased with increasing concentration. As in the case of DPPH radical scavenging, CEE exhibited the highest ABTS antiradical properties, followed by CAE with an inhibition of 50.3 % for the ABTS radical at 1.2 mg mL^{-1}. In addition, SEE possessed a strong scavenging capacity for the ABTS radical, which was a little lower than that of CEE. The order of ABTS radical scavenging activity of all extracts was similar to that observed for DPPH. The differences in the ABTS scavenging activities exhibited by the various extracts indicated that the extracting solvent and extraction method influenced the antioxidant ability of the extracts.

Hydroxyl radical scavenging activity

The hydroxyl radical scavenging activity of the various extracts was investigated (Fig. 3). All extracts exhibited strong concentration-dependent scavenging

abilities for the hydroxyl radical. CEE was found to be the most powerful scavenger of the hydroxyl radical, with an inhibition of up to 90.5 % at a concentration of 1.2 mg mL^{-1}. It is worth mentioning that CEE showed an inhibition of 10.9 % at a concentration as low as 0.2 mg mL^{-1}. The weakest scavenger was found to be SPE, the inhibition of which, however, reached 52.3 % at 1.2 mg mL^{-1}. The results showed that the extracts obtained by both cold-extraction and by Soxhlet extraction had excellent scavenging activities for the hydroxyl radical. Furthermore, the order of antiradical ability for the hydroxyl radical was similar to those for ABTS and DPPH radicals and the TP content.

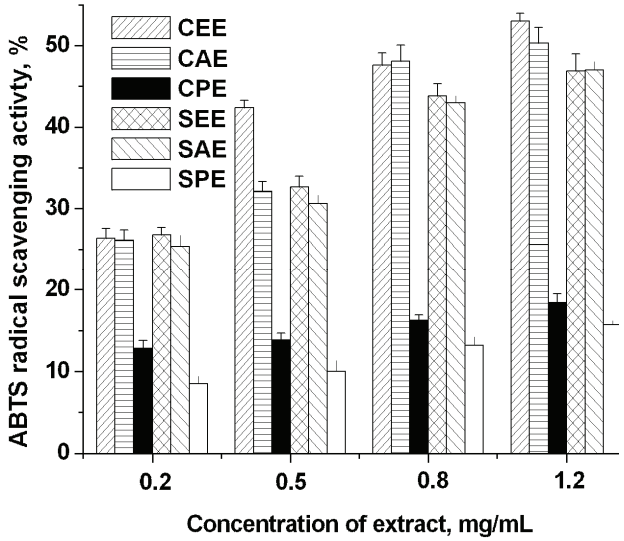

Fig. 2. ABTS radical scavenging activity of the various solvent extracts from *Pouzolzia zeylanica*. The values are the mean±*SD* of three parallel measurements. The values are significantly different ($P < 0.05$) when compared to the control.

Reducing power

The reducing powers of the various solvent extracts from *Pouzolzia zeylanica* are shown in Fig. 4. Different extracts exhibited different degrees of electron donating capacities in a concentration-dependent manner, whereby CEE was the most outstanding at the various concentrations. The reducing capacities at 700 nm for CEE, CAE, CPE and SEE were 1.14, 0.72 0.38 and 0.93, respectively. Therefore, reducing power order was: CEE > SEE > CAE > CPE. The trend in reducing power of the various solvent extracts from *Pouzolzia zeylanica* was similar to that observed for DPPH, ABTS, hydroxyl radical scavenging activities and the content of TP, indicating that there is a correlation between the TP content and the antioxidant activities of the various solvent extracts from *Pouzolzia zeylanica.*

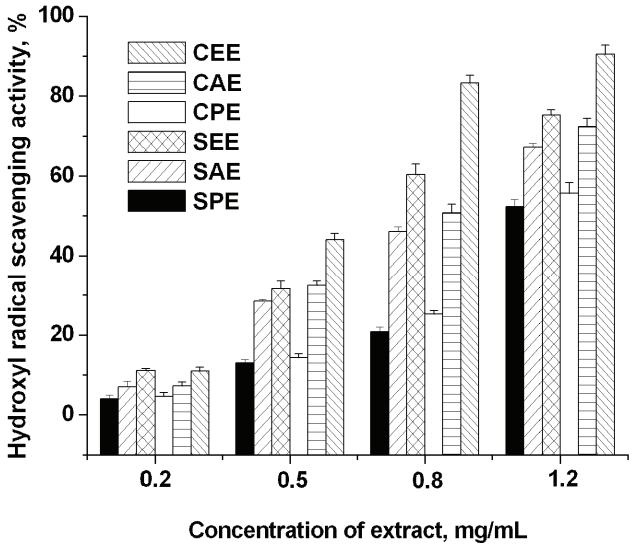

Fig. 3. Hydroxyl radical scavenging activity of the various solvent extracts from *Pouzolzia zeylanica*. The values are the mean±*SD* of three parallel measurements. The values are significantly different ($P < 0.05$) when compared to the control.

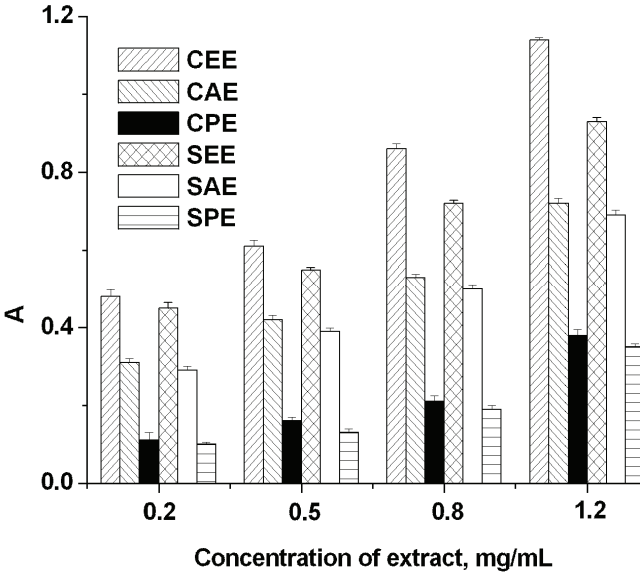

Fig. 4. Reducing power of the various solvent extracts from *Pouzolzia zeylanica*. The values are the mean±*SD* of three parallel measurements. The values are significantly different ($P < 0.05$) when compared to the control.

CONCLUSIONS

In the present investigation, extracts of *Pouzolzia zeylanica* exhibited outstanding scavenging effects on DPPH, ABTS and hydroxyl radicals, and pronounced reducing powers. It is one of the few members of the Urticaceae family which have been investigated for their antioxidant activities and showed a high antioxidant capacity compared to the intensive research of members of other families, such as Lamiaceae, Asteraceae, Fabaceae, Geraniaceae and Rosaceae. CEE proved to be the most efficient extract and was superior to butylated hydroxytoluene. It contained the highest total phenolic content (TP) of 90.5 mg g^{-1} DW, expressed as the gallic acid standard (determined by the Folin-Ciocalteu method). The TP content and antioxidant activities in both tested systems of different extracts followed the same order: CEE > SEE > CAE > SAE > CPE > SPE, showing there were significant correlations between the antioxidant activities and the TP content of *Pouzolzia zeylanica*. The results indicated that all extracts from *P. zeylanica*, obtained by cold-extraction under stirring or Soxhlet extraction, contained phenolic compounds and exhibited excellent antioxidant activities. However, cold-extraction under stirring seemed to be the more efficacious method of acquiring antioxidants exhibiting capacities. Since this investigation is a preliminary study, a detailed study of the antioxidant mechanisms of specific phenolic components is an absolute necessity, and is in progress. Nevertheless, based on the above presented results, various solvent extracts of *P. zeylanica*, especially the CEE extract, could be investigated as a possible new source of natural antioxidants in the food, nutraceuticals and cosmetic industry.

Acknowledgements. The authors thank the National Natural Science Foundation of China (Grant No. 20961001), the Key Project of the Chinese Ministry of Education. (Grant No. 2010168), the Guangxi Natural Science Foundation (Grant No. 2010GXNSFB013014), the Scientific Research Fund of Guangxi Provincial Education Department (Grant No. 200911MS146) for financial support.

ИЗВОД

КАПАЦИТЕТ УКЛАЊАЊА СЛОБОДНИХ РАДИКАЛА, АНТИОКСИДАТИВНА АКТИВНОСТ И САДРЖАЈ ФЕНОЛА У *Pouzolzia zeylanica*

PEIYUAN LI[1], LINI HUO[1], WEI SU[2], RUMEI LU[1], CHAOCHENG DENG[1], LIANGQUAN LIU[2], YONGKUN DENG[1], NANA GUO[2], CHENGSHENG LU[1] и CHUNLING HE[1]

[1]*College of Pharmacy, Guangxi Traditional Chinese Medical University и* [2]*College of Chemistry and Life Science, Guangxi Teachers Education University, Nanning, China*

Састојци *Pouzolzia zeylanica* су екстраховани различитим растварачима (ацетон, етил-ацетат, петролетар) применом две методе (хладна екстракција и Сокслетовом апаратуром). За процену антирадикалске и антиоксидативне способности екстраката коришћена су четири *in vitro* система: DPPH, ABTS, тест уклањања хидроксилних радикала и тест одређивања редукционе способности. Сви екстракти су испољили изузетну антиоксидативну активност, која је била већа и од активности бутилованог хидрокси-толуена. Екстракти у етил-ацетату

су имали највећу антиоксидативну активност, а метода хладне екстракције уз мешање је била најефикаснија за изоловање антиоксиданаса. Антиоксидативна активност је била у директној корелацији са укупним фенолним садржајем екстраката. Резултати су показали да ови екстракти, а нарочито етил-ацетатни, могу послужити као извор природних антиоксиданаса који се могу користити за терапију обољења насталих као последица оксидативних реакција у организму.

(Примљено 18. августа, ревидирано 1. новембра 2010)

REFERENCES

1. M. M. Al-Dabbas, T. Suganuma, K. Kitahara, D. X Hou, M. Fujii, *J Ethnopharmacol.* **108** (2006) 287
2. R. Tsao, Z. Deng, *J. Chromatogr. B* **812** (2004) 85
3. E. Hayet, M. Maha, A. Samia, M. Mata, P. Gros, H. Raida, M. M. Ali, A. S. Mohamed, L. Gutmann, Z. Mighri, A. Mahjoub, *World J. Microbiol. Biotechnol.* **24** (2008) 2933
4. Y. Y. Lim, J. Murtijaya, *LWT-Food Sci. Technol.* **40** (2007) 1664
5. A. Scalbert, C. Manach, C. Morand, C. Remesy, *Crit. Rev. Food Sci. Nutr.* **45** (2005) 287
6. K. Wang, Y. Pan, H. Wang, Y. Zhang, Q. Lei, Z. Zhu, H. Li, M. Liang, *Med. Chem. Res.* **19** (2010) 166
7. I. Gulcin, R. Elias, A. Gepdiremen, K. Taoubi, E. Koksal, *Wood Sci. Technol.* **43** (2009) 195
8. M. Namiki, *Crit. Rev. Food Sci.* **29** (1990) 273
9. O. Politeo, M. Jukic, M. Milos, *Food Chem.* **101** (2007) 379
10. B. Tepe, D. Daferera, A. Sokmen, M. Sokmen, M. Polissiou, *Food Chem.* **90** (2005) 333
11. C. S. Ku, S. P. Mun. *Bioresour. Technol.* **99** (2007) 2852
12. I. Gulcin, M. E. Buy ukokuroglu, M. Oktay, O. I. Kufrevio glu, *J. Ethnopharmacol.* **86** (2003) 51
13. T. M. Rababah, N. S. Hettiarachy, R. Horax, *J. Agric. Food Chem.* **52** (2004) 5183
14. N. Gámez-Meza, J. A. Norieg a-Rodríguez, L. Ley va-Carrillo, J. Ortega-García, L. Bringas-Alvarado, H. S. García, L. A. Medina-Juárez, *J. Food Process. Pres.* **33** (2009) 110
15. G. Jiang, Y. Jiang, B. Yang, C. Yu, R. Tsao, H. Zhang, F. Chen, *J. Agric. Food. Chem.* **57** (2009) 9293
16. M. Terashima, I. Nakatani, A. Harima, S. Nakamura, M. Shiiba, *J. Agric. Food. Chem.* **55** (2007) 165
17. Z. Wu, D. Hong, *Flora of China*, Vol. 5, Science Press, Beijing, China, 2003, p. 175
18. K. S. Kumar, K. Ganesan, P. V. Subba Rao, *Food Chem.* **107** (2008) 289
19. Y. Pan, K. Wang, S. Huang, H. Wang, X. Mu, C. He, X. Ji, J. Zhang, F. Huang, *Food Chem.* **106** (2008) 1264
20. C. Delgado-Andrade, J. A. Ru fián-Henares, F. J. Morale s, *J. Agric. Food Chem.* **53** (2005) 7832
21. I. N. Beara, M. M. Lesjak, E. D. Jovin, K. J. Balog, G. T. Anackov, D. Z. Orcić, N. M. Mimica-Dukić. *J. Agric. Food Chem.* **57** (2009) 9268.

Journal of the Serbian Chemical Society
JSCS-info@shd.org.rs • www.shd.org.rs/JSCS
J. Serb. Chem. Soc. 76 (5) 719–731 (2011)
JSCS–4153
UDC 546.562+546.732:547.586.2
Original scientific paper

New Cu(II) and Co(II) octaazamacrocyclic complexes with 2-amino-3-phenylpropanoic acid

GORDANA VUČKOVIĆ[1*#], MIRJANA ANTONIJEVIĆ-NIKOLIĆ[2#], SLAĐANA B. TANASKOVIĆ[3#] and VUKOSAVA ŽIVKOVIĆ-RADOVANOVIĆ[1#]

[1]Faculty of Chemistry, University of Belgrade, P.O. Box 118, 11158 Belgrade, [2]Higher Technological School of Professional Studies, 15000 Šabac and [3]Faculty of Pharmacy, Vojvode Stepe 450, 11000 Belgrade, Serbia

(Received 1 December 2010, revised 27 January 2011)

Abstract: New cationic Cu(II) and Co(II) complexes with *N*,*N*',*N*'',*N*'''-tetrakis(2-pyridylmethyl)-1,4,8,11-tetraazacyclotetradecane (tpmc) and the anion of 2-amino-3-phenylpropanoic acid (*S*-phenylalanine) were prepared. The complexes were analyzed and characterized by elemental analysis, conductometric, polarimetric, magnetic and cyclic voltammetric measurements, as well as by spectroscopic data (UV/Vis, IR). Both complexes are binuclear with the general formula $[M_2(S\text{-Phe})tpmc](ClO_4)_3 \cdot nH_2O$; *S*-PheH = *S*-phenylalanine, M(II) = Cu, n = 7; Co, n = 0. Based on previously reported data for some familiar complexes and the present results, pentacoordinated geometry was proposed. Both of the central metal ions are coordinated with two pyridyl and two cyclam nitrogens and bridged with $–N–(CH_2)_3–N–$ portions of the cyclam ring and oxygen atoms of the *S*-phenylalaninate ion. Antimicrobial screening of the complexes, solvent, starting salts and ligands alone was performed against fungi, mould and some bacteria. In certain cases, enhanced activity of Co(II) complex towards bacteria compared with the relevant free ligands and starting salts was detected.

Keywords: Cu(II) and Co(II) complexes; pendant octaazamacrocycle; *S*-phenylalanine.

INTRODUCTION

Metal aminocarboxylate complexes have been the subject of extensive research for many years. They are used to study phenomenon of the structure, stability, magnetic properties and non-covalent interactions important in chemical reactions, molecular recognition and regulation of biochemical processes, for a better understanding of enzyme–metal ion–substrate complexes, which play an

* Corresponding author. E-mail: gordanav@chem.bg.ac.rs
# Serbian Chemical Society member.
doi: 10.2298/JSC101201062V

important role in metalloenzyme-catalysed biochemical reactions.[1–13] The antimicrobial activity of such types of complexes was also the subject of some investigations.[11,13] Mixed-ligand mononuclear complexes of Cu(II) and Co(II)/(III) with *S*-/*R*-phenylalanine and *N*-donor ligands: 2,2'-bipyridyl, 1,10-phenantroline, imidazole, *N*,*N*'-diethylethylenediamine-*N*,*N*'-di-α-butyrato dianion, 3,3',4,5,5'--pentamethyl-4'-ethyl-2,2'-dipyrrolyl-methene were prepared and described.[6–10] The aminocarboxylato ligands in these complexes are bidentate chelates connected to the metal ions *via* the carboxylate oxygen and the amino group, *N*,*O* mode. In Co(III) complexes with *N*,*N*-bis(carboxymethyl)-*S*-phenylalanine including as the secondary ligand aliphatic or aromatic aminocarboxylates *S*-/*R*-phenylalanine/*S*-tryptophan, NH–π interaction was observed as an important factor for molecular recognition and stabilisation of their crystal molecular structures.[7] In the same paper, this interaction was also studied in solution for Co(III) ternary complexes with *N*,*N*-bis(carboxymethyl)-*S*-phenylalanine or nitrilotriacetic acid including one of the following amino acids / derivatives: glycine, *S*-proline/phenylglycine/alanine/leucine/4-methylphenylalanine/tyrosine or *S*,*R*-chlorophenyl--alanine. Bis(aminocarboxylato) square-planar Cu(II) complexes of *N*,*O*-bonded *S*-methionine/phenylalanine/tryptophan were isolated and investigated by thermal and spectroscopic (UV/Vis, IR, EPR) methods.[10] In the complexes of transition metal ions with *N*-substituted *S*-phenylalanine the COO^- group is coordinated to Co(II) and Cd(II) as bidentate *O*,*O*'- (thus forming chelate rings) or to Zn(II) as *O*-monodentate.[11]The formation of pentanuclear Cu(II) complexes with *S*-phenylalanine/tryptophanhydroxamic acid was also studied in solution and the structure was predicted using a combined potentiometric, spectrophotometric, CD and ESI–MS study and X-ray data of similar species of β-alaninehydroxamic acid.[12] Mononuclear complexes of divalent Co, Cu, Ni and Zn with amino acid-derived compounds were also described.[13]

On the other hand, polyazamacrocyclic ligands and their metal complexes are an attractive field of investigation due to their numerous unusual structural, spectral, redox and biological properties and possible applications as catalysts, new magnetic materials, ion selective potentiometric sensors, antimicrobial or agents for nucleic acid cleavage.[14–23]

In previous papers, a series of binuclear Co(II) complexes with pendant arm octaazamacrocycle *N*,*N*',*N*'',*N*'''-tetrakis(2-pyridylmethyl)-1,4,8,11-tetraazacyclotetradecane (tpmc) and an additional aliphatic α-/β-aminocarboxylate having linear or branched chain (glycine, *S*-alanine, *S*-aminobutyric/α-aminoisobutyric/β-aminobutyric/β-aminoisobutyric acid, *S*-norvaline/*S*-valine), or *N*-methyl glycine derivatives (*N*-methyl/*N*,*N*-dimethylglycine), were described. The general formula was $[Co_2(A)tpmc]B_3$; A^- = anion of the corresponding amino acid/derivative, $B = ClO_4^-/BF_4^-$. It is supposed that the A ligands are coordinated with Co(II) *via* the COO^- group in bridged[17–19] or a combined chelate-bridged

mode,[19] whereas the $–NH_2$ group remains uncoordinated. Metal centres are also bridged with $N–(CH_2)_3–N$ fragments of the cyclam ring.

The aim of the present study was the preparation, characterization and antimicrobial testing of Co(II)/Cu(II) tpmc complexes with *S*-phenylalanine, as a representative of aromatic amino acids and the comparison of the results with data for the related described complexes containing aliphatic amino acids or aliphatic/aromatic carboxylates.[16–22]

EXPERIMENTAL

Metal–organic perchlorate salts must be handled with caution! Since they contain both oxidizing and reducing groups and metal ions are sometimes effective catalysts, serious explosions are possible! Use only the absolute minimum of material required and never heat more than a few crystals!

Preparation

$Cu(ClO_4)_2·6H_2O$,[24] $Co(ClO_4)_2·6H_2O$,[25] tpmc[26] and $[Cu_2tpmc](ClO_4)_4$[27] were prepared and purified by the procedures described elsewhere. All other chemicals, as *p.a.* commercial products, were used as received.

$[Cu_2$(S-Phe)tpmc$](ClO_4)_3·7H_2O$ (1)

$[Cu_2tpmc](ClO_4)_4$ (50 mg; 0.046 mmol) was dissolved in 5 mL of 4:1 mixture CH_3CN–$–H_2O$ (v/v). To this solution, *S*-phenylalanine (15 mg; 0.091 mmol) dissolved in 4 mL of 1:1 mixture $CH_3CN–H_2O$, (v/v) previously neutralized with NaOH (0.1 mol L^{-1}) to pH ≈ 7.0 (controlled with pH strips 6.4–8.0) was slowly added. The colour gradually changed from blue–violet to blue. The reaction mixture was refluxed and stirred at ≈ 80 °C for the following 3 h, then concentrated to 1/3 of its initial volume on a water bath. It was allowed to cool to room temperature, covered with parafilm and left in a refrigerator undisturbed to crystallize slowly. The blue precipitate was vacuum-filtered, washed with small portions of cold CH_3CN and deionised water and air-dried. The product was then powered and recrystallized from deionised water. The blue microcrystalline product was removed by suction, washed with small portions of deionised water and left in a desiccator over silica gel. The product was stable to open air. Decomposition occurred at ≈190 °C (checked with a hot plate equipped with a microscope). Yield: 70 %.

/Co_2(S-Phe)tpmc$](ClO_4)_3$ (2)

$Co(ClO_4)_2·6H_2O$ (260 mg, 0.709 mmol) and tpmc (200 mg, 0.355 mmol) were dissolved in a minimum volume of CH_3CN. The mixture was warmed on a water bath to 80 ° C and stirred. An aqueous solution of *S*-phenylalanine (72 mg; 0.355 mmol) previously neutralized with NaOH (0.1 mol L^{-1}) to pH ≈ 7.0 (controlled with pH strips 6.4–8.0) was gradually added dropwise to the first solution. The reaction mixture was refluxed with stirring for 2.5 h (at 80 °C). The obtained brownish–purple solution was evaporated on a water bath to 1/2 of its initial volume. It was left in a refrigerator well closed overnight, whereby a dark purple precipitate contaminated with a small amount of violet side-product $[Co_2(OH)tpmc](ClO_4)_3$ appeared. The precipitate was removed by suction, dried, recrystallized from CH_3CN and washed properly with small portions of cold CH_3OH. This procedure was repeated until a pure purple microcrystalline compound was obtained, which was dried and stored in a dessicator over silica gel. The compound was stable in the solid state to open air at room temperature and on

heating to 200 °C, but on prolonged standing of its solution, dark brown $Co(OH)_3$ formed. Yield: 63 %.

Analytical methods and applied instruments

Elemental analyses were performed by standard methods in the Centre for Instrumental Analyses, ICTM, Belgrade. The Cu content in complex **1** was determined by atomic absorption spectrophotometry using a Perkin-Elmer AAS-5100/PC instrument. The electronic absorption spectra of the complexes in CH_3CN/DMF solutions (1.0×10^{-3} mol L^{-1}) were recorded on a GBC UV/Vis Cintra 20 spectrophotometer. The reflectance spectrum of complex **2** was recorded on a CARY 17D spectrophotometer using MgO as the standard. The position of the broad maxima were corrected using the Kubelka–Munks function.[28] Magnetic susceptibility measurements were realised at room temperature (20±2 °C) using an MSB-MKI balance calibrated with $Hg[Co(SCN)_4]$ (Sherwood Scientific Ltd., England). The data were corrected for diamagnetic susceptibilities using Pascal constants.[29] The IR spectra were run on a Nicolet 6700 FTIR spectrometer (ATR technique) in the range 400–4000 cm^{-1}. Molar electrical conductivities in CH_3CN/DMF (1.0×10^{-3} mol L^{-1}) were measured at room temperature on a Hanna instruments HI 8820N conductometer. The optical rotation for the complexes and *S*-phenylalanine alone were measured at 589 nm at ambient temperature (20±2 °C) using a tube of 1 dm on a Rudolf Research Analytical Autopol IV automatic polarimeter (c = 2.2×10^{-4} for complex **1**, 2.4×10^{-4} for **2** and 2.4×10^{-3} mol L^{-1} for *S*-phenylalanine). Electrochemical measurements on complex **1** were performed using electronic equipment Metrohm 797 VC Computrace in a standard three-electrode cell: a Pt disc as the working electrode, standard Ag/AgCl as the reference electrode and Pt as the auxiliary one. Measurements were performed in 10 mL of CH_3CN. The concentration of complex **1** was 1.0×10^{-4} mol L^{-1}. Cyclic voltammetry (CV) was performed with sweep rates of 50, 100 and 200 mV s^{-1} in the potential range from –1 to 1 V *vs.* Ag/AgCl. Electrochemical measurements on complex **2** were also performed in a standard three-electrode cell but with a glassy carbon (GC) as the working electrode, saturated calomel (SCE) as a reference and Pt as the auxiliary electrode. The measurements were realised in 100 mL of a mixture of CH_3CN: aqueous NaOH (1.0 mol L^{-1}) solution (3:7, v/v). CV was performed by changing the potential in the range from –0.5 to 0.4 V *vs.* SCE at a sweep rate of 100 mV s^{-1}. The change in the potential was achieved using a sweep generator, EDT Research, the impulses of which were brought to a potentiostat, Bruker Potentio-Galvanostat EI30. An *XY* plotter, Hewlett Packard 7015 X–Y, was used. All measurements were performed at room temperature (20±2 °C). Oxygen was removed from the system by continuous bubbling with oxygen-free N_2.

For the preliminary antimicrobial test, the agar well diffusion method was applied.[30] The screening was performed against the following 6 cultures of microorganisms: the Gram-(+) bacteria *Micrococcus lysodeikticus* ATCC 4698 and *Staphylococcus aureus* ATCC 25923, the Gram-(+) bacterium forming spores, *Bacillus subtilis* ATCC 6633, the Gram -(–) bacterium *Escherichia coli* ATCC 25922, the fungi *Candida albicans* ATCC 24433 and the mould *Aspergillus niger* ATCC 12066. Nutrition (cultivation) medium was Mueller–Hinton agar for the bacteria and Sabouraud dextrose agar for the fungi. The incubation temperature was 37 °C for the bacteria and 28 °C for the fungi. The solvents: CH_3CN, DMSO and CH_3OH, ligands *S*-PheH in CH_3OH and a suspension of tpmc in CH_3CN, aqueous solutions of $Co(ClO_4)_2\cdot6H_2O$ and $Cu(ClO_4)_2\cdot6H_2O$ and the complexes **1** and **2** in DMSO (1.0 mg mL^{-1}) were tested separately. In the holes of agar plates (Ø 0.8 cm), 100 µL of each compound solution were applied. Neither of the complexes showed antifungal activity. The antibacterial activities of complexes **1** and **2** were quantified by the dilution method in agar (the minimum inhibition con-

centration was determined, *MIC*).[31,32] The initial concentration of the complexes was 8 mg mL^{-1} in DMSO. This solution was doubly diluted to give concentrations in the range 8–0.125 mg mL^{-1}. 0.5 mL of the solution of the tested substances was mixed with 9.5 mL of melted and cooled nutrition agar. The bacteria were seeded on the surface of the agar plate. After incubation for 24 h, the *MIC* values were determined as the lowest concentration of the complex preventing visible growth of the bacteria.

ACD/ChemSketch (Freeware version) was employed for drawing Figs. 1 and 4 and prediction of the relative M···M distances within the complexes described in this paper.

RESULTS AND DISCUSSION

New cationic binuclear Cu(II) and Co(II) complexes with pendant arm octaazamacrocyclic ligand tpmc and *S*-phenylalanine, representing an aromatic aminocarboxylate ligand, were successfully isolated. The Cu(II) complex was prepared by the expansion of the coordination sphere of $[Cu_2tpmc](ClO_4)_4$ with the anion of *S*-phenylalanine in the molar ratio of reactants ≈1:2. The yield of the target complex was thus approximately two times higher than in the case of the direct synthesis starting from the reactants. The Co(II) complex was prepared by direct synthesis using the reactants $Co(ClO_4)_2·6H_2O$, tpmc and neutralized *S*-phenylalanine in the molar ratio ≈2:1:1. In both syntheses, *S*-phenylalanine was neutralized to pH ≈ 7.0 to enhance its donor ability and to suppress the formation of violet $[Co_2(OH)tpmc](ClO_4)_3$ during the synthesis of the Co(II)complex, which was always present as a side-product, even in pure aqueous solution.

Complex **1** (t = 20±2 °C) was well soluble in CH_3CN, H_2O, CH_3OH and DMSO but insoluble in C_2H_5OH. Complex **2** (t = 20±2 °C) was well soluble in CH_3CN, DMSO and DMF and sparingly in H_2O and CH_3OH.

The analytical results obtained for the prepared complexes were as follows.

*Complex **1***. Anal. Calcd. for $Cu_2C_{43}H_{68}N_9O_{21}Cl_3$ (FW 1280.58): C, 40.33; H, 5.35; N, 9.84; Cu, 9.91 %. Found: C, 40.34; H, 4.97; N, 9.72; Cu, 9.52 %.

*Complex **2***. Anal. Calcd. for $Co_2C_{43}H_{56}N_9O_{15}Cl_3$ (FW 1145.27): C, 45.10; H, 4.75; N, 11.01 %. Found: C, 44.92; H, 4.92, N, 10.68 %.

The values of molar electrical conductivities measured in CH_3CN and DMF for both complexes are given in Table I. In CH_3CN, for both complexes, they were between those found for 1:3 (literature range 340–420 S cm^2 mol^{-1}) and for 1:4 (500 S cm^2 mol^{-1}) type of electrolytes. In DMF, the value was slightly higher for complex **1**, while complex **2** in DMF corresponded to a 1:3 type (literature range 200–240 S cm^2 mol^{-1}) (Table I).[33]

Considering the results of elemental analyses and conductivity measurements, the general formulas of the complexes were proposed as $[M_2(S\text{-Phe})tpmc](ClO_4)_3·nH_2O$, *S*-PheH = *S*-phenylalanine, M(II) = Cu, n = 7; Co, n = 0.

The electronic absorption spectrum of the blue Cu(II) complex **1** recorded in CH_3CN has a broad absorption maximum in the visible region corresponding to d–d transitions. The position and intensity of the maximum was similar to those

found for congeneric described binuclear Cu(II)tpmc complexes containing benzoate/hydrogenphthalate instead of *S*-phenylalanine ligand.[20] X-Ray structure analyses[16] of these complexes confirmed a coordination number 5 and the chromophore CuN_4O, which are also supposed for complex **1**. In addition, in UV part of the spectra, very intensive dented bands at 220–305 nm (ε from 4700 to 13596 L mol^{-1} cm^{-1}) could be ascribed to charge transfer (CT) transitions. In DMF, the position of the absorption maximum was similar but more intense; CT dented bands were found at 275–318 nm (ε from 4748 to 5769 L mol^{-1} cm^{-1}).

TABLE I. Electronic spectral data for complexes **1** and **2** in CH_3CN[a]/DMF[b], reflectance spectrum[c], molar conductivities (Λ_M) and magnetic moments (μ_{eff}) at room temperature compared with some relevant published analogues

Complex[d]	λ_{max} / nm (ε / L mol^{-1} cm^{-1})	ΛM S cm^2 mol^{-1}	μeff μ_B per M(II)
$[Cu_2tpmc](ClO_4)_4$[27]	680 (340)[a] 594[c]	510[a]	1.90
$[Cu_2(S\text{-Phe})tpmc](ClO_4)_3\cdot 7H_2O$	650 (235)[a] 648(381)[b]	445[a] 276[b]	2.05
$[Co_2(OH)tpmc](ClO_4)_3\ H_2O$[35]	489 (60), 574 (80)[a]	–	–
$[Co_2(S\text{-Ala})tpmc](ClO_4)_3\cdot H_2O$[17]	459 (60), 512 (75), *sh* 551(58)[a]; 452, 508, *sh* 560[c]	–	4.62
$[Co_2(S\text{-Phe})tpmc](ClO_4)_3$	460 (66), 512(85), *sh* 555(61)[a]; 471 (67), 510 (77), *sh* 559(59)[b]; 425, 482, 538[c]	476[a] 219[b]	4.21

[a]in CH_3CN; [b]in DMF, [c]reflectance spectrum; [d]tpmc = *N*,*N*',*N*'',*N*'''-tetrakis(2-pyridylmethyl)-1,4,8,11-tetraazacyclotetradecane; *S*-PheH = *S*-phenylalanine; *S*-AlaH = *S*-alanine; sh-shoulder

The magnetic moment of 2.05 μ_B per Cu(II) at room temperature (Table I) was in the range 1.75 –2.20 μ_B found previously for similar five-coordinated Cu(II) complexes with one unpaired electron and in which there is no significant magnetic interaction.[20–22,34]

In binuclear complexes, the phenylalaninate-bridged ligand has, theoretically, the possibility for coordination in several modes represented in Fig. 1.[34]

In the electronic absorption spectrum of complex **2** recorded in CH_3CN/DMF (Table I), two maxima and one shoulder corresponding to d–d transitions for high-spin Co(II) complexes were observed. From Table I is obvious that maxima positions and the ε values for complex **2** are comparable with the given data for $[Co_2(S\text{-ala})tpmc](ClO_4)_3\cdot H_2O$[17] in CH_3CN, which contains the aliphatic *S*-alanine, suggesting the same CoN_4O chromophore but differ from those for $[Co_2(OH)tpmc](ClO_4)_3$.[35] The coordination number 5, as the most probable due to the lower symmetry than for coordination number 6, found in congeneric complexes is assumed.[36] However, there is a bathochromic shift of all maxima in the spectra of complex **2** in solution (recorded both in CH_3CN and DMF) compared

with the reflectance spectrum of the complex, which was not the case for the *S*-alaninate analogue. This fact implies some changes in the geometry, conformation or coordination sphere upon dissolution of the complex containing *S*-phenylalanine. The reason might be the introduction of the more bulky phenyl group in the aminocarboxylato ligand.

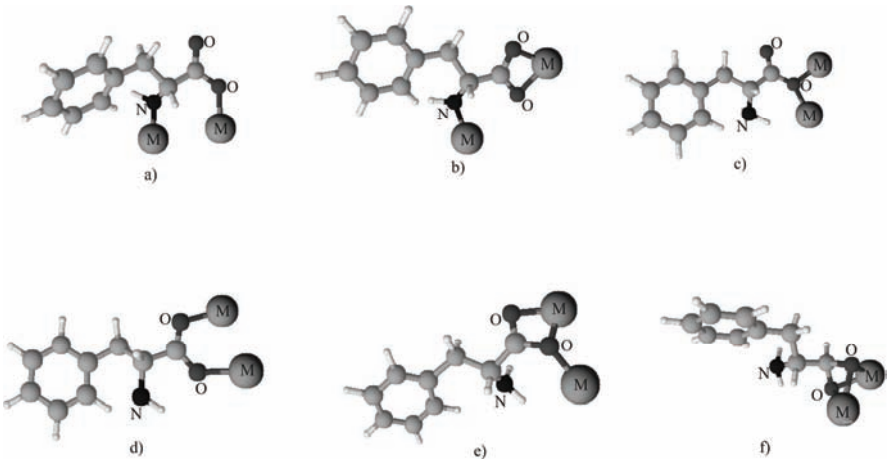

Fig. 1. Some of the theoretically possible coordination modes of the phenylalaninate ligand in binuclear bridged complexes: a) *N*,*O*-; b) combined chelate-bridged, *O*,*O*',*N*-; c) monoatomic *O*,*O*-; d) *O*,*O*'-; e) combined chelate-bridged *O*,*O*,*O*'-; f) combined chelate-bridged *O*,*O*,*O*',*O*'-.

The UV part of the spectrum of complex **2** in CH_3CN contains several unresolved maxima in the range 250–290 nm, with ε around 4350 L mol^{-1} cm^{-1}, belonging to CT transitions. In the spectrum recorded in DMF, there is sharp maximum at 276 nm (ε = 4730 L mol^{-1} cm^{-1}), originating also from CT. The magnetic moment at room temperature for the complex **2** (Table I) of 4.21 μ_B falls in the range 3.96–4.75 μ_B/Co(II) found for high-spin analogous complexes with 3 unpaired electrons.[18,29]

In IR spectra of the complexes, the following bands (in cm^{-1}) were present: a medium broad band with maxima ≈3573 of ν(O–H) from the crystal bonded molecules of H_2O overlapping the valence vibrations of $-NH_2$ in the spectrum of **1** and a doublet at 3313 and 3279 from ν(NH_2) in the spectrum of **2**; a strong sharp band ≈1610 in both complexes, originating from skeletal valence vibrations of the pyridine ring from tpmc included in coordination, which was found at 1588 in the spectrum of free tpmc, a strong band of ν(ClO_4^-) which was not included in the coordination at 1101 for **1**, *i.e.*, 1065 for **2**, as well as a medium sharp band from δ(ClO_4^-) at 624 for **1**, *i.e.*, at 619 for **2**. Finally, weak bands at 473 corresponding to ν(M–N) for **1** and 463 for **2** and at 407 are ascribed to ν(M–O).[37]

The bands of the asymmetrical and symmetrical vibrations of the $–COO^–$ group, $\nu_{as}(OCO^–)$ and $\nu_s(OCO^–)$ and the values $\Delta\nu = \nu_{as} - \nu_s$ for the free ligand and both complexes, together with the corresponding values for the analogous Co(II) *S*-alaninate complex are given in Table II. The shift of ν_{as} and ν_s in the spectra of complexes **1** and **2** was evidence for the participation of the carboxylic group in the coordination. The electronic absorption spectral data (Figs. 1a and 1b) excluded *N*,*O*-chelate coordination of the *S*-phenylalaninate anion. Furthermore, the electronic spectra for the Co(II) tpmc *S*-alaninate and *S*-phenylalaninate complexes and the increasing of their $\Delta\nu$ values compared with those found for the uncoordinated ligands were similar, suggesting the same coordination mode. This together with the absence of a band over 1650 cm^{-1} indicated the participation of both O atoms in the coordination, *i.e.*, the *O*,*O*'-bridged coordination mode, hence the mode in Fig. 1c could be excluded.

TABLE II. IR spectral data values (cm^{-1}) of ν(OCO) for the free aminocarboxylate, complexes **1** and **2** and the Co(II)tpmc *S*-alaninate analogue[17]

Compound[a]	$\nu_{as}(OCO^-)$	$\nu_s(OCO^-)$	$\Delta\nu$
S-PheH	1562	1408	154
$[Cu_2(S\text{-Phe})tpmc](ClO_4)_3\cdot 7H_2O$ (**1**)	1573	1398	175
$[Co_2(S\text{-Phe})tpmc](ClO_4)_3$ (**2**)	1578	1357	221
S-AlaH	1594	1413	181
$[Co_2(S\text{-Ala})tpmc](ClO_4)_3\cdot H_2O$[17]	1575	1350	225

[a]Abbreviations as in Table I

The $\Delta\nu$ value for both complexes was higher than that for uncoordinated *S*-phenylalanine (154 cm^{-1}). For the complex **1**, it was 175 and for **2,** 221 cm^{-1}, meaning a stronger bond in the latter case. Moreover, the $\Delta\nu$ value of the Co(II) complex was comparable with that found for the analogous *S*-alaninate Co(II) complex, 225cm^{-1},[17] suggesting almost the same strength of the Co–O bonds.

For complex **1**, $[M]_{589}$ is –1408.64°, and for complex **2,** +498.59°, which is significantly higher than the value for the corresponding *S*-alaninato Co(II) complex of +168°,[17] while for the *S*-phenylalanine alone $[M]_{589}$ is –20.63° at room temperature. The origin of the optical rotation in the *S*-alaninate complex was ascribed to the "vicinal effect" alone.[17] The value of the molar optical rotation is most probably increased in complex **2** due to the conformational and configurational contribution to the overall activity, as well as due to the greater asymmetry in the complex ion. As for the complex **1**, representing the first Cu(II)tpmc complex with an optically active aminocarboxylate, there is no comparable published data for familiar complexes, although its value of $[M]_{589}$ is also rather high.

The electrochemical behaviour of the synthesized complexes was studied by cyclic voltammetry. First the voltammograms of the starting complex $[Cu_2tpmc](ClO_4)_4$, tpmc and the aminocarboxylate salt were recorded in CH_3CN.

Measurements were performed in the range of –1.0 to +1.0 V at scan speeds of 50, 100 and 200 mV s^{-1}. A representative CV of complex **1** at 200 mV s^{-1} is shown in Fig. 2. The same correlation was observed using a lower rate of potential change but with increasing rate, the cyclic voltammogram was broader, showing that the adsorption of the complex on the working electrode was a relatively slow process. The absence of peaks on both voltammograms suggests the electrochemical stability of the complex under the investigated conditions. The electrochemical behaviour of similar dicarboxylato Cu(II)tpmc complexes was previously studied using lower rates, when it was observed that with decreasing the rate of potential change on the electrodes and by holding the potential, some peaks appeared or became more intensive.[21]

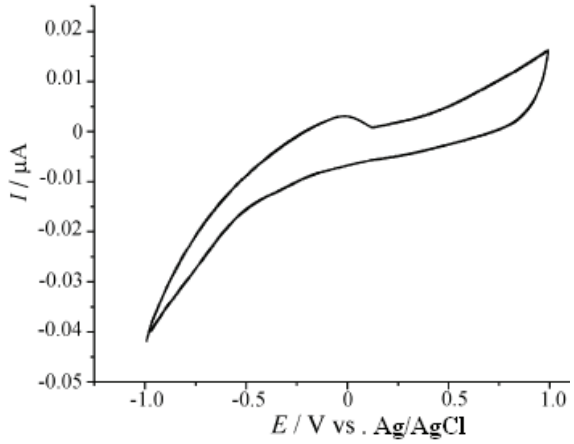

Fig. 2. Cyclic voltammogram of the complex: $[Cu_2(S\text{-Phe})tpmc](ClO_4)_3 \cdot 7H_2O$ in CH_3CN (scan rate: of 200 mV s^{-1}).

The state of the working electrode in the second experiment was first determined by potentiodynamic measurement in the basic electrolyte in the absence of complex **2**. Then complex **2** was added, for which the cyclic voltammogram is presented in Fig. 3. As the obtained curves are identical, it was concluded that the Co(II) complex is electrochemically stable in this electrolyte in the potential range –0.5 to +0.4 V *vs.* SCE and that there is no "charge transfer". On expanding the potential range towards more negative potential than –0.6 V *vs.* SCE, there were no essential changes, except the start of H_2 evolution. On expanding the potential range towards more positive potential than +0.65 V *vs.* SCE, the complex was completely decomposed and peaks due to the oxidative decomposition of its products appeared.

A computer program was applied for the optimization of the possible geometries and coordination modes of aminocarboxylato ligands. Thereby it was seen that in the Cu(II)tpmc complex with *S*-phenylalanine with bridged *O*,*O*'-coordination, the approximate Cu···Cu distance was larger (≈5.1 Å) than in the case of the analogous *μ*-*O*,*O*'-benzoato complex (≈4.5 Å), for which such a coordi-

nation was confirmed by X-ray analysis. This is quite understandable due to the steric hindrance of the more bulky benzyl than phenyl group and introduction of amino group in the first complex. Unfortunately, for the corresponding Co(II)tpmc complex, no comparable X-ray analyses data exist for analogous complexes. However, by using the same program, the Co···Co distance in this complex was estimated to be ≈5.0 and ≈4.8 Å in the related complex with *S*-alanine.

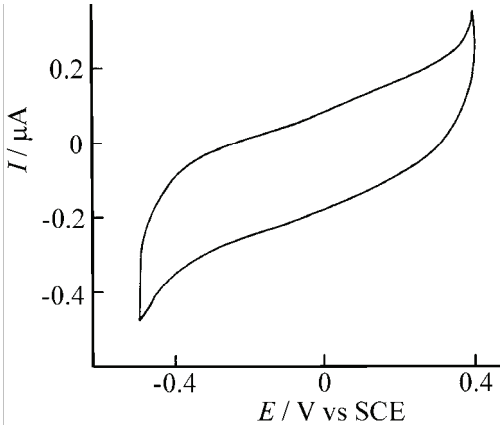

Fig. 3. Cyclic voltammogram of the complex $[Co_2(S\text{-Phe})tpmc](ClO_4)_3$ (scan rate: 100 mV s^{-1}).

Based on all the above reported results, the asymmetrical *μ-O,O'* manner of coordination is proposed as the most probable, with one oxygen in the base of a square-pyramidal geometry and the other in the axial position of a trigonal-bipyramid (Fig. 4).

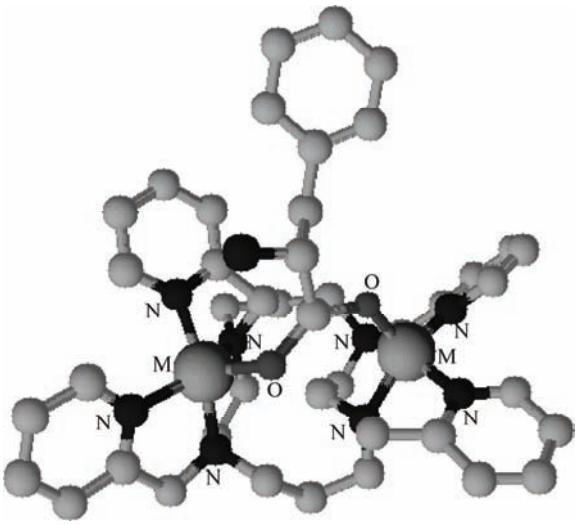

Fig. 4. Proposed geometry of the complex cation $[M_2(S\text{-Phe})tpmc]^{3+}$, M(II) = Co/Cu within complexes **1** and **2**.

The antimicrobial study showed that the solvents, ligands, simple salts and complex **1** were inactive up to 400 μg mL^{-1} against all the studied microorganisms. Both complexes were inactive against the tested fungi and mould. Complex **2** had moderate activity towards some of the studied bacteria (Table III). The Co(II) complex was more active than the analogous Cu(II) complex, suggesting that it is kinetically less stable under the investigated conditions.

TABLE III. Minimum inhibitory concentration (*MIC*), in μg mL^{-1}, of the complexes **1** and **2**

Complex	Solvent	M.L.[a]	S.A.[a]	E.C.[a]	B.S.[a]
$[Cu_2(S\text{-Phe})tpmc](ClO_4)_3 \cdot 7H_2O$	DMSO	>400	>400	>400	>400
$[Co_2(S\text{-Phe})tpmc](ClO_4)_3$		50	100	200	>400

[a]M.L, *M. lysodeikticus* ATCC 4698; S.A, *S. aureus* ATCC 25923; E.C, *E. coli* ATCC 25922; B.S, *B. subtilis* ATCC 6633

CONCLUSIONS

In this paper, the first Cu(II)tpmc complex with an aminocarboxylate ligand and the first Co(II)tpmc complex with an aromatic aminocarboxylate were described. Their composition was consistent with binuclear 3+ cationic complexes. The molar ratio of tpmc and *S*-phenylalanine anion was 1:1. Based on spectral analyses, conductometric and magnetic measurements, cyclic voltammetry and previously published congeneric complexes, pentacoordinated geometry with an *exo* coordination mode of the octaazamacrocyclic ligand in the boat conformation, with a *μ-O,O'*-bonded *S*-phenylalaninato ion is proposed. The cobalt(II) complex showed moderate antibacterial activity against some strains. The complexes were compared mutually and with some related already published complexes.

Acknowledgements. We gratefully acknowledge the financial support of the Ministry of Education and Science of the Republic of Serbia (Project No. 172014), Dr. Dragan Manojlović of the Faculty of Chemistry, Belgrade, Serbia, for the CV measurements and Dr. Gordana Gojgić-Cvijović from ICTM – Centre for Chemistry Belgrade, Serbia, for the antimicrobial test.

ИЗВОД

НОВИ Cu(II) И Co(II) ОКТААЗАМАКРОЦИКЛИЧНИ КОМПЛЕКСИ СА 2-АМИНО-3-ФЕНИЛ-ПРОПАНСКОМ КИСЕЛИНОМ

ГОРДАНА ВУЧКОВИЋ[1], МИРЈАНА АНТОНИЈЕВИЋ-НИКОЛИЋ[2], СЛАЂАНА Б. ТАНАСКОВИЋ[3] и ВУКОСАВА ЖИВКОВИЋ-РАДОВАНОВИЋ[1]

[1]Хемијски факултет, Универзитет у Београду, п.пр. 118, 11158 Београд, [2]Висока технолошка школа струковних студија, 15000 Шабац и [3]Фармацеутски факултет, Универзитет у Београду, Војводе Степе 450, 11000 Београд

Добијена су два нова комплекса Cu(II) и Co(II) са *N,N',N'',N'''*-тетракис(2-пиридилметил)-1,4,8,11-циклотетрадеканом (tpmc-ом) и анјоном 2-амино-3-фенил-пропанске киселине (*S*-фенилаланина). Они су анализирани и окарактерисани: елементалном анализом, кондуктометријским, поларимет ријским, магнетним и циклично-волтаметријским мерењима, као и

спектроскопским подацима (UV/Vis, IR). Оба комплекса су динуклеарна опште формуле $[M_2(S\text{-Phe})tpmc](ClO_4)_3 \cdot nH_2O$; *S*-PheH = *S*-фенилаланин, M(II) = Cu, $n = 7$; Co, $n = 0$. На основу раније добијених података за сродне комплексе и нових резултата претпостављена је пентакоординациона геометрија. Оба централна метална јона су координована за по два пиридил и два цикламова азота и премошћена $–N–(CH_2)_3–N–$ фрагментима цикламовог прстена и кисеониковим атомима *S*-фенилаланинато јона. Антимикробни тест комплекса, растварача, полазних соли и самих лиганада је извршен на гљивице, плесни и бактерије. У извесним случајевима нађена је повећана активност комплекса Co(II) према појединим бактеријама у односу на одговарајуће слободне лиганде и полазне соли.

(Примљено 1. децембра 2010, ревидирано 27. јануара 2011)

REFERENCES

1. P. Emseis, D. E. Hibbs, P. Leverett, N. Reddy, P. A. Williams, *J. Coord. Chem*. **56** (2003) 661
2. A. J. Blake, B. B. De, W.-S. Li, N. R. Thomas, *Acta Crystallogr*. **C58** (2002) 570
3. S. H. Seda, J. Janczak, J. Lisowski, *Inorg. Chim. Acta* **359** (2006) 1055
4. A. Böhm, H. Brunner, W. Beck, *Z. Anorg. Allg. Chem.* **634** (2008) 274
5. P. Kannan, K. Rathinavelu Sankaran, *React. Kinet. Catal. Lett*. **85** (2005) 231
6. L. H. Abdel-Rahman, L. P. Battaglia, M. R. Mahmoud, *Polyhedron* **15** (1996) 327
7. H. Kumita, T. Kato, K. Jitsukawa, H. Einaga, H. Masuda, *Inorg. Chem.* **40** (2001) 3936
8. I.-K. Lee, M.-J. Jun, *Bull. Korean Chem. Soc*. **17** (1996) 433
9. E. V. Rumyantsev, I. E. Kolpakov, Yu. S. Marfin, E. V. Antina, *Russ. J. Gen. Chem*. **79** (2009) 482
10. A. Stanila, A. Marcu, D. Rusu, M. Rusu, L. David, *J. Mol. Struct.* **834–836** (2007) 364
11. D. Mitić, M. Milenković, S. Milosavljević, D. Gođevac, Z. Miodragović, K. Anđelković, Dj. Miodragović, *Eur. J. Med. Chem.* **44** (2009) 1537
12. F. Dallavalle, M. Tegoni, *Polyhedron* **20** (2001) 2697
13. Z. H. Chohan, M. Arif, M. A. Akhtar, C. T. Supuran, *Bioinorg. Chem. Appl.* (2006) 1 and references cited therein
14. M. C. B. Oliveira, M. S. R. Couto, P. C. Severino, T. F oppa, G. T. S. Martins, B. Szpoganicz, R. A. Peralta, A. Neves, H. Terenzi, *Polyhedron* **24** (2005) 495
15. G. Vučković, S. B. Tanasković, U. Ry chlewska, D. D. Radanović, J. Mroziński, M. Korabik, *J. Mol. Struct.* **827** (2007) 80
16. G. Vučković, M. Antonijević-Nikolić, T. Lis, J. Mroziński, M. Korabik, D. D. Radanović, *J. Mol. Struct.* **872** (2008) 135
17. G. Vučković, D. Opsenica, S. P. Sovilj, D. Poleti, *J. Coord. Chem.* **47** (1999) 331
18. G. Vučković, D. Opsenica, S. P . Sovilj, D. Poleti, M. Avramov-Ivić, *J. Coord. Chem.* **42** (1997) 241
19. G. Vučković, S. B. Tanaskovi ć, M. Antonij ević-Nikolić, V. Živkovi ć-Radovanović, G. Gojgić-Cvijović, *J. Serb. Chem. Soc*. **74** (2009) 629
20. G. Vučković, M. Antonijević, D. Poleti, *J. Serb. Chem. Soc*. **67** (2002) 677
21. Z. M. Miodragović, G. Vučković, S. P. Sovilj, D. D. Manoj lović, M. J. Malinar, *J. Serb. Chem. Soc.* **63** (1998) 781
22. G. Vučković, M. Antonij ević-Nikolić, M. Korabik, J. Mroziński, D. D. Manojlović, G. Gojgić-Cvijović, N. Matsumoto, *Pol. J. Chem.***79** (2005) 679

23. B. B. Petković, S. P. Sovilj, M. V. Budimir, R. M. Simonović, V. M. Jovanović, *Electroanalysis* **22** (2010) 1894
24. R. Portillo, L. Albertola, *Anales Soc. Espan. Fis. Quim.* **28** (1930) 1117
25. A. Kiss, Z. M. Gerendas, *Z. Phys. Chem.* **180** (1937) 117
26. S. Chandrasekhar, W. L. Waltz, L. Prasad, J. W. Quail, *Can. J. Chem.* **75** (1997) 1363
27. E. Asato, H. Toftlund, S. Kida, M. Mikuriya, K. S. Murray, *Inorg. Chim. Acta* **165** (1989) 207
28. W. Wendlandt, H. Hecht, *Reflectance Spectroscopy*, Wiley, New York, 1966
29. E. König, *Magnetic Properties of Coordination and Organometallic Transition Metal Compounds*, Springer-Verlag, Berlin, 1966
30. J. F. Acar, F. W. Goldstein, in *Antibiotics in Laboratory Medicine*, 4th ed., V. Lorian, Ed., Williams and Wilkins, Baltimore, 1996, p. 1
31. D. Amsterdam, in *Antibiotics in Laboratory Medicine*, 4th ed., V. Lorian, Ed., Williams and Wilkins, Baltimore, MD, 1996, p. 52
32. H. M. Ericsson, J. C. Sherris, *Acta Pathol. Microbiol. Scand. Suppl.* **217** (1971) 3
33. W. J. Geary, *Coord. Chem. Rev.* **33** (1980) 227
34. F. A. Cotton, G. Wilkinson, *Advanced Inorganic Chemistry*, 6th ed., Wiley, New York, 1999
35. H. Harada, M. Kodera, G. Vučković, N. Matsumoto, S. Kida, *Inorg. Chem*. **30** (1991) 1190
36. B. P. Lever, *Inorganic Electronic Spectroscopy*, 2nd ed., Elsevier, Amsterdam, 1984, p. 480
37. a) K. Nakamoto, *Infrared and Raman Spectra of Inorganic and Coordination Compounds*, Part B, 5th ed., Wiley, New York, 1997; b) G. B. Deacon, R. J. Philips, *Coord. Chem. Rev.* **33** (1980) 227.

Journal of the Serbian Chemical Society
JSCS-info@shd.org.rs • www.shd.org.rs/JSCS
J. Serb. Chem. Soc. 76 (5) 733–741 (2011)
JSCS–4154
UDC 547.686:54.02+66.095.252.5:547.52
Original scientific paper

Effect of benzocyclobutadieno-annelation on cyclic conjugation in fluoranthene congeners

IVAN GUTMAN[1]*#, BORIS FURTULA[1#] and ALEXANDRU T. BALABAN[2]

[1]*Faculty of Science, University of Kragujevac, P. O. Box 60, 34000 Kragujevac, Serbia and* [2]*Texas A&M University at Galveston, 5007 Avenue U, Galveston, TX 77551, USA*

(Received 1 December 2010)

Abstract: Earlier studies revealed that benzo-annelation has a peculiar effect on the intensity of cyclic conjugation in the five-membered ring of fluoranthene congeners. Now, the analogous effect of benzocyclobutadieno-annelation was examined and it was found show it is opposite to the effect of benzo-annelation: a benzocyclobutadiene fragment in angular (resp. linear) position with regard to the five-membered ring, decreases (resp. increases) the intensity of cyclic conjugation in the five-membered ring.

Keywords: fluoranthenes; Kekulé structure; polycyclic aromatic hydrocarbon; benzo-annelation; benzocyclobutadieno-annelation.

INTRODUCTION

Attaching a benzene ring to a carbon–carbon bond of a polycyclic conjugated molecule can be performed in two different ways: either as an ordinary benzo-annelation or by connecting the benzene ring *via* two new carbon–carbon bonds, referred to as a benzocyclobutadieno-annelation (or, abbreviated, BCBD-annelation), Fig. 1.

The effect of benzo-annelation on cyclic conjugation in various polycyclic conjugated systems was much studied: in acenaphthylene and fluoranthene congeners,[1–8] in other non-alternant conjugated molecules,[9,10] and in benzenoid hydrocarbons,[11–17] and a general theory thereof was developed.[18] The analogous effect of benzocyclobutadieno-annelation has until now not been examined at all.

In previous works, particular attention was paid to the effect of benzo-annelation on the intensity of cyclic conjugation in the five-membered ring of acenaphthylene and fluoranthene congeners.[1–8] Within these studies, the following five generally valid regularities could be established:

* Corresponding author. E-mail: gutman@kg.ac.rs
# Serbian Chemical Society member.
doi: 10.2298/JSC101201061G

Rule 1. Benzo-annelation in an angular position to the five-membered ring increases the intensity of cyclic conjugation in the five-membered ring.

Rule 2. Benzo-annelation in a linear position to the five-membered ring decreases the intensity of cyclic conjugation in the five-membered ring.

Rule 3. The effects specified in Rules 1 and 2 are proportional to the number of benzo-annelated rings.

Rule 4. The effect of an angular benzo-annelation on the intensity of cyclic conjugation in the five-membered ring is significantly stronger than the analogous effect of linear benzo-annelation.

Rule 5. The effect of annelation at the "male" part of fluoranthene (positions a_3, a_4 and l_3, Fig. 2) is much weaker than the effect of annelation at the "female" part (positions a_1, a_2, l_1, and l_2, see Fig. 2).

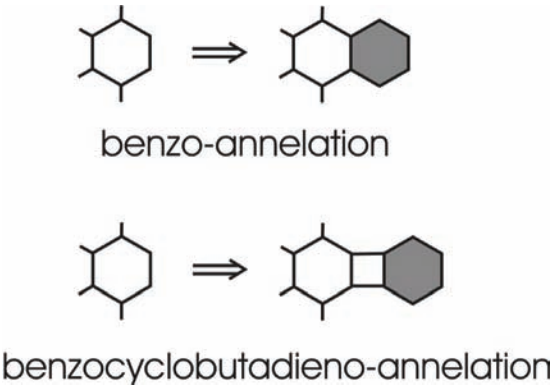

Fig. 1. Two ways in which a benzene ring can be annelated to a polycyclic conjugated system. In this work, the effects of the benzocyclobutadieno (BCBD) annelation on the intensity of cyclic conjugation in a ring of the parent conjugated system were studied for the first time (*cf.* Fig. 2).

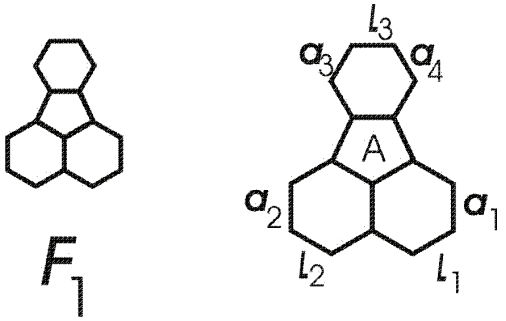

Fig. 2. Fluoranthene **F$_1$** and the sites where a benzo- or BCBD-annelation can occur. Sites marked by *a* and *l* pertain, respectively, to angular and linear annelation relative to the five-membered ring (A).

The intensity of cyclic conjugation can be assessed by means of the energy-effect (*ef*) of the respective ring. The theory of the *ef*-method has been outlined in two reviews.[19,20] For additional details see an older paper,[21] more recent articles,[16,17,22,23] and elsewhere.[4,11] For the present considerations it is sufficient to recall that the *ef*-values are expressed in units of the HMO carbon–carbon resonance integral β. Therefore, positive *ef*-values indicate thermodynamic sta-

bilization caused by cyclic conjugation, and the greater is *ef*, the stronger is the cyclic conjugation in the considered ring.

It should be noted that in previous works,[1–8] instead of "angular" constellation of a five- and a six-membered ring, their "PCP" constellation (where PCP is the abbreviation of "phenyl-cyclopentadienyl") was used. In these works,[1–8] RuAle 1 was referred to as the "PCP rule" or the "PCP effect". Since in the present work, we are going to consider benzocyclobutadieno-annelation will be considered, the term "PCP" would be misleading, and, therefore, the more plausible term "angular" is used (*cf*. Fig. 1).

The regularities stated here as Rules 1–4 were first discovered by calculating the *ef*-values of the five-membered ring. Eventually, these regularities were confirmed by a number of other, independent, theoretical approaches.[3,6,8,13]

In this paper, the regularities analogous to Rules 1–4 in BCBD-derivatives of fluoranthene (**F$_1$**) are studied. BCBD-annelation in fluoranthene may occur in the angular or in the linear mode, relative to the five-membered ring, as shown in Fig. 2.

NUMERICAL WORK

There exist four monobenzocyclobutadieno- (**F$_2$**–**F$_5$**), ten dibenzocyclobutadieno- (**F$_6$**–**F$_{15}$**), nine tribenzocyclobutadieno- (**F$_{16}$**–**F$_{24}$**), and three tetrabenzocyclobutadieno-fluoranthenes (**F$_{25}$**–**F$_{27}$**), *i.e.*, a total of 26 BCBD-annelated species. These, together with the labeling of their rings, are depicted in Figs. 3a and 3b.

The calculated energy effects of the five-membered ring (A) and of the attached benzene rings (R, S, T, U) of fluoranthene and its 26 BCBD-annelated derivatives are given in Table I. The analogous data for benzo-annelated fluoranthenes can be found in the literature.[2]

SOME REGULARITIES OBSERVED

By examining the data given in Table I, a number of regularities for the cyclic conjugation in BCBD-annelated fluoranthene-derivatives can be recognized.

The main observed regularities are the following.

Rule 1*. BCBD-annelation in an angular position to the five-membered ring decreases the intensity of cyclic conjugation in the five-membered ring.

Rule 2*. BCBD-annelation in a linear position to the five-membered ring increases the intensity of cyclic conjugation in the five-membered ring.

Rule 3*. The effects specified in Rules 1* and 2* are proportional to the number of benzo-annelated rings.

Rule 4*. The effect of an angular BCBD-annelation on the intensity of cyclic conjugation in the five-membered ring is significantly weaker than the analogous effect of linear BCBD-annelation.

Rule 5*. The same difference between "male" and "female" effects, as stated in Rule 5, exists also in the case of BCBD-annelation.

Rules 2* and 3* are convincingly illustrated by the following data: *ef*(**F$_1$**,A) = = 0.0031 (no BCBD-annelation); *ef*(**F$_3$**,A) = 0.0047, *ef*(**F$_5$**,A) = 0.0036 (one BCBD-

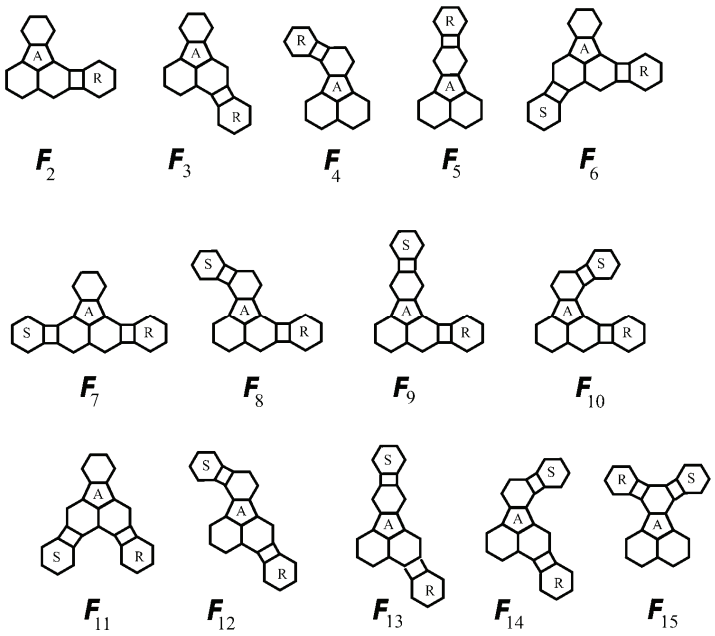

(a)

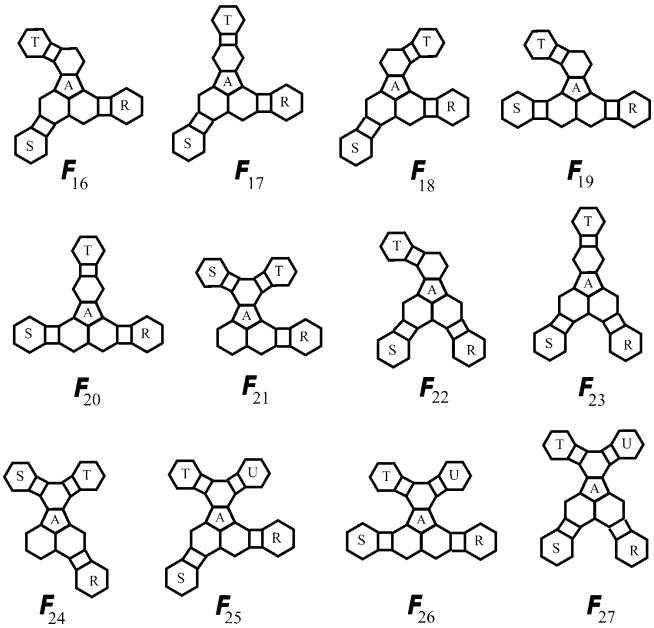

(b)

Fig. 3. a) Mono- and di-benzocyclobutadieno-annelated fluoranthenes, and b) tri- and tetra-benzocyclobutadieno-annelated fluoranthenes and the labeling of the attached benzene rings.

annelation); *ef*(**F**$_{11}$,A) = 0.0081 , *ef*(**F**$_{13}$,A) = 0.0060 (two BCBD-annelations); *ef*(**F**$_{23}$,A) = 0.0110 (three BCBD-annelations, maximum possible). Thus, due to Rule 2*, the cyclic conjugation in the five-membered ring of **F**$_{23}$ is roughly three times greater than in fluoranthene (**F**$_1$).

TABLE I. The energy effects (in β units) of the five- and six-membered rings of fluoranthene and its benzocyclobutadieno-annelated congeners (depicted in Figs. 2, 3a and 3b)

Molecule	*ef*(**F**,A)	*ef*(**F**,R)	*ef*(**F**,S)	*ef*(**F**,T)	*ef*(**F**,U)
F$_1$	0.0031				
F$_2$	0.0031	0.3439			
F$_3$	0.0047	0.5086			
F$_4$	0.0023	0.4459			
F$_5$	0.0036	0.4356			
F$_6$	0.0042	0.3183	0.5524		
F$_7$	0.0028	0.3705	0.3705		
F$_8$	0.0023	0.3433	0.4451		
F$_9$	0.0036	0.3431	0.4344		
F$_{10}$	0.0023	0.3438	0.4458		
F$_{11}$	0.0081	0.4287	0.4287		
F$_{12}$	0.0033	0.5225	0.4407		
F$_{13}$	0.0060	0.4903	0.4247		
F$_{14}$	0.0033	0.5245	0.4432		
F$_{15}$	0.0020	0.3375	0.3375		
F$_{16}$	0.0030	0.3180	0.5667	0.4434	
F$_{17}$	0.0052	0.3188	0.6316	0.4262	
F$_{18}$	0.0030	0.3184	0.5636	0.4416	
F$_{19}$	0.0022	0.3701	0.3705	0.4453	
F$_{20}$	0.0031	0.3703	0.3703	0.4343	
F$_{21}$	0.0020	0.3434	0.3371	0.3376	
F$_{22}$	0.0049	0.4463	0.4477	0.4371	
F$_{23}$	0.0110	0.4143	0.4143	0.4078	
F$_{24}$	0.0025	0.5359	0.3355	0.3370	
F$_{25}$	0.0023	0.3182	0.5759	0.3369	0.3358
F$_{26}$	0.0018	0.3702	0.3702	0.3373	0.3373
F$_{27}$	0.0034	0.4626	0.4626	0.3352	0.3352

Analogously, Rules 1* and 3* are illustrated by the following data: *ef*(**F**$_1$,A) = = 0.0031 (no BCBD-annelation); *ef*(**F**$_2$,A) = 0.003 1, *ef*(**F**$_4$,A) = 0.002 3 (one BCBD-annelation); *ef*(**F**$_7$,A) = 0.00 28, *ef*(**F**$_8$,A) = 0.00 23, *ef*(**F**$_{10}$,A) = 0.0023, *ef*(**F**$_{15}$, A) = 0.0020 (two BCBD-annelations); *ef*(**F**$_{19}$,A) = 0.002 2, *ef*(**F**$_{21}$,A) = = 0.0020 (three BCBD-annelations); *ef*(**F**$_{26}$,A) = 0.018 (four BC BD-annelations, maximum possible). Thus, due to Rule 1*, the cyclic conjugation in the five-membered ring of **F**$_{26}$ is roughly two thirds that in fluoranthene (**F**$_1$).

From these examples, it can be seen that linear BCBD-annelation has a much stronger effect on cy clic conjugation in the five-mem bered ring than angula r BCBD-annelation, as claimed by Rule 4*.

If both linear and angular BCBD-annelations are present, then their effect is a delicate combination of the effects described by Rules 1 and 2; for details see Table I. In all studied cases, the (magnifying) effect of linear annelation dominates over the (attenuating) effect of angular annelation. A characteristic example is **F6** (one linear and one angular annelation), in which the cyclic conjugation in the five-membered ring is by some 33 % more intense than in fluoranthene itself.

There exist three pairs of isomers that differ in the position of an annelation at the sites a_3 and a_4 (Fig. 2). These are **F8**–**F10**, **F12**–**F14**, and **F16**–**F18**. These isomers of *cis*-like and *trans*-like types have almost identical modes of cyclic conjugation, which is just another manifestation of isoarithmicity.[2,24,25] For instance, for **F16**, one has *ef*(A) = 0.0063, *ef*(R) = 0.1157, *ef*(S) = 0.1652 and *ef*(T) = 0.1308, whereas for **F18**, they are *ef*(A) = 0.0062, *ef*(R) = 0.1169, *ef*(S) = = 0.1653 and *ef*(T) = 0.1321.

On comparing Rules 1–4 with Rules 1*–4*, it was immediately recognized that BCBD-annelation and benzo-annelation affect cyclic conjugation in exactly the opposite ways. In order to show the quantitative aspects of this opposite tendency, the correlation between the *ef*-values of the five-membered rings of benzo-annelated fluoranthenes and the *ef*-values in the analogous BCBD-annelated species is presented in Fig. 4.

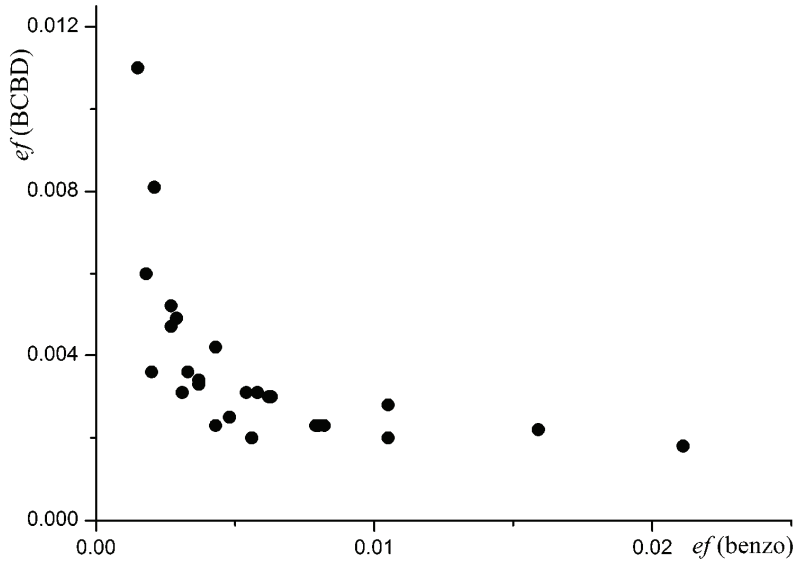

Fig. 4. The energy effects (*ef*) of the five-membered rings of BCBD-annelated fluoranthenes plotted *versus* the corresponding *ef*-values of the benzo-annelated species.

Plots of the energy effects of the benzene rings in BCBD-annelated fluoranthenes *versus* the analogous *ef*-values of the benzo-annelated species are shown in Figs. 5 and 6.

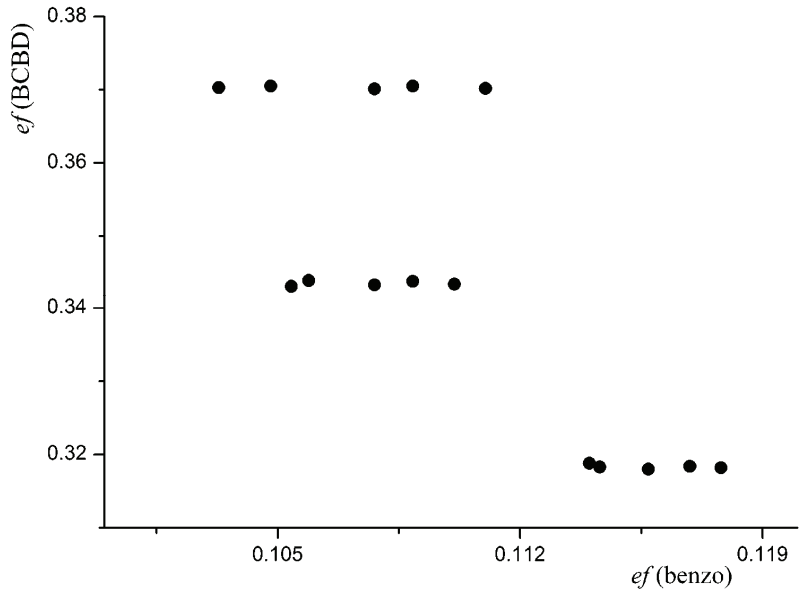

Fig. 5. The energy effects (*ef*) of the benzene rings of BCBD-annelated fluoranthenes in positions a_1 and/or a_2 (*cf.* Fig. 2), plotted *versus* the corresponding *ef*-values of the benzo-annelated species. For details see text.

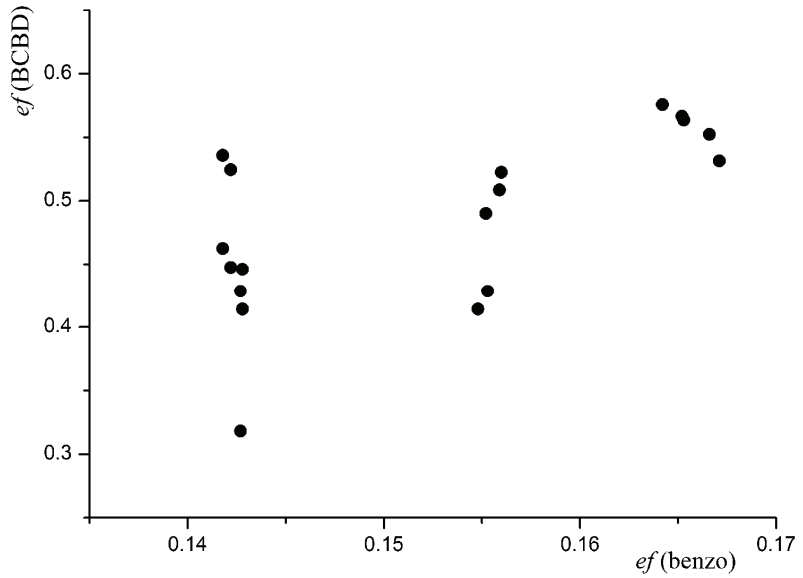

Fig. 6. The energy effects (*ef*) of benzene rings of BCBD-annelated fluoranthenes in positions l_1 and/or l_2 (*cf.* Fig. 2), plotted *versus* the corresponding *ef*-values of the benzo-annelated species. For details see text.

Figure 5 pertains to the angularly annelated benzene rings. Only annelation in the "female" positions, a_1 and/or a_2, are considered because of Rules 5 and 5*. In harmony with Rules 1 and 1*, it can be seen that benzo-annelation has a much stronger structure-dependency than BCBD-annelation. The data points are grouped into three clusters, depending on whether in the "female" part of the respective molecule there are two angular annelations (bottom), an angular and a linear annelation (top), or just a single angular annelation (middle).

Figure 6 pertains to the linearly annelated benzene rings. Again, in view of Rules 5 and 5*, only annelation in the "female" positions, l_1 and/or l_2, are considered. In harmony with Rules 2 and 2*, this time BCBD-annelation has a much stronger structure-dependency than benzo-annelation. The data points are grouped into three clusters, depending on whether in the "female" part of the respective molecule there are two linear annelations (right), a linear and an angular annelation (left), or just a single linear annelation (middle).

The data in Figs. 4–6 may be viewed as illustrations of the previously established Rules 1–4, the presently established Rules 1*–4*, and the fundamental differences between benzo- and benzocyclcobutadiene-annelations.

Acknowledgement. I. G. and B. F. thank the Ministry of Science and Technological Development of the Republic of Serbia for partial support of this work, through Grant No. 144015G.

ИЗВОД

УТИЦАЈ БЕНЗОЦИКЛОБУТАДИЕНСКЕ АНЕЛАЦИЈЕ НА ЦИКЛИЧНУ КОЊУГАЦИЈУ У ЈЕДИЊЕЊИМА ФЛУОРАНТЕНСКОГ ТИПА

ИВАН ГУТМАН[1], БОРИС ФУРТУЛА[1] и ALEXANDRU T. BALABAN[2]

[1]Природно–математички факултет Универзитета у Крагујевцу и [2]Texas A&M University at Galveston, Galveston, USA

Ранија истраживања показала су да бензоанелација на специфични начин утиче на интензитет цикличне конјугације у петочланом прстену једињења флуорантенског типа. У овом раду проучен је аналогни утицај бензоциклобутадиенске анелације, и показано је да је он супротан утицају бензоанелације: бензоциклобутадиенски фрагмент у ангуларном (одн. линеарном) положају у односу на петочлани прстен, умањује (одн. увећава) интензитет цикличне конјугације у петочланом прстену.

(Примљено 1. децембра 2010)

REFERENCES

1. I. Gutman, J. Đurđević, A. T. Balaban, *Polycyclic Aromat. Compd.* **29** (2009) 3
2. J. Đurđević, I. Gutman, J. Terzić, A. T. Balaban, *Polycyclic Aromat. Compd.* **29** (2009) 90
3. J. Đurđević, I. Gutman, R. Ponec, *J. Serb. Chem. Soc.* **74** (2009) 549
4. I. Gutman, J. Đurđević, *J. Serb. Chem. Soc.* **74** (2009) 765
5. S. Radenković, J. Đurđević, I. Gutman, *Chem. Phys. Lett.* **475** (2009) 289
6. J. Đurđević, S. Radenković, I. Gutman, S. Marković, *Monatsh. Chem.* **140** (2009) 1305

7. B. Furtula, I. Gutman, S. Jeremić, S. Radenković, *J. Serb. Chem. Soc.* **75** (2010) 83
8. A. T. Balaban, T. K. Dickens, I. Gutman, R. B. Mallion, *Croat. Chem. Acta* **83** (2010) 209
9. I. Gutman, S. Jeremić, V. Petrović, *Indian J. Chem.***48A** (2009) 658
10. A. T. Balaban, J. Đurđević, I. Gutman, *Polycyclic Aromat. Compd.* **29** (2009) 185
11. I. Gutman, N. Turković, J. Jovičić, *Monatsh. Chem.* **135** (2004) 1389
12. S. Radenković, W. Linert, I. Gutman, S. Jeremić, *Indian J. Chem.* **48A** (2009) 1657
13. I. Gutman, S. Radenković, W. Linert, *Monatsh. Chem.* **141** (2010) 401
14. S. Jeremić, S. Radenković, I. Gutman, *J. Serb. Chem. Soc.* **75** (2010) 943
15. S. Jeremić, S. Radenković, I. Gutman, *Maced. J. Chem. Chem. Eng.* **29** (2010) 63
16. A. T. Balaban, J. Đurđević, I. Gutman, S. Jeremić, S. Radenković, *J. Phys. Chem.* **A 114** (2010) 5870
17. A. T. Balaban, I. Gutman, S. Jeremić, J. Đurđević, *Monatsh. Chem.* **142** (2011) 53.
18. I. Gutman, *J. Math. Chem.* **47** (2010) 1309
19. I. Gutman, *Monatsh. Chem.* **136** (2005) 1055
20. I. Gutman, in *Mathematical Methods and Modelling for Students of Chemistry and Biology*, A. Graovac, I. Gutman, D. Vukičević, Eds., Hum, Zagreb, 2009, pp. 13–27.
21. I. Gutman, S. Bosanac, *Tetrahedron* **33** (1977) 1809
22. I. Gutman, S. Stanković, J. Đurđević, B. Furtula, *J. Chem. Inf. Model.* **47** (2007) 776
23. I. Gutman, S. Stanković, *Monatsh. Chem.* **139** (2008) 1179
24. A. T. Balaban, *MATCH Commun. Math. Chem.* **24** (1989) 29
25. I. Gutman, A. T. Balaban, M. Randić, C. Kiss-Tóth, *Z. Naturforsch., A: Phys. Sci.* **60** (2005) 171.

Journal of the Serbian Chemical Society
JSCS-info@shd.org.rs • www.shd.org.rs/JSCS

J. Serb. Chem. Soc. *76* (5) 743–749 (2011)
JSCS–4155

UDC 547.313.2+541.124:
66.095.252.091.7:536.722
Original scientific paper

An *ab initio* study of the mechanism of the cycloaddition reaction forming bicyclic compounds between vinylidene (H_2C=C:) and ethylene

XIUHUI LU*, ZHENXIA LIAN and YONGQING LI

School of Chemistry and Chemical Engineering, University of Jinan, Jinan, Shandong, 250022, P. R. China

(Received 20 August, revised 21 September 2010)

Abstract: The mechanism of the cycloaddition reaction forming a bicyclic compounds between singlet vinylidene (H_2C=C:) and ethylene was investigated using the CCSD(T)//MP2/6-31G* method. From the potential energy profile, it can be predicted that this reaction has one dominant channel. The presented rule of this reaction, a [2+2] cycloaddition reaction between the two reactants occurred forming a four-membered ring carbene (INT1), in which the sp lone electron of the C atom from carbene in INT1 and the π^* unoccupied orbital of ethane form the sp→π^* donor–acceptor effect, resulting in the formation of intermediate (INT2). Due to the further sp^3 hybridization of C atom from carbene in INT1, INT2 isomerizes to the bicyclic compound (P2) *via* the transition state (TS2).

Keywords: vinylidene; reaction mechanism; potential energy surface.

INTRODUCTION

Since unsaturated carbene was recognized as an active intermediate in the 1960s, it has not only attracted much attention from theoretical chemists but has also been practically applied in organic chemistry.[1,2] For example, it was shown that the cycloaddition reaction of unsaturated carbine can provide a simple and direct way for the synthesis of small-ring, highly strained compounds, as well as those that can hardly be synthesized through conventional ways.[2] Hitherto, in depth exploration of the rearrangement reaction of alkylidene carbine has been realized,[3,4] and the insertion reactions of alkylidene carbene have also been studied.[5,6] Apeloig and Fox performed experimental and theoretical studies on the 3-dimensional selectivity of substitute groups from the products of the vinylidene–olefins addition reactions of alkylidene carbene.[7,8] In previous papers, the

* Corresponding author. E-mail: lxh@ujn.edu.cn
doi: 10.2298/JSC100820065L

mechanism of cycloaddition reaction between alkylidene carbene and asymmetric π-bonded compounds was explored.[9–12] However, no report on the mechanism of the cycloaddition reactions between alkylidene carbene and symmetric π-bonded compounds, in which bicyclic compounds are formed, was found. It is quite difficult to investigate the mechanisms of these cycloaddition reactions directly by experimental methods due to the high activity of alkylidene carbene; therefore, a theoretical study is more practical. To explore the mechanism of cycloaddition reactions between alkylidene carbene and symmetric π-bonded compounds, in which bicyclic compounds are formed, vinylidene (H_2C=C:) and ethylene were selected as model molecules. Its mechanism (considering simultaneous hydrogen transfer) was investigated and analyzed theoretically. The results showed that the cycloaddition reaction has two possible pathways, as follows:

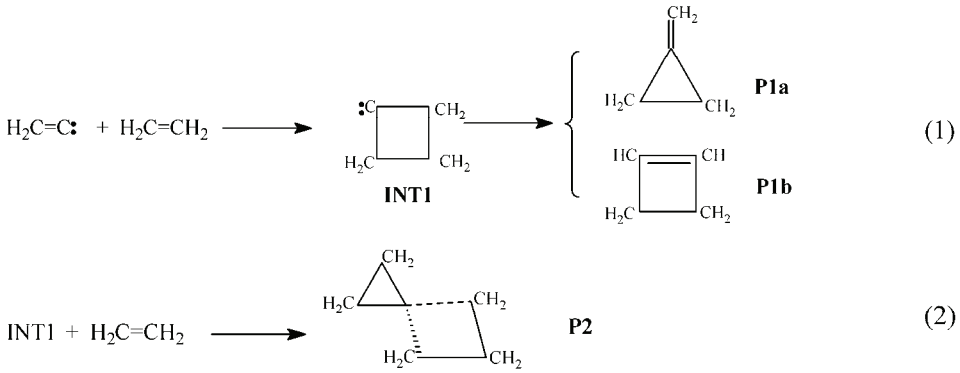

CALCULATION METHOD

MP2/6-31G*[13] implemented in the Gaussian 98 package was employed to locate all the stationary points along the reaction pathways. Full optimization and vibrational analysis were realized for the stationary points on the reaction profile. Zero-point energy and CCSD (T) corrections were included in the energy calculations. The CCSD(T) method consists of a coupled-cluster calculation with single, double and perturbative triple excitations. Thus, this method could generate more accurate energies than the MP2 method. In order to explicitly establish the relevant species, the intrinsic reaction coordinates (IRC)[14,15] was also calculated for all the transition states appearing on the potential energy profile.

RESULTS AND DISCUSSION

Reaction (1): channels for forming the four-membered ring intermediate (INT1), the H-transfer product (P1b) and the three-membered ring product (P1a)

Theoretical calculations show that the ground state of vinylidene is singlet state. The geometrical parameters of the intermediate (INT1), transition states (TS1a, TS1b) and products (P1a, P1b) which appear in reaction (1) between vinylidene and ethene are given in Fig. 1. The energies are listed in Table I, and

the potential energy surface for the cycloaddition reaction is shown in Fig. 2. The unique imaginary frequencies of the transition states TS1a and TS1b are 525.3 and 684.9 cm^{-1}, and consequently these transition states can be affirmed as real ones. According to the calculations of the IRC of TS1a and TS1b, further optimization for the primary IRC results, TS1a connects INT1 with P1a and TS1b connects INT1 with P1b.

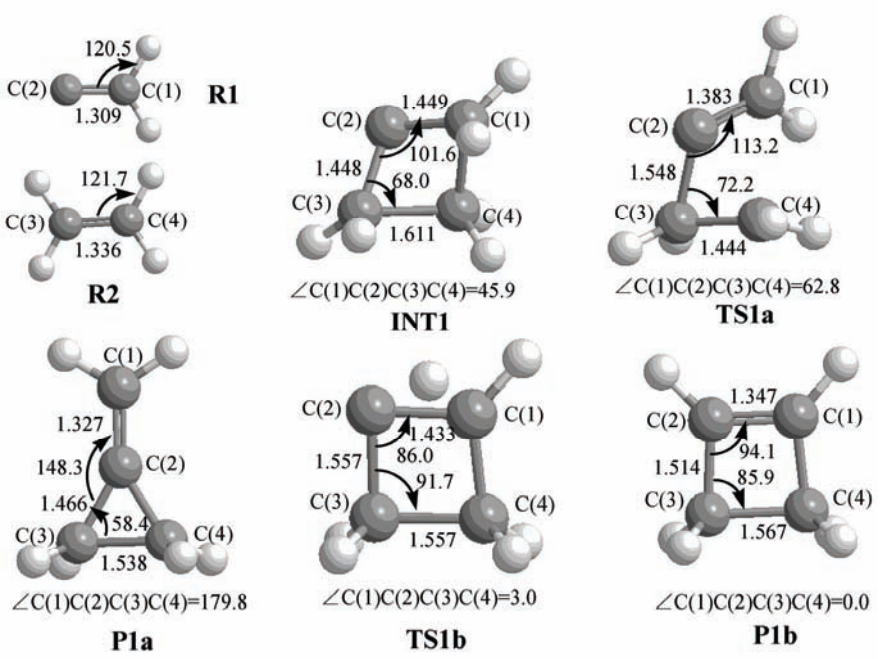

Fig. 1. Optimized MP2/6-31G* geometrical parameters and atornic numbering for the species in the cycloaddition reaction (1), in which the bond lengths and bond angles are given in angstroms and degrees, respectively.

According to Fig. 2, it can be seen that Reaction (1) has two reaction pathways a and b, both of which are composed of two steps, the first step is that the two reactants (R1, R2) form a four-membered ring intermediate (INT1), which is a barrier-free exothermic reaction of 22.9 kJ mol^{-1}; the second step is that INT1 isomerizes to a three-membered ring product (P1a) and a H-transfer product (P1b) *via* transition states TS1a and TS1b, with energy barriers of 45.1 and 43.4 kJ mol^{-1}, respectively. As the barrier difference is only 1.7 kJ mol^{-1}, Reactions **a** and **b** mutually compete.

Reaction (2): the channel for forming the bicyclic compound (P2)

In Reaction (2), INT1 further reacts with ethylene (R2) to form a bicyclic compound (P2). The geometrical parameters of the intermediate (INT2), transi-

tion state (TS2) and the product (P2) appearing in Reaction (2) are given in Fig. 3. The energies are listed in Table I and the potential energy surface for the cycloaddition reaction is shown in Fig. 2. The unique imaginary frequencies of the transition state TS2 is 180.1 cm^{-1} and, consequently, the transition state can be affirmed as a real one. According to the calculations of the IRC of TS2 and further optimization for the primary IRC results, TS2 connects INT2 with P2.

TABLE I. Zero point energy (*ZPE* / a. u.), total energies (E_T / a. u.) and relative energies (E_R / kJ·mol^{-1}) for the species from various theoretical methods ($^aE_T = E$ (Species)+*ZPE*, $^bE_R = = E_T - E_{(R1+R2)}$, $^bE_R = E_T - E_{(INT1+R2)}$)

Reaction	Species	*ZPE*	MP2/6-31G*		CCSD(T)//MP2/6-31G*	
			^aE_T	^bE_R	^AE_T	^BE_R
Reaction (1)	R1+R2	0.07620	–155.19440	0.0	–155.27029	0.0
	INT1	0.08701	–155.21863	–63.62	–155.27902	–22.9
	TS1a (INT1–P1a)	0.08502	–155.20073	–16.62	–155.26185	22.2
	P1a	0.08726	–155.30944	–302.04	–155.36961	–260.8
	TS1b (INT1–P1b)	0.08372	–155.19920	–12.60	–155.26250	20.5
	P1b	0.08838	–155.32180	–334.49	–155.38185	–292.9
Reaction (2)	INT1+R2	0.13905	–233.45162	0.0	–233.54891	0.0
	INT2	0.13961	–233.45378	–5.7	–233.55087	–5.1
	TS2 (INT2–P2)	0.14093	–233.45086	–2.0	–233.54875	0.4
	P2	0.14823	–233.59602	–379.1	–233.68358	–353.6

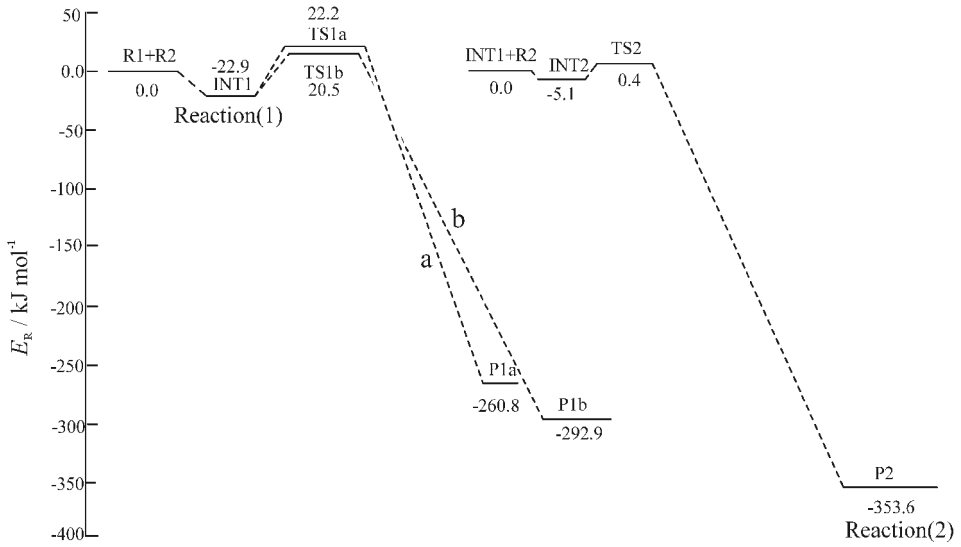

Fig. 2. The potential energy surface for the cycloaddition reactions of vinylidene and ethylene at the CCSD(T)//MP2/6-31G* level.

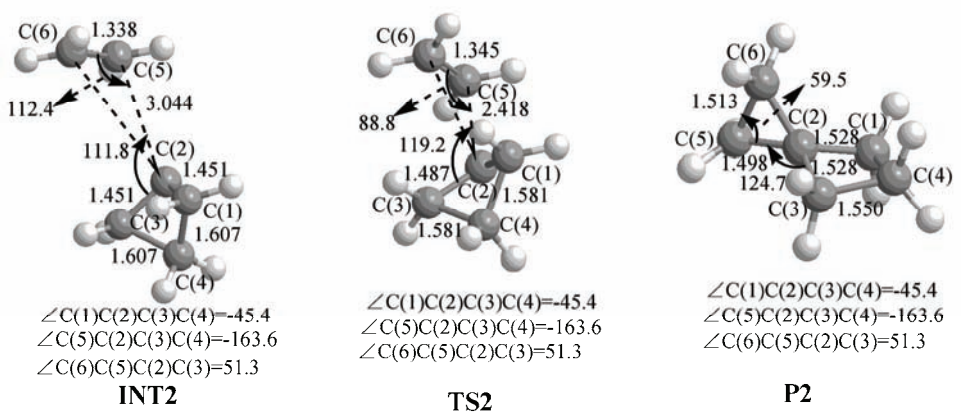

Fig. 3. Optimized MP2/6-31G* geometrical parameters and atomic numbering for INT2, TS2 and P2 in the cycloaddition reaction (2), in which the bond lengths and bond angles are given in angstroms and degrees, respectively.

According to Fig. 2, it can be seen that the reaction pathway of reaction (2), based on the two reactants (R1, R2) forming the intermediate (INT1), involves INT1 further reacting with ethylene (R2) to form the intermediate INT2, which is also a barrier-free exothermic reaction of 5.1 kJ mol^{-1}. In the next step, the intermediate (INT2) isomerizes to the bicyclic compound (P2) *via* a transition state (TS2), with an energy barrier of 5.5 kJ mol^{-1}. Comparing reaction (2) with reaction (1), two reactions mutually compete for INT1 but because INT1 →P1a and INT1→P1b have to climb over barriers of 45.1 and 43.4 kJ mol^{-1}, respectively, while INT1+R2→INT2 can directly reduce the system energy by 5.1 kJ mol^{-1}, reaction (2) is the dominant reaction pathway.

Theoretical analysis and explanation of the dominant reaction pathway

According to the above analysis, the dominant reaction pathway of the cycloaddition reaction between singlet state vinylidene and ethylene as follows:

$$R1 + R2 \rightarrow INT1 \xrightarrow{+R2} INT2 \xrightarrow{TS2} P2 \qquad \text{Reaction (2)}$$

The frontier molecular orbitals of R1, R2 and INT1 in these reactions are shown in Fig. 4. According to Fig. 4, the mechanism of the reaction can be explained with the schematic frontier molecular orbitals diagrams (Figs. 5 and 6) and Figs. 1 and 3. According to Figs. 1 and 5, when the vinylidene (R1) interacts with ethane (R2), due to the two π orbital in the reactants; a [2+2] cycloaddition reaction occurs, forming the four-membered ring carbene (INT1). In INT1, because of the unsaturated character of the C(2) atom from carbene, INT1 reacts further with ethylene (R2) to form the bicyclic compound (P2). The mechanism of the reaction can be explained by Figs. 3 and 6 as: INT1 initially interacts with ethane (R2), the sp lone electron of C(2) in INT1 and the π^* unoccupied orbital

of ethene forming a sp→π* donor–acceptor effect, resulting in the formation of the intermediate INT2; as the reaction proceeds, the C(2)–C(5) bond (INT2: 3.044 Å; TS2: 2.418 Å; P2: 1.498 Å) gradually shortens after the transition state (TS2) due to further sp^3 hybridization of the C(2) atom from carbene in INT1. Finally, INT2 isomerizes to the bicyclic compound P2.

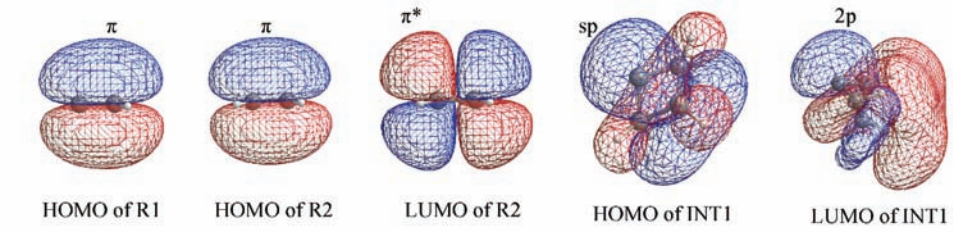

Fig. 4. The frontier molecular orbitals of R1, R2 and INT1.

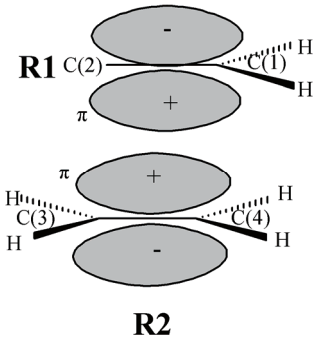

Fig. 5. A schematic interaction diagram for the frontier orbitals of H_2C=C: (R1) and H_2C=CH_2 (R2).

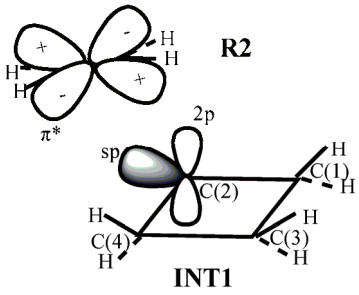

Fig. 6. A schematic interaction diagram for the frontier orbitals of INT1 and H_2C=CH_2 (R2).

CONCLUSIONS

From the potential energy profile of the cycloaddition reaction between singlet vinylidene (H_2C=C:) and ethane, forming a bicyclic compound, it can be predicted that this reaction has one dom inant channel. The dominant channel of this reaction consists of three steps: *i*) the two reactants first form a four-membered ring carbene (INT1) through a barrier-free exothermic reaction of 22.9 kJ mol^{-1};

ii) the four-membered ring carbene INT1 further reacts with ethane (R2) to form an intermediate (INT2) through a barrier-free exothermic reaction of 5.1 kJ mol^{-1}; *iii*) INT2 isomerizes to a bicyclic compound (P2) *via* a transition state (TS2) with an energy barrier of 5.5 kJ mol^{-1}.

И З В О Д

AB INITIO ПРОУЧАВАЊЕ МЕХАНИЗМА РЕАКЦИЈЕ ЦИКЛОАДИЦИЈЕ КОЈОМ НАСТАЈЕ БИЦИКЛИЧНО ЈЕДИЊЕЊЕ ВИНИЛИДЕНА (H_2C=C:) И ЕТИЛЕНА

XIUHUI LU, ZHENXIA LIAN и YONGQING LI

School of Chemistry and Chemical Engineering, University of Jinan, Jinan, Shandong, 250022, P. R. China

Механизам реакције циклоадиције којом настаје бициклично једињење синглетног винилидена (H_2C=C:) и етилена испитиван је коришћењем CCSD(T)MP2/6-31G* методе. На основу профила потенцијалне енергије може да се предвиди да ова реакција има један доминантан пут. Приказани реакциони пут, [2+2] реакција циклоадиције између два реактанта, која се одиграва стварањем четворочланог карбенског прстена (INT1), у којем неспарени sp електрон C атома из карбена у INT1 и π* непопуњена орбитала етана остварују sp→π* донор–акцептор ефекат, што резултује настајањем интермедијара (INT2). Због даље sp^3 хибридизације C атома из карбена у INT1, INT2 се изомеризује у бициклично једињење (P2) преко прелазног стања (TS2).

(Примљено 20. августа, ревидирано 21. септембра 2010)

REFERENCES

1. P. Stang, *Acc. Chem. Res.* **15** (1982) 348
2. P. Stang, *Chem. Rev.* **78** (1978) 384
3. R. Krishnan, M. J. Frisch, J. A. Pople, *Chem. Phys. Lett.* **79** (1981) 408
4. M. J. Frisch, R. Krishnan, J. A. Pople, *Chem. Phys. Lett.* **81** (1981) 421
5. D. J. Wardrop, W. Zhang, *Tetrahedron Lett.* **43** (2002) 5389
6. K. S. Feldman, A. L. Perkins, *Tetrahedron Lett.* **42** (2001) 6031
7. Y. Apeloig, M. Karni, P. J. Stang, D. P. Fox, *J. Am. Chem. Soc.* **105** (1983) 4781
8. D. P. Fox, P. J. Stang, Y. Apeloig, M. Karni, *J. Am. Chem. Soc.* **108** (1986) 750
9. X. H. Lu, Y. X. Wang, *J. Phys. Chem. A* **107** (2003) 7885
10. X. H. Lu, W. R. Wu, H. B. Yu, X. L. Yang , Y. H. Xu, *J. Mol. Struct. (Theochem.)* **755** (2005) 39
11. X. H. Lu, H. B. Yu, W. R. Wu, Y. H. Xu, *Int. J. Quantum Chem.* **107** (2007) 451
12. X. H. Lu, P. P. Xiang, W. R. Wu, X. Che, *J. Mol. Struct. (Theochem.)* **853** (2008) 82
13. L. A. Curtis, K. Raghavachari, J. A. Pople, *J. Chem. Phys.* **98** (1993) 1293
14. K. Fukui, *J. Chem. Phys.* **74** (1970) 4161
15. K. Ishida, K. Morokuma, A. Komornicki, *J. Chem. Phys.* **66** (1977) 2153.

Journal of the Serbian Chemical Society
JSCS-info@shd.org.rs • www.shd.org.rs/JSCS
J. Serb. Chem. Soc. 76 (5) 751–756 (2011)
JSCS–4156
UDC 621.383.51:546.181.1–151+
541.135.1:541.147
Original scientific paper

Phosphonium iodide as a donor liquid electrolyte for dye-sensitized solar cells

HUI LI*, HONGSHI JIANG, CHENZHONG YAO and JIAN WANG

Department of Applied Chemistry, Yuncheng University, Yuncheng, Shanxi 044000, P. R. China

(Received 1 December 2009, revised 30 July 2010)

Abstract: An efficient triphenylmethylphosphonium iodide-based liquid electrolyte was synthesized and used for the first time as an electrolyte in dye-sensitized solar cells (DSSCs). With the as-synthesized electrolyte, the DSSC yielded an overall light to electricity conversion efficiency of 5.34 to 7.10 %, when the radiant power was tuned from 100 to 10 mW cm^{-2}. This may be attributed to the limitation of mass transport in the DSSC. The electronic and ionic processes in the DSSC were investigated by electrochemical impedance spectroscopy and linear voltammography, respectively.

Keywords: dye-sensitized solar cells; tripheny lmethylphosphonium iodide; mass transport; conversion efficiency.

INTRODUCTION

Dye-sensitized solar cells (DSSCs), which are usually composed of an interconnected nanocrystalline TiO_2 electrode anchored with photosensitizers, a liquid electrolyte typically containing I_3^-/I^- as the redox couple and a Pt counter electrode,[1] have drawn much interest in the past decade. This kind of DSSCs were considered as potential high-efficient and low-cost alternatives to conventional inorganic photovoltaic modules.[2] Their photovoltage is determined by the difference between the Fermi level of the TiO_2 electrode under illumination and the Nernst potential of I_3^-/I^- in the electrolyte.[3] It was concluded that tuning the composition of the electrolyte enhances the open-circuit voltage. Meanwhile, the properties (conductivity, viscosity, *etc.*) of the electrolyte are believed to play a role in the photovoltaic performance of DSSCs by affecting the kinetics of electronic and ionic processes.[4,5] The designing and preparation of a suitable electrolyte component iodide is critically necessary to improve the performance of DSSCs.

* Corresponding author. E-mail: lihuiwf@gmail.com
doi: 10.2298/JSC091201055L

Recently, imidazolium salt-based electrolytes were successfully applied to dye-sensitized solar cells,[2,4–7] and sulfonium salts also showed potential application as electrolytes in DSSCs.[8] However, phosphonium salts as electrolytes for DSSCs have received limited attention, even though they have been used in supercapacitors.[9] There has only been one paper reporting phosphonium salts, excluding triphenylmethylphosphonium iodide, as electrolytes in DSSCs, and the highest light to electricity conversion efficiency under a light intensity of 8.9 mW cm^{-2} was 5.7 %.[10] Furthermore, it was found that triphenylmethylphosphonium iodide was more air-stable than the expensive and water-sensitive LiI,[11] which is mostly used in DSSCs. Herein, triphenylmethylphosphonium iodide (TPMI) was synthesized and used for the first time in the electrolyte for DSSCs. Electric impedance spectroscopy was used to investigate the ionic and electronic processes in the DSSC under varied light intensities.

EXPERIMENTAL

Triphenylmethylphosphonium iodide (TMPI) was synthesized according to a literature method.[12–14]. Briefly, a solution of tripheny lphosphine (PhP3) (19 mmol, 5.0 g) in dry tetrahydrofuran (THF) was added dropwise to a solution of CH_3I (20 mmol, 2.9 g) in dry THF at room temperature. The reaction mixture was stirred for 12 h and filtered. The white precipitate was then rinsed with dry THF and recrystallized from ethanol/ether. ^{1}H-NMR (300 MHz; CCl_3D, δ / ppm): 7.61–7.86 (15H, *m*), 1.24 (3H, *m*). The as-synthesized TMPI at a concentration of 0.5 M togeth er with 0.05 M I_2 and 0.6 M 4-tertb utylpyridine (TBP) in acetonit rile was used as the electrolyte for the DSSCs.

A mesoporous TiO_2 electrode was prepared by depositing a paste containing TiO_2 nanoparticles (P25, Degussa) and ethyl cellulose in terpineol onto a conducting glass substrate (F--doped SnO_2, FTO) using a screen-printing technique. The coated substrate was sintered at 450 °C in air for 0.5 h. Then, the sintered porous thin film with a thickness of *ca.*12 μm was immersed into a 3×10^{-4} M solution of the dye *cis*-dithiocyanate-*N,N*'-bis(4,4'-dicarboxylate--2,2'-bipyridine) ruthenium(II) (N3) in dry ethanol for about 12 h, after which the dye-anchored film was rinsed with dry ethanol. A platinized counter electrode was prepared by spin-coating an H_2PtCl_6 solution (50 mM in 2-propanol) onto FTO glass and sintering at 390 °C for 0.5 h. A sandwich-type solar cell was fabricated by clamping the TiO_2/N3/electrolyte with a counter electrode with two clips. The active electrode area was 0.16 cm^2.

The electrochemical impedance spectra (EIS) and linear sweep voltammograms were both obtained with an AutoLab model PGSTAT 30 potentiostat. The EIS was obtained in the frequency range of 0.1 Hz to 10^6 Hz with an AC amplitude of 5 mV. Linear sweep voltammograms of symmetric electrochemical cells consisting of two identical platinized FTO separated by Scotch tape of 45 μm were used to estimate the apparent diffusion coefficient of I_3^- in the electrolytes of TPMI in acetonitrile. The photovoltaic performance of the DSSC was measured with a Keithley 2400 digital source meter controlled by a computer and a 500 W xenon lamp as the light source to give simulated AM 1.5 irradiation.

RESULTS AND DISCUSSION

The photocurrent-voltage curves of a DSSC employing the N3 dye and the TPMI-based electrolyte under different light intensities are shown in Fig. 1. The

photovoltaic performance parameters under different radiant power are listed in Table I. The highest conversion efficiency of 7.10 % was obtained at a moderate radiant power of 10 mW cm^{-2}. This is the highest efficiency that has been achieved so far for DSSCs under moderate power irradiation with phosphonium salts as the electrolyte. When the light intensity was increased to 100 mW cm^{-2}, the overall energy conversion efficiency was 5.34 %. The reduction of conversion efficiencies with increasing light intensity is related to limitation in the mass transport of triiodide ions between the electrodes in DSSCs.[15]

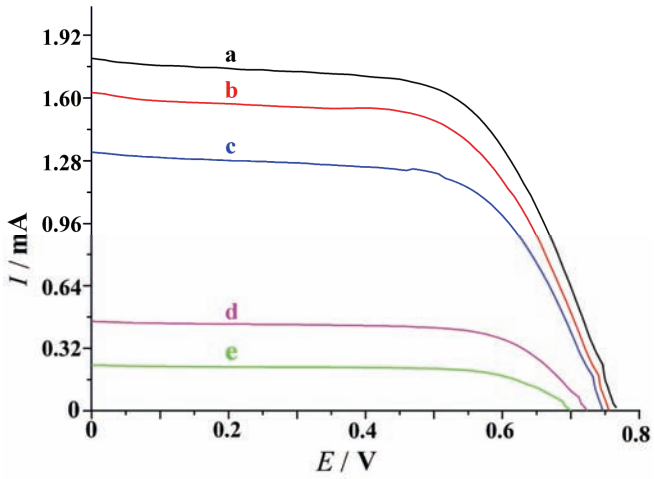

Fig. 1. Photocurrent–voltage characteristics of the DSSC under varied light intensities (AM 1.5): a) 100; b) 80; c) 60; d) 20; e) 10 mW cm^{-2}.

The electric impedance spectra of a DSSC measured at open circuit voltage (–0.75 V) with and without irradiation in the frequency range 0.1–10^6 Hz are presented in Fig. 2. The three semicircles in the high frequency, intermediate and low frequency regions in each impedance spectrum of Fig. 3 can be assigned to the impedance of charge transfer at the Pt/electrolyte interface (Z_1), electron transfer occurring at the TiO_2/dye/electrolyte interface (Z_2), and Nernst diffusion within the electrolyte (Z_3), respectively. The charge-transfer resistance Z_1 in the dark and at 40 mW cm^{-2} were both less than 10 Ω cm^2, indicating a good catalytic performance of the Pt counter electrodes for the reduction of triiodide ions. The impedance Z_2, characterizing electron transfer from the conduction band of the mesoscopic TiO_2 film to triiodide ions in the electrolyte, was much smaller at 40 mW cm^{-2} than that in the dark even though the potential of the film was the same. The smaller is the impedance Z_2, the faster is electron recombination under irradiation, which can reduce the efficiency of electron injection from the sensitizer N3 to the conduction band of TiO_2.[4] In comparison with the internal resis-

tance of the DSSC,[16] the Warburg diffusion impedance Z_3 can be neglected. In addition, the impedance over 10^6 Hz cannot be measured due to instrumental limitations. The resistances R_S with and without irradiation in the high frequency range $>10^6$ Hz due to the resistance of electrolyte and sheet resistance of FTO were almost the same in Fig. 3, which confirms that R_S was dominated by the sheet resistance of FTO. From Fig. 3 and Table I, it may be proposed that fast electron recombination in the DSSC with irradiation is detrimental to the power conversion efficiency.

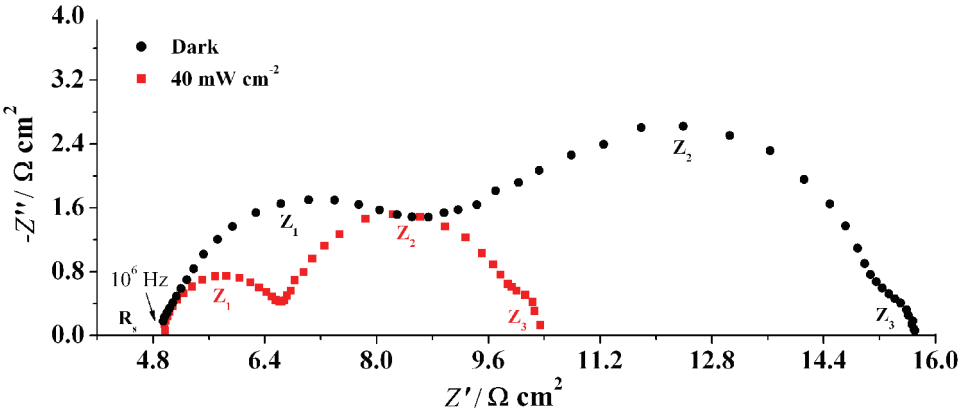

Fig. 2. Electrochemical impedance spectra of a DSSC. Z_1, Z_2 and Z_3 correspond to the frequency regions: 10^6 – 470 Hz, 470 – 1.7 Hz and 1.7 – 0.1 Hz, respectively, at –0.75 V and 40 mW cm^{-2} (■) and in the dark (●).

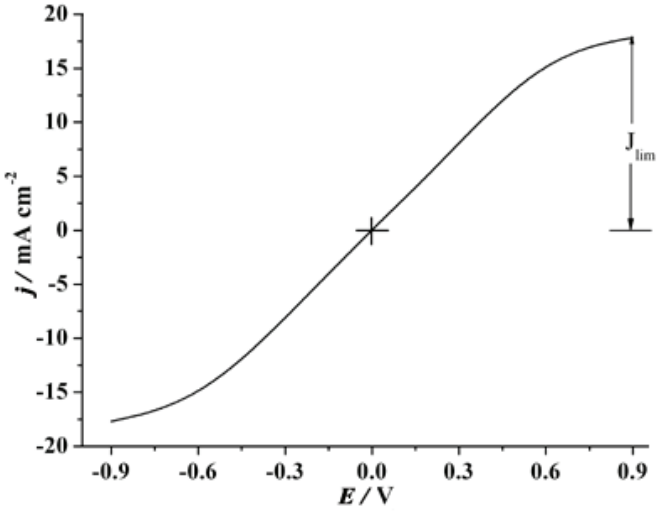

Fig. 3. Characteristic voltammogram for the symmetrical electrochemical cells. Scan rate: 10 mV s^{-1}.

TABLE I. Photovoltaic performance of the DSSC with TPMI-based electrolyte under various irradiation powers (AM 1.5), P, incident power; V_{oc}, open circuit voltage; j_{sc}, short circuit current density; η, power conversion efficiency

P / mW cm^{-2}	V_{oc} / mV	j_{sc} / mA cm^{-2}	FF	η / %
10	700.9	1.4	0.69	7.10
20	724.5	2.9	0.68	7.09
60	747.5	8.3	0.63	6.52
80	755.9	10.3	0.61	5.94
100	765.5	11.3	0.62	5.34

In order to further elucidate the mass transport in the DSSC, a symmetric FTO/Pt/electrolyte/Pt/FTO electrochemical cell was employed to determine the apparent diffusion coefficient of triiodide, which was considered as the current-limiting species due to their lower concentration in the electrolyte (the molar ratio of I^- to I_3^- is 1:10). The characteristic linear sweep voltammetry curve of the TPMI based electrolyte is presented in Fig. 3. The resemblance between the anodic and cathodic limiting current plateaus indicates steady-state conditions. The apparent diffusion coefficient (D_{app}) of triiodides can be calculated from the limiting current densities according to the equation, $J_{lim} = 2nFC_0D_{app}/d$,[17] where $n = 2$ is the electron-transfer number required for the reduction of triiodide to iodide, F is the Faraday constant, C_0 the bulk concentration of triiodide ions and d the thickness of the cell. From the data shown in Fig. 3, the diffusion coefficient of triiodide in the TPMI based electrolyte at room temperature was determined to be about 7.6×10^{-6} cm^2 s^{-1}, which is roughly half of that of the LiI electrolyte in acetonitrile giving a larger current density of 16.8 mA cm^{-2}.[18,19] This sheds light on the cause of the smaller current density of 11.3 mA cm^{-2} in the DSSC based on TPMI liquid electrolyte and, consequently, the relatively low power conversion efficiency of 5.34 % at 100 mW cm^{-2}, AM 1.5.

CONCLUSIONS

In conclusion, triphenylmethylphosphonium iodide as an I^- donor in acetonitrile was for the first time used in a DSSC and the energy conversion efficiency at 10 mW cm^{-2} (AM 1.5) was up to 7.10 %. The ionic and electronic processes in the DSSC were investigated *via* electric impedance spectroscopy and cyclic voltammogram. It was found that the rapid electron recombination at high intensities of irradiation was detrimental to the power conversion efficiency. The short-circuit current densities at high intensity irradiation were related to the mass transport of I_3^-, which has a diffusion coefficient of 7.6×10^{-6} cm^2 s^{-1}. This is valuable information for the design and improvement of the electrolyte components for DSSCs.

Acknowledgement. We thank the College Research Program of Yuncheng University [2008114] for funding.

И З В О Д

ФОСФОНИЈУМ-ЈОДИД КАО ДОНОР У ТЕЧНОМ ЕЛЕКТРОЛИТУ ЗА СОЛАРНЕ ЋЕЛИЈЕ СЕНЗИБИЛИСАНЕ БОЈОМ

HUI LI, HONGSHI JIANG, CHENZHONG YAO и JIAN WANG

Department of Applied Chemistry, Yuncheng University, Yuncheng, Shanxi 044000, P. R. China

Синтетисан је ефикасан течан електролит на бази трифенилметилфосфонијум-јодида и по први пут је коришћен као електролит за соларне ћелије сензибилисане бојом. Са овим електролитом соларна ћелија је показала укупан степен конверзије светлосне енергије у електричну између 5,34 и 7,10 %, при снази зрачења у опсегу од 100 до 10 mW cm^{-2}. Овај резултат се може приписати ограничењима у преносу масе у соларној ћелији. Електронски и јонски процеси у соларној ћелији су испитивани спектроскопијом електрохемијске импеданције и линеарном волтаметријом, респективно.

(Примљено 1. децембра 2009, ревидирано 30. јула 2010)

REFERENCES

1. B. O'Regan, M. Grätzel, *Nature* **353** (1991) 737
2. H. Kim, G. P. Kushto, C. B. Arnold, Z. H. Kafafi, A. Piqué, *Appl. Phys. Lett.* **85** (2004) 464
3. F. Pichot, B. A. Gregg, *J. Phys. Chem. B* **104** (2000) 6
4. Q. Wang, J. E. Moser, M. Grätzel, *J. Phys. Chem. B* **109** (2005) 14945
5. Y. Wang, Y. Sun, L. Kang, *Mater. Lett.* **63** (2009) 1102
6. K. Hara, T. Nishikawa, K. Sayama, K. Aika, H. Arakawa, *Chem. Lett.* **32** (2003) 1014
7. J. H. Park, J. H. Yum, S. Y. Kim, M. S. Kang, Y. G. Lee, S. S. Lee, Y. S. Kang, *J. Photochem. Photobiol. A* **194** (2008) 148
8. H. Paulsson, A. Hagfeldt, L. Kloo, *J. Phys. Chem. B* **107** (2003) 13665
9. E. Frackowiak, G. Lota, J. Pernak, *Appl. Phys. Lett.* **86** (2005) 164104
10. R. E. Ramírez, E. M. Sánchez, *Sol. Energy Mater. Sol. Cells* **90** (2006) 2384
11. J. Kiddle, *Tetrahedral Lett.* **41** (2000) 1339
12. K. Alem, G. Belder, G. Lodder, H. Zuilhof, *J. Org. Chem.* **70** (2005) 179
13. G. K. Mor, O. K. Varghese, M. Paulose, K. Shankar, C. A. Grimes, *Sol. Energy Mater. Sol. Cells* **90** (2006) 2011
14. J. B. Baxter, E. S. Aydil, *Appl. Phys. Lett.* **86** (2005) 53114
15. P. Wang, B. Wenger, R. Humphry-Baker, J. Moser, J. Teuscher, W. Kantlehner, J. Mezger, E. V. Stoyanov, S. M. Zakeeruddin, M. Grätzel, *J. Am. Chem. Soc.* **127** (2005) 6850
16. L. Han, N. Koide, Y. Chiba, T. Mitate, *Appl. Phys. Lett.* **84** (2004) 2433
17. N. Papageorgiou, Y. Athanassov, M. Ar mand, P. Bonhôte, H. Pettersso n, A. Aza m, M. Grätzel. *J. Electrochem. Soc.* **143** (1996) 3099
18. A. Hauch, A. Georg, *Electrochim. Acta* **46** (2001) 3457
19. K. Hara, T. Nishikawa, M. Kurashige, H. Kawauchi, T. Kashima, K. Sayama, K. Aika, H. Arakawa, *Sol. Energy Mater. Sol. Cells* **85** (2005) 21.

Journal of the Serbian Chemical Society
JSCS-info@shd.org.rs • www.shd.org.rs/JSCS
J. Serb. Chem. Soc. 76 (5) 757–768 (2011)
JSCS–4157
UDC 666.762.8+541.183+546.21:
544.723.3+544.032.4
Original scientific paper

Characterisation of surface oxygen groups on different carbon materials by the Boehm method and temperature-programmed desorption

ANA M. KALIJADIS[1*#], MARIJA M. VUKČEVIĆ[2#], ZORAN M. JOVANOVIĆ[1#], ZORAN V. LAUŠEVIĆ[1#] and MILA D. LAUŠEVIĆ[2#]

[1]*Laboratory of Physics, Vinča Institute of Nuclear Sciences, P. O. Box 522, 11000 Belgrade and* [2]*Faculty of Technology and Metallurgy, University of Belgrade, Karnegijeva 4, 11000 Belgrade, Serbia*

(Received 24 December 2009, revised 27 October 2010)

Abstract: The surface characteristics of different carbon materials: activated carbon, carbon felt, glassy carbon and a porous carbon monolith were investigated. The specific surface area was examined by the BET method with N_2 adsorption, the amount and the type of surface oxygen groups by Boehm titration as well as by temperature-programmed desorption (TPD). By comparing the results obtained using BET analysis with those of TPD and the Boehm method, it was found that the number of surface groups was not proportional to the specific surface area. The total amount of oxygen groups, obtained by TPD, is higher than the amount obtained by Boehm's method for porous samples. The inconsistencies between these results originate from the fact that the Boehm method is limited to the determination of acidic and basic groups, whereas TPD provides information on the total number of all surface oxygen groups. In addition, the presence of porosity could reduce the solvent-accessible surface in the Boehm method. The TPD profiles of CO evolution showed the presence of a low temperature maximum, below 650 K, which originates from CO_2 reduction on the carbon material surface.

Keywords: carbon materials; surface oxygen groups; temperature programmed desorption.

INTRODUCTION

Many applications of carbon materials are strongly influenced by their surface chemistry. Thus, their uses in catalysis,[1] adsorption in solution or electrochemical processes[2,3] are the examples of the influence of surface chemistry on

* Corresponding author. E-mail: anaudovicic@vinca.rs
# Serbian Chemical Society member.
doi: 10.2298/JSC091224056K

the performance of materials. Many properties of carbon materials are decisively influenced by chemisorbed oxygen, which can be bound in the form of various functional groups. The surface of carbons is heterogeneous and consists of the faces of basal planes and of edges of such layers. The edge sites are much more reactive than the atoms in the interior of the basal planes, and they represent active sites for oxygen chemisorptions. Therefore, surface oxygen groups are predominantly located on the edges.[4,5]

Surface oxygen groups on carbon materials are usually determined by titrations in aqueous solutions. One of the standard methods is the Boehm method.[5–7]. Additionally, temperature programmed desorption (TPD),[8–12] X-ray photoelectron spectroscopy (XPS),[13,14] or methods involving diffuse reflectance FTIR (DRIFTS)[15,16] can also be used.

In the present study, both the Boehm titration and the TPD method were employed for the determination of oxygen groups on the surface of different carbon materials: activated carbon (AC), carbon felt (CF), glassy carbon (GC) and porous glassy carbon monolith (CM). TPD provides quantitative information on the total number of surface oxygen groups, while the Boehm titration method gives both qualitative and quantitative information only about basic and acidic groups (in the form of carboxyl, lactone and phenol). Surface oxygen complexes on carbon materials decompose upon heating by releasing CO and CO_2, thus, the TPD peaks of CO and CO_2 at different temperatures correspond to specific oxygen groups. For example, CO_2 is released by decomposition of carboxylic groups at 373–673 K,[17,18] or lactone groups at 463–923 K.[18,19] Both CO and CO_2 peaks originate from the decomposition of carboxylic anhydrides in the temperature range of 623–900 K.[17,18] Phenols, ethers, carbonyls and quinones give rise to CO at 973–1253 K.[18,20] The quantities of CO and CO_2 released during the TPD experiments correspond to the total amount of surface oxygen groups. The decomposition temperature is related to the bound strength of specific oxygen-containing groups. Thus, the position of the peak maximum at a defined temperature corresponds to a specific oxygen complex at the surface. Deconvolution of the TPD profiles gives qualitative information about surface oxygen groups.

The surface oxygen groups on a carbon with acidic (carboxyl, lactone, phenol) as well as basic properties can be determined by the Boehm method. These groups differ in their acidities and can be distinguished by neutralisation with different solutions:HCl (for basic groups) and $NaHCO_3$, Na_2CO_3 and NaOH (for acidic groups).

The objective of this work was to characterize the active sites at the surfaces of different carbon materials by comparison of the results obtained by these two methods.

EXPERIMENTAL

Materials

Four different carbon materials were used:

– activated carbon was obtained from Trayal (Krusevac, Serbia) with granulation of 0.25–1 mm;

– carbon monolith was purchased from Fractal Carbon (London, UK) in the shape of a cylinder (L = 3.0 cm, d = 1.8 cm) containing 8600 capillaries inside the material. This is a composite material consisting of glassy carbon bed and activated carbon on the inner capillary walls;

– carbon felt and glassy carbon were produced at the Institute "Vinča" (Serbia). Viscose felt was impregnated with $ZnCl_2$ and NH_4Cl, carbonised at 1173 K in order to obtain carbon felt, and activated with CO_2 from 873 K to 1173 K.

– GC plates (10 mm×5 mm×0.8 mm) were produced by polymerisation of poly(furfuryl alcohol) and carbonisation of the polymer in an electric oven at 1273 K under a nitrogen atmosphere with a heating rate of 0.2 K min^{-1}.

Measurements

The TPD method in combination with mass spectrometry was used to investigate the nature and thermal stability of the surface oxygen groups of the carbon materials. A custom-built set-up for temperature programmed desorption was used. A quartz tube was placed inside an electrical furnace and coupled with an Extorr 3000 quadrupole mass spectrometer (Extorr Inc.), which was used as a detector for the gases evolved from the surface of the carbon materials. Data acquisition during the heating time was achieved using appropriate software (Extorr Inc.). The signals, as partial pressures (torr), at m/z 28 and 44 (CO and CO_2) were simultaneously recorded as a function of time (s). The instrument was calibrated using analytical grade calcium carbonate and calcium oxalate (amounts in the range of 15–60 μmol). Accurately measured amounts of the chemicals were placed in the quarts tube, outgassed at room temperature to 10^{-7} torr and then subjected to TPD at a linear heating rate of 10 K min^{-1} to 1173 K. A calibration of the instrument was necessary to calculate the constants of the experimental system (K_{co2} and K_{co}). These constant represent the coefficient of proportionality between the amount of examined evolved gases (mol g^{-1}) and the integration area under the corresponding TPD profiles (torr s). The constants of the experimental system were calculated from the obtained results as described in the literature.[21] The TPD profiles of samples of the carbon material (0.1 g) were obtained under identical experimental conditions as those employed for the calibration measurements. The TPD plots obtained were deconvoluted using multiple Gaussian functions, taking the position of the peak centre as the initial estimate. CO_2 reduction during TPD experiment was examined by comparing TPD profile of $CaCO_3$ and of the same amount of $CaCO_3$ in the presence of GC. For this purpose, the GC was preheated to remove all surface oxygen groups and to obtain a reasonably clean carbon surface before mixing with $CaCO_3$.

The specific surface areas of carbon materials were determined by nitrogen adsorption at liquid nitrogen temperature using a Micromeritics ASAP 2020 MP apparatus. The nitrogen adsorption isotherms were analysed using the Brunnauer, Emmett and Teller (BET) method.[22]

The oxygen groups on a carbon material surface that has acidic or basic properties are conveniently determined by titration methods. The surface groups of the studied carbon materials were determined by the Boehm method. The acidic sites were determined by mixing small quantities (0.1 g) of each carbon material with 10 ml of different bases (0.1 M NaOH,

0.1 M $NaHCO_3$ or 0.05 M $NaCO_3$) in 25 ml beakers. The beakers were sealed and shaken for 24 h. The solutions were then filtered and titrated with 0.05 M H_2SO_4. Similarly, the basic sites were determined by mixing 0.1 g of each carbon material with 10 ml of 0.1 M HCl. The obtained solutions were titrated with 0.1 M NaOH.

RESULTS AND DISCUSSION

Surface characteristics of different carbon materials were investigated by comparing the results obtained by BET, the Boehm method and TPD.

Initially, the possibility of CO_2 reduction, as a secondary reaction on a carbon surface, was investigated by recording TPD profiles of $CaCO_3$ and $CaCO_3$ mixed with GC ($CaCO_3$/GC). For this experiment, the GC was preheated. Thus, the total amounts of CO_2 and CO released could only originate from $CaCO_3$ decomposition. Two possible reactions could be the source of CO evolution. One is CO_2^+ fragmentation in the ion source of the mass spectrometer and the second is the reduction of CO_2 gas on the carbon material in the furnace of the TPD apparatus. A typical TPD profile for the thermal decomposition of calcium carbonate is shown in Fig. 1. The major peak at $m/z = 44$, originates from the parent ion CO_2^+ and the minor peak at $m/z = 28$ represents CO^+ formed by fragmentation of CO_2^+ in the ion source.

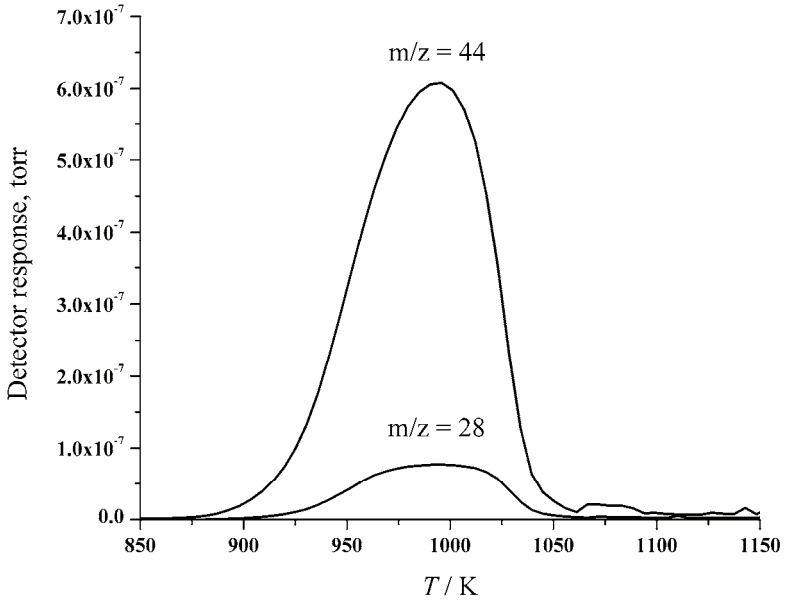

Fig. 1. TPD Profiles for the thermal decomposition of calcium carbonate.

The TPD results for $CaCO_3$ and $CaCO_3$/GC decomposition are compared in Fig. 2. TPD Profile of $CaCO_3$/GC mixture showed an increase in CO evolution and a simultaneous decrease in CO_2 evolution, compared to pure $CaCO_3$. The

peak areas of CO (I_{CO}) and CO_2 (I_{CO_2}) were calculated for both measurements. For $CaCO_3$ decomposition, I_{CO}/I_{CO_2} was 0.13 and in the presence of GC, the ratio was 0.22, due to the increased amount of CO released. Thus, it can be assumed that CO_2 reduction on the carbon surface occurred.

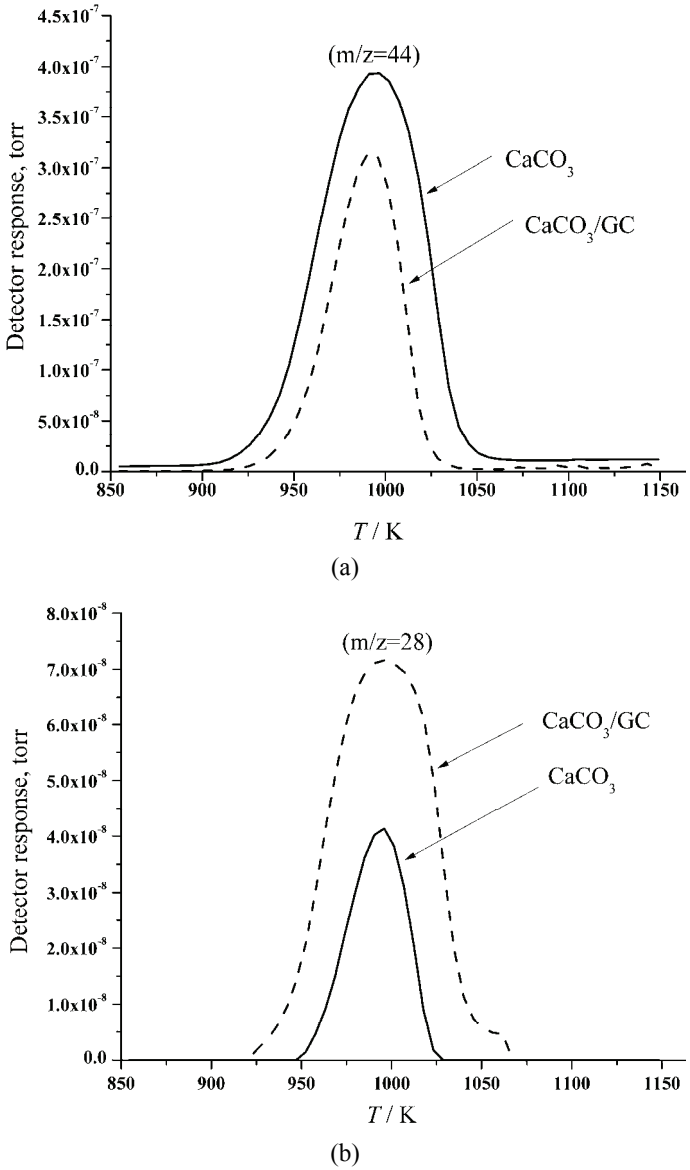

Fig. 2. A comparison of the TPD profiles for the thermal decomposition of $CaCO_3$ and $CaCO_3$/GC; a) m/z = 44 and b) m/z = 28.

The TPD profiles of the examined carbon materials are presented in Figs. 3–6. The CO_2 profiles of all samples show a first maximum in the temperature range from 580 to 640 K, which is very likely due to the decomposition of carboxylic groups. The second maximum appears in the range 880–1030 K, which originates from the more stable anhydrides or lactone groups.

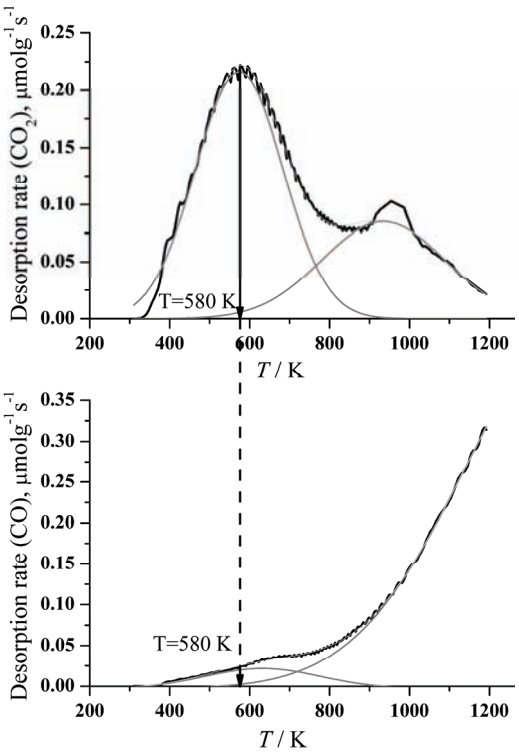

Fig. 3. Deconvoluted CO_2 and CO profiles for activated carbon.

The CO profiles for all carbon material samples had a maximum above 1100 K, which could suggest the existence of anhydride, although it could also be attributed to phenols, ethers, carbonyls or quinones.[17,18,20] TPD profiles also show a local CO maximum at a relatively low temperature, around 600 K (Figs. 3–6), which is unlikely to originate from the decomposition of oxygen complexes. This appearance of this peak could be related to CO_2 reduction on the carbon surface. At higher temperatures, the amount of CO released was relatively high; hence, the overall contribution of CO from CO_2 reduction was not significant and it has a negligible effect on quantitative representation of the TPD results. The origin of the incomplete high temperature process of CO evolution is the temperature limitation of the instrument. The employed instrumental setup has a temperature limit of 1173 K, although surface oxygen groups, that give rise to CO, thermally decompose in temperature range 973–1253 K.[18,20]

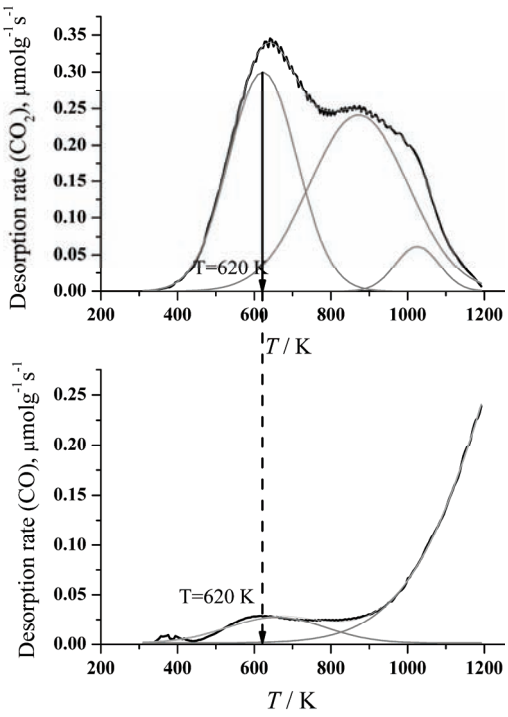

Fig. 4. Deconvoluted CO_2 and CO profiles for carbon monolith.

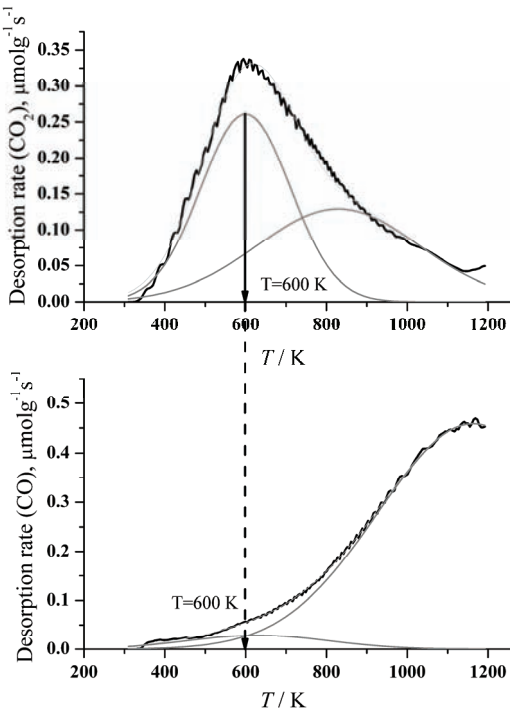

Fig. 5. Deconvoluted CO_2 and CO profiles for carbon felt.

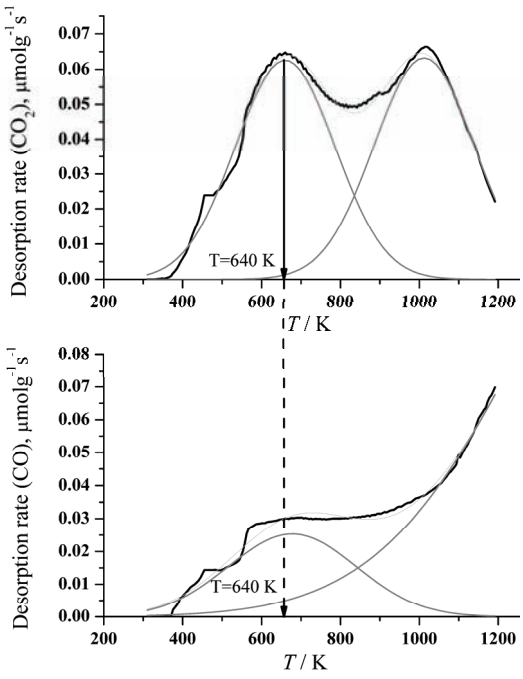

Fig. 6. Deconvoluted CO_2 and CO profiles for glassy carbon.

The decomposition temperature is related to the bound strength of specific oxygen-containing group. Thus, the peak maximum at the defined temperature corresponds to a specific oxygen complex at the surface. In order to separate the amounts of several types of oxygen groups, the acquired TPD profiles were deconvoluted. The obtained results are given in Table I.

TABLE I. Amounts of CO_2 and CO obtained by deconvolution of the TPD profiles

Carbon material	T / K	CO_2 mmol g^{-1}	ΣCO_2 mmol g^{-1}	T / K	ΣCO mmol g^{-1}
AC	580	0.415	0.616	≈ 1150	2.081
	940	0.201			
CM	620	0.454	1.006	≈ 1150	2.005
	870	0.497			
	1020	0.055			
CF	600	0.505	0.919	≈ 1150	2.152
	830	0.414			
GC	640	0.241	0.370	≈ 1150	0.671
	1010	0.129			

The results obtained by the Boehm method and the specific surface areas obtained by the BET method are presented in Table II.

TABLE II. Surface characteristics of the carbon materials obtained by the BET and Boehm method

Carbon material	BET $m^2 g^{-1}$	Basic groups mmol g^{-1}	Acidic groups, mmol g^{-1}			
			Total	Carboxyl	Lactone	Phenol
AC	960	0.683	0.282	0.210	0.043	0.029
CM	150	0.776	0.388	0.228	0.050	0.110
CF	831	0.842	0.684	0.342	0.207	0.135
GC	< 5	0.683	0.434	0.401	0	0.034

Due to the lack of the open porosity, the specific area of the GC sample was below the detection limit of the instrument. From the results obtained by the Boehm titration method, it can be observed that the amount of basic groups was significantly higher than total amount of acidic groups. These results suggest that all carbon materials had a basic character. The largest amount of oxygen groups obtained by the Boehm method was found at the carbon felt surface and the smallest at the activated carbon surface.

The total amount of CO and CO_2 ($\Sigma CO_2 + \Sigma CO$) released in TPD measurements due to decomposition of oxygen complexes follows the order CF > CM > > AC > GC, while the total amount of surface groups obtained in the Boehm titrations follows the order CF > CM > GC > AC (Table III).

TABLE III. Total amount of surface groups obtained by TPD and the Boehm method

Carbon material	TPD method $\Sigma CO_2 + \Sigma CO$, mmol g^{-1}	Boehm method Basic + acidic groups, mmol g^{-1}
AC	2.697	0.965
CM	3.011	1.164
CF	3.071	1.526
GC	1.041	1.117

Comparing the results obtained by these two methods, agreement for the total amount of oxygen groups was found only for the porous materials (AC, CM and CF). Although the TPD results follow the same trend as those of the Boehm method, total amounts of surface groups found were twofold higher than those obtained by the Boehm method. The difference in the results can originate from limitations of the Boehm titration method, which enables the detection of acidic group in the form of carboxylic, lactones, phenols and basic species. However, this method cannot assess the other acidic and neutral groups.

Another reason for the discrepancies in the quantitative results could originate from the fact that in the Boehm method, the presence of porosity could reduce the solvent-accessible surface. Only the GC sample gave comparable results obtained using both methods. GC has no open porosity, and solution can react with the whole surface. In addition, the Boehm method showed that there were no lactone groups at the GC surface; therefore, the CO_2 released from the GC

surface at higher temperatures during the TPD experiments could be assigned to the decomposition of anhydrides. Because anhydride groups can be hydrolysed (Fig. 7) in aqueous solution, as in the Boehm method, rendering two carboxylic groups,[23] it was concluded that the results obtained by TPD and the Boehm method showed acceptable agreement for the carboxylic groups.

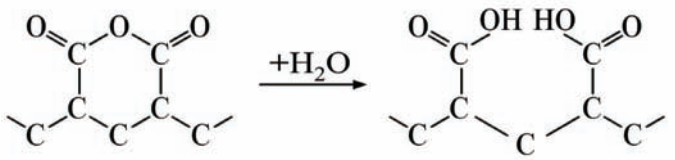

Fig. 4. Hydrolysis of anhydride groups in aqueous solution

The values of the specific surface areas of the different samples were compared with the amounts of surface oxygen groups obtained by the Boehm's method and TPD. It can be observed that the number of oxygen groups was not proportional to the specific area, since the expected increase of the amount of the oxygen groups with the increased specific surface area was not observed. For example, the GC sample, with a low specific area, encloses a large number of oxygen containing groups. According to obtained results, it was found that the specific surface area has no crucial influence on the amount of surface oxygen groups. The number of active sites located at the edges of the basal plane defines the amount of chemisorbed oxygen and has more influence on the amount of surface oxygen groups than the specific surface area.

CONCLUSIONS

The objective of this work was to characterize the surface chemistry of different carbon materials with different porous textures. All the tested carbon materials had a basic character. The results obtained by the Boehm method showed the highest amount of surface oxygen groups on the carbon felt and the lowest on the activated carbon. Comparing the results obtained using BET analysis with those obtained by TPD and the Boehm titration method, it was found that the number of surface groups was not proportional to the specific surface area, but more likely influenced by the number of active sites located at the edges of basal planes. For the non-porous GC sample, the total amount of all oxygen groups obtained by both methods was similar. However, the total amounts of oxygen groups on the porous carbon surface (AC, CM and CF) obtained by TPD were higher than the amounts obtained by the Boehm titration method because of limitations of the latter method. The secondary reaction of CO_2 reduction on the carbon surface had a negligible effect on the determination of the surface oxygen groups. The integration of the results obtained by both the Boehm method and

TPD enabled the provision of unique i nformation about the surface chemistry of the samples.

Acknowledgements. Authors acknowledge the financial support of this work provided by the Ministry of Scienc e and Technological Development of the Republic Serbia through t he projects "Physics and Chemistry with Ion Bea ms", No. 15 1005B, and "Basic Research in Chemistry", No. 142002.

ИЗВОД

КАРАКТЕРИЗАЦИЈА ПОВРШИНСКИХ КИСЕОНИЧНИХ ГРУПА РАЗЛИЧИТИХ КАРБОНСКИХ МАТЕРИЈАЛА БЕМОВОМ (BOEHM) МЕТОДОМ И ТЕМПЕРАТУРСКИ ПРОГРАМИРАНОМ ДЕСОРПЦИЈОМ

АНА М. КАЛИЈАДИС[1], МАРИЈА М. ВУКЧЕВИЋ[2], ЗОРАН М. ЈОВАНОВИЋ[1], ЗОРАН В. ЛАУШЕВИЋ[1] и МИЛА Д. ЛАУШЕВИЋ[2]

[1]*Лабораторија за физику, Институт за нуклеарне науке Винча, п. пр. 522, 11000 Београд и* [2]*Технолошко–металуршки факултет, Универзитет у Београду, Карнегијева 4, 11000 Београд*

Испитиване су површинске особине различитих карбонских материјала: активног угља, карбонског филца, стакластог угљеника и порозног карбон монолита. Специфична површина узорака испитивана је BET методом, а количина и тип површинских група Бемовим титрацијама и температурски програмираном десорпцијом (TPD). Поредећи резултате добијене BET методом са резултатима TPD-а и Бемове титрације, закључено је да број површинских група није пропорционалан специфичној површини узорака. Укупан број кисеоничних група код порозних узорака, добијен на основу TPD-а, је већи него у случају Бемових титрација. Разлог неслагања резултата ових двеју метода потиче из чињенице да је Бемов метод ограничен на одређивање само киселих и базних група, док TPD даје информацију о укупном броју свих кисеоничних група. Такође, код Бемовог метода, постојање порозности може смањити раствору доступну површину. TPD спектри издвајања CO показали су ниско-температурски максимум, испод 650 K, који потиче од редукције CO_2 на површини карбонског материјала.

(Примљено 24. децембра 2009, ревидирано 27. октобра 2010)

REFERENCES

1. A. F. Pérez-Cadenas, F. Kapt eijn, J. A. Moulijn, F. J. Maldonado-Hódar, F. Carrasco-Marín, C. Moreno-Castilla, *Carbon* **44** (2006) 2463
2. C. Brasquet, B. Rousseau, H. Estrade-Szwarckopf, P. Le Cloirec, *Carbon* **38** (2000) 407
3. B. F. Abramović, V. J. Guz svány, F. F. Gaál, Z. V. Lauševi ć, *J. Serb. Chem. Soc.* **66** (2001) 179
4. K. Kinoshita, *Carbon, electrochemical and physicochemical properties*, 1st ed., Wiley, New York, 1988, p. 86
5. H. P. Boehm, *Carbon* **40** (2002) 145
6. H. P. Boehm, *Carbon* **32 (**1994) 759
7. T. Vasiljević, M. Baćić, M. Laušević, A. Onjia, *Mat. Sci. Forum* **453** (2004) 163
8. S. Haydar, C. Moreno-Castilla, M. A. Ferro-García, F. Carrasco-Marín, J. Rivera-Utrilla, A. Perrard, J. P. Joly, *Carbon* **38** (2000) 1297
9. G. S. Szymański, Z. Karpiński, S. Biniak, A. Świątkowski, *Carbon* **40** (2002) 2627
10. M. F. R. Pereira, S. F. Soares, J. J. M. Órfão, J. L. Figueiredo, *Carbon* **41** (2003) 811

11. J.-H. Zhou, Z.-J. Sui, J. Zhu, P. Li, D. Chen, Y.-C. Dai, W .-K. Yuan, *Carbon* **45** (2007) 785
12. A. A. Perić-Grujić, O. M. Neškovi ć, M. V. V eljković, Z. V. Laušević, M. D. Laušević, *Bull. Mater. Sci.* **30** (2007) 587
13. C. Kozlowski, P. M. A. Sherwood, *Carbon* **24** (1986) 357
14. J. B. Donnet, G. Guilpain, *Carbon* **27** (1989) 749
15. A. Dandekar, R. T. K. Baker, M. A. Vannice, *Carbon* **36** (1998) 1821
16. J. L. Figueiredo, M. F. R. Pereira, M. M. A. Freitas, J. J. M. Órfão, *Carbon* **37** (1999) 1379
17. Y. Otake, R. G. Jenkins, *Carbon* **31** (1993) 109
18. U. Zielke, K. J. Hüttinger, W. P. Hoffman, *Carbon* **34** (1996) 983
19. B. Marchon, J. Carrazza, H. Heinemann, G. A. Somorjai, *Carbon* **36** (1988) 507
20. D. M. Nevskaia, A. Santianes, V. Muñoz, A. Guerrero-Ruíz, *Carbon* **37** (1999) 1065
21. J. Wang, B. McEnaney, *Thermochim. Acta* **190** (1991) 143
22. S. Brunauer, P. H. Emmett, E. Teller, *J. Am. Chem. Soc.* **60** (1938) 309
23. M. Domingo-García, F. J. López Garzón, M. J. Pérez-Mendoza, *J. Colloid. Interface Sci.* **248** (2002) 116.

Journal of the Serbian Chemical Society
JSCS-info@shd.org.rs • www.shd.org.rs/JSCS
J. Serb. Chem. Soc. 76 (5) 769–780 (2011)
JSCS–4158
UDC 66.061+54.06:544.354–128.2–039.6+504.53
Original scientific paper

A comparison of sample extraction procedures for the determination of inorganic anions in soil by ion chromatography

SVETLANA M. STANIŠIĆ[1], LJUBIŠA M. IGNJATOVIĆ[1*#], MILICA C. STEVIĆ[1#] and ALEKSANDAR R. ĐORĐEVIĆ[2]

[1]*Faculty of Physical Chemistry, University of Belgrade, Studentski Trg 12–16, Belgrade and* [2]*Faculty of Agriculture, University of Belgrade, Nemanjina 6, Zemun, Serbia*

(Received 11 September, revised 26 October 2010)

Abstract: Three different extraction techniqu es were used for aqueou s extraction of anions from soil of the type Ranker that was sampled from a serpentine site. The first technique involved the use of a rotary mixer (rotary mixer assisted extraction), the sec ond, a microwave digestion system (microwave assisted extraction), with different extraction te mperatures for every cycle during th e procedure as follows: 50, 100 and 150 °C. An ultrasonic bath (ultrasonic assisted extraction) was used for the last technique in which the durations of the extraction process were: 10, 20, 30, 40 and 50 min. The concentrations of inorganic anions in the soil extracts after filtration were determined by ion chromatography. The results showed that the microwave-assisted extraction was highly efficient, giving, at a te mperature of 150 ° C, several times higher amounts of extracted anions in water than the other two technique s. Moreover, the extracted amounts of anions obtained by means of an ultrasonic bath with an extraction time ranging from 10 to 50 min were similar to those obtained by means of the rotary mixer with an extraction time of 22 h. However, extraction using the rotary mixer was more reliable, since the extracted amounts of anions obtained by means of an ultrasonic bath do not correlate with prolongation of the extraction time.

Keywords: soil sample extraction; inorganic anions extraction; ion c hromatography.

INTRODUCTION

The contents of inorganic anions and the mineral composition of soil are the results of different biological, physicochemical, chemical and physical processes, which are themselves the results of the influence of pedogenetic factors.[1] Bonma-

* Corresponding author. E-mail: ljignjatovic@ffh.bg.ac.r
# Serbian Chemical Society member.
doi: 10.2298/JSC100911069S

rito *et al.*[2] demonstrated, by analyzing 120 samples of soil from rural, suburban and urban areas, *via* HPLC and IC, that different concentration of inorganic anions in soil, which vary in their spatial and temporal parameters, was the consequence not only the chemical composition of the soil, but also of anthropogenic and natural influences.

The more important inorganic anions in soil, NO_3^-, NO_2^-, Cl^-, HCO_3^-, SO_4^{2-}, $H_2PO_4^-$, HPO_4^{2-}, PO_4^{3-} and F^-, are found as soil constituents. In this role, they are a matter of interest in environmental science. Additionally, they can act as pollutants, as in the case of the increased concentration of sulphates due to atmospheric deposition in developed industrial areas. It should be pointed out that anions as soil constituents and their concentrations are especially significant for agriculture, not only as components in plant nutrition, but also as a restrictive factor in vegetable production in the case of increased concentrations, *i.e.*, carbonates, sulphates and chlorides in naturally saline soils, such as solonchaks.[3]

All the above mentioned indicates the considerable importance of the determination of the concentrations of anions in soil. This is equally important for a large number of scientific and practical fields, such as water-use management, registration and monitoring of the concentration of chemical species in soil, the monitoring of industrial and mining areas, environmental protection, agricultural crop improvement, preservation of forest ecosystems and the development of ecology.

The determination of the concentrations of inorganic anions can be realized by the analysis of soil solutions *in situ*[4] (by using porous cups, porous plates, capillary wicks, resin boxes and lysimeters), the analysis of solutions extracted from soil using the techniques of drainage, centrifugation or liquid–liquid substitution[5] or, as is the case with the method used in this study, by analyzing soil extract obtained through applying different techniques for the extraction of anions from mixtures of soil and water or some other extraction solvent.

The quantity of anions extracted from soil depends, among other factors, on the type of solvent used for the extraction, the extraction time, temperature and pressure, soil/solvent ratio and composition and characteristics of the soil from which the sample was taken.

Previous studies dealt, largely, with the possibility of extracting separate anions from soil samples using different extraction solvents. Fluoride extraction was realized using aqueous $CaCl_2$, KCl or $AlCl_3$ solutions, within the concentration values from 1.0×10^{-3} to 1.0×10^{-1} mol l^{-1}. The studies showed that the highest amount of fluorides was extracted by the use of $AlCl_3$, while the results obtained from the employment of the other two extraction solvents depended on the pH value of the soil sample.[6] Several studies[7] showed that the use of an exchange resin resulted in 6 to 20 times more fluorides being extracted than the use of water or an aqueous $CaCl_2$ solution regardless of the soil type from which the

sample was taken. Soft extraction solvents[8] that were used include 0.01 mol l^{-1} HCl, 1.0 mol l^{-1} and 0.02 mol l^{-1} NH_4Cl and 1.0 mol l^{-1} $CaCl_2$, giving varying results depending on the soil type, while 5 mol l^{-1} NaOH, 70 % $HClO_4$, concentrated HCl and H_3PO_4,[9] were used as concentrated extraction solvents. The conclusion was that two times more fluorides were extracted when NaOH and H_3PO_4 were used than with the other mentioned solvents. The extraction of sulphates was realized using aqueous solutions of LiCl, $CaCl_2$, $Ca(H_2PO_4)_2$,[10] with no significant difference in the obtained extraction results, while an analysis of extractions from a gypsum-free soil sample using water, 0.1 mol l^{-1} NaCl, 0.016 mol l^{-1} KH_2PO_4 and 0.5 mol l^{-1} $NaHCO_3$ showed that water was the most efficient extraction solvent for soils with pH < 6.[11] Nitrates were extracted from soil using saturated (0.35 %) $CaSO_4 \cdot 2H_2O$ in solution with 0.03 mol l^{-1} NH_4F and 0.015 mol l^{-1} H_2SO_4, 0.01 mol l^{-1} $CaCl_2$, 0.5 mol l^{-1} $NaHCO_3$ and 2.0 mol l^{-1} KCl, of these KCl, at different molarities was used for nitrate extraction more often than the others.[12]

In relation to the simultaneous extraction of several anions from soil sample, studies[13] were performed using soft extraction solvents, 0.01 mol l^{-1} H_3PO_4, deionised water and 0.01 mol l^{-1} NaOH, with the conclusion that NaOH was the most efficient system for fluoride, bromide and sulphate extraction, while chloride extraction gave varying results depending on the soil type.

In addition to the comparison of the efficiency of different extraction solvents, the influence of extraction time on the achieved results was investigated. However, no study has hitherto involved the use of a rotary mixer, microwave digestion system or ultrasonic bath for soil sample preparation with aim of increasing the efficiency of inorganic anions extraction.

Deionised water that was used as a soft extraction solvent has hydrolytic and dissolving effect on salts contained in soil samples. This dissolving effect is present to a greater extent when simple inorganic salts that are highly soluble (nitrates, nitrites, chlorides and sulphates of sodium and magnesium and sodium carbonate), fairly soluble (gypsum) and sparingly soluble (Ca and Mg carbonates and Ca, Fe and Al phosphates), and to a lesser extent with complex salts (alumino-silicates) and organic compounds.[14]

In this study, different extraction techniques were employed to extract the anions from soil using water as the extractant. The efficiencies of the techniques were investigated by ion chromatographic determination of the extracted anions.

EXPERIMENTAL

Chemicals and procedures

The soil sample was taken from a site covered with natural vegetation that had been exposed to minimal influences of anthropogenic pollution at the location Bubanj Potok near Belgrade, Serbia. The soil sample, weighing 1.0 kg in total, was obtained by combining samples taken from the surface horizon, rich in humus, from 30 different sites, at a depth of 20 cm.

The depth of the total soil profile at this location is 50 cm. The sample was air dried for 72 h. Then, large fractions were removed, crushed in a mortar and sieved through a 1.0 mm pore diameter sieve. The basic pedological analysis included: the potentiometric determination of the pH in H_2O and 1.0 mol l^{-1} KCl, the humus content after the Turin method, the adsorptive complex of the soil (H, T, S) after Kappen, determination of the soil texture by the pipette method, the hydrolytic acidity after Kappen, the hygroscopic moisture by drying at 105 °C, the moisture loss after heating at 700 °C for 30 min and the soil conductivity by the conductometric method.

Deionised water from a Milli-Q Gradient system (Millipore, USA) was used for the extraction and preparation of all mixtures. The resistivity of the deionised water used was 18.2 MΩ·cm (at 25 °C). The substances used for analysis were of high analytical purity grade. The eluent was prepared by dissolving 3 mmol of Na_2CO_3 (Fluka, Switzerland), previously dried for 2 h at 105 °C) in a litre of deionised and degassed water. The eluent was made on a daily bases and then filtered through a 0.20-µm pore size membrane filter (Phenomenex, USA). A primary multi-anion standard solution, produced by Fluka, Switzerland, (Cat. No. 89886, Lot 1265008) was used for calibration.

The extraction mixtures were prepared in normal flasks, 50 ml volume, by mixing soil sample with deionised water in the ratio 1:10, *i.e.*, 2 g / 20 ml.

Two series, four extractions each, were performed using a rotary mixer (rotary mixer assisted extraction, RAE in the further text) in which the mixture was processed for 22 h at 10 rpm at 20 °C.

The second technique involved the use of an ultrasonic bath (ultrasonic assisted extraction, UAE in the further text) with the mixture positioned at the same place in the bath and at same initial water temperature, 17 °C. Two extractions were made for each of the following extraction times: 10, 20, 30, 40 and 50 min.

The third technique involved the use of a microwave digestion system (microwave assisted extraction, MAE in the further text). Five extractions at each of the following temperatures: 50, 100 and 150 °C, were performed. The given temperature was achieved in 15 min for each extraction cycle, while the extraction itself lasted 15 min. Subsequently, the samples were cooled to room temperature.

In addition, two further extractions were performed on soil that had been dried at 700 °C for 30 min using the ultrasonic bath for a duration of 15 min.

A blank extraction was performed for each of the employed extraction techniques.

When the extraction processes were finished, each of the extraction mixtures was first centrifuged, then filtered through a medium wide pore sized filter paper and finally through a 0.20-µm pore-sized membrane syringe filter (Phenomenex, USA). The soil extracts were preserved at 4 °C in a laboratory refrigerator for the further analyses.

Equipment

An overhead mixer Reax 20/8 (Carl Roth, Germany) rotary mixer and a Transsonic T 760 DH (Elma, Germany) ultrasonic bath with an ultrasonic frequency of 40 kHz and an effective ultrasound power of 170 W were employed for the extractions. The type of the microwave digestion system consisted of an ETHOS 1, Advanced Microwave Digestion Labstation (Milestone, Sorisole, Italy), equipped with 10 Teflon containers. The capacity of the containers was 75 ml each, and the maximum pressure and temperature that could be achieved were 10 MPa and 300 °C. The extraction mixtures were centrifuged using Sigma 2-5 centrifuge (Sigma, Germany) at 2500 rpm.

The employed ion chromatography system was a Metrohm, type 761 Compact IC (Switzerland) with a conductometric detector. The conductometric detection was realized after suppression of the conductivity of the eluent, for which the packed-bed Metrohm Suppressor Module (MSM) was used. The principle of the conductivity suppression is the exchange of Na^+ from the eluent with H^+ from the suppressor module. The result of this is that low conductive species, H_2O and CO_2, are formed in the eluent instead of primary present high conductive Na^+. The separation column used was Metrosep A Supp1-250, with carrier material polystyrene–divinylbenzene copolymer (particle size 7 μm, column dimensions 4.6 mm×250 mm), and with guard column (Metrosep A Supp 1 Guard). The eluent was 3 mM Na_2CO_3 at a flow rate of 1.0 mL min^{-1}. The full-scale range was 50 μS and the injected sample volume was 20 μL for each probe.

RESULTS AND DISCUSSION

A sample of soil, type Ranker, taken from a serpentine site in Bubanj Potok, a rural area near Belgrade, was used as the substrate. The measured pH value in KCl (5 g soil:10 ml KCl) was 6.0, and in deionised water, the pH value was (5 g soil:10 ml water) 6.9. The results of other pedological analysis are given in Table I. The basic pedological analyses were performed not only to determine the chemical properties of the soil, but also to investigate the possible presence of factors that could influence the adsorption of inorganic anions by positively charged colloid particles in the solution. The investigated soil was characterized as rich in humus, with weakly acidic reaction. As other studies demonstrated, the chemical properties of soil can have, to some extent, an influence on extraction results, which should also be considered.

TABLE I. The results of the basic pedological analysis of the soil

Soil parameter	Measurement			
	1	2	3	Mean
Humus, %	5.15	5.23	5.12	5.16
Total C, %	2.99	3.03	2.97	2.99
The sum of base cations, meq 100 g^{-1}	34.6	33.5	39.6	35.9
Large sand particles, %	4.87	6.22	6.83	5.97
Small sand particles, %	30.1	30.8	31.6	30.8
Colloid clay, %	45.8	43.6	41.0	43.4
Silt, %	19.3	19.3	20.6	19.7
Hygroscopic moisture, %	3.1	3.1	3.1	3.1
Heating loss, %	14.2	14.6	14.4	14.4

The results of the determinations of the amounts of fluorides, chlorides, nitrates, phosphates and sulphates present in the extracts obtained using RAE, UAE and MAE are presented in Tables II–IV, respectively.

After accuracy evaluation of the obtained results, it was concluded that the employed analytic method presented an relative standard deviation *RSD* for fluorides of 4.85 %, for chlorides 1.19 %, for nitrates 2.13 %, for phosphates 1.24 % and for sulphates 1.00 %.

TABLE II. The results of determinations of anions after RAE (mg 100 g^{-1} soil)

Sample series No.	No. of extraction	Fluorides	Chlorides	Nitrates	Phosphates	Sulphates
1	1	0.39	3.56	2.22	0.35	1.79
	2	0.43	3.66	2.13	0.21	1.68
	3	0.37	3.38	2.06	0.27	1.76
	4	0.49	3.32	2.35	0.33	1.73
	Mean	0.42±0.07	3.48±0.27	2.19±0.04	0.29±0.14	1.74±0.03
2	1	0.37	3.63	2.17	0.62	1.73
	2	0.27	3.81	2.08	0.34	1.82
	3	0.35	3.85	2.11	0.89	1.75
	4	0.29	3.59	2.00	0.51	1.82
	Mean	0.32±0.05	3.72±0.29	2.09±0.04	0.59±0.29	1.78±0.03
Average concentration		0.37±0.06	3.60±0.28	2.14±0.04	0.44±0.22	1.76±0.03

TABLE III. The results of determinations of anions after UAE (mg 100 g^{-1} soil)

Extraction time min	No. of extraction	Fluorides	Chlorides	Nitrates	Phosphates	Sulphates
10	1	0.41	2.23	1.47	0.34	1.39
	2	0.29	2.79	1.89	0.24	2.41
	Mean	0.35±0.06	2.51±0.20	1.68±0.03	0.29±0.14	1.90±0.03
20	1	0.03	2.53	0.00	0.00	1.50
	2	0.28	3.23	1.27	0.22	1.22
	Mean	0.13±0.02	2.88±0.23	0.63±0.03	0.11±0.14	1.36±0.02
30	1	0.13	4.54	2.13	0.34	1.87
	2	0.25	2.04	1.09	0.00	2.91
	Mean	0.19±0.03	3.29±0.26	1.61±0.03	0.17±0.14	2.39±0.04
40	1	0.21	2.09	1.37	0.00	1.64
	2	0.07	4.97	1.53	0.26	1.82
	Mean	0.14±0.02	3.53±0.28	1.45±0.03	0.13±0.14	1.73±0.03
50	1	0.13	4.23	1.30	0.00	2.63
	2	0.29	2.95	1.72	0.07	1.29
	Mean	0.21±0.03	3.59±0.28	1.51±0.03	0.03±0.14	1.96±0.04

The extraction of fluorides by means of the rotary mixer gave the results presented in Table II, which were, on average, similar to the results of extraction realized using the ultrasonic bath with an extraction time of 10 min. As shown in Table 1, prolongation of the UAE time was not in positive correlation with the amount of extracted fluoride. By using MAE (Table IV, Fig. 1), a significant increase in the amount of extracted anions occurred at a temperature of 150 °C, even up to 4.5 times more than the amount extracted at the lower temperatures.

The UAE of chlorides demonstrated (Table III) that prolongation of the extraction time led initially to an increased amount of extracted ions, first by 10 % and finally to an insignificant 1.7 % when the extraction was extended from 40 to

50 min. Compared to the UAE, the RAE (Table II) was more efficient for the extraction of chloride ions.

TABLE IV. The results of determinations of anions after MAE (mg 100 g^{-1} soil)

Extraction temperature, °C	No. of extraction	Fluorides	Chlorides	Nitrates	Phosphates	Sulphates
50	1	0.18	2.10	12.7	0.43	1.38
	2	0.18	1.71	34.4	0.45	2.69
	3	0.18	2.65	13.0	0.38	5.14
	4	0.18	2.43	18.6	0.41	3.65
	5	0.18	1.87	21.6	0.43	2.45
	Mean	0.18±0.03	2.15±0.17	20.1±0.4	0.42±0.21	3.05±0.06
100	1	0.18	8.25	69.1	0.49	3.94
	2	0.13	5.81	320	0.71	7.66
	3	0.14	9.47	272	1.46	8.16
	4	0.14	8.52	212	0.97	5.36
	5	0.16	7.16	229	0.81	7.82
	Mean	0.15±0.02	7.84±0.15	221±4	0.89±0.44	6.59±0.13
150	1	0.71	37.5	415	1.69	18.5
	2	0.89	45.7	606	1.97	15.3
	3	0.69	32.7	523	2.03	13.9
	4	0.73	35.7	483	1.83	16.7
	5	0.79	41.6	546	1.97	15.2
	Mean	0.76±0.13	38.6±1.5	515±10	1.90±0.95	15.9±0.3

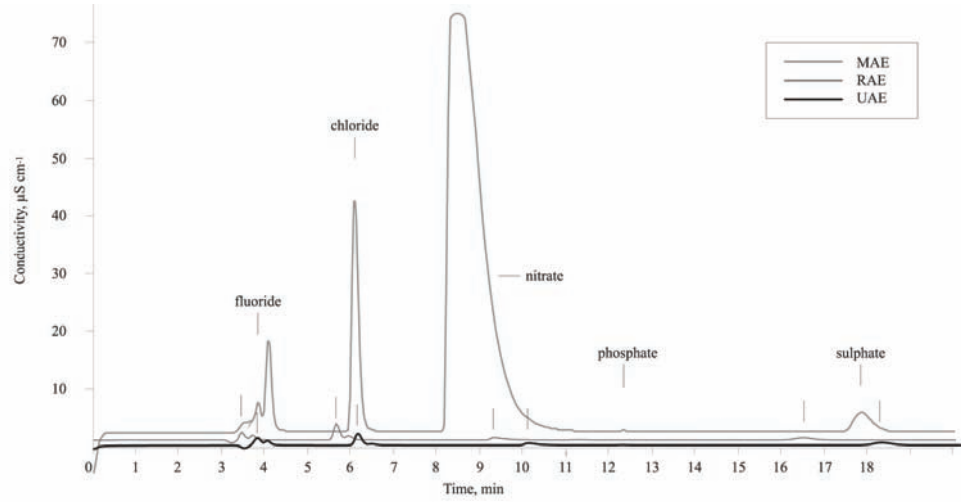

Fig. 1. A comparison of the chromatograms of the soil extracts provided by each of the three extraction techniques.

The average value from the two RAEs was higher than the value obtained by UAE after the longest extraction time, 50 min, which gave the highest extract ed

amount. The concentration of extracted chloride ions by MAE at 100 °C was about two times higher than the highest concentrations obtained by the other two techniques. On increasing the temperature to 150 °C, the obtained concentration was about 12 times higher than the highest concentrations resulting from the use of RAE and UAE.

The UAE of nitrates (Table III) showed the extracted amount of these anions did not vary with changing extraction time. The obtained amount was less than the one obtained by RAE (Table II). Given the fact that nitrates are highly soluble, their concentration determined in the soil solution obtained by centrifugation was almost equal to the amount obtained by extraction with water.[15] The amounts of nitrates obtained by MAE were 10 times higher at a temperature of 50 °C, and even up to 100 times higher at 100 °C, than the amounts obtained using the other two techniques. MAE at a temperature at 150 °C gave concentrations of nitrate ions that were beyond the given measurement range for all probes obtained. After dilution of the extracts, the IC results showed that the extracted amount of nitrate ions obtained at 150 °C was 2.4 times higher than that obtained by extraction at 100 °C (Table IV, Fig. 1).

The UAE of sulphate ions (Table III) gave results demonstrating that the extracted ion amount did not depend on the extraction time. At the same time, the amount of sulphate ions extracted by RAE was almost equal to the average amount of sulphate ions extracted by UAE with extraction times of 10, 20, 30, 40 and 50 min. The MAE results demonstrated (Table IV) also in the case of sulphate ions that significantly increased amounts of extracted ions occurred with increasing extraction temperature. Although there were some variations in the results of each of extractions as the extraction temperature was changed, the average amount of the extracted sulphates at 150 °C was 7 times higher than the highest amount of sulphates extracted by the other two extraction techniques (Fig. 2).

The UAE of phosphates demonstrated that with prolongation of the extraction time to 20 or more minutes, the previously low concentrations of extracted phosphates went beyond the detection threshold. The average concentration of the extracted phosphates obtained by RAE was higher than the concentration extracted by UAE for10 min. The use of MAE at a temperature of 150 °C gave an almost five times higher amount of phosphate ions than the average amount obtained by RAE. The extracted amount of phosphate ions was low, since the investigated soil was formed on a substrate (serpentine) with a low level of P_2O_5. Generally, the average concentration of phosphates in this type of soil ranges from 1–3 mg 100 g^{-1} of soil.[12]

The results of extracted anions from soil sample using the MAE technique showed (Table IV, Fig. 2) that the extracted amounts were higher with increasing extraction temperature.

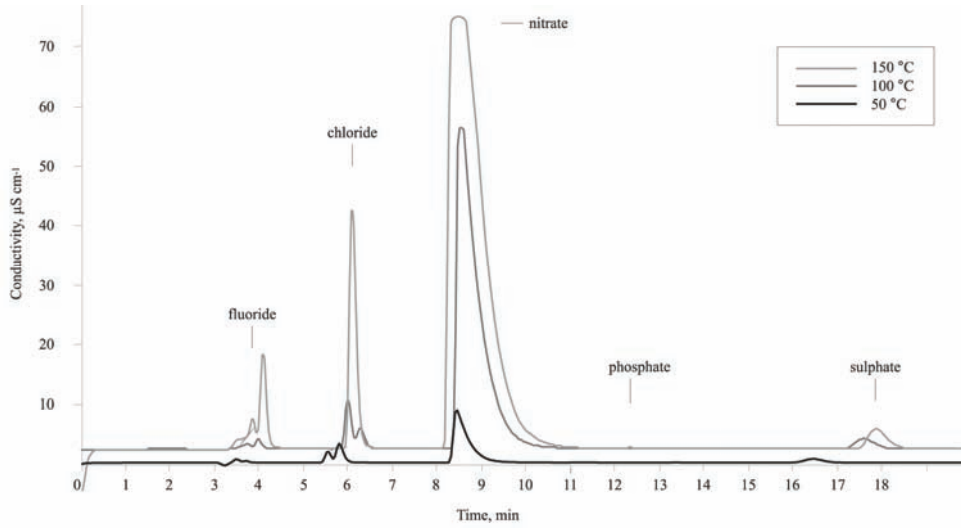

Fig. 2. A comparison of chromatograms of the soil extracts provided by MAE at different temperatures.

Ranker found on serpentine sites is characterized by a low ratio of Ca:Mg of less than one, high concentrations of Ni, Cr and Mn, and a lack of the essential nutrients, such as available nitrogen, potassium and phosphorus, necessary for the growth of agricultural crops.[16] Compared to other soil types, Ranker on serpentine sites has increased concentrations of magnesium that influences the generation of simple inorganic salts which are more soluble, containing a high percentage of crystallized water.

A significant amount of Ni in a soil sample, which gives insoluble $Ni_3(PO_4)_2$ $7H_2O$, can be one of the limiting factors for the extraction of phosphates. Unlike phosphates, the fluorides, chlorides and sulphates of Ni demonstrate relatively high solubilities in water. In addition to this, an investigation of the colloid fraction of the soil (particles ≤ 0.2 µm) evidenced that a certain amount of positively charged colloid particles was present in the soil. These particles have the ability to adsorb anions. The adsorption of anions in soil, that can have negative influence on their extraction, is also influenced by the properties of anions (in accordance with their increasing ability to be adsorbed $Cl^- = NO_3^- < SO_4^{2-} < PO_4^{3-} <$ $< OH^-$), the presence of sesquioxides to a greater extent and the acidic reaction of the soil.[17]

The extraction of anions from a soil sample previously heated at 700 °C for 30 min was realized by means of the ultrasonic bath, with an extraction time of 15 min (Fig. 3). The results showed that the extracted amount of nitrate was 5 times less than the amount extracted under the same conditions from a soil sample that had not been heated. The reason for this can be the conversion of nitrates

of heavy and alkaline earth metals, by heating, into metal oxide, nitrogen dioxide and oxygen. The chromatograms of heated soil samples showed a significant increase of sulphates peak due to sulphur conversion during the combustion of organic matter into sulphate, but also to the possibility that dissolution of sulphate salts occurred.

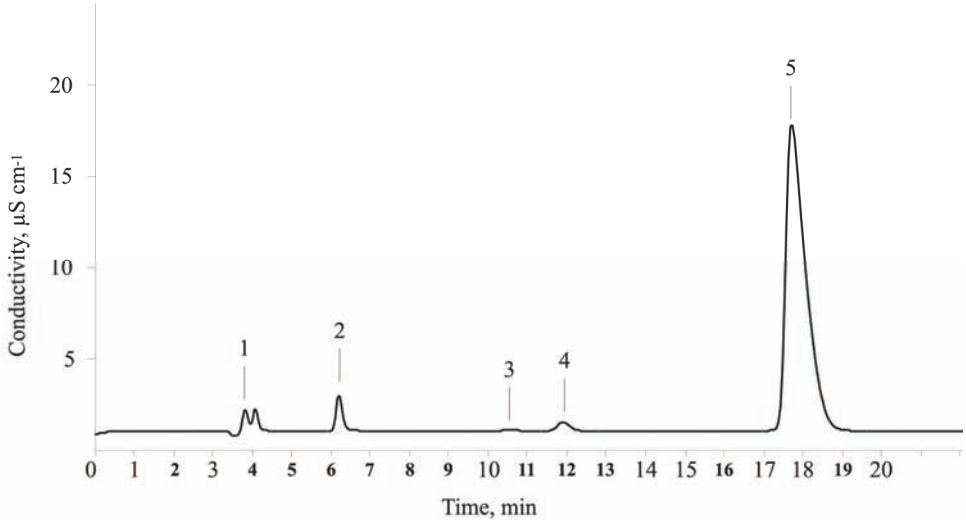

Fig. 3. The chromatogram of the extract of the previously heated soil. Anions concentrations (mg 100 g^{-1} soil; peak number): F^- (0.33; peak 1), Cl^- (3.13; peak 2), NO_3^- (0.31; peak 3), PO_4^{3-} (4.58; peak 4) and SO_4^{2-} (77.0; peak 5).

CONCLUSIONS

The conclusions that can be drawn from the obtained results are that the extraction technique involving the use of an ultrasonic bath was less reliable and less efficient for the simultaneous extraction of inorganic anions from soil than the extraction technique that uses a rotary mixer. In addition, the results of the ultrasonic bath assisted extractions showed that prolongation of the extraction time did not influence the amount of extracted anions, except in case of chloride ions. On the other hand, the ultrasonic assisted extraction is less time consuming and minimizes the expenditure of extraction solvent.

Unlike these two extraction techniques, the microwave-assisted extraction of inorganic anions for later chromatographic determination was efficient, reliable and less time consuming. The amount of anions obtained by microwave-assisted extraction correlated with the increasing extraction temperature and was significantly higher compared to the amounts obtained by conventional techniques for soil sample preparation.

The techniques employed in this study for the preparation of soil samples for analysis can also be applied to other types of soil, and are significant for esti-

mating the concentration of inorganic anions in soil, originating from highly soluble salts. In addition, the results of such preparations of soil samples for ion chromatographic analysis give a certain insight into the concentration of anions in the soil solution, *i.e.*, in the soil liquid phase.

Applying these new techniques for the extraction of anions from soil samples combined with different extraction solvents, *e.g.*, soft extractants, concentrated acid, base or salt solutions, can be considered and requires further investigation. The aim was to improve the extraction procedures and soil analyses, which is important for many scientific and practical reasons.

Acknowledgement. This study was financially supported by the Ministry of Education and Science of the Republic of Serbia (Grant 172030).

ИЗВОД

УТИЦАЈ ПРИПРЕМЕ УЗОРКА ЗЕМЉИШТА НА ОДРЕЂИВАЊЕ НЕОРГАНСКИХ АНЈОНА МЕТОДОМ ЈОНСКЕ ХРОМАТОГРАФИЈЕ

СВЕТЛАНА М. СТАНИШИЋ[1], ЉУБИША М. ИГЊАТОВИЋ[1], МИЛИЦА Ц. СТЕВИЋ[1] и АЛЕКСАНДАР Р. ЂОРЂЕВИЋ[2]

[1]*Факултет за физичку хемију, Универзитет у Београду, Студентски трг 12–16, Београд и* [2]*Пољопривредни факултет, Немањина 6, Земун*

Вршена је екстракција анјона у дејонизованој води, из узорка земљишта типа серпентинита, употребом три различите технике екстракције: употребом ротационе мућкалице у трајању од 22 сата, микроталасне пећнице, уз промену температуре за сваки од циклуса екстракције: 50, 100 и 150 °C и ултразвучне каде, са екстракционим временом од 10, 20, 30, 40 и 50 min. У екстракту земљишта добијеном након филтрације су одређиване концентрације неорганских анјона методом јонске хроматографије. Извршена су поређења резултата за сваку од техника екстракције, чиме је закључено да се екстракција потпомогнута микроталасима показала као веома ефикасна, дајући на температури од 150 °C неколико пута већу количину екстрахованих анјона у поређењу са друге две технике екстракције. Количина екстрахованих анјона употребом ултразвучне каде, са екстракционим временом у распону од 10 до 50 min, је била приближна количини добијеној екстракцијом која користи ротациону мућкалицу, у трајању од 22 h. Ипак, екстракциона техника која користи ротациону мућкалицу се показала као поузданија од технике екстракције потпомогнуте ултразвуком, јер количина екстрахованих анјона при екстракцији уз помоћ ултразвука није у корелацији са продужењем екстракционог времена.

(Примљено 11. септембра, ревидирано 26. октобра 2010)

REFERENCES

1. M. Jakovljević, M. Pantović, *Soil and Water Chemistry*, Faculty of Agriculture, University of Belgrade, Belgrade, Serbia, 1991, p. 144 (in Serbian)
2. C. R. Bonmarito, A. B. Sturdevant, D. W. Szymanshy, *J. Forensic Sci.* **1** (2007) 52
3. G. Sposito, *The Chemistry of Soils*, Oxford University Press, New York, USA, 2008, p. 227
4. L. Weichermüller, J. Siemens, M. Deurer, S. Knoblauch, H. Rupp, A. Göttlein, T. Pütz, *J. Environ. Qual.* **36** (2007) 1735

5. J. Jakmunee, J. Junsomboon, *Talanta* **79** (2009) 1076
6. S. Larsen, A. E. Widdowson, *J. Soil Sci.* **2** (1971) 210
7. S. Supharunsun, M. Wrainwright, *Bull. Environ. Contamin. Toxicol.* **28** (1982) 632
8. C. G. Rodriguez, E. A. R odriguez, M. L. F. Marcos, *Commun. Soil Sci. Plant. Anal.* **32** (2001) 2503
9. A. Phuphatana, E. H. Carlson , R. W. Manus, *Econ. Geol. Bull. Soc. Econ. Geol.* **71** (1976) 661
10. H. A. Ajwa, M. A. Tabatabai, *Commun. Soil Sci. Plant Anal.* **24** (1993) 1817
11. V. Schmalz, T. Griesche k, G. Gerstac ker, E. Worch, *J. Plant Nutr. Soil Sci.* **164** (2001) 577
12. A. R. Đorđević, *Ph.D. Thesis*, Faculty of Agriculture, University of Belgrade, Belgrade, Serbia, 1997, p. 120 (in Serbian)
13. S. E. J. Buykx, M. A. G. T. van den Hoop, P. de Joode, *J. Environ. Monit.* **6** (2004) 552
14. H. L. Bohn, B. L. McNeal, *Soil Chemistry*, 3rd ed., Wiley, New York, USA, 2001, p. 44
15. P. R. Hesse, *A Textbook of Soil Chemical Analysis*, William Clowes, London, 1971, p. 112
16. A. Chiarucci, A. J. M. Baker, *Plant Soil* **293** (2007) 1
17. D. L. Sparks, *Environmental Soil Chemistry*, 2nd ed., Elsevier, San Diego, CA, USA, 2003, p. 174.

Journal of the Serbian Chemical Society
JSCS-info@shd.org.rs • www.shd.org.rs/JSCS
J. Serb. Chem. Soc. 76 (5) 781–794 (2011)
JSCS–4159
UDC 631.452+633+541.183:546.722/.726(497.11)
Original scientific paper

Distribution and forms of iron in the vertisols of Serbia

MIODRAG Ž. JELIĆ[1]*, JELENA Ž. MILIVOJEVIĆ[2], SREĆKO R. TRIFUNOVIĆ[3]**, IVICA G. ĐALOVIĆ[4#], DRAGIŠA S. MILOŠEV[5] and SRĐAN I. ŠEREMEŠIĆ[5]

[1]University of Kosovska Mitrovica, Faculty of Agriculture, Jelene Anžujske, 38228 Zubin Potok, [2]Center for Small Grains of Kragujevac, Save Kovacevica 31, 34000 Kragujevac, [3]Department of Chemistry, Faculty of Science, University of Kragujevac, Radoja Domanovića 12, 34000 Kragujevac, [4]Institute of Field and Vegetable Crops, Maksima Gorkog 30, 21000, Novi Sad and [5]University of Novi Sad, Faculty of Agriculture, Dositeja Obradovića 8, 21000, Novi Sad, Serbia

(Received 19 July, revised 26 October 2010)

Abstract: Soil of arable land and meadows from the Ap horizon, taken from ten different localities, were investigated for different forms of Fe, including total (HF), pseudo-total (HNO_3), 0.1 M HCl extractable and DTPA (diethylenetriaminepentaacetic acid)-extractable. A sequential fractional procedure was employed to separate the Fe into fractions: water soluble and exchangeable Fe (I), Fe specifically adsorbed with carbonates (II), reducibly releasable Fe in oxides (III), Fe bonded with organic matter (IV) and Fe structurally bonded in silicates (residual fraction) (V). The soil pH, cation exchange capacity, and size fractions (clay and silt) had a strongest influence on the distribution of the different forms of Fe. The different extraction methods showed similar patterns of the Fe content in arable and meadow soils. However, the DTPA iron did not correspond with the total iron, which confirms the widespread incidence of iron-deficiency in vertisols is independent of the total iron in soils. The amount of exchangeable (fraction I) and specifically adsorbed (II) iron showed no dependence on its content in the other fractions, indicating low mobility of iron in vertisols. The strong positive correlation (r = 0.812 and 0.956) between the content of iron in HNO_3 and HF and its contents in the primary and secondary minerals (fraction – V) indicate a low content of plant accessible iron in the vertisol. The sequential fractional procedure was confirmed as suitable for accessing the content and availability of iron in the vertisols of Serbia.

Keywords: soil; iron solubility; plant availability; adsorption; distribution of iron.

* Corresponding authors. E-mail: *miodragjelic@yahoo.com; **srecko@kg.ac.rs
# Serbian Chemical Society member.
doi: 10.2298/JSC100619068J

INTRODUCTION

Vertisols are the predominant soils in Central and western Serbia and cover 780 000 ha, which is 8.93 % of the total land area in Serbia. [1] These soils, developed through degradation of lake sediment, are suitable for vegetable, fruit and vine crops production. However, the unfavourable characteristics induced by high clay contents, poor structure (a prismatic polyedric structure with the frequent occurrence of angled aggregates) and generally high acidity could limit their productivity potential.

The distribution and availability of heavy metals in soils is important when assessing the environmental quality of an area, since increased concentrations in soil, water and plants pose a serious threat to human and animal health. The origin of heavy metals in the soil is mainly geochemical (originating from the parent substrate) and partly anthropogenic (various sources of pollution). The soil solution contains considerably small amounts of the microelements, thus heavy metals occur in soil in water-soluble, exchangeable forms, bound to specific sites of the organic and inorganic soil components and in the structure of primary and secondary minerals.[2–5]

The bioavailability, mobility and chemical reactivity of heavy metals in soils are often associated with their distribution among certain soil fractions and the dynamic equilibrium among them.[6,7]

Iron is an important micronutrient which availability could be significantly affected by the soil properties. Generally, the total iron increases with increasing cation exchange capacity (*CEC*) and the clay and silt content. [8] Complexation of iron by soil organic matter may result in increased plant availability, and microbial exudates can supply additional iron to plant routes.[2] Likewise, exchangeable iron adsorbed onto inorganic sites and diethylenetriaminepentaacetic acid (DTPA) extractable iron increase with increasing soil organic matter but decrease with higher soil pH and calcium carbonate content.[4,28]

The determination of the mobile and potentially mobile iron forms is the key issue in the estimation of iron availability to plants. However, the simple selection of methods for their extraction is not sufficient for conceptualisation of their availability, sources or interconnection with a phase of a soil. Accordingly, iron distribution among the different fraction is essential an understanding of their chemistry in soils. Many authors suggested the employment of a sequential extraction procedure for investigation of heavy metals in the environment, sediment of natural origin or in substrates secondarily enriched with heavy metals (*e.g.*, agriculture, industry, road traffic).[7,9–12] These method eliminate the disadvantages of individual extraction procedures and provide information on the total and available content of selected heavy metals in soils, the strength of the bonding and their relationship with specific compounds in the solid phase of soil. [10] Hitherto in Serbia, many single or sequential extraction procedures, mainly based

on the Tessier procedure or different versions thereof, have been applied to soils and sediments to fractionate metals by using different extractants or reagents to obtain more useful information about the bioavailability and mobility of metals.[1,14–16]

The aim of this study was to assess the distribution and forms of iron in the environmental conditions of vertisols soils in Serbia by utilizing different extraction methods and a sequential extraction procedure.

EXPERIMENTAL

The investigations were conducted on vertisols (smonitza) type of soils taken from the Ap horizon at ten different localities in Serbia (Fig. 1): (1) Milutovac, (2) Priština, (3) Trnava, (4) Rekovac, (5) Vranje (Neradovac), (6) Zaječar, (7) Bela Crkva, (8) Blace, (9) Salaš and (10) Kragujevac. The sub-samples were taken from field and meadow ecosystems at a depth of 0 to 20 cm, after which they were air-dried, crushed in a porcelain mortar and sieved through stainless steel screens. Particles 2 mm in size were used for soil characterization and Fe-fraction analyses.

Fig. 1. Geographical locations of the investigated soil samples in the Republic of Serbia.

Determination of the soil characteristics

Soil pH was determined in a suspension in water and 1 M KCl at the ratio of soil:solution ratio of 1:2.5 after a 0.5 h equilibration period; the organic content was determined using the humus method of Kotzmann[27] and the available P_2O_5 and K_2O content was determined using the Egner-Riehm Al method.[13,14] The *CEC* was determined using the method with 1 M NH_4OAc, pH 7, and the particle size distribution was determined by a pipette method. The total iron was determined by atomic adsorption spectrophotometry (AAS, Model Carl Zeis Jena AAS 1N). A cold extraction method was used for the determination of the total and pseudo-total iron in which 0.5±0.001 g of sample was transferred into a centrifuge tube and then 10 mL of 0.5 M HCl was added. The solution was shaken, subjected to vortex for a short time and placed on a shaking-table for agitation for 1 h. After agitation, the solution was centrifuged at 3000 rpm (1,900×g) for 15 min, and then filtered through a 0.45-μm syringe filter to remove particulates.

The total iron was determined by AAS after digestion of the soil sample (0.5 g), which had previously been heated in Pt dishes for 2 h at 450 °C with a mixture of acids (HF, HNO_3 and $HClO_4$). The pseudo-total content of iron was determined by AAS spectrometry after the finely grounded soil sample (2 g) had been digested for 2 h with 20 ml conc. HNO_3 and then treated with 3 ml 30 % H_2O_2 and heated for 15 min.[13]

Sequential fractional procedures

Iron (Fe) in different soil fractions was extracted using the procedure proposed by Tessier *et al.*[10] The methods followed for the fractionation procedures are outlined below:

1. Water soluble and exchangeable metals were determined by extraction with 0.1 M $CaCl_2$ (pH 7.0). 10 g of soil was agitated in plastic pots with 100 cm^3 of solution for 20 min, and then filtered.

2. Specifically adsorbed metals and metals bound to carbonates were determined by extraction with 1.0 M NaOAc (pH 5.0). Again, 10 g of soil was added to 100 cm^3 of solution, agitated for 5 h at room temperature and then filtered. In this case, the sum of 1) and 2) was obtained and by subtraction, fraction 2 was obtained.

3. Reductant releasable Fe occluded in oxides of Fe and Mn was determined in the following manner. 2.5 mg of soil was placed in a centrifuge tube and, after extraction of fractions 1 and 2, 50 cm^3 of 0.04 M hydroxylamine hydrochloride in 25 % of HOAc, pH 3, was added. The tubes were then kept in a water bath for 6 h at 85 °C and stirred. Subsequently, the total volume was set to 50 cm^3 by addition of distilled water, closed and then agitated for 10 min, and centrifuged for 10 min at 3000 rpm. The clear solution was removed into reagent bottles, while the remaining soil was washed with 20 cm^3 of distilled water.

4. Metals bound to the organic matter were determined in the following way. 7.5 cm^3 of 0.02 M HNO_3 and 12.5 ml of H_2O_2 pH 2.0 were added to the test tubes with the soil remaining from the previous three extractions. The tubes were kept in a water bath at 86 °C for 2 h, under stirring. After cooling, 7.5 cm^3 of 30 % H_2O_2 was added and the mixture was again kept at 86 °C for 3 h. After cooling, 12.5 cm^3 of 3.2 M NH_4OAc in 20 % HNO_3 was added. The final volume was set by adding distilled water and then the tubes were closed. They were then shaken for 30 min and centrifuged for 10 min at 3000 rpm. The clear solution was transferred into reagent bottles.

5. Metals structurally bound in silicates (residual fraction) were determined by calculation as the difference between the total content determined with HNO_3–HF–$HClO_4$ and the sum of the first four fractions.

The distribution of iron in the chemical fractions 1–4 was determined by flame AAS (atomic absorption spectrometry).

Statistical analysis

The results obtained for the different contents of iron (total, accessible and different chemical fractions) in the vertisols were statistically evaluated by the Student's *t*-test and the Pearson correlation coefficients.[18]

RESULTS AND DISCUSSION

Basic characteristics of examined Serbian vertisols are given in Table I.

TABLE I. Examined physico-chemical characteristics of vertisols in Serbia (mean, range and standard deviation); *t*-test field: meadow; NS – application of the Student *t*-test showed that there is no statistical significance between the examined characteristics of field and meadow soils

Soil characteristic	Field			Meadow		
	Mean	Range	Standard deviation	Mean	Range	Standard deviation
pH (H_2O)	7.1	5.8–8.1	0.9	6.9	5.6–8.1	0.9
pH (KCl)	6.0	4.6–6.9	0.9	5.8	4.7–7.0	0.9
Humus content, %	3.3	2.5–4.0	0.5	3.5	2.0–5.6	1.1
P_2O_5 mg/100 g	7.7	0.6–28.0	8.5	4.2	0.8–17.8	5.0
K_2O mg/100 g	34.4	19.0–59.6	11.8	31.1	20.4–53.5	10.4
CEC meq/100 g	25.1	15.5–31.5	5.6	23.8	16.9–34.7	6.6
Sand, %	29.6	21.4–36.0	4.8	32.2	22.3–50.5	9.0
Silt, %	24.6	18.8–31.2	3.6	22.8	11.9–29.4	5.6
Clay, %	45.8	33.5–54.4	7.2	44.9	28.9–64.3	11.1
Silt + Clay, %	70.4	64.0–78.6	4.8	67.7	49.5–77.7	9.0

The examined vertisols showed marked heterogeneity in terms of pH, and most of the studied soil samples were acid to slightly alkaline. In terms of the readily available phosphorus content, the selected locations belong to the class of soils with lower availability of this element but the observed level of P_2O_5 varied widely between the different samples: 0.6–28.0 mg/100 g soil for samples from fields and 0.8–17.8 mg/100 g soil for the samples under meadows. The investigated soils showed a moderate to high content of available K_2O. The selected sites of vertisols also differed in their humus contents, with an average of 3.3 (field) and 3.5 % (meadow), and had a high capacity for cation adsorption, range from 15.5 to 34.7 meq/100 g soil.

The average value of total iron (HNO_3–HF–$HClO_4$ extraction) in the tested vertisols was 3.7 (field) and 3.6 % (meadows), ranging from 0.5 to 5 % which are typical values for "normal" land. The variations between the samples could be explained by the differences in the basic physical and chemical properties of the soil. Thus, soils with higher clay contents and higher values of *CEC* contained higher levels of iron. This indicates that the metals in soils with the higher values

of CEC are strongly bounded and could not be subjected to leaching out in the deeper layers. Consequently, the total content of the iron was the higher compared with soils with a less pronounced CEC thus metals are not in form that could be easily adopted by plants, what determines their low accessibility.[5,19]

The extraction of accessible forms of iron using mild extraction agents (0.1 M HCl and 0.005 M DTPA) showed extremely low contents of soluble iron compared to the total iron contents. The solution of 0.1 M HCl extracted two times more iron compared with the 0.005 M DTPA solution, ranging from 53.5 (field) to 60.6 mg/100 g soil (meadow). This observation confirms that the application of 0.1 M HCl solution also transformed the part of iron cations specifically adsorbed on organic and mineral components (oxides, carbonates and silicates), as well as occluded and precipitated iron. The acids also released coordinated bound iron ions from the surface of silica, but these amounts vary considerably depending on the mineralogical composition of soil.[20–22]

Lindsay and Norvell[23] using the DTPA-accessible content of microelements (iron) successfully separated Colorado soils into deficient and well supplied.. Based on the plants response to the application of microfertilizers (Fe), the critical content of DTPA-extracted iron was determined, which was 4.5 mg kg^{-1} for corn and 2.5 mg kg^{-1} for sorghum (sorghum plants are less susceptible to a lack of microelements). Below these values, plants responded to the application of iron, hence it could be considered that this soil was deficient in Fe. Above the value of 4.5 mg kg^{-1} extracted iron, the plants showed no response to the application of iron microfertilizers, therefore these soils were characterized as well supplied.

The relative values of the extracted iron in HNO_3 solution, obtained from the pseudo-total metal contents,[13] show a similar variation in both groups of vertisols, since the decomposition of the crystal lattice of the primary and secondary minerals was not complete. From the vertisol of arable soils, 84.9 % of its total content was extracted by HNO_3, while from the meadows 83.4 %. These data indicate that at least 15–17 % of the total iron content is most likely located in the structures of primary and secondary minerals. These results correspond with those of Hang *et al.*,[25] who found that the average extractability of 4 M HNO_3 for iron was between 76 to 85 % of that of HF for vertisols of the Mississippi River Delta.

In the case of vertisols originating from the fields that are richer in iron, HNO_3 extracts a greater part of the total iron, compared with vertisols from the meadows. However, it was observed that the relative values of the extraction of iron show similar variation in both groups of soil. Based on this, it could be concluded that the higher concentrations of iron in the arable soil was not a prerequisite for its greater solubility and its greater occurrence in the weaker forms of bondage.

In the vertisol of the fields, 0.1 M HCl solution extracted 0.15 % of the total content of iron, whereas 0.005 M DTPA extracted 0.07 %. Considering the indi-

vidual samples, the relative values obtained by extraction with 0.1 M HCl showed greater variation, ranging from 0.06 to 0.22 %, which is in accordance with the greater variation in the total iron content of these soil samples. The relative amounts of iron extracted by 0.1 M HCl solution decreased with increasing total iron content. However, among the individual samples, there were differences in the relative distribution of iron, which is the result of the differences in the pH of the observed soils samples. Particularly important are the samples with the lowest pH values in which the relative iron content, compared to the other samples, was up to nine times higher. Considering the fact that DTPA also extracted the labile forms of microelements from the soil, the amounts of specifically adsorbed iron and iron bound to carbonates was significantly higher in these samples.

Compared to the vertisol of fields, the average value of the relative iron content in the meadow samples extracted with 0.1 M HCl solution was higher (0.18 %), although the average total iron content was lower. The individual samples of vertisol from the meadows showed marked heterogeneity with respect to the relative iron content in the extraction medium (0.03 to 0.38 %), which is most likely caused by differences in the total content of iron and related with variability in the chemical properties of the samples, since the higher prevalence of iron occurs in the samples with the lower pH values. In addition, several soil samples from the meadows, the pH values (in 1 M KCl) of which ranged from 4.7 to 7.0, contained up to 2–6 times more iron. The DTPA iron was not in accordance with the total iron, which confirms the wide incidence of iron-deficiency despite the total amount of iron in the soils.[8,25]

According to the results of the *t*-test (Table II) between the total and accessible iron contents in the tested vertisols, no statistically significant differences in the distribution of iron between the field and meadows was found, as a result of the similar mineralogical composition of the parent material on which these soils are formed.[26,27]

TABLE II. Iron content in the tested vertisols of Serbia determined using different extraction methods (X±sd and interval, mg kg^{-1})

Location	HF	HNO_3	0.1 M HCl	0.005 M DTPA
Field (n = 10)	37000±4516	31200±4036	53.5±14.3	24.6±19.1
	31000–44000	24500–36900	28.0–69.0	7.0–56.0
Meadow (n = 10)	36000±5869	30300±6015	60.6±43.1	30.3±25.3
	28000–44000	22200–36900	25.0–144.0	8.0–86.0
t-Test	0.2117[a]	0.3709[a]	0.7726[a]	1.5102[a]

[a]There is no statistical significance at $p < 0.05$

The analysis of the correlation coefficients showed that the total iron content and capacity for the adsorption of cations (*CEC*) depended moderately (r = 0.49), which correspond with the supposition that soils with higher *CEC* values may

have a greater total content of heavy metals (Table III).[19] In addition, a strong dependence of the total iron content on the clay content and clay content + dust content (r = 0.72 and 0.76, respectively) was observed, due to the capacity of the mechanical fraction to adsorb cations and considerably contribute in the capacity of the whole soil. Accordingly, a negative correlation of the iron content and amount of sand (r = –0.76) was found, since a coarsening of the soil particles results in a decrease of soil sorption capacity and less iron in the structure of the minerals (silicates, quartz) in the larger soil particles [12]. In general, the observed total iron content in soil was almost entirely controlled by its mechanical composition.[8]. The pseudo-total content of iron, in addition to the observed relationships for the total iron content, has a positive correlation with the pH value.[28]

TABLE III. The relative content of iron in different extraction agents (in % of HF-total)

Extraction method/Locality	HF	HNO_3	0.1 M HCl	0.005 M DTPA
Field				
Milutovac	35000	91.1	0.15	0.03
Priština	44000	83.9	0.06	0.03
Trnava	41000	79.5	0.11	0.03
Rekovac	38000	78.9	0.14	0.03
Vranje	35000	91.4	0.19	0.02
Zaječar	34000	78.8	0.10	0.04
Bela Crkva	32000	76.5	0.21	0.17
Blace	35000	94.0	0.15	0.07
Salaš	43000	85.3	0.15	0.10
Kragujevac	31000	89.3	0.22	0.18
X	37000	84.9	0.15	0.07
Meadow				
Milutovac	28000	84.6	0.36	0.07
Priština	41000	90.0	0.35	0.02
Trnava	40000	74.8	0.06	0.04
Rekovac	39000	89.0	0.09	0.06
Vranje	38000	95.8	0.06	0.02
Zaječar	29000	76.6	0.18	0.12
Bela Crkva	28000	80.0	0.38	0.31
Blace	36000	89.3	0.12	0.12
Salaš	44000	83.6	0.03	0.02
Kragujevac	39000	70.4	0.15	0.14
X	36000	83.4	0.18	0.09

The amount of iron extracted from vertisols with a solution of 0.1 M HCl showed no dependence on any set of properties of this type of soil (Table IV).

The greatest influence on the DTPA accessible iron in the Serbian vertisols had the acidity (r = –0.92) and potential acidity (r = –0.89), and to a lesser extent, the content of available potassium and the *CEC*, the correlation coefficients of which were 0.57 and 0.69, respectively. Regarding the fact that the obtained cor-

relation coefficients were negative, it can be concluded that increasing soil acidity increases the solubility of iron, while an increasing content of clay increases the strength of the binding between the clay and iron, and consequently reduces its solubility.

TABLE IV. Correlation coefficients between the total and available content of iron and some soil properties

Soil property	Iron	
	Total (HF)	Pseudo–total (HNO_3)
pH (H_2O)	NS[a]	0.51[b]
pH (1 M KCl)	NS	0.51[b]
Humus content	NS	NS
$CaCO_3$	NS	NS
P_2O_5	NS	NS
K_2O	NS	NS
CEC	0.49[c]	0.52[b]
Sand	–0.76[c]	–0.66[b]
Silt	NS	NS
Clay	0.72[c]	0.52[b]
Silt + Clay	0.76[c]	0.66[c]
	Available content (0.1 M HCl)	Available content (DTPA)
pH(H_2O)	NS	–0.92[c]
pH(nKCl)	NS	–0.89[c]
Humus content	NS	NS
$CaCO_3$	NS	NS
P_2O_5	NS	NS
K_2O	NS	–0.57[b]
CEC	NS	–0.69[c]
Sand	NS	NS
Silt	NS	0.64[c]
Clay	NS	–0.60[c]
Silt + Clay	NS	NS

[a]There was no statistical significance; [b]statistically significant at the probability level 0.05; [c]statistically significant at the probability level 0.01

A similar result was presented in Sharma *et al.*[8] Additionally, they observed a positive correlation with the content of organic matter, following the formation of chelates and the reduction of iron(III) to iron(II), which upon oxidation, precipitates as amorphous iron compounds thereby increasing the solubility of the iron. The DTPA soluble iron in the vertisols showed a statistically significant positive correlation with the content of the mechanical silt fraction, which indicates that coarsening of the soil particles could potentially provide a readily available fraction of iron.

Sequential extraction analysis

Considering the fact that the tested vertisols in Serbia were established at locations with deficient iron content in the parent material, from their sequential extraction (Table V), it is possible to determine the form of their location in the soil, allowing for a clear understanding of their potential mobility and accessibility for plants.

TABLE V. Distribution of iron in the different fractions of vertisols obtained by sequential analyses procedures (mg kg^{-1})

Fraction	I	II	III	IV	V
Field Fe ±*SD*	0.11±0.32	2.62±2.04	4024±1777	221±127	32552±4301
Meadow Fe ±*SD*	0.18±0.22	4.0±5.07	4094±1181	231±146	31970±58881

Based on statistical correlation analysis (Table VI), a highly significant correlation was found between the exchangeable and specifically adsorbed iron (r = = 0.89), which indicates mutual influences of these two fractions. The quantities of exchangeable (fraction I) and specifically adsorbed iron (fraction II) in the investigated vertisols of Serbia showed no dependence on its contents in the other extracted fractions, indicating low mobility of iron in these soils. The negative correlations between the total and residual Fe (fraction V) with the Fe in fraction II (r = –0.46 and –0.51, respectively) and the positive correlation of the total with the residual Fe (r = 0.96) indicate that the mobility of iron is small and that the stable fraction V is correlated with the total iron content. The content of iron in the first fraction has no significant correlation with any soil properties, except pH (Table VII).

TABLE VI. Correlation coefficient between the iron content in different chemical fractions in soil from fields and meadows

Fraction	I	II	III	IV	V	Fe content total (HF)
I	1,00					
II	0.89[a]	1.00				
III	NS[b]	NS	1.00			
IV	NS	NS	NS	1.00		
V	NS	–0.51[c]	NS	NS	1.00	
Fe content total	NS	–0.46[c]	NS	NS	0.96[c]	1.00

[a]Statistically significant at the probability level 0.01; [b]there was no statistical significance; [c]statistically significant at the probability level 0.05

Specifically adsorbed iron and iron related to carbonates (fraction II) gave significant differences and negative correlations with some soil properties, such as pH, clay content and *CEC*. The positive correlation with the silt implies that these factors had a dominant influence on the distribution of iron in this fraction. The negative correlation between the iron content in the specifically adsorbed

iron fraction and the pH value of the soil indicates that the solubility of iron in this fraction decreases with increasing soil pH because high pH values favour the oxidation of Fe^{2+} to Fe^{3+}, which results in the precipitation of iron(III) salts and oxides. The significant negative correlation between the specifically adsorbed iron and the clay content indicates that with increasing clay content, the CEC value increases and hence the association of iron and the solid soil phase, which resulted in reduced mobility and accessibility of the iron in this fraction.

TABLE VII. Correlation coefficients between the iron content in different chemical fractions and some soil characteristics

Soil characteristics	Fraction					
	I	II	III	IV	V	Fe content total
pH (H_2O)	–0.48[a]	–0.70[b]	–0.45[a]	NS[c]	0.54[a]	NS
pH (1M KCl)	NS	–0.64**	–0.46[a]	NS	0.54[a]	NS
Humus content	NS	NS	NS	NS NS		NS
P_2O_5	NS	NS	–0.66[b]	NS	NS	NS
K_2O	NS	NS	–0.70[b]	NS	0.53[a]	NS
CEC	NS	–0.55[b]	–0.49[a]	0.50[a]	0.63[b]	0.49[a]
Sand	NS	NS	NS	NS	–0.78[b]	–0.76[b]
Silt	NS	0.55[b]	NS	NS NS		NS
Clay	NS	–0.50[a]	NS	0.43[a]	0.80[b]	0.72[b]
Silt + Clay	NS	NS	NS	NS	0.78[b]	0.76[b]

[a]Statistically significant at the probability level 0.05; [b]statistically significant at the probability level 0.01; [c]there was no statistical significance

The positive correlation between the iron content in Fraction II and the silt content indicates iron unstably bound with the silt particles, since increasing particle size led to increasing solubility of the iron in this fraction.

The content of extracted iron from the oxide fractions of Fe (Fraction III) is negatively correlated with some soil properties, such as pH value, content of available P_2O_5 and K_2O and the values of *CEC*. Increasing soil pH values decreased the iron content in the third fraction due to the high degree of oxidation of Fe^{2+} compounds and depositions with phosphate. The negative correlation between the iron content in this fraction and the *CEC* value indicates that the increase in surface adsorption increases the bond strength between the solid soil phase and iron, which affects the lower solubility of iron in this fraction.

The amount of iron extracted from the organic matter was positively correlated with the *CEC* values and the clay content. This indicates that the clay and the *CEC* are the dominant factors affecting the distribution of iron in this fraction.

The iron associated with the residual fraction was negatively correlated with sand content and positively with the soil pH values, readily available K_2O, clay, *CEC* and the silt + clay fractions. The negative correlation between the residual iron and sand and a positive correlation with the clay content and silt + clay indi-

cates that most of iron in this fraction is bound to clay particles and silt. The clay fractions usually contain high amounts of metals (Fe) due to high adsorption, as well as the content present in the cry stal lattice. These variations in the a mounts of residual iron with cl ay are in a ccordance with the con clusions of other authors.[28,29]

The positive correlation between iron i n residual fractions and soil pH indicates that base oxidation and environm ental conditions cause iron deposition but reducing conditions its hydrolysis.[4]

Based on the attained results of correla tion coefficients given in Table VIII, DTPA extracted iron gives highl y significant positive correl ations with the iro n content in Fractions I and II ($r = 0.689$ and 0.907, respectively) and a negativ e correlation with the content in fraction V.

TABLE VIII. The correlation coefficients between the content of iron in different chem ical fractions of soil and its contents obtained using different extraction procedures

Extraction procedures	Fraction				
	I	II	III	IV	V
HF	NS[a]	–0.463[b]	NS	NS	0.956[c]
HNO_3	NS	–0.519[b]	NS	NS	0.812[c]
0.1 M HCl	NS	–0.441[b]	NS	NS NS	
0.005 M DTPA	0.689[c]	0.907[c]	NS	NS	–0.557[c]

[a]There was no statistical signif icance; [b]statistically significant at the probability level 0.05; [c]statistically significant at the probability level 0.01

Since the DTPA extractan t gives highly significant correlation coefficients with fractions I and II, it can be us ed to evaluate the accessibility of iron for plants, and this interpretation agrees with the negative correlat ion ($r = –0.557$) between the DTPA extracted iron and the iron content in the structures of the p rimary and secondary minerals.

Unlike the DTPA extracta nt, 0.1 M HCl showed less pronounced statistical significance ($r = 0441$) only with the i ron content in the second fraction and, therefore, cannot be used as a reliable factor in the interpretation the bioavailability of the iron in soils.

The less pro nounced but significant ne gative correlation coefficients ($r =$ $= –0.519$ an d $–0.463$) found between the HNO_3 and HF extract ed iron and it s contents in fractions I and II, respectiv ely, showed that the iron extracted with these acids is not weakly bound iron which is easily accessible to plants. Moreover, this interpretation agrees with the existence of strong posit ive correlations ($r = 0.812$ and 0.95 6) between the con tent of iron i n HNO_3 and HF and its co ntents within the structure of primary and secondary minerals (residual fraction V).

CONCLUSIONS

Analyses using the procedures of sequential extraction showed that the soil samples from arable soils and meadows were similar in the relative distribution of iron among the different fractions. The sequential extraction procedures showed that the iron was mostly built into the lattice of primary and secondary minerals and in the clay minerals of the residual fraction. The iron content in the soils was correlated with the pH value, *CEC* and the aggregate size fraction of silt and clay. The low plant availability of the iron in the vertisols could be explained by its occurrence in the least soluble fraction (Fraction V). The appropriate selection of genotype, foliar application and liming are required for the successful growth of agricultural crops on the examined soils.

Acknowledgment. This research was supported by grants from the Ministry of Science and Technological Development of the Republic of Serbia (Project Nos. TR 31054 and OI 172016).

И З В О Д

ДИСТРИБУЦИЈА И ФОРМЕ ГВОЖЂА У ВЕРТИСОЛИМА СРБИЈЕ

МИОДРАГ Ж. ЈЕЛИЋ[1], ЈЕЛЕНА Ж. МИЛИВОЈЕВИЋ[2], СРЕЋКО Р. ТРИФУНОВИЋ[3], ИВИЦА Г. ЂАЛОВИЋ[4], ДРАГИША С. МИЛОШЕВ[5] и СРЂАН И. ШЕРЕМЕШИЋ[5]

[1]Пољопривредни факултет, Универзитет у Косовској Митровици, Јелене Анжујске, 38228 Зубин Поток, [2]Центар за стрна жита, Саве Ковачевића 31, 34000 Крагујевац, [3]Институт за хемију, Природно–математички факултет,Универзитет у Крагујевцу, Радоја Домановића 12, 34000 Крагујевац, [4]Институт за ратарство и повртарство, Максима Горког 30, 21000 Нови Сад и [5]Пољопривредни факултет, Универзитет у Новом Саду, Доситеја Обрадовића 8, 21000 Нови Сад

У циљу одређивања различитих облика гвожђа у неким варијететима вертисола са подручја Србије (оранице и ливаде) пореклом са десет различитих локалитета анализиран је укупан садржај гвожђа (HF), псеудо-укупан садржај (HNO_3), 0,1 M HCl растворљиво и DTPA растворљиво гвожђе. Секвенцијалном екстракцијом извршено је раздвајање фракција гвожђа на растворљиво у води и размењиво Fe (I), специфично абсорбовано гвожђе са карбонатима (II), оклудовано Fe у оксидима (III), Fe везано за органску материју (IV) и Fe структурно везано у силикатима (резидуални део, V). pH вредност земљишта, CEC и величина фракција (глина и прах) имали су значајан утицај на дистрибуцију различитих облика гвожђа. Различите методе екстракције су показале сличан облик садржаја Fe у обрадивом земљишту и ливади. Међутим, садржај DTPA растворљивог гвожђа не одговара укупном садржају, што потврђује да је учесталост недостатка гвожђа у вертисолима на подручју Србије независна од укупног гвожђа у земљиштима. Износ размењивог гвожђа (фракција I) и адсорбовованог (II) гвожђа није показала зависност од његовог садржаја у другим фракцијама, што указује на ниску мобилност гвожђа у проучаваним вертисолима. Јака позитивна корелација (p = 0,812 и 0,956) између садржаја гвожђа у HNO_3 и HF и његов садржај у примарним и секундарним минералима (фракција V) показују низак ниво гвожђа доступног биљкама у испитиваним вертисолима. Коришћењем секвенцијалне екстракције могуће је утврдити садржај и приступачност гвожђа у вертисолима Србије.

(Примљено 19. јула, ревидирано 26 октобра 2010)

REFERENCES

1. J. Milivojević, M. Jakovljević, M. Jelić, *Acta biologica Jugoslavica: Plant Soil* **54** (2005) 73
2. C. L. MacKowiak, P. R. Grossl, B. G. Bugbee, *Soil Sci. Soc. Am. J.* **65** (2001) 1744
3. G. W. Brümmer, in *The Importance of Chemical "Speciation" in Environmental Processes*, M. Bernhard, F. E. Brinckman, P. J. Sadler, Eds., Springer Verlag, Berlin 1986, p. 169
4. A. Kabata-Pendias, A. Pendias, *Trace elements in soils and plants*, 2nd ed., CRC Press, Boca Raton, FL, USA, 2001
5. D. C. Adriano, *Trace Elements in the Terrestrial Environment*, Springer Verlag, New York, 1986
6. S. M. Kraemer, *Aquat. Sci*. **66** (2004) 3
7. C. R. M. Rao, A. Sahuquillo, J. F. Lopez Sanchez, *Water, Air, Soil Pollut*. **189** (2008) 291
8. B. D. Sharma, D. S. Chahal, P. Singh, K. Raj-Kumar, *Commun. Soil Sci. Plant Anal.* **39** (2008) 2550
9. J. T. Sims, *Soil Sci. Soc. Am. J.* **50** (1986) 367
10. A. Tessier, P. G. C. Campbell, M. Bisson, *Anal. Chem.* **51** (1979) 844
11. B. Kim, M. B. McBride, *Environ. Pollut*. **144** (2006) 475
12. M. J. Sánchez-Martín, M. García-Delgado, L. F. Lorenzo, M. S. Rodríguez-Cruz, M. Arienzo, *Geoderma* **142** (2007) 262
13. A. M. Ure, in *Heavy metals in soils*, 2nd ed., B. J. Allovay, Ed., Blackie Academic & Professional, Glasgow, UK, 1995, p. 58
14. P. S. Polić, *PhD dissertation*, University Belgrade, 1991
15. D. Relić, D. Đorđević, A. Popović, T. Blagojević, *Environ. Int.* **31** (2005) 661
16. Đ. Petrović, M. Todorović, D. Manojlović, V. D. Krsmanović, *J. Serb. Chem. Soc.* **75** (2010) 1005
17. H. Egner, H. Riehm, W. R. Domingo, *Kungl. Lantbrukshögskolans Annaler* **26** (1960)
18. R Mead, R. N. Curnow, A. M. Hasted, *Statistical methods in agricultural and experimental biology*, Chapman & Hall, London, 1996, p. 410
19. H. S. Jassal, P. S. Sidhu, B. D. Sharma, S. S. Mukhopadhyay, *J. Indian Soc. Soil Sci.* **48** (2000) 163
20. F. X. Han, W. L. Kingery, J. E. Hargreaves, T. W Walker, *Geoderma* **142** (2007) 96
21. J. P. Singh, S. P. S. Karwasra, M. Singh, *Soil Sci*. **146** (1988) 359
22. M. Petrovic, M. Kastelan-Macan, A. J. M. Horvat, *Water, Air, Soil Pollut.* **111** (1999) 43
23. W. L. Lindsay, W. L. Norvell, *Soil Sci. Soc. Am. J.* **42** (1978) 421
24. J. L. Sims, W. H. Patrick, *Soil Sci. Soc. Am. Proc*. **42** (1978) 258
25. X. Hang, H. Wang, J. Zhou, C. Du, X. Chen, *J. Hazard. Mater*. **163** (2009) 922
26. A. Chen, C. Lin, W. Lu, Y. Ma, Y. Bai, H. Chen, J. Li, *J. Hazard. Mater*. **175** (2010) 638
27. L. D. Colombo, S. B. Mangione, A. Figlioglia, *Agr. Med. Intern. J. Agric. Sci*. **128** (1998) 273
28. M. Jakovljević, M. Kresović, S. Blagojević, S. Antić-Mladenović, *J. Serb. Chem. Soc.* **70** (2005) 765
29. Y. K. Soon, S. Abboud, *Can. J. Soil Sci*. **70** (1990) 277
30. C. Kabala, B. R. Singh, *J. Environ. Qual*. **30** (2001) 485
31. M. Jakovljevic, M. Pantovic, S. Blagojevic, *Laboratory Manual of Soil and Water Chemistry*, Faculty of Agriculture, Belgrade, 1995, p. 57 (in Serbian).

Journal of the Serbian Chemical Society
JSCS-info@shd.org.rs • www.shd.org.rs/JSCS
J. Serb. Chem. Soc. 76 (5) 795–803 (2011)
JSCS–4160
UDC 627.157+546.36+539.163:627.8.034.7
(282.243.743)
Original scientific paper

Distribution and accumulation of heavy metals in the water and sediments of the River Sava

ŽIVORAD VUKOVIĆ[1], MIRJANA RADENKOVIĆ[1], SRBOLJUB J. STANKOVIĆ[1]* and DUBRAVKA VUKOVIĆ[2]

[1]*Institute of Nuclear Sciences Vinča, P. O. Box 522, Belgrade 11001 and* [2]*Institute of Veterinary Medicine, Vojvode Toze 24, Belgrade 11000, Serbia*

(Received 20 April 2010, revised 7 January 2011)

Abstract: The distribution and accumulation of assorted heavy metals and a long-lived radionuclide (Cu, Zn, Pb, Cd, U, Th and ^{137}Cs) in the water and sediment of the River Sava (in Serbia) were investigated at three locations in the vicinity of industrial and urban settlements (Sabac, Obrenovac, Belgrade). The concentrations of heavy metals in the sediment were found to be in the ranges (mg kg^{-1}): 29.6–145.1 for Cu, 53.2–253.6 for Zn, 14.2–78.6 for Pb, 0.3––24.6 for Cd, and 4.0–12.5 Bq l^{-1} for ^{137}Cs. These values correlate to the concentrations in the river water if expressed by equilibrium distribution coefficients K_d (dm^3 g^{-1}) between the solid and liquid phases. The degrees of accumulation and enrichment of tracer metals were determined.

Keywords: accumulation; cesium; enrichment; heavy metals; K_d; sediment.

INTRODUCTION

The studies of heavy metals and other pollutants in river water and sediments have multiplied in recent years, especially for large rivers such as the Danube,[1] Po[2] and Tisza.[3]

Discharges of inorganic and organic micro-pollutants and radioactivity from various industrial, agricultural and municipal sources have resulted in permanently contaminated water, polluted sediments and the accumulation of chemicals in the aquatic food-chain.

In view of the persistence of many micro-pollutants and their potential for bioaccumulation, sediments are regarded as an important source that seriously threatens natural ecosystems[2]. Unlike organic pollutants, heavy metals are not removed by natural processes of decomposition. Heavy metals entering natural waters become part of the water sediment system and their distribution processes

* Corresponding author. E-mail: srbas@vinca.rs
doi: 10.2298/JSC100420067V

are controlled by a dynamic set of physical and chemical interactions and equilibria.[4]

Heavy metals are among the most common environmental water and biota pollutants, indicating the presence of both natural and the anthropogenic sources. Heavy metals of anthropogenic origin are generally introduced into the river system as inorganic complexes or hydrated ions, which are easily adsorbed on the surfaces of sediment particles through relatively weak physical or chemical bonds. Thus, heavy metals of anthropogenic origin are found predominantly as a labile extractable fraction in sediments.[5]

The trend of heavy metal accumulation over the last hundred years[6] shows increasing concentrations of heavy metals in surface sediments, which mainly result from anthropogenic activities. The trace metal levels in sediments usually displayed marked seasonal and regional variations, which were attributed to anthropogenic influences and natural processes.[7,8]

An analysis of the River Po sediment quality identified three major factors which explained the observed variance.[2] The first and second factors corresponded to anthropogenic inputs and geological factors, while the third one included seasonal processes of minor importance.

The Sava became an international river in 1992. It drains 95.700 km^2 of land in former Yugoslavia, before entering the Danube at Belgrade in Serbia. For the supply of potable water, both large cities and small villages in the Sava catchment area rely on ground water. Only Belgrade, the Serbian capital, uses ground water and river water conjunctively. The other uses of the river and its surroundings include agriculture, forestry, power generation, recreation *etc*. Increasing industrialization and the growth of large urban centers have been accompanied by increased pollution of the aquatic environment. Furthermore, the changes in the water environment effected by human activity have affected the ecological system of the Sava catchments. Notwithstanding the investigations performed on the upper stretches of River Sava in Slovenia and Croatia,[9,10] little attention has been paid to the quality of its water in Serbia.[11] In this study, the contents of assorted heavy metals and long-lived radionuclides were analyzed with the objective to predict the level and trends of River Sava water and sediment pollution in Serbia.

EXPERIMENTAL

From the autumn of 2005 to the spring of 2009, samples of both river sediment and water were collected at three locations: Sabac (marked with 1), Obrenovac (2) and Belgrade (3). A map of the final stretch of the Sava River with sample collection locations marked is shown in Fig. 1.

The specimens were taken for analysis in proper dishes, according to the standard procedure.[12] The sediment samples were collected with a grab sampler.

Fig. 1. Location of sampling stations on the Sava River: Šabac – location No. 1, Obrenovac – location No. 2 and Belgrade – location No. 3.

The sediment samples were dried in an oven at 105 °C to constant weight. The caked sediment material was then finely ground and 2.5 g samples were dissolved in 25 cm^3 of 1/1 HNO_3. For investigation of the river water quality parameters, standard analytical methods[13] were used, as well as atomic absorption spectrometry.[14] The concentrations of heavy metals were determined by flame atomic absorption spectrometry in an air/acetylene flow, using a Perkin Elmer AA 200 spectrometer. The cadmium concentration was determined by the graphite furnace technique using Perkin Elmer AA 600 with a transversely-heated graphite atomizer (THGA) and a Zee man Effect background correction system. THGA provides a uniform temperature distribution over the entire length of the tube length, rapid heating and an integrated L'vov platform, resulting in an improved signal/interference ratio and high analytical sensitivity. The analytical injection (20 µl) and the atomization were realized in five steps, controlled by appropriate software and an auto-sampler.

For both techniques, adequate hollow cathode lamps (HCL) were used for irradiation and mixed reference standard solutions were prepared for analysis, using Merck certified atomic absorption stock standards (1000 µg ml^{-1}) and Mili-Q purified water. No modifiers were added.

The activity of the gamma-ray emitter was analyzed by a multichannel analyzer using a reverse electrode HPGe detector of 23 % relative efficiency. The radioactivity of sediment samples was measured on the fraction of particles that passed through a 1.0 mm sieve, after establishment of the radioactive equilibrium between ^{220}Rn and its daughter products.

RESULTS AND DISCUSSION

The concentrations of heavy metals in the river sediment at the three studied locations, marked Fig. 1, are presented in Table I. There were no large fluctuations in the concentrations of heavy metals in the sediments. Differences in the concentrations existed between the spring and autumn seasons, which were more then 20 % higher in the autumn in the case of Pb and Cd, but negligibly higher for Cu and Zn. The mean values of the concentrations for all the samples amounted to: 56.0 mg kg^{-1} for Zn; 39.0 mg kg^{-1} for Cu; 27.0 for Pb and 4.6 mg kg^{-1} for Cd. In the upper stretch of the Sava River, about 450 km from its confluence, these values were: 136.0 mg kg^{-1} for Zn; 29.0 mg kg^{-1} for Cu, and 22.5

mg kg^{-1} for Pb.[9] Thus, a large discrepancy was obtained only for Zn. In the Sava River sediment in Slovenia, the concentrations of Cd were below 0.8 mg kg^{-1}.[10]

TABLE I. Concentrations of heavy metals in sediment (mg kg^{-1}) from autumn 2005 to spring 2009, min. – minimum, max. – maximum, mean – mean value

Heavy metal	Location No. 1 concentration, mg kg^{-1}			Location No. 2 concentration, mg kg^{-1}			Location No. 3 Concentration, mg kg^{-1}		
	Min.	Mean	Max.	Min.	Mean	Max.	Min.	Mean	Max.
Zn (autumn)	52.0	66.2	83.3	56.5	68.1	78.1	51.5	72.3	86.5
Zn (spring)	28.2	38.9	45.8	48.9	57.5	71.4	49.2	61.8	72.3
Cu (autumn)	28.2	34.3	43.3	45.8	51.4	59.3	39.3	48.2	58.6
Cu (spring)	25.2	31.5	39.1	33.6	47.6	57.3	35.5	46.1	56.0
Pb (autumn)	14.7	20.3	29.1	38.3	42.6	52.0	36.7	43.5	58.2
Pb (spring)	13.9	17.1	19.6	15.4	17.4	19.5	15.3	20.2	22.4
Cd (autumn)	3.9	5.7	8.5	3.8	5.8	7.3	5.8	7.7	8.6
Cd (spring)	2.8	3.8	5.6	3.6	4.9	6.6	3.7	5.1	6.9

The concentrations of heavy metals in the river water at the same three sites are presented in Table II. These concentrations in both the solid and the liquid phases are relatively low. The concentrations of Cd in the river water surmounted the limiting value of 5 μg dm^{-3} for class A surface waters only in a few cases. Pb as well was above its limiting value of 50 μg dm^{-3} in a few cases.[11]

TABLE II. Concentrations of heavy metals in water (μg dm^{-3}) from autumn 2005 to spring 2009, min. – minimum, max. – maximum, mean – mean value

Heavy metal	Location No. 1 concentration, mg kg^{-1}			Location No. 2 concentration, mg kg^{-1}			Location No. 3 Concentration, mg kg^{-1}		
	Min.	Mean	Max.	Min.	Mean	Max.	Min.	Mean	Max.
Zn (autumn)	14.3	41.2	72.1	17.5	46.5	64.2	22.6	56.1	78.4
Zn (spring)	14.5	29.3	45.2	19.5	36.0	44.9	32.3	48.4	64.8
Cu (autumn)	13.2	20.9	32.6	9.2	15.8	24.5	11.7	15.3	17.2
Cu (spring)	16.7	21.2	29.1	7.3	13.6	17.5	5.5	12.8	16.1
Pb (autumn)	2.9	4.1	5.6	3.8	4.7	6.2	4.3	6.5	7.2
Pb (spring)	2.8	3.8	4.9	2.2	3.9	6.1	3.2	5.8	6.3
Cd (autumn)	0.5	2.1	4.1	0.4	0.7	1.0	0.4	0.8	1.3
Cd (spring)	0.3	0.5	0.7	0.3	0.5	0.9	0.3	0.6	0.8

Heavy metals are among the most common environmental pollutants in water and biota, which indicate the presence of natural and anthropogenic sources. The reason for the small fluctuations of the concentrations is the absence of heavy metals in the Sava water originating from point sources at the tested locations. Diffuse pollution originates from many small sources. Most diffuse pollutants stem from the use of land for agriculture, forestry, industry, and urban settlements.[15]

The anthropogenic impact can be quantified by calculating the enrichment factor. Enrichment factors (*EF*) were used to evaluate possible anthropogenic intakes of the observed sediment metals and were calculated according to the formula:

$$EF = (M_{sample} / A_{sample}) / (M_{crust} / A_{crust}) \quad (1)$$

where M_{sample} and M_{crust} are the levels of the targeted metals in the sediment samples and local uncontaminated crust minerals, respectively, and A_{sample} and A_{crust} are the corresponding values for a normalizing element presumed not enriched due to local contamination. The baseline values for M_{crust} were taken from published data.[1,14]

The values of heavy metals sediment concentrations correlate to their concentrations in the river water. The heavy metal enrichment factor (*EF*) usually suggests concentrations above the background level in the study area. An element concentration higher than twice the background content implies anthropogenic pollution; *EF*s higher than 2 indicate contaminated sites.[1] A similar approach was used in many studies.[3,6,14,16] The present approach to the interpretation of the experimental results was different. In this paper, the partitioning of heavy metals between suspended matter and water is described in terms of the equilibrium distribution coefficient K_d (dm^3 g^{-1}), expressed as the concentration ratio under equilibrium conditions. The processes of heavy metals and radionuclides sorption and desorption by suspended particles and bottom sediments are instantaneous, reversible, and described by a constant distribution coefficient K_d.[17,18] The values of distribution coefficients of the examined four metals are presented in Figs. 2–4 for locations 1–3, respectively. The values of the K_d coefficients fall in the direction Cd > Pb > Cu ≈ Zn. The distribution coefficient for each heavy metal demonstrates the capability of the sediment to accumulate it. In the absence of anthropogenic influences, distribution coefficients reflect the background levels of trace elements in a river sediment, according to the distribution law.

The expanding industrial activity over the post-WW2 years regularly introduced heavy and toxic metals into the river ecosystems. Studies demonstrate that surface water quality has deteriorated noticeably in many countries over past decades, due to poor land use practices.[19]

However, the industrial activity in Serbia slowed down during the past two decades, which is the reason for the weakly noticeable anthropogenic input of heavy metals in the Sava River system from the nearby environment. In spite of this, the high values of K_d for the four examined heavy metals indicate their accumulation in the sediment.

In our opinion, the enrichment factor (*EF*) is more correctly evaluated by comparing the minimal and maximal values of K_d, because a K_d value expresses the real state of a river system, based on the distribution law.

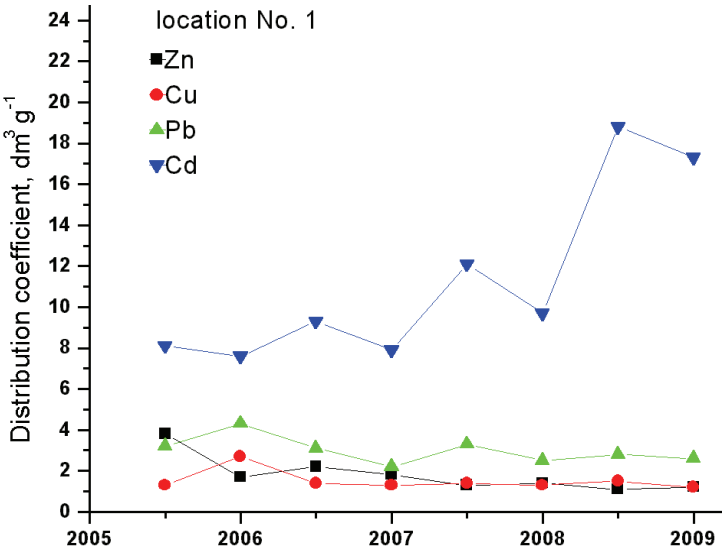

Fig. 2. Distribution coefficient K_d (dm^3 g^{-1}) for location No. 1 in the four-year period.

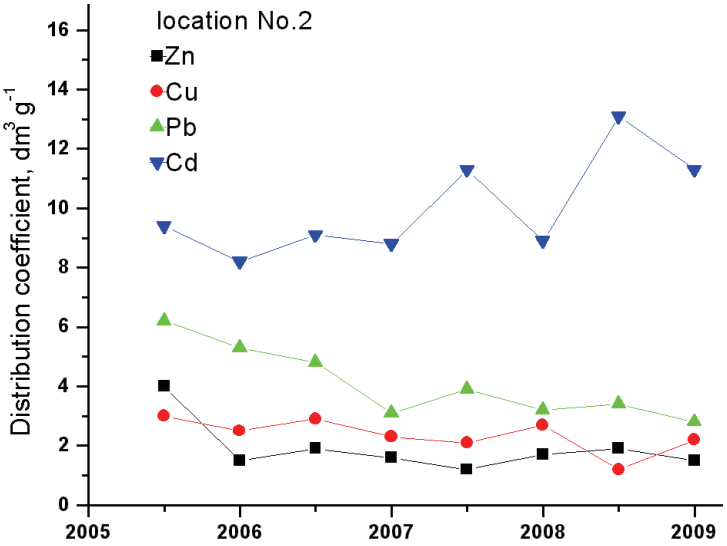

Fig. 3. Distribution coefficient K_d (dm^3 g^{-1}) for location No. 2 in the four-year period.

Experimental results of many studies showed high sorption of heavy metals in sediments, but there were cle ar differences among the sediments and soil samples.

Hydraulic processes are mainly responsible for the transport and diffusion of toxic substances through water, whereas geochemical processes influence the interaction of dissolved tracer metals with suspended matter an d bottom sedi-

ment.[18] River sediment is an integral and dynamic part of a river basin. It originates from the weathering of minerals and soil upstream and is susceptible to transport downstream by the river water.

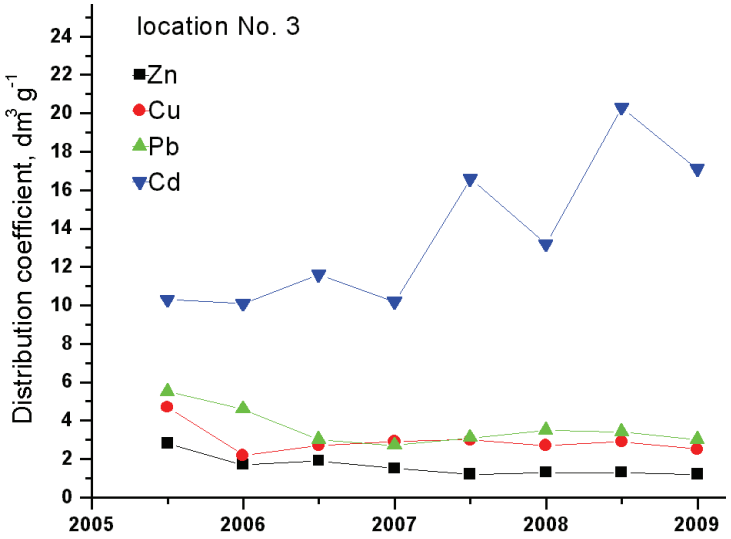

Fig. 4. Distribution coefficient K_d (dm^3 g^{-1}) for location No. 3 in the four-year period.

The reason for the weakly noticeable accumulation of heavy metals in the Sava River sediment lies in the fact that the suspension load of sediment varies broadly depending on the traits of the river streams. The International Atomic Energy Agency default value for rivers[20] is 5.0×10^{-2} kg m^{-3}. The high value of the suspension load, resulting in higher mass loading, arises because the flow of the River Sava is greater down-stream. In this way, large amounts of tracer heavy metals are transported by the Sava River stream to the River Danube and the Black Sea.

The long lived natural radionuclides behaved similar to the investigated heavy metals.[17,18] The results of long-lived radionuclide accumulation in the ecosystem of the Sava River were the subject of a previous study.[21] It was proven that the natural radioactivity of the Sava sediment reflects the natural background (the activity is 26–33 Bq kg^{-1} for ^{238}U and 28–49 Bq kg^{-1} for ^{232}Th). In contrast to the heavy metals, the natural radionuclides do not show seasonal variations because there are no identified point or diffuse sources of natural radionuclides. In addition to the natural radioactivity, there is also anthropogenic radioactivity present in the Sava River ecosystem, as a result of nuclear weapons tests and the Chernobyl nuclear accident. As a consequence of the Chernoby l fallout, ^{137}Cs concentrations of between 4 and 13 Bq kg^{-1} were also detected in the Sava sediment. In earlier findings, the ^{137}Cs radioactivity was below 0.01 Bq l^{-1} in the

river water, and between 12 and 41 Bq kg $^{-1}$ ^{21} in the sediment. The present results show an absence of radionuclide accumulation in the Sava River sediment. In this case, the flux of Cs radionuclide from sediment to water, due to sediment re-suspension and direct exchange of radionuclide from the bottom sediment, prevails over the radionuclide flux from the water to the sediment.[22]

CONCLUSIONS

The levels of heavy metals in the Sava River water and sediment displayed seasonal fluctuations, which were attributed mainly to natural processes, with a barely noticeable accumulation. The influences of anthropogenic sources are not pronounced. The concentrations of heavy metals in the bottom sediment are in correlation with their concentration in the river water. The degree of accumulation was calculated by comparing the minimal and maximal values of the distribution coefficients for each heavy metal.

The low level of radioactivity from anthropogenic radionuclides (^{137}Cs) originates from the Chernobyl accident and gradually decreases without evidence of any new contamination.

ИЗВОД

РАСПОДЕЛА И АКУМУЛАЦИЈА ТЕШКИХ МЕТАЛА У ВОДИ И СЕДИМЕНТУ РЕКЕ САВЕ

ЖИВОРАД ВУКОВИЋ[1], МИРЈАНА РАДЕНКОВИЋ[1], СРБОЉУБ Ј. СТАНКОВИЋ[1] и ДУБРАВКА ВУКОВИЋ[2]

[1]Институт за нуклеарне науке "Винча", п .пр. 522, 11001 Београд и [2]Институт ветеринарске медицине, Војводе Тозе 24, 11000 Београд

Тешки метали (Cu, Zn, Pb и Cd) и дугоживећи радионуклиди (U, Th и ^{137}Cs) испитивани су у води и седименту реке Саве у току кроз Србију на три локације у близини индустријских и урбаних насеља (Шабац, Обреновац и Београд). Концентрације тешких метала у седименту варирале су у опсегу (mg kg^{-1}): 28,1–145,1 за бакар, 53,2–253,6 за цинк, 14,2––78,6 за олово и 3,0–24,6 за кадмијум. Ове вредности су у корелацији са концентрацијама тешких метала у речној води изражене преко коефицијента дистрибуције K_d (dm^3 g^{-1}) између чврсте и течне фазе. Одређивани су степени акумулације и концентрисања трасерских количина тешких метала.

(Примљено 20. априла 2010, ревидирано 7. јануара 2011)

REFERENCES

1. P. Woitke, J. Wellmitz, D. Helm , M. Kube, P. Lepom , P. Litheraty, *Chemosphere* **51** (2003) 633
2. M. Camusso, S. Galassi, D. Vignati, *Water Res.* **36** (2002) 2491
3. S. M. Sakan, D. S. Djordevic, D. D. Manojlovic, P. S. Polic, *J. Environ. Manage.* **90** (2009) 3382
4. C. K. Jain, *Water Res.* **38**(2004) 569
5. K. P. Singh, A. Malik, N. Basant, V. K. Sing , A. Basant, *Chemom. Intell. Lab. Syst.* **87** (2007) 185

6. B. Xu, X. Yang, Z. Gu, Y. Zhang, Y. Chen, Y. Lv, *Chemosphere* **75** (2009) 442
7. A. L. Tuna, F. Yilmaz, A. Demirak, N. Ozdemir, *Environ. Monit. Assess.* **125** (2007) 47
8. A. Sood, K. D. Singh, P. Pandey, S. Sharma, *Ecol. Indic.* **8** (2008) 709
9. V. Orescanin, L. Mikelic, S. Lulic, G. Pavlovic, N. Coumbassa, *Nucl. Instrum. Meth. B* **263** (2007) 85
10. S. Murko, R. Milačić, M. Veber, J. Ščančar, *J. Serb. Chem. Soc.* **75** (2010) 113
11. J. Krizan, M. Vojinovic-Miloradov, *Water Res.* **31** (1997) 2914
12. N. D. Drndarski, S. Maric, *J. Radioanal. Nucl. Chem.* **130** (1989) 287
13. R. N. Reeve, *Environmental Analysis*, Wiley, Chichester, UK, 1994, p. 200
14. S. Olivares Rieumont, D. Rosa, L. Lima, D. W. Graham, K. D. Alessandro, J. Borroto, F. Martinez, J. Sanchez, *Water Res.* **39** (2007) 3945
15. R. C. Ferrier, B. J. D. Arci, J. MacDonald, M. Altken, *Water Environ. J.* **19** (2005) 361
16. A. Kaushik, A. Kansal, S. Meena, S. Kumari, C. P. Kaushik, *J. Hazard. Mater.* **164** (2009) 265
17. I. Kryshev, P. Boyer, L. Monte, J. E. Brittain, N. N. Dzyuba, A. L. Krylov, A. I. Kryshev, A. V. Nosov, K. D. Sanina, M. I. Zheleznyak, *Sci. Total Environ.* **407** (2009) 2349
18. L. Monte, P. Boyer, J. E. Brittain, L. Hakanson, S. Lepicard, J. T. Smith, *J. Environ. Radioactiv.* **79** (2005) 273
19. S. Li., S. Gu, X. Tan, Q. Zhang, *J. Hazard. Mater.* **165** (2009) 317
20. A. Aguero, *Sci. Total Environ.* **348** (2005) 32
21. Ž. Vukovic, V. Sipka, D. Todorovic, S. J. Stankovic, *J. Radioanal. Nucl. Chem.* **268** (2006) 129
22. J. T. Smith, R. T. Clarke, M. Saxén, *J. Environ. Radioactiv.* **49** (2000) 65.